The automatic detection and rectification of surface and aesthetic defects in the production of wooden panels

Kuehn, Marc Oliver

Award date:
2016

Awarding institution:
Coventry University

The Automatic Detection and Rectification of Surface and Aesthetic Defects in the Production of Wooden Panels

Marc Oliver Kühn

A thesis submitted in partial fulfilment
of the University's requirements
for the Degree of Doctor of Philosophy

September 2015

Coventry University

In collaboration with: Baumer

Abstract

The trend in production of furniture, flooring, housing parts and similar is to repair and upgrade defective feedstock rather than scrap it. The corresponding task of rectification is mainly based on manual labour with a clearly visible need for automation to reduce costs. This thesis shows that it is possible to automatically carry out defect rectification on softwood panels by first detecting unwanted defects of various kinds, second assessing them correctly also by pre-determined aesthetic aspects and thirdly generating instructions for correspondingly an aesthetically acceptable repair.

A novel approach based on pixel-wise registered multi-dimensional images, cascaded unsupervised and supervised learning and an expert system based on a fuzzy knowledge base has been tested. It is shown that automated patching under aesthetic aspects can be achieved by modelling the human wood worker's implicit and explicit knowledge. Support Vector Machines (SVMs) are able to deal with the high dimensional registered image data and the associated non-linear classification problem that addresses the local aesthetics without the need for feature engineering. An expert system generates rectification instructions for the detected defects with respect to the final panel appearance and acts as a user interface to adjust the process. Satisfactory results in terms of aesthetically acceptable panels of Nordic Spruce patched with different types of solid and liquid fillers have been achieved.

The feasibility of machines being able to assess, preserve, modify or create aesthetics is demonstrated for the first time on wooden panels. The application in a productive, industrial environment has successfully been shown, therefore filling a gap in the automation of wooden panel production.

Keywords: *automated patching, intelligent automation, wooden panels, putty, dowels Nordic Spruce, Pine Radiata, patching rules, aesthetic appearance, defect detection, image sensor fusion, Deep Learning, SVM, SOM, Expert System, knowledge base,*

Acknowledgements

Firstly, I must express my warmest gratitude to my Director of Studies, Dr. Raymond Jones for his superb guidance over all these years. I could not have asked for a better support, advice and motivation in setting up, writing and editing this thesis from the very beginning. I am equally grateful to my supervisors John Owen for his patience and the discussions related to arts and Dr. James Shuttleworth for joining the project in a critical stage and for his technical input from computer science in the diverse topic of this thesis.

My PhD research project would not have been set up without the visions and belief of my supervisor at Baumer Inspection GmbH, Professor Dr. Jörg Eberhardt. The numerous discussions we had in Carinthia further influenced my work greatly. Of course I want to express equal gratitude to Professor Dr. Robert Massen for his great and visionary support from the early beginning of the project and I wish much more time could have been spent on our exchange of ideas. I would like to thank also his wife for the marvellous evenings on the terrace we had during the supervisor meetings.

Many thanks go to my former colleagues: to Michael Göttlicher for his great practical contribution to the project with his diploma thesis and for the discussions we had in Austria, Chile and Finland, to Andrzej Stefanski for his engineering and support in Austria and also to Stephan Kubalek for his tireless commitment and the discussions during our testing in Finland.

It would take many more lines to thank individually everyone who has helped and supported me. Nevertheless, I would like to extend my thanks to all the helping hands at Coventry University, to Professor Dr. Matthias Franz at University of Applied Sciences, Constance and to the employees at Tilly GmbH, Finnforest / Metsä Group, Arauco S.A. and Fill GmbH.

Finally my heartfelt thanks go to my girlfriend Mandy, my friends and to my parents for their encouragement, my father not being able to witness the accomplishment this work.

Marc Oliver Kühn, August 2015

Table of contents

ABSTRACT ..... **I**

ACKNOWLEDGEMENTS ..... **II**

TABLE OF CONTENTS ..... **III**

LIST OF FIGURES ..... **VII**

LIST OF TABLES ..... **XIV**

LIST OF FORMULAS ..... **XV**

ABBREVIATIONS ..... **XVI**

TERMINOLOGY ..... **XVIII**

1 INTRODUCTION **1**

1.1 BACKGROUND OF THE PROBLEM 2
1.2 STATEMENT OF THE PROBLEM 2
1.3 AIM AND OBJECTIVES 3
1.4 RESEARCH QUESTIONS 4
1.5 SCOPE OF THE STUDY 5
1.5.1 Delimitations and limitations *6*
1.6 STRUCTURE OF THE THESIS 7

2 CONTEXTUAL BACKGROUND **8**

2.1 INDUSTRY SIGNIFICANCE 8
2.1.1 Wood-based panels *10*
2.1.2 Economical aspects - market development *11*
2.2 DEFECTS ON WOODEN PANELS 13
2.2.1 Physical defects *14*
2.2.1.1 Three-dimensional defects 14
2.2.1.1.1 Knothole 15
2.2.1.1.2 Glue-filled knothole 16
2.2.1.1.3 Cracks 16
2.2.1.1.4 Pinhole/wormhole 17
2.2.1.1.5 Roughness 17
2.2.1.1.6 Shells 18
2.2.1.1.7 Resin pocket 18
2.2.1.1.8 Cracked Knots 19
2.2.1.2 Structural defects 20
2.2.1.2.1 Dark knot, dry not & loose knot 20
2.2.1.2.2 Bark, Knot with bark, Ringed Knot 21
2.2.1.2.3 Rot 22
2.2.1.2.4 Reaction wood (compression wood) 23
2.2.1.2.5 Pressed-in particle 23
2.2.2 Pure aesthetic defects *24*
2.2.2.1 Discoloration 24
2.2.2.2 Grain structure 25
2.2.2.3 Blue stain 26
2.2.2.4 Needleflex / Needleinfusion 27
2.2.2.5 Knots 28
2.2.2.5.1 Sound knots 28
2.2.2.6 Clusters of knots 29
2.2.3 Quality standards *30*
2.2.3.1 Standards and norms 30
Company specific standards 32
2.2.4 Summary *33*
2.3 METHODS OF PATCHING WOODEN PANELS 33
2.3.1 Types of patching on wooden panels *33*

2.3.1.1 Solid fillers 35
2.3.1.2 Liquid fillers 36
2.3.1.2.1 One-component putty 37
2.3.1.2.2 Two-component putty 37
2.3.1.3 Hotmelts 38
2.3.2 Investigation into manual processes 38
2.3.2.1 Patching with dowels 38
2.3.2.2 Patching with putty 40
2.3.3 Aesthetic aspects when patching 44
2.4 TECHNOLOGY DEMANDS 45

3 LITERATURE REVIEW 46

3.1 MACHINE VISION AND WOOD BASED PRODUCTS 46
3.1.1 Imaging techniques 46
3.1.2 Multi-channel image processing 53
3.1.3 Classification techniques in defect detection 54
3.1.4 Features for wood defect classification 56
3.2 WOOD APPEARANCE AND AESTHETICS 57
3.3 AUTOMATED PHYSICAL RECTIFICATION OF WOOD BASED PRODUCTS 61
3.4 AUTOMATED AESTHETICAL RECTIFICATION OF WOOD BASED PRODUCTS 62
3.5 SUMMARY OF REVIEW 62

4 RESEARCH METHODS 64

4.1 CLASSIFICATION OF DEFECTS UNDER LOCAL AESTHETIC ASPECTS 64
4.1.1 Combined unsupervised and supervised learning 69
4.1.2 SOM – Self Organizing Map 70
4.1.2.1 Discussion of SOM 72
4.1.3 SVM- Support Vector Machine 73
4.1.3.1 A geometrical interpretation of SVM margins 75
4.1.3.2 Discussion of Support Vector Machines 78
4.2 DECISION MAKING FOR PATCHING UNDER APPEARANCE ASPECTS 79
4.2.1 Expert Systems 83
4.2.2 FIS – Fuzzy Inference System 84
4.2.3 Discussion of FIS 85
4.3 SUMMARY OF RESEARCH METHODS 85

5 SYSTEM DESIGN 86

5.1 A DEDICATED CLUSTER ARCHITECTURE FOR AUTOMATED PATCHING 88
5.1.1 Layer 1: Sensor data fusion - creating the global image 93
5.1.2 Layer 2: Detection & evaluation 96
5.1.2.1 Segmentation 96
5.1.2.2 Classification 99
5.1.3 Layer 3: Decision making & patching data generation 99
5.1.3.1 User interface and interface to machinery 100
5.1.4 Summary 100
5.2 DEFECT DETECTION TECHNIQUES 101
5.2.1 Standard detection techniques 101
5.2.2 Demanding defect types 103
5.2.2.1 Glue-filled knothole 103
5.2.2.2 Resin pocket 104
5.2.2.3 Pressed-in particle 105
5.2.3 Specifically optimized detection techniques 106
5.2.3.1 Analysis of spectral data 106
5.2.3.2 Fluorescence evaluation 110
5.2.3.3 UV remission evaluation 110
5.2.3.4 UV absorption evaluation 111
5.2.4 Summary 111
5.3 DEFECT CLASSIFICATION SYSTEM 114
5.3.1 Principle of cascaded training 115
5.3.2 Classification of raw pixel data 117
5.3.3 Incorporating a priori knowledge 118

5.3.4 Summary *119*
5.4 DECISION MAKING 120
5.4.1 Information flow *120*
5.4.2 Definition of fuzzy rules at the example of Knothole with bark *123*
5.4.3 Spanning the decision surface *126*
5.4.4 Summary *138*
5.5 PATCHING DATA GENERATION 138
5.5.1 Patching with dowels *139*
5.5.2 Patching with putty *142*
5.6 SUMMARY 144

6 SYSTEM DEVELOPMENT & PERFORMANCE 146

6.1 DETECTION PERFORMANCE 147
6.1.1 Training of the classification system *147*
6.1.1.1 Training experiment setup 148
6.1.1.2 Training and testing 149
6.1.1.2.1 Bark 150
6.1.1.2.2 Dark Knot 152
6.1.1.2.3 Ringed Knot 153
1.1.1.1.1 Sound Knot 154
6.1.1.2.4 Cracked Knot 157
6.1.1.2.5 Resin Pocket 158
6.1.1.2.6 Judgement on local aesthetics 159
6.2 PATCHING PERFORMANCE 161
6.2.1 Decision making *161*
6.2.1.1 Patching with dowels 163
6.2.1.2 Patching with putty 167
6.2.1.2.1 Optimization approaches 171
6.3 SUMMARY 173

7 DISCUSSION AND CONCLUSIONS 174

7.1 REVIEW 174
7.2 DISCUSSION 176
7.2.1 Interpretation of findings *176*
7.2.2 Interpretation in context of literature *180*
7.2.3 Generalisation and implications *184*
7.2.4 Limitations of the study *185*
7.3 CONCLUSIONS 188
7.4 FURTHER RESEARCH 192

REFERENCES 197

APPENDIX 208

A.1. FUNCTION PRINCIPLE OF SOM 208
A.2. FUNCTION PRINCIPLE OF SVM 211
A.2.1 Linear learning machines *211*
Hyperplane margin optimization 212
Maximum margin 213
Optimization strategy 213
Convexity 215
Application of optimization strategy 215
Extended optimization theory 216
Support Vectors 219
A.2.2 The Kernel Trick *221*
A.2.3 Soft margin extension *223*
A.3. FUZZY LOGIC 226
A.3.1 Membership functions *226*
A.3.2 Fuzzy logic operators *227*
A.3.3 If-then rules *228*
A.4. ALGORITHMS AND CALIBRATIONS FOR IMAGE SENSOR DATA FUSION 231
A.4.1 Calibrations *231*

A.4.2 Image stitching *232*
A.4.3 Image registration *233*
A.5. ELIMINATION OF INTERNAL & EXTERNAL DISTURBING EFFECTS 235
A.5.1 Elimination of dynamic effects from vibration *235*
A.5.2 Elimination of dynamic effects from panel warping *236*
Shaded images 236
Displacement of image plane in triangulation 238
Derivation of tilted image plane satisfying the Scheimpflug rule 239
A.6. ETHICAL APPROVAL CERTIFICATE 241

List of figures

Figure 2-1: Wood working industry sectors. (Data: *[CEI*-Bois2011*]*).....9
Figure 2-2: Links between the different sectors in the wood-working industry in terms of production and material flow. The furniture sector plays an important and central role among the different sectors and as it consumes several of the other sectors' outputs.....9
Figure 2-3: Sub-sectors within the wood-based panels sector. (Data: *[CEI-Bois 2011]*).....10
Figure 2-4: Plywood panels and blockboards end user markets (data: *[CEI-Bois 2011]*).....10
Figure 2-5: Plywood production rates EU & China (data: *[FAOSTAT 2014]*).....12
Figure 2-6: Plywood: import quantities EU, export quantities China (data: *[FAOSTAT 2014]*).....12
Figure 2-7: Production rate & price trends of Finish plywood (data: *[FAOSTAT 2014]*).....13
Figure 2-8: Knothole (showing some bark on the right side) in pine plywood top layer veneer (4mm). The application of glue in fine lengthwise lanes with the use of spray nozzles is visible as brown vertical lines on the core layer at the bottom of the hole.....15
Figure 2-9: Knothole (showing some bark on the right side) in top layer lamella (5mm) of solid wood spruce panel. The application of glue by extensive coating of the core layer is visible as a white bottom of the hole.....15
Figure 2-10: Knothole in top layer lamella (5mm) of solid wood spruce panel. The application of glue by extensive coating of the core layer is visible as a white bottom. Knothole is located at lamella's border, therefore showing a sharp edge.....15
Figure 2-11: Glue-filled knothole on three-layer solid wood panel (spruce).....16
Figure 2-12: Crack in top layer veneer (pine) of plywood panel, 700mm of length.....16
Figure 2-13: Rough surface of plywood veneer from Nordic Spruce due to very soft earlywood torn out in the peeling process.....17
Figure 2-14: Shells on plywood panel (Pine Radiata) – torn loose earlywood.....18
Figure 2-15: Resin pocket on peeled veneer of spruce. Thin wood often covers parts of the resin pocket (left side).....18
Figure 2-16: Resin pocket on sawn lamella of spruce, only partially opened and with lake from flew-out resin.....19
Figure 2-17: Cracked Knot on plywood panel of spruce.....19
Figure 2-18: Dark knot on sawn lamella from spruce, still quite attached to the surrounding sound wood.....20
Figure 2-19: Dry knot on peeled veneer from spruce showing partial detachment. The surrounding wood already formed some bark to isolate the knot.....20
Figure 2-20: Fallen out loose knot (showing the dark brown homogenous applied glue on the underlying veneer sheet.....21
Figure 2-21: Ingrown bark on plywood of pine, most likely due to former damage.....21
Figure 2-22: Ingrown bark at fold on plywood of spruce.....21
Figure 2-23: Bark around dead knot on plywood of spruce.....22
Figure 2-24: Soft rot (darker area) on veneer from spruce.....22
Figure 2-25: Compression wood on plywood panel of Pine Radiata. Abnormal growth of the wood fibres due to presence of tensile respectively compression on the tree (wind, grown crooked, grown on a slope, etc.).....23
Figure 2-26: Particle pressed into the surface of a spruce plywood panel.....24
Figure 2-27: Pressed-in particle, when removed by sanding, the indentation will remain.....24
Figure 2-28: Discoloration (red) of plywood veneer from Pine Radiata (close-up view).....24
Figure 2-29: Discoloration (red) of plywood veneer panel from Pine Radiata (panel view). Although defect-free in terms of knots and similar, the unusual appearance may be a severe issue in industrial production.....25
Figure 2-30: Examples of different grain structures. Grain structure influences the perception of the wood colour.....25
Figure 2-31: Blue stain on sawn lamella of spruce, the crosswise cut shows the infestation of the outer sapwood.....26
Figure 2-32: Blue stain on plywood panel of Pine Radiata.....26
Figure 2-33: Needleflex on Pine Radiata.....27
Figure 2-34: Sound grown knot on panel of Pine Radiata, fully bonded to the fibres of the surrounding wood, showing a reddish colour.....28

Figure 2-35: Sound grown knots on panel of Pine Radiata, tightly bonded to the surrounding wood, showing brownish colour. 28
Figure 2-36: Knot-free surface preferred by South-American market. 29
Figure 2-37: Regular sound knots preferred in Scandinavian and Austrian market. 29
Figure 2-38: Clusters of sound knots, aesthetically undesired, being also a structural issue. 29
Figure 2-39: Company specific (related to European Norm EN 12017-1) definition of appearance characteristics for multi-layered solid wood panel *[Tilly Naturholzplatten GmbH n.d.]* 32
Figure 2-40: Box/finger joint of sound areas after cutting out crosswise the defective area on a lamella. 33
Figure 2-41: Types of patching on wooden panels: a first distinction is made between patching based on the generous removal vs. local replacement of defective areas with different types of fillers. Camouflaging is an imaginable alternative/extension. 34
Figure 2-42: Circular dowels (spruce) made from branches to reproduce the characteristic age-ring appearance and therefore the best choice for insertion into knotholes. 35
Figure 2-43: Circular dowels (spruce) made from solid sound wood. Various appearances can be produced which favours them for defective areas besides knotholes, depending on the grain structure. 35
Figure 2-44: Elliptic/elongated dowels (spruce) made from solid/sound wood for elongated defect areas like cracks. 35
Figure 2-45: Inlay (pine) produced and inserted with a punch press. 35
Figure 2-46: One-component (1K), water based putty without colorant used to fill area of fallen-out bark on spruce plywood. Result after sanding. 36
Figure 2-47: One-component (1K), water based putty with beige/light brown colouring used to fill pre-processed (routed) defective area on spruce plywood. Result after sanding. 36
Figure 2-48: Two-component (2K) polyurethane filler with beige/light brown pigmentation used to fill knotholes on plywood panel of spruce, applied with a nozzle. Image shows result before sanding; no shrinking is recognizable but the effect of an air bubble in the low viscous filler can be seen. 36
Figure 2-49: Polyurethane-Reactive (PUR) transparent Hotmelt used to patch cracked knot in parquet slab of oak. The application is normally carried out using a solid metal punch to ensure backfill and fast cooling down by evacuation of heat. Image shows result before sanding. 36
Figure 2-50: Manual patching of solid wood panels of spruce with dowels by four workers in two teams. Picture taken in a production facility for multi-layered solid wood panels in Austria. 39
Figure 2-51: Sequence of actions and decisions when patching manually with dowels. Parallelisation of tasks at Austrian panel production facility using teams consisting of two workers responsible for routing respectively filling. 40
Figure 2-52: Patching plywood panels of pine with two-component putty in a Chilean plywood production facility. Pre-processing: every defect area is routed to remove any glue on the underlying veneer to ensure optimal adhesion of the filler. 41
Figure 2-53: Patching plywood panels of pine with two-component putty in a Chilean plywood production facility. Using a nozzle, the filler is applied to the previously routed defect area and if necessary smoothened with the use of a scraper. To prevent blockage of the nozzle lots of putty is wasted by flushing in idle times. 42
Figure 2-54: Patching plywood panels of pine with one-component, water-based putty using simple scraper for application. This is the third and final step in the process, carried out after patching with the two-component filler and related routing in a Chilean plywood production. 43
Figure 2-55: Sequence of actions and decisions for patching with different types of putty and appropriate pre-processing in a Chilean plywood production facility. The process is completely serialized for one board to avoid mixture of different putty types in wrong order. 44
Figure 4-1: Dark knot. 66
Figure 4-2: Ringed knot. 66
Figure 4-3: Knot with bark. 66
Figure 4-4: Acceptable looking dark knot. 67
Figure 4-5: Unattractive looking dark knot. 67
Figure 4-6: Unsupervised learning model. 70
Figure 4-7: Supervised learning model. 70
Figure 4-8: SOM clustering of image tiles. The map organizes the samples in terms of similarity. Blue lines indicate class boundaries in terms of similarity to cluster centres. 71
Figure 4-9: Principle of SVM-training in analogy to two-layer perceptron: Transformation of input vector (symbolized by character 'A') to a higher dimensional feature space via nonlinear function,

construction of optimal hyperplane by finding support vectors, classification according to position relative to hyperplane. 74
Figure 4-10: Geometrical interpretation of SVM classifier. Example of training set with linear separable classes $\omega 1$ and $\omega 2$. For each class the convex hull is shown. The hyperplane classifier is perpendicular to the line between the closest points of the two convex hulls. 77
Figure 4-11: Example of plywood panel (spruce) satisfying ISO 2426-3-2000 appearance class E. (image represents approx. 1m^2). 80
Figure 4-12: Example of plywood panel (spruce) satisfying ISO 2426-3-2000 appearance class I. (image represents approx. 1m^2). 81
Figure 4-13: Example of plywood panel (spruce) satisfying ISO 2426-3-2000 appearance class II. Class II due to unsound knots (image represents approx. 1m^2)....81
Figure 4-14: Example of plywood panel (spruce) satisfying ISO 2426-3-2000 appearance class II. Class II due to huge amount of knots (image represents approx. 1m^2). 82
Figure 4-15: Example of plywood panel (spruce) satisfying ISO 2426-3-2000 appearance class II. Class II due to size of sound knots (image represents approx. 1m^2). 82
Figure 4-16: Schematic diagram of Fuzzy Inference System (FIS). 84
Figure 5-1: Backward view along automated patching line for plywood panels. From rear to front: Scanner system, routing tool portal, 2K-putty tool portal and 1K-putty tool portal in the foreground. Each portal consists of x/y axes with two tools of same type (left/right). Maximum panel size is 2.5m x 5m. 86
Figure 5-2: Routing tools and suction for pre-processing in automated patching using putty. 86
Figure 5-3: 1K putty insertion tool: stamp with nozzle. 86
Figure 5-4: 2K putty insertion tool with nozzle and waste bin for flushing. 86
Figure 5-5: View on automated patching line for solid wood panels. In the foreground the portal with four aggregates with tools for different sized and shaped dowels can be seen. The panel is scanned forward (from rear to front in image) and is then turned to scan the backside in backward movement. Then the panel is moved to left onto the transportation through the portals. 87
Figure 5-6: Aggregate with tools for insertion of circular dowels. The view from below shows router (left) and punch (centre), both using a stencil mounted on a slide. The transparent hose on the right side is used to feed the dowel. 87
Figure 5-7: Block diagram of conventional system architecture for image processing 89
Figure 5-8: Block diagram of new system architecture for image processing 91
Figure 5-9: Schematic diagram of the new scanner's modular processing cluster. 93
Figure 5-10: Partitioning of image sensor fusion principles into fusion on pixel level, feature level or symbol level. 94
Figure 5-11: Basic image data processing chain in proposed image sensor data fusion. 95
Figure 5-12: Non-segmenting approach based on classification of image tiles from the uniformly sub-divided overall image including background (sound wood). 97
Figure 5-13: Segmenting approach generating image tiles of different size only for defect candidates that are then classified. 97
Figure 5-14: Connection of tiles/object fragments is necessary to complete defect regions in the non-segmenting approach. Problems arise with thereby connected defects for the further processing for patching. 98
Figure 5-15: Glue-filled knothole on three-layered solid wood panel of spruce. 104
Figure 5-16: Resin pocket on solid wood panel (sawn lamella). Bottom side of panel showing lake of leaked resin. 104
Figure 5-17: Resin pocket on plywood panel (peeled veneer) showing crystallized resin. Left part showing nearly no indentation. 104
Figure 5-18: Pressed-in particle on plywood panel of spruce. 105
Figure 5-19: Determination of Signal-to-Noise-Ratios (SNRs) over the spectrum to identify interesting spectral bands for a specifically optimized imaging technique. 106
Figure 5-20: Complete spectrum of the used ultra-violet lamp with significant peaks around 367nm, 406nm and 436nm. 107
Figure 5-21: Fluorescence at glue: VIS-range of the spectrum comparing excitation and emission spectra, Red circled peaks result from fluorescence effect at surrounding wood (reddish colour). (Blue circled peak indicated remission). 108
Figure 5-22: Photography (VIS) of glue-filled knothole. 108

Figure 5-23: Photography (UV) of glue-filled knothole showing fluorescence at area with glue (note the light bluish, white colour) and fluorescence at the surrounding wood (reddish colour), refer to the measured emission spectrum in Figure 5-21. 108
Figure 5-24: Fluorescence at resin: VIS-range of the spectrum comparing excitation and emission spectra. Red circled peaks result from fluorescence effect at surrounding wood (curve around 550nm is perceived as yellowish colour at resin and around 700m as reddish at sound wood). 109
Figure 5-25: Photography (VIS illumination) of resin pocket and leaked resin. 109
Figure 5-26: Photography (UV illumination) of resin pocket and leaked resin showing fluorescence at area with resin. Note the yellowish colour. 109
Figure 5-27: Image showing glue-filled holes (1&2), smeared glue (3) and lake of resin (4) on a wooden panel (spruce) in VIS spectrum as the result of fluorescence....110
Figure 5-28: Image showing glue (1, 2 &3) as the result of remission of UV light on wooden panel (spruce). Note that the resin (4) is showing less remission. 110
Figure 5-29: Image snippet of wooden panel (larch) showing UV absorption on resin (1 & 2).....111
Figure 5-30; Principle of cascaded training. 115
Figure 5-31: Pre-sorting of training data (images) using *ColourBrain® SOM* user interface. 116
Figure 5-32: Principle of multi-channel raw pixel data serialized to feature vector.....117
Figure 5-33: Illustration of raw pixel data used for SVM-classification. The input pattern is compared to the support vectors (red arrows) by mapping and calculating the inner product in one step using kernel function. 118
Figure 5-34: Principle of feature vector extended by a priori knowledge....119
Figure 5-35: Information flow in the decision layer: decision making.....120
Figure 5-36: Resolving assignment of pre-processing and filling material.....121
Figure 5-37: Knothole with bark (no glue on knothole bottom/core veneer due to bottom side of the panel). Needs routing due to soft/loose bark. 122
Figure 5-38: Knothole with glue on knothole bottom/core veneer (due to top side of panel). Needs routing due to adhesion when filling with 2K putty.....122
Figure 5-39: Knothole on top side of panel, therefore showing glue on core veneer and having additionally bark. Needs routing in any case.....122
Figure 5-40: Decision process for routing knotholes incorporating neighbourhood evaluation.....122
Figure 5-41: Membership functions for “bark”. 125
Figure 5-42: Membership functions for “glue”.....125
Figure 5-43: Membership functions for “diameter”.....125
Figure 5-44: Membership functions for "shape".....125
Figure 5-45: Membership functions for "grain". 126
Figure 5-46: Membership functions for "clustering". 126
Figure 5-47: Membership functions for "target appearance" (overall panel appearance).....126
Figure 5-48: Decision surface (pre-processing) bark – glue. 127
Figure 5-49: Decision surface (pre-processing) bark – diameter.....127
Figure 5-50: Decision surface (pre-processing) bark – shape.....127
Figure 5-51: Decision surface (pre-processing) bark – grain. 127
Figure 5-52: Decision surface (pre-processing) bark – clustering.....128
Figure 5-53: Decision surface (pre-processing) bark – panel appearance (overall).....128
Figure 5-54: Decision surface (pre-processing) glue – diameter. 128
Figure 5-55: Decision surface (pre-processing) glue – shape. 128
Figure 5-56: Decision surface (pre-processing) glue – grain. 129
Figure 5-57: Decision surface (pre-processing) glue – clustering. 129
Figure 5-58: Decision surface (pre-processing) glue - panel appearance (overall).....129
Figure 5-59: Decision surface (pre-processing) diameter – shape.....129
Figure 5-60: Decision surface (pre-processing) diameter - grain.....130
Figure 5-61: Decision surface (pre-processing) diameter – clustering.....130
Figure 5-62: Decision surface (pre-processing) diameter – panel appearance (overall).....130
Figure 5-63: Decision surface (pre-processing) shape – grain.....130
Figure 5-64: Decision surface (pre-processing) shape – clustering.....131
Figure 5-65: Decision surface (pre-processing) shape – panel appearance (overall). 131
Figure 5-66: Decision surface (pre-processing) grain – clustering.....131
Figure 5-67: Decision surface (pre-processing) grain – panel appearance (overall).....131
Figure 5-68: Decision surface (pre-processing) clustering – panel appearance (overall).....132

Figure 5-69: Decision surface (filling) bark –glue. 132
Figure 5-70: Decision surface (filling) bark –diameter. 132
Figure 5-71: Decision surface (filling) bark –shape. 133
Figure 5-72: Decision surface (filling) bark – grain. 133
Figure 5-73: Decision surface (filling) bark – clustering. 133
Figure 5-74: Decision surface (filling) bark - panel appearance (overall). 133
Figure 5-75: Decision surface (filling) glue – diameter. 134
Figure 5-76: Decision surface (filling) glue – shape. 134
Figure 5-77: Decision surface (filling) glue – grain. 134
Figure 5-78: Decision surface (filling) glue – clustering. 134
Figure 5-79: Decision surface (filling) glue - panel appearance (overall). 135
Figure 5-80: Decision (filling) surface diameter – shape. 135
Figure 5-81: Decision surface (filling) diameter – grain. 135
Figure 5-82: Decision surface (filling) diameter – clustering. 135
Figure 5-83: Decision surface (filling) diameter - panel appearance (overall). 136
Figure 5-84: Decision surface (filling) shape – grain. 136
Figure 5-85: Decision surface (filling) shape – clustering. 136
Figure 5-86: Decision surface (filling) shape - panel appearance (overall) 136
Figure 5-87: Decision surface (filling) grain – clustering. 137
Figure 5-88; Decision surface (filling) grain - panel appearance (overall). 137
Figure 5-89: Decision surface (filling) clustering - panel appearance (overall) 137
Figure 5-90: Information flow in the decision layer: generation of patching instructions and data. 139
Figure 5-91: Initial test with 15mm circular dowel: coverage not reached. 140
Figure 5-92: Test: 20mm dowel is sufficient / promising to start position optimization. 140
Figure 5-93: Calculation of shift vectors based on uncovered areas. 140
Figure 5-94: Movement of dowel according to added shift vectors and re-testing the coverage (result: insufficient at multiple positions). 140
Figure 5-95: Testing & shifting a combination of one circular and one elliptical dowel (result: insufficient at the left). 140
Figure 5-96: Testing and shifting a combination of one circular and two elliptical dowels results in sufficient coverage of the defect. 140
Figure 5-97: Small diameter router applied to defect contour. Red path is needed to fully cover/mill the defect contour. White contour is the resulting synthetic defect contour. 142
Figure 5-98: Large diameter router applied to defect contour. Red path is needed to fully cover/mill the defect contour. White contour is the resulting synthetic defect contour. 142
Figure 5-99: Low viscosity guarantees homogenous filling of the narrowings. 144
Figure 5-100: Higher viscosity requires nozzle to move into the narrowings. 144
Figure 5-101: Depending on expanse of the defect and the viscosity of the putty the filling path needs extension. 144
Figure 6-1: Support Vectors of SVM for defect type “Bark”. Every 15th SV is shown including its scoring by the hyperplane, red line indicating decision boundary. 150
Figure 6-2: RPC for defect type “Bark”, Average Precision (AP) is 96.39%. Red dotted line represents random classifier. 151
Figure 6-3: Support Vectors of SVM for defect type “Dark Knot”. Every 15th SV is shown including its scoring by the hyperplane, red line indicating decision boundary. 152
Figure 6-4: RPC for defect type “Dark Knot”, Average Precision (AP) is 97.16%. Red dotted line represents random classifier. 152
Figure 6-5: Support Vectors of SVM for defect type “Ringed Knot”. Every 15th SV is shown including its scoring by the hyperplane, red line indicating decision boundary. 153
Figure 6-6: RPC for defect type “Ringed Knot”, Average Precision (AP) is 94.63%. Red dotted line represents random classifier. 153
Figure 6-7: Support Vectors of SVM for defect type “Sound Knot”. Every 15th SV is shown including its scoring by the hyperplane, red line indicating decision boundary. 154
Figure 6-8: RPC for defect type “Sound Knot”, Average Precision (AP) is 65.42%. Red dotted line represents random classifier. 154
Figure 6-9: Colour image snippet of Cracked Knot. 155
Figure 6-10: Scatter image snippet of the same Cracked Knot. 155
Figure 6-11: 3D image snippet of the same Cracked Knot. 155

Figure 6-12: Fused image snippet of Cracked Knot for crack width estimation. 155
Figure 6-13: Support Vectors of SVM for defect type “Sound Knot” based on improvement with crack width incorporated in the a priori knowledge extension. 156
Figure 6-14: RPC for defect type “Sound Knot”, based on improvement with crack width incorporated in the a priori knowledge extension. Average Precision (AP) is improved to 95.75%. Red dotted line represents random classifier. 156
Figure 6-15: Support Vectors of SVM for defect type “Cracked Knot”. Every 15th SV is shown including its scoring by the hyperplane, red line indicating decision boundary. 157
Figure 6-16: RPC for defect type “Cracked Knot”, Average Precision (AP) is 94.57%. Red dotted line represents random classifier. 157
Figure 6-17: Support Vectors of SVM for defect type “Resin Pocket”. Every 15th SV is shown including its scoring by the hyperplane, red line indicating decision boundary. 158
Figure 6-18: RPC for defect type “Resin Pocket”, Average Precision (AP) is 99.14%. Red dotted line represents random classifier. 158
Figure 6-19: Support Vectors of SVM in aesthetic judgement on Dark Knots. Every 15th SV is shown including its scoring by the hyperplane, red line indicating decision boundary. 160
Figure 6-20: RPC for local aesthetics judgement yielding in an AP of 91.93%. Red dotted line represents random classifier. 160
Figure 6-21: User interface visualizing the result of the decision making and patch data generation for validation. UV channel image of solid wood panel undergoing patching (knothole with glue) using a dowel is shown. Green circle represents circular dowel true to scale. 162
Figure 6-22: User interface visualizing the result of decision making and patch data generation for validating the patching on a plywood panel. Colour image channel is shown with overlays indicating routing path, resulting synthetic defect contour and filling path true to scale. 162
Figure 6-23: Screenshot of combination of circular and elliptic dowel placed on a knothole addressing the requirement to align the elliptical dowel to the lamella border (indicated by red line). Cyan contour is indicating a defect in 3D channel. 163
Figure 6-24: Photography of result from patching with combination of circular and elliptical dowels, refer to Figure 6-23. 164
Figure 6-25: Screenshot of combination of circular and two elliptic dowels placed on a glue-filled knothole addressing the requirement to align the elliptical dowel to the lamella border (indicated by red line). Cyan contour is indicating a combination of defect segmentation partially in UV channel (dark blue contour) and partially in 3D channel, being merged. 164
Figure 6-26: Resin pocket on solid wood panel of spruce with leaked resin forming resin lake. 165
Figure 6-27: Same resin pocket on panel of spruce patched correctly with one elliptic dowel. 165
Figure 6-28: Statistical validation of decision making and patching instruction generation on a solid wood panel patched with dowels only (48 panels with 624 defective areas). 167
Figure 6-29: Combined patching with 1K and 2K putty on plywood panel of spruce (note strong Needleflex that is tolerated in this setting. Panel not sanded, therefore no evaluation is possible yet. 168
Figure 6-30: Example of putty (1K) filled defect without pre-processing, after sanding. 168
Figure 6-31: Example of putty (2K) filled defect with pre-processing by routing, after sanding. 168
Figure 6-32: Statistical validation of decision making and patching instruction generation on plywood panels of spruce (50 panels with 3535 defects). 169
Figure 6-33: Example of low-quality (C-quality) plywood panel (spruce) posing high demands especially on segmentation, classification and decision making. Red circles highlight selection of patched defects shown below (from left to right). 170
Figure 6-34: Patch ok, although insufficient routing results in poor appearance. (Left highlighting circle in Figure 6-33). 170
Figure 6-35: Path intentionally not carried out completely at the panel’s edge, combined with crack. 170
Figure 6-36: Proper patched defect without pre-processing. (Right highlighted circle in Figure 6-33). 170
Figure 6-37: Resin pocket that has to be repaired by routing first and then filling with 2K putty. 172
Figure 6-38: Example for a corresponding repair instruction (red track: router, blue track: filling tool) where the preference is set to the preservation of sound wood and less usage of putty, resulting in complex, time-consuming movements. Area is 2926.5mm^2. 172
Figure 6-39 Example for a corresponding repair instruction (red track: router, blue track: filling tool) where the preference is set to the least time-consuming execution of both tools which is achieved by smoothed and straight movements. Area to process increases to 3650mm^2. 172

Figure 7-1: Plywood panel patched with putty does not allow assessment and replicability using markings made previous to scanning. 187
Figure 7-2: Defect marked previous to scanning and patching with dowels for replicability purposes and evaluation before sanding. 187
Figure 7-3: Defect free surface of plywood panel quality 'A'. This result would be achievable also with large-scale overprinting on lower quality panels while local patching is able to remove only some defects and cannot radically change the appearance. 193
Figure 7-4: Panel of marble patched with epoxy resin (not yet sanded) in a similar manual way like plywood. *[GHGGroup 2010],* image used with kind permission. 194
Figure 7-5: Oak board with tin used for filling cracked knots with the purpose to emphasize aesthetically. *[LUNA-DESIGN n.d.], i*mage used with kind permission. 195
Figure 7-6: Walnut board with tin used for filling knot holes with the purpose to emphasize aesthetically. *[Buck 2015*], image used with kind permission. 195
Figure 7-7: Fluorescent resin used for filling immersions on a panel of Pecky Cypress. Pecky Cypress shows pockets that reside from heartwood which is destroyed by a fungus [Saurus 2014]. Image used with kind permission. 196
Figure A-1: SOM principle: initially equally distanced nodes in the mesh holding weight vector with length equal to the feature space's dimension. 208
Figure A-2: SOM principle: mesh bended to best matching unit (BMU) adapting to similarity among the samples. 209
Figure A-3: Separating hyperplane (*w, b*) for a two-dimensional training set. 211
Figure A-4: Margin γ_i, γ_j of two samples s_i, s_j, each from one of the two classes, as Euclidian distance to a hyperplane. 212
Figure A-5: Margin of training set defined by closest sample(s). 213
Figure A-6: Maximal margin hyperplane, support vector highlighted. 220
Figure A-7: Comparison of maximal margin classifier and soft margin classifier working on linearly nonseparable data: 223
Figure A-8: Comparison of maximal margin classifier and soft margin classifier working on linearly nonseparable data: 223
Figure A-9: Crisp value of membership to class *B* when threshold is applied. 226
Figure A-10: Fuzzy value of membership to *B* (sigmoidal membership function). 227
Figure A-11: Principle application of fuzzy rules to the input space, top view illustrating the segmentation of the input space by the rules. 229
Figure A-12: Principle application of fuzzy rules to the input space spanned by three fuzzy variables, surface plot visualizing the degrees of membership. 230
Figure A-13: Scanner calibration plates used to carry out various calibrations. Right calibration plate showing laser alignment, white balancing and geometrical calibration using column-wise binary-coded real world coordinates. 232
Figure A-14: Exemplary registration (translation, scaling and interpolation of lower resolution 3D channel image to high resolution colour image, channel images are the product of stitching the channel's single overlapping camera images. 234
Figure A-15: Elimination of disruptive impulse disturbance. 235
Figure A-16: Warped plywood panel introducing disturbing dynamic effect 236
Figure A-17: Elimination of disruptive shading using low-pass (LP) filter and either an additive of multiplicative shading model. Grey values represent depth/height. 237
Figure A-18: Displacement of focus/image plane with variation of depth in object plane. 238
Figure A-19: Optical setup satisfying the Scheimpflug rule. 239

List of tables

Table 2-1: Excerpt from norm ISO 2426-3:2000 defining three appearance classes (E, I, II) for plywood from softwood by limiting amount of defects, knots and other common defects *[ISO 2426-3:2000]*.....31
Table 4-1: Examples of four different defective knot types from plywood of spruce. 65
Table 4-2: Example of typical feature-based discrimination between different knot defect types. 66
Table 4-3: Summary and comparison of potential classification methods according to requirements stated for defect detection on wooden panels including aesthetic aspects. 69
Table 5-1: Image resolutions of the different sensors used in a dedicated scanner for automated repair and resulting data rates to be handled (acquisition) and processed (after registration). Values at production speed of 35m/min. 92
Table 5-2: Verification matrix for a typical detection of defects on solid wood panels using colour, 3D and scatter imaging.....102
Table 5-3: Verification matrix for a typical detection of defects on plywood panels using colour, 3D and scatter imaging.....102
Table 5-4: Colour coding for verification matrix of standard defect detection techniques. 102
Table 5-5: Legend tor verification matrix of standard defect detection techniques. 102
Table 5-6: Verification matrix for detection of defects on solid wood panels incorporating specifically optimized detection techniques.....112
Table 5-7: Colour coding and legend for verification matrix, incorporating specifically optimized defect detection techniques.....112
Table 5-8: Verification matrix for detection of defects on plywood incorporating specifically optimized detection techniques.....113
Table 5-9: Rule set group 1.x on *if* and *how* to patch knothole with bark in principle. 123
Table 5-10: Rule set group 2.x on appearance (decision between dowels, putty and options).....124
Table 5-11: Rule set group 3.x incorporating overall panel appearance. 125
Table 5-12: Membership function used for modelling rules concerning Knothole with bark.....126
Table 5-13: Segmentation of decision space towards output “pre-processing” 132
Table 5-14: Segmentation of decision space towards output “filling”.....137
Table 5-15: Exemplary patching data set for patching with dowels on solid wood panels including dowel type (circular, elliptical), position with reference to panel edges, orientation and information containing preferred colour and/or texture. 139
Table 5-16: Sequence of finding appropriate dowel size/ dowel combination including position optimization.....140
Table 6-1: Evaluation of standard panel for validation of patching performance. Each defect is compared according to detection, classification, decision making (system vs. expert) and patching. CD=circular dowel, ED=elliptic dowel. 166
Table 7-1: Summary of average precisions achieved in the classification of defect types.....181

List of formulas

Formula 4-1: Definition of convex hull on set of points (e.g. training data set). 76
Formula 4-2: Geometrical interpretation of margin optimization problem based on convex hulls of two data sets. 76
Formula 4-3: Formulation of margin optimization problem based on convex hulls of two data sets. 77
Formula A-1: SOM principle: Euclidian norm for identification of BMU. 208
Formula A-2: SOM principle: identification of BMU in terms of Euclidian distance to input sample. 208
Formula A-3: SOM principle: adaption of BMU and neighbours according to lateral inhibition. 209
Formula A-4: SOM principle: neighbourhood kernel $\boldsymbol{h}$ and learning rate $\boldsymbol{\alpha}$ decrease during convergence. 210
Formula A-5: Hyperplane in n-dimensional space. 211
Formula A-6: Margin to hyperplane calculation for sample point (x_i, y_i). 212
Formula A-7: Primal optimization problem with objective function and constraints. 214
Formula A-8: Codomain (feasible region) of the objective function. 214
Formula A-9: Formulation of convex optimization problem for maximum margin classifier. 216
Formula A-10: Primal optimisation problem. 216
Formula A-11: Lagrangian dual function for optimization problem statement, magnifying the objective function with weighted sum of constraint functions. 217
Formula A-12: Lagrangian dual optimisation problem. 217
Formula A-13: Kuhn-Tucker theory: Lagrangian dual optimization problem with inequality constraints solved via Karush-Kuhn-Tucker conditions for optimal point. 218
Formula A-14: Primal Lagrangian for Support Vector Machine margin optimization. 219
Formula A-15: Constraint on optimal solution - meaning of Support Vectors in the SVM optimization concept/strategy. 220
Formula A-16: Dual Lagrangian for Support Vector Machine margin optimization. 221
Formula A-17: Dual Lagrangian incorporating kernel function for implicit mapping of feature space. 222
Formula A-18: Primal optimization problem extended by slack variables to produce a soft margin classifier 224
Formula A-19: crisp threshold example, class dark 226
Formula A-20: crisp threshold example, class bright 226
Formula A-21: light ray line. 239
Formula A-22: Image scale. 239
Formula A-23: Mapping function. 239
Formula A--24: Tilted detector plane satisfying the Scheimpflug rule. 240

Abbreviations

1K	One-component
2K	Two-component
3D	Three-dimensional
ANN	Artificial Neural Network
ANSI	American National Standards Institute
AOI	Area Of Interest
AP	Average Precision
APKFVE	A Priori Knowledge Feature Vector Extension
BMU	Best Matching Unit
CAR	Causal Auto-Regressive
CD	Circular dowel
CPU	Central Processing Unit
DCM	Defect Candidate Map
DCM	Defect Candidate Map
DIN	Deutsche Industrie Norm (German Industry Norm)
ED	Elliptic dowel
EN	European Norm
ERP	Enterprise Resource Planning
FIS	Fuzzy Inference System
FPGA	Field Programmable Gate Array
GLCM	Grey Level Co-occurrence Matrix
GPGPU	Computation on Graphics Processing Units
GUI	Graphical User Interface
HVCCS	Hierarchical Vector Connected Components Segmentation
HVS	Human Visual System
IR	Infra-Red
ISO	International Standards Organisation
K-NN	K-Nearest Neighbour
LBP	Local Binary Pattern
LVQ	Learning Vector Quantization
MDF	Medium-Density Fibreboard
MLP	Multi-Layer Perceptron
Mm	Millimetre
NIR	Near Infra-Red
OSB	Oriented Strand Board
OVA	One-Versus-All
PC	Personal Computer
PCA	Principle Component Analysis
PI	Polyester Isophytal
PPS	Production Planning System
PU	Poly-Urethane
RAM	Random Access Memory
RB	Red, Blue
RFID	Radio-Frequency Identification

RGB	Red Green Blue
RGB	Red, Green, Blue
ROC	Receiver-Operator-Characteristics
RPC	Recall-Precision Curve
SOM	Self Organizing Map
SVD	Singular Value Decomposition
SVM	Support Vector Machine
UV	Ultra-Violet
VIS	Visible (part of the spectrum)

Terminology

ΔE	Colour distance metric used in *CIE-Lab* colour space.
1K putty	One-component putty, usually water-based.
2K putty	Two-component putty, usually Polyurethane (PU) or Polyester Isophytal (PI).
Accuracy	Proximity of measurement results to the true value, offset or bias.
CIE *L*a*b**	Perceptionally uniform colour space (also *CIE-Lab*).
Classification	In this context: the task of determination between several possible classes a segmented object can belong to with the aim to assign a specific label.
Colorimetry	Science and technology to characterize physically the human perception of colour.
Detection	In this context: the task of finding and segmenting an object from image data.
Evaluation	In this context: the task of applying measures to a detected object, e.g. diameter, depth, mean colour, etc.
Feature engineering	Area of engineering and research dealing with finding and extraction of explicit features for classification from the raw data. This involves filter operations and dimensionality reduction, e.g. by de-correlating the features using PCA.
Kansei Engineering	Product development and design incorporating the customers' psychological aspects and needs.
Lamella	Thin (1-10mm) sawn but long piece of wood used to build face veneer of solid wood panels by butt-jointing.
Patch	Material applied to a defective area, eventually after removal of defective material.
Patching	Application of a patch with the aim to remove the disadvantageous defective area (physical patching) and/or to hide it respectively to make it less visible (aesthetic Patching).
Pixel	Single element of a spatially resolved digital image.
Plywood panel	Wooden panel made from rotary sliced veneers glued in a sandwich construction.
Portal	A section in the automated production line where a type of certain tools is applied.
Precision	Reproducibility of the measurement, random error.
Putty	Liquid or low-viscosity material used for Patching.
Radial Projection	Clockwise accumulation of pixel values along a scanline (watch hand) to gain a two-dimensional diagram indicating the presence of an object and its position in terms of 0°-360° to the centre of projection.

Raw features	Uncondensed sensor data, e.g. image (contrary to handcrafted features derived explicitly from the image).
Registration	Task of aligning images from different perspectives, of different spatial resolutions and of different type in a way that pixels belonging to the same physical coordinate in the scene are related to each other.
Segmentation	Task of separating pixels in an image belonging to an object from those belonging to background.
Solid wood panel	Wooden panel made from lengthwise sawn lamellas glued on both sides of an edge-glued solid wood core.
Stitching	Task of joining images that together form a panoramic view of a scene.
Thresholding	Image data manipulation, for example a pixel having an intensity value above the threshold is set to white; an intensity value below the threshold is set to black.
Undistortion	Process in image processing removing distortion, e.g. from lens aberration or illumination variance.
Veneer	Very thin sheet of wood peeled from stem rotationally.

1 Introduction

Wood is an important resource for a large variety of goods like furniture, flooring, timber components, housing parts, etc. Like other natural materials wood products show imperfections of various kinds. Automated inspection systems exist that can grade the feedstock according to these imperfections. It is economically and ecologically beneficial to rectify a workpiece showing imperfections instead of discarding it. Benefit could be gained with a system automating such procedures beyond the task of grading, be it for the purpose of reducing human labour and therefore reduction of costs or the purpose of reproducibility and more reliable results. No such system is currently available to the industry.

In highly automated plants for furniture (decorated particle boards) and laminate flooring, automated visual inspection is frequently used for grading the final product under appearance aspects. As these systems inspect well-defined synthetic printed decors, the algorithms for both physical and aesthetical flaws can use a considerable amount of a priori knowledge. This facilitates the task of detecting surface defects like scratches, dents and blisters and aesthetic defects like colour contaminations, colour instabilities and irregularities in texture. These algorithms are of little use when analyzing random multicoloured patterns such as from real wood. The necessity for algorithms that do not draw on the a priori knowledge about the exact appearance of the device under test but give reliable detection results also for unseen surfaces is therefore clearly evident. Furthermore, with a model of human visual perception in mind that always combines several sensations in the sense of features *[Gregory 2001]*, it is necessary to promote the combination of different signals from different sensors to create a more complete image of the inspected surface. The principles of sensor fusion play a major role in the design of a system addressing this requirement but are under-developed for the specific task. Investigations into new sensor fusion techniques and their corresponding algorithms which are expected to be custom-tailored for the purpose of defect detection on natural surfaces are necessary to close this gap.

1.1 Background of the problem

Machine vision is an engineering branch that incorporates the science of computer vision in the context of manufacturing *[Steger, Ulrich and Wiedemann 2008]* with computer vision as the science and the set of technologies that enable machines to retrieve information from images *[Graves and Bachelor 2003]* which is necessary to solve specific tasks. Therefore "a generally accepted definition of machine vision is (...) the analysis of images to extract data for controlling a process or activity" *[Relf 2004]*. The automated visual inspection of surfaces as a branch of machine vision is well-developed for a large number of inspection tasks in the production line. Replacing the human eye for quality control and process monitoring on a huge variety of products is state-of-the art for both the scientific basis and industrial production processes. Based on information gained from these automated tasks, the automatic control of handling tools and production tools is simple to apply. Machine Vision does therefore further mean "(...) recognizing the actual objects in an image and assigning properties to those objects - understanding what they mean" *[Hapgood 2007]*. The automated visual inspection in the production of panels based on natural materials such as wood, stone etc. is specially challenging due to the natural variety of the appearance of these materials and the further added complexity of the perceived visual quality of their surfaces.

1.2 Statement of the problem

The first and main task of any automatic surface inspection is the robust and precise detection and localisation of all kinds of surface flaws and their separation into physical defects and aesthetic defects. Physical defects reduce the functionality and aesthetic defects offend human perception: "Product material integrity and surface appearance are important attributes that will affect product operation, reliability and customer confidence" *[Smith 2001]*. While simple manual sorting-out has largely been used to guarantee the required overall quality of a production charge, from the ecological perspective additional processes that target the repair and upgrade of a product whenever applicable are desirable. However, with today's ever faster operating production plants this currently mostly manual labour process is not an economical option. For example, the common manual repair of wooden panels, generally called patching, may improve the exploitation of wood, but it is tending to become uneconomical due to the huge amount of human labour which is required.

Sustainable recovery of wood resources is furthermore an ecologically sensible approach. The limited availability of stock and the need to improve its value creates demand for automated patching technologies to resolve the lack of automation in this field.

1.3 Aim and objectives

The aim of this research is to find a solution for the automated generation of instructions for defect rectification on natural surfaces and to show that this task can satisfactorily be automated.

An automated rectification process in principle includes the proper detection of defects as well as the decision of what and how to repair. In the application on wooden panels, detection techniques furthermore need to be evaluated for their applicability in terms of decision making also on the aesthetics of the defects. Suitable existing detection techniques together with newly developed detection techniques can then be integrated into a working prototype system.

- The first objective is to identify defect detection techniques and to assess their adaptability for the specified task of automated repair on wooden panels.
- The second objective is then to establish research methods for the purpose of defect detection on wooden panels including the requirement of aesthetic assessment of the defects by adapting the identified existing detection techniques or newly develop detection techniques.

Different aspects of automated repair need to be investigated for rectification. The common patching techniques used to repair wooden panels and the possibilities of an automated generation of the associated patching instructions also from an aesthetic point of view should to be evaluated.

- The third objective is to identify suitable common patching techniques used to repair different types of wooden panels
- The fourth objective is to develop a concept to generate patching data in an automated manner for the incorporated patching techniques, to implement it and integrate it into the prototype systems.

For a system suitable for industrial applications, capable of carrying out automated rectification and therefore substantially influencing the overall production process, user control on the panels' quality is required.

- The fifth objective is therefore to devise possibilities for adjusting quality also in terms of the final appearance of the panels incorporating wood working expert knowledge.

The focus of this study is on knowledge driven technologies for both detection and rectification of defects on surfaces of wooden panels. The results of an integrated system for automated rectification are compared to manually carried-out repair and are assessed with respect to the possibilities of a machine to control the product's final appearance in terms of customer satisfaction.

1.4 Research questions

The statement made in this thesis concerns the feasibility of an industrial-suited machine vision system that can be built to satisfy the requirements stated by the superimposed tasks of automated inspection and automated repair of natural surfaces. Two major topics are thereby addressed: (a) the model of visual perception of defects on natural surfaces including aesthetic issues, applicable for the defect detection. (b) The accomplishment of automated patching with regard to the final overall appearance of a panel. The following research questions were therefore identified:

- Is it possible to automatically discriminate defects on wood surfaces by physical and aesthetic properties?
- How can human expert knowledge be modelled to be used by a system for automated patching of wood surfaces?
- Is it possible to achieve aesthetically satisfying results with automated patching in relation to the capabilities of humans?
- Is it possible to apply aesthetic patching by retouching a defect in an automatic manner such that it is no longer visually perceptible?

A quite comprehensive set of research aspects is spanned by these four research questions as each of them has its own large set of second level aspects. Hence it becomes clear, that it

is not reasonable to address all initial research questions and therefore it is not reasonable to cover all topics in the scope of this research project. Following the logical order of the issues addressed by each of the initial questions, it was decided to focus on the first three questions which deal with the perception and appearance properties of defects and the knowledge involved with mainly physical patching under aesthetic aspects. The main reason for this decision is the industry-driven nature of this applied research project and the fact that the research is initiated by a company working on automated inspection and patching systems. Therefore an action oriented approach as covered by the first and second question is necessary. Further it is important to recognize the importance of the third initial research question for the company *Baumer Inspection GmbH* whose inspection and repair systems are studied. The fourth research question implies the development of new technologies, e.g. printing technologies that raise many questions by themselves, e.g. colour calibration and automated generation of patterns, which might be worth a separate research project and which are not in the scope of this study. The main research question addressed by this thesis is therefore given the following formulation:

How is it possible to detect and repair surface and aesthetic defects on natural surfaces like wooden panels in an automated manner such that it can replace human labour?

1.5 Scope of the study

The underlying research project has a strong interdisciplinary character. Besides a clearly dominating engineering domain the project spans over parts of the fields of physiology and arts as well.

The engineering domain consists of two branches: Information engineering with its specialization into machine vision on the one hand and wood engineering from the primary and secondary wood industry on the other. The primary wood manufacturing industry is the sector consisting of organisations that are involved in the development and production of wooden feedstock like timber, plywood, panels, structural composite lumber, and glued laminated timber and similar. The secondary wood manufacturing sector represents the manufacture of this feedstock into finished goods, such as furniture, toys, containers, or construction components like house frames *[Maryland's SFLA 2003]*.

Questions concerning appearance of natural surfaces range more into the field of psychology when it comes to analyze and explain certain perception-related phenomena and range more into the field of philosophy and arts when it comes to characterize and (re-) produce aesthetics.

1.5.1 Delimitations and limitations

This study deals with the detection and rectification of defects on panels. Non-flat surfaces of objects define their own requirements which may be similar to those of flat ones but show additional complexity in all stages of the targeted process and are therefore excluded from this research. Due to the industrial context defined by the core competency of company *Baumer Inspection GmbH*, the main focus is on wood-based panels but the outcome of the research may be generalisable to natural surfaces in common, for instance stone panels. The common characterization of the appearance of these surfaces is therefore *multicoloured and visually textured* which includes the subset of naturally looking surfaces having synthetic surface decors as well. These surfaces are highly common in the production of furniture for example.

While for the rectification step an approach as generic and adaptive as possible is targeted, which seems to be feasible at least for a large variety of different kinds of wood, the detection and decision making steps are restricted to softwoods due to the limitations of the underlying industrial project. Therefore hardwoods are excluded from the investigations regarding the detection techniques and decision making for the generation of patching data. Nevertheless the principles of both detection and patching data generation are the same for hardwoods and might likely be adapted to natural surfaces in common. The main focus concerning softwoods is on the European/Nordic Spruce (*picea abies*) which is the main raw material for the production of multilayered panels and edge-glued panels in Europe and Radiata/Monterey Pine (*pinus radiata*) which is the major raw material for the production of plywood worldwide *[Woodexplorer 2014]*.

The sense-perception plays an important role for the appearance of a surface. This fact involves aesthetics: “Aesthetics (...) is a branch of philosophy dealing with the nature of beauty, art and taste and with the creation and appreciation of beauty” *[Merriam Webster Dictionary 2015]*. To investigate into the meaning of art from the philosophic point of view is out of the scope of this research. The first and third initial research question is therefore not

meant to answer the philosophic question of "*what is aesthetics?"* rather than "*what is a good practice?"* derived from applied arts to ensure an aesthetic pleasing result. Sense-perception on surfaces in this context is limited to visual perception and excludes the additional information like odours, acoustics or haptics a person may retrieve from such an object.

As aesthetics is also a reflection of culture *[Riedel and Stahl 1999]* the scope of this research has to be limited to the European culture due to the fact that the prototype systems are developed for the European market. Even the European cultural sphere shows regionally substantial differences, but in the underlying context this generalisation seems to be tolerable.

1.6 Structure of the thesis

To further outline the issues addressed in the underlying research a ***Contextual Background*** is presented which covers background knowledge from the production of wooden panels including a defect catalogue and a comprehensive overview on patching to understand the motivation and needs of the wood working industry and to derive the requirements stated for automated repair. A ***Literature Review*** and survey on existing inspection systems identifies the state-of-the-art in automated inspection of wooden panels explaining the existing detection principles and their limitations. For the application of such systems to automated patching also under aesthetic aspects, defect classification based on feature extraction seems to be inappropriate and the need for sensor data fusion and knowledge based approaches is explained. ***Research Methods*** chapter 4 will introduce the methods and technologies available to create and deal with high-dimensional registered image data of wooden panels and to model human expert knowledge by incorporating machine learning and expert systems. The combination of these methods leads to a ***System Design*** introduced in chapter 5 covering the overall processing chain from proper acquisition techniques to defect segmentation, defect evaluation and classification to the decision making for patching and the generation of patching instructions. In the ***System Development and Performance*** chapter experiments are carried out to test the performance of the chosen methods and of the overall system compared also to manual repair. A critically carried out analysis of the capabilities and possibilities of the developed technology is followed in the final chapters for ***Discussion*** and ***Conclusions*** including suggestions for further research work.

2 Contextual background

This chapter addresses the initial statements from the introduction chapter concerning economical, ecological and technical needs for intelligent automation and more specifically for intelligent, automated rectification processes in the wood-working industry. The importance of this industry sector is explained as well as the fundamental technical comprehension of the production of wood-based panels on which this research is focused. The contextual background chapter is therefore the separation of background knowledge from the introduction chapter and a comprehensive collection of important additional information necessary to understand the assumptions, references and findings in the following chapters.

2.1 Industry significance

The European wood-working industry provides more than 2.7 million jobs *[CEI-Bois 2011]*. Besides playing the role of a major employing industry in many member states, the wood-working industry is among the top three industries in Austria, Finland, Portugal and Sweden *[CEI-Bois 2011]*. Being a diversified industry, the covering activities range from sawmilling to the production of wood-based panels like plywood, multi-layered wooden panels or parquet veneers, from construction components like structural composite lumber and house frames to packaging with pallets and boxes, from joinery to all kinds of furniture. With only a few large groups, mostly in the sawmill sector and the panel sector, this industry is mainly formed by approximately 131.000 Small and Medium Sized Enterprises (SMEs) having a total production value of €165.000 million *[CEI-Bois 2011]*.

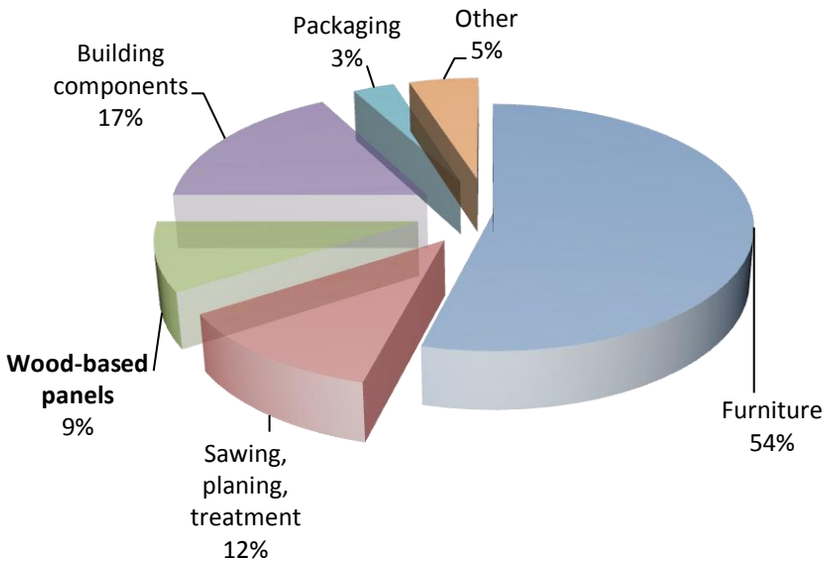

Figure 2-1: Wood working industry sectors. (Data: *[CEI*-Bois2011*]*).

As can be seen from Figure 2-1, the biggest sector inside the wood working industry is clearly the furniture sector. The furniture sector in turn is a major consumer of wood-based panels and sawn wood, therefore the whole wood-working industry is closely linked to the furniture sector as illustrated in Figure 2-2:

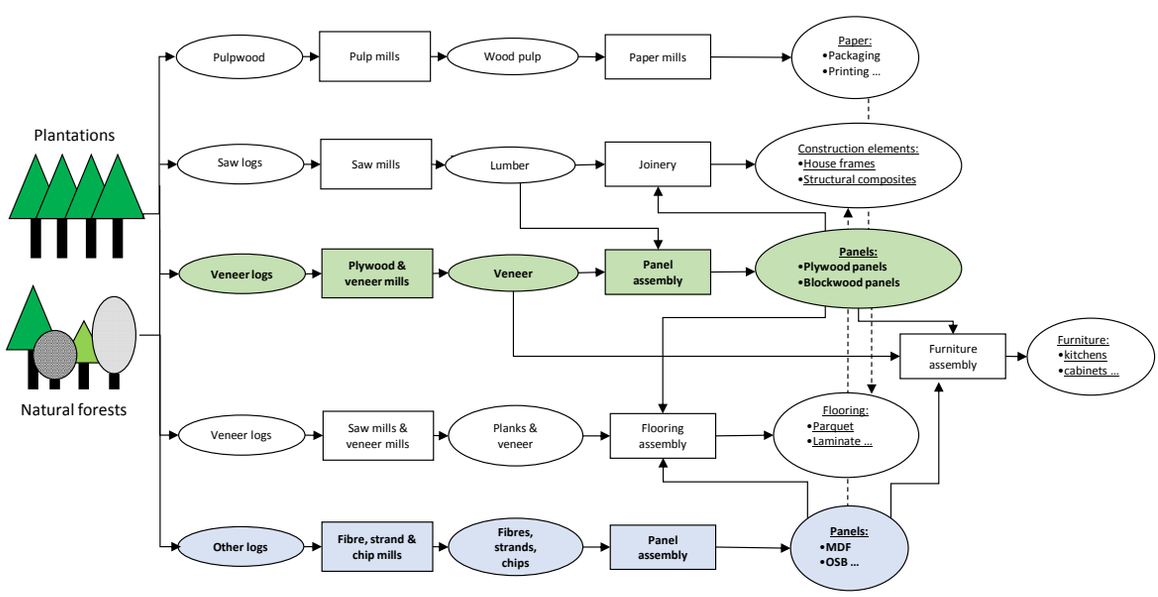

Figure 2-2: Links between the different sectors in the wood-working industry in terms of production and material flow. The furniture sector plays an important and central role among the different sectors and as it consumes several of the other sectors' outputs.

2.1.1 Wood-based panels

A closer look into the industry producing wood-based panels shows the importance of this sub-sector: this sector has been accounting for 9% respectively €13 billion of total industry production in 2011 *[CEI-Bois 2011]*. Wood-based panels are a starting product for a huge amount of applications, ranging from the furniture industry to the building industry to the packaging industry. All kinds of wood-based panels, particleboards (Oriented Strand Board, OSB), fibreboards (Medium-Density Fibreboard, MDF) or plywood-/multi-layered wooden panels are used in the production of kitchens and cabinets. The construction and building industry show a massive need of panels, e.g. plywood panels or OSB boards used for the concrete formwork or used to construct complete house frames. The production of flooring, which is commonly attributed to the building industry, incorporates all kinds of panels and veneers for the production of multiply parquet slabs too, while the production of laminate flooring is a big market for MDF boards as they are used as carrier plates.

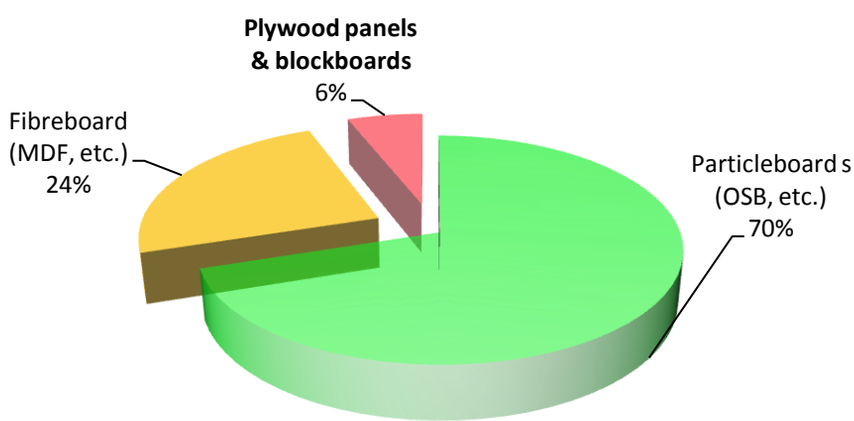

Figure 2-3: Sub-sectors within the wood-based panels sector. (Data: *[CEI-Bois 2011]*).

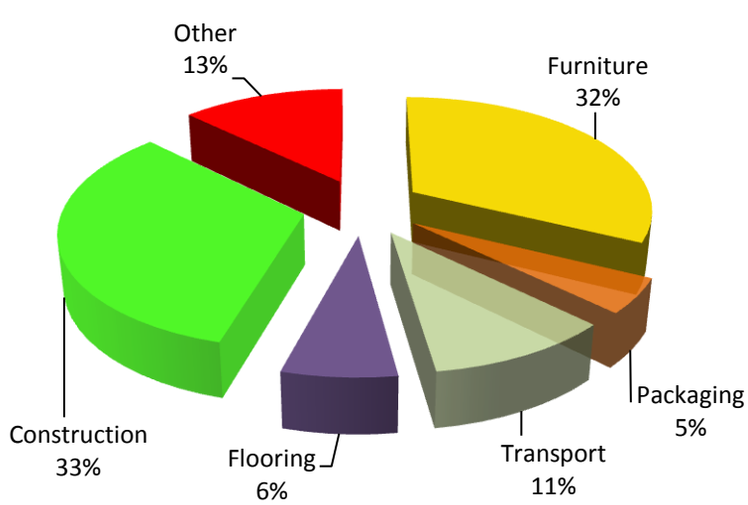

Figure 2-4: Plywood panels and blockboards end user markets (data: *[CEI-Bois 2011]*).

2.1.2 Economical aspects - market development

The wood working industries in Western Europe experience high feedstock and labour costs, forcing them to adopt leading edge technologies to remain competitive and profitable. Technical development has been led mainly by the major exporters like Finland and Sweden, and is now widely spread within the wood-working industry, driving cost efficiency and development of more value-added products. Industry consolidation from numerous smaller businesses to large-scale companies is leading to higher production from fewer units, as well as to greater specialization.

In the MDF, OSB and particleboard industries for example, the most important technical development over the last decades has been the continuous pressing technology (Siempelkamp[1]) that has dramatically reduced production costs through economies of scale and better process control. In the production of multi-layered wooden panels the development of band saws being able to cut veneer with a thickness of only 1.8mm and minimum loss due to ultra-thin saw blades and computer controlled feeding (Fill GmbH[2]*)* in combination with high efficient automated sorting of the cut-out veneer led to an increase of the added value.

As labour is a major cost element for the European furniture businesses for example, European companies had to adopt leading edge technologies like computer aided processes to remain competitive and profitable. This resulted in shifting the emphasis from the primary processing of wood to the finishing and assembly of products. The increasing possibilities of intelligent automation in the other sectors of the wood-working industry are furthermore still enormous and their implementations become more and more viable with the consolidation of the plywood and multi-layered wooden panel businesses into fewer but bigger companies while facing an ever-increasing competition especially from Asia. To illustrate this fact, Figure 2-5 shows exemplarily the production rates of European plywood panels in the last twenty years compared with the production rates of China.

[1] http://www.siempelkamp.com
[2] http://www.fill.co.at/

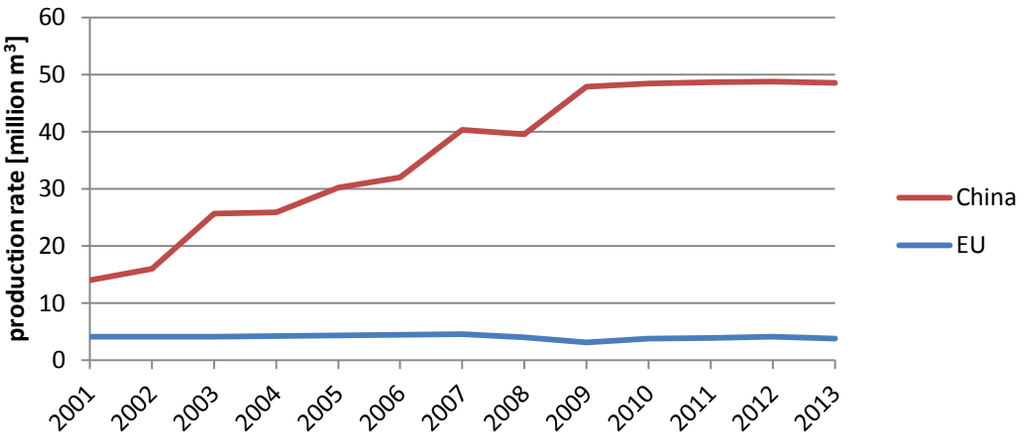

Figure 2-5: Plywood production rates EU & China (data: *[FAOSTAT 2014]*).

Figure 2-6 shows the European import quantities of plywood panels compared with the Chinese export quantities of plywood panels. The finding from these figures is the fact that while the demand for plywood panels grew by factor 2-3 from approximately 6 to more than 16 million square meters in the last ten years in Europe, the European production stagnated while the demand has been mainly satisfied with Chinese imports.

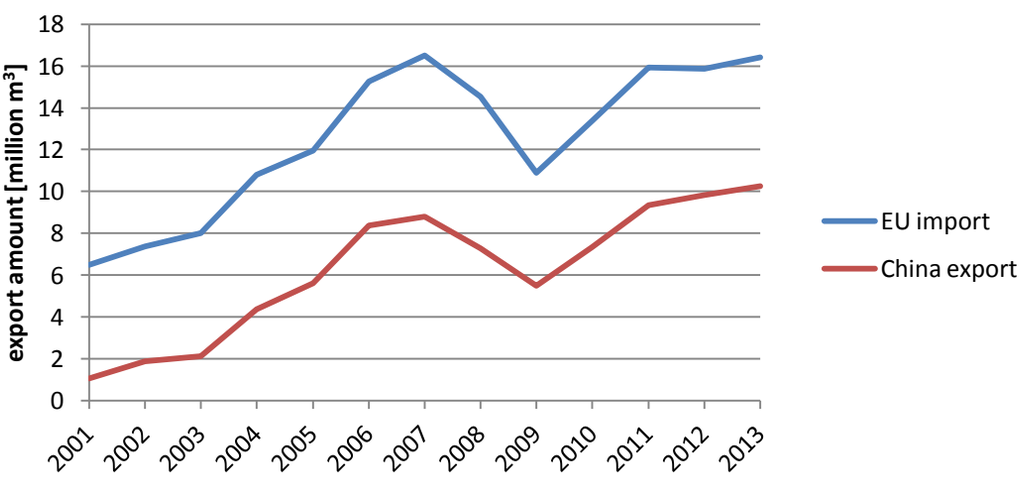

Figure 2-6: Plywood: import quantities EU, export quantities China (data: *[FAOSTAT 2014]*).

Besides the clearly visible impact of the economic crisis on the European production and import of plywood panels in the years 2008 & 2009 one can see that in the years before substantial market shares were lost to China.

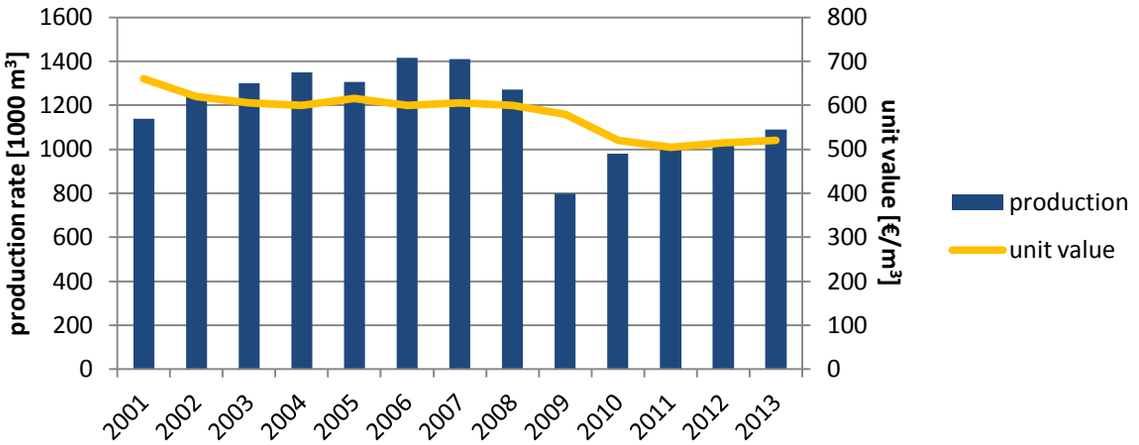

Figure 2-7: Production rate & price trends of Finish plywood (data: *[FAOSTAT 2014]*).

The development of the price for Finish plywood is exemplary for this development on the plywood market. Figure 2-7 displays the situation of rising production quantities (except during the economic crisis in 2008/2009) while the value per unit is continuously decreasing over more than the last ten years.

The decreasing prices for plywood panels due to the steadily increasing production output especially of the Chinese facilities, make it necessary not only for European but also for Scandinavian and (Southern) American producers to constantly improve the production processes by developing and investing into latest technology and equipment. This has already been realized in the mid eighties, for example Baldwin *[Baldwin 1981]* stated that "..the key to escape the profitability crisis is high yield management, a management concept that seeks the most veneer from the log and the optimum result from the workers and their equipment". From an economical point of view the main goals are to reduce the amount of waste, maximize the yield of the natural resources and therefore increase the added-value and profit.

2.2 Defects on wooden panels

This subchapter gives an overview over the different types of defects in terms of areas on wooden panels with unwanted characteristics. "Unwanted" in this sense refers to a degraded quality depending on more or less standardised quality definitions depending on the intended use of the wooden product. For example on formwork panels no indentations are tolerated while on load-bearing parts no structural defects and only a certain amount of knots are allowed. These rules from the area of constructional timber differ greatly from

those applied to flooring and furniture parts, where appearance characteristics are to the fore. There exists a variety of norms, from single countries (German industrial norms *DIN*), economic zones (North America Lumber Standard, European Norm EN) as well as proprietary norms issued by the major companies. The latter are normally a refinement to the superordinated national or regional definitions with respect to the particularities of the used raw materials (for example special cultivation of Pine Radiata in big South American plantations). The study of the most important norms and the experience from the industrial projects led to a superior categorization of defects which is presented in the following paragraphs. This categorization is then also the basis for the identification of a suitable set of modular detection techniques in the following chapter, as the physical and optical characteristics of the defects are also investigated. Therefore this categorization corresponds to the view of an automated inspection system while intuitively often a defect categorization based on the cause is applied by human wood workers. Nevertheless in the following description of the defects their cause is explained too, as this creates a better understanding.

2.2.1 Physical defects

Physical defects in this context are those defects that can be separated from a sound surrounding by a simple method of metrology and where a common measurement unit (e.g. millimetres) can be applied. It is important to distinguish between a measurement the separation from the surrounding (segmentation) is based on and a measurement which is used in the second-level characterization of an otherwise segmented area. Once segmented, any defect is normally characterized by measurements like width, length and diameter, but only the physical defects can be identified as such by a simple measurement like depth.

2.2.1.1 Three-dimensional defects

The simplest measurement of defects on panels is the measurement of either depth or height. It is also the most intuitive measurement as the first and most important quality requirement in the production of panels is a planar surface. The discrimination between depth and height is thereby very important, as elevations often result from loose particles especially on the top side of panels that result from the handling in the production process and which are not necessarily to be repaired. Therefore the indentation is of greater interest, examples are presented in the following.

2.2.1.1.1 Knothole

Knotholes result from fallen-out (dry) knots. As the wood of knots contains much more lignin *[Richter 2014]* it is therefore much harder but also shows a different shrinkage during drying as the grain direction in knots is not parallel to the grain direction in the wood of the trunk. Together, this can result in a detachment of the knot *[Peck 1957]* which will then simply drop out from the veneer or lamella at all stages of the production process where mechanical influence is given, or will be pulled out in the sawing (refer to Figure 2-8).

Figure 2-8: Knothole (showing some bark on the right side) in pine plywood top layer veneer (4mm). The application of glue in fine lengthwise lanes with the use of spray nozzles is visible as brown vertical lines on the core layer at the bottom of the hole.

Figure 2-9: Knothole (showing some bark on the right side) in top layer lamella (5mm) of solid wood spruce panel. The application of glue by extensive coating of the core layer is visible as a white bottom of the hole.

Figure 2-10: Knothole in top layer lamella (5mm) of solid wood spruce panel. The application of glue by extensive coating of the core layer is visible as a white bottom. Knothole is located at lamella's border, therefore showing a sharp edge.

Other factors for the occurrence of knotholes are the type of wood (fir shows higher, pine shows lower occurrence) and the age and condition of the branch. Dead branches almost always produce loose knots, often with bark as a result of the trunk isolating the remains as can be seen in Figure 2-8 and Figure 2-9, refer also to 2.2.1.2.1 *Dark knot, dry not & loose knot*. Typical diameters differ with the type of wood. E.g. lamellas and veneer from spruce show knotholes ranging from 5-25mm while those on fast growing Monterey Pine (Pine Radiata) typically show diameters from 30-90mm.

2.2.1.1.2 Glue-filled knothole

Figure 2-11: Glue-filled knothole on three-layer solid wood panel (spruce).

A special variant of the knothole can be found on solid wood panels. During pressing the excessive glue (often white appearing Kauramin, refer to Figure 2-11) is pressed through the openings of the face veneer resulting in glue-filled holes.

2.2.1.1.3 Cracks

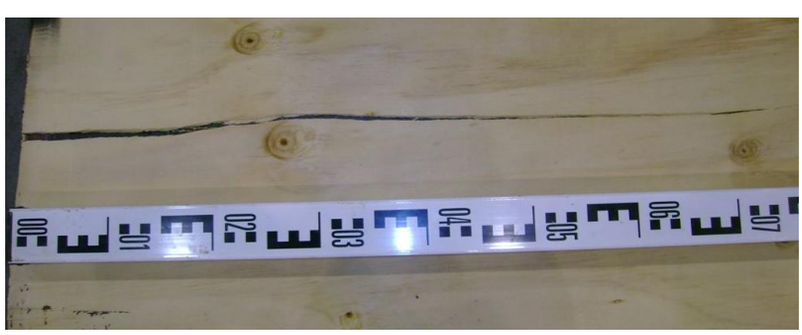

Figure 2-12: Crack in top layer veneer (pine) of plywood panel, 700mm of length.

Cracks are an immediate result of the drying process as the amount of shrinkage is much higher in radial direction than in longitudinal direction. This effect is intensified by short drying times and extreme moisture differences respectively wrong moisture content during storage and handling. It only leads to cracks on the single lamella or veneer sheet, never on a glued and pressed panel which will rather bend and warp under these forces. The rate of

crosswise cracks orthogonal to the grain direction (longitudinal shrinkage) is much lower than the rate of cracks in grain direction (radial shrinkage) but its presence is much more critical to the load capacity which is important in the production of lumber. Typical lengthwise cracks range from 50mm to several hundred millimetres in length and up to 20mm in width; crosswise cracks are typically below 100mm in length.

2.2.1.1.4 Pinhole/wormhole

The term pinhole or often also wormhole is commonly used for holes in wood with a diameter typically below 5mm (small diameter and very circular shape are the only discriminative characteristics). In most cases these holes are caused by insects of different types, not necessarily worms, depending on the geographic origin of the wood.

2.2.1.1.5 Roughness

During the seasons, the tree forms more or less dense wood, called earlywood and latewood. Earlywood referring to the wood cells grown first in the season shows thin cell walls and large cell cavities. Contrary the latewood, which is much denser due to thick-walled cells with very small cavities, is created to the end of the season. As the strength of the wood is defined more by the cell walls and less by the cavities, stiffness and strength are defined by the amount of latewood. The much softer earlywood can be torn out, especially by a blunt knife or saw blade. This effect on veneer on spruce is shown in Figure 2-13 at the much brighter part of the annual ring containing the softwood. With a typical mean depth of 0.2 - 0.3mm this effect is usually called Roughness.

Figure 2-13: Rough surface of plywood veneer from Nordic Spruce due to very soft earlywood torn out in the peeling process.

2.2.1.1.6 Shells

Figure 2-14: Shells on plywood panel (Pine Radiata) – torn loose earlywood.

Analogous to the Roughness on spruce (refer to previous section), in the peeling of stems from Pine it may happen that the earlywood gets torn loose, leaving large areas of slight indentation as well as large loose areas as shown in Figure 2-14 which are called Shells.

2.2.1.1.7 Resin pocket

Figure 2-15: Resin pocket on peeled veneer of spruce. Thin wood often covers parts of the resin pocket (left side).

The resin pocket is cut horizontally or vertically in the production process (depending on whether the trunk has been peeled for plywood or sawn for lumber) and therefore either is forming a flat but wide indentation, refer to Figure 2-15 or a narrow but deep crack, refer to Figure 2-16.

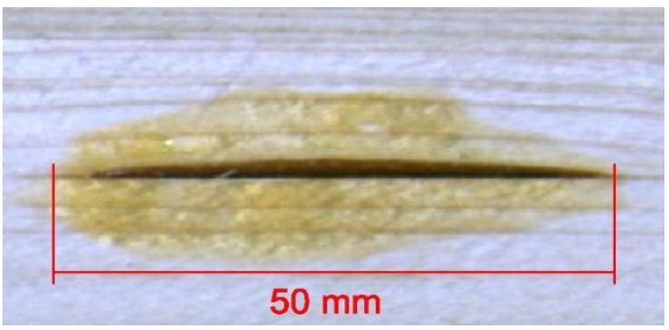

Figure 2-16: Resin pocket on sawn lamella of spruce, only partially opened and with lake from flew-out resin.

When being hot pressed, the resin becomes fluid and might form a resin lake around the opening (e.g. on the bottom side of the panel). The resin pocket's true size normally cannot be determined correctly from the view on the surface, often the pocket is still covered with some thin wood like shown for peeled plywood in Figure 2-15, left side or is cut at the border leaving the longer part of the pocket beneath, refer to Figure 2-16 on sawn lumber

2.2.1.1.8 Cracked Knots

Sound knots that are principally connected to the surrounding wood but show cracks are called Cracked Knots. The cracks occur during drying of the peeled veneer and due to the fact that the grain direction in the knot is different to the grain direction of the surrounding wood resulting in divergently oriented forces in the shrinking. This may lead to a fragmentation of the knot as can be partially seen in Figure 2-17, resulting in a bigger hole in the worst case.

Figure 2-17: Cracked Knot on plywood panel of spruce.

Cracked knots may be tolerated for some purposes of plywood panels. The cracks are nevertheless problematic due to penetration by moisture and water in outdoor applications. They are intolerable with panels that are coated with foils as they normally shine through the coating.

2.2.1.2 Structural defects

The class of structural defects generally is formed by any defect interrupting the sound wood and its normal grain structure, which would include as well the knotholes and cracks, etc. In this context the structural defects exclude the previously introduced *physical defects* and limit the class to defects that result from abnormal or destroyed fibres in the wood either from biological processes of the plant or by external influence.

2.2.1.2.1 Dark knot, dry not & loose knot

Figure 2-18: Dark knot on sawn lamella from spruce, still quite attached to the surrounding sound wood.

Figure 2-19: Dry knot on peeled veneer from spruce showing partial detachment. The surrounding wood already formed some bark to isolate the knot.

Figure 2-20: Fallen out loose knot (showing the dark brown homogenous applied glue on the underlying veneer sheet.

As already described in *2.2.1.1.1 Knothole*, the higher amount of lignin and the different grain orientation of the knot's influence the amount of shrinkage in that way that the knot can detach from its surrounding. Often the living tree attempts to isolate an already dead knot resulting from a dead branch with the creation of bark which is shown in Figure 2-23.

2.2.1.2.2 Bark, Knot with bark, Ringed Knot

Figure 2-21: Ingrown bark on plywood of pine, most likely due to former damage.

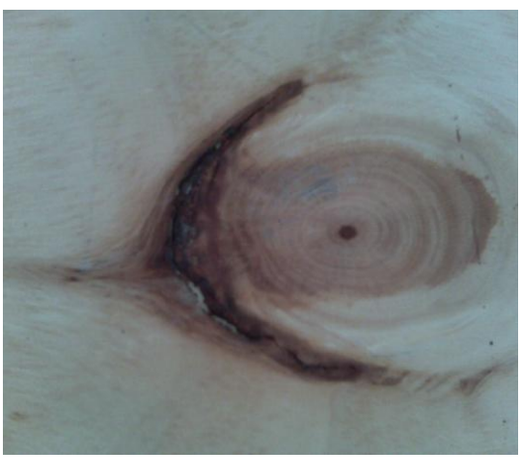

Figure 2-22: Ingrown bark at fold on plywood of spruce.

Figure 2-23: Bark around dead knot on plywood of spruce.

Bark may become ingrown when either folds on the stem coalesce or due to a mechanically caused damage at the outside of the trunk during lifetime, this is shown in Figure 2-21 and Figure 2-22. As already mentioned in *2.2.1.1.1 Knothole* and *2.2.1.2.1 Dark knot & loose knot*, the tree grows bark around dead knots to isolate them from the sound wood of the trunk which is shown in Figure 2-23.

2.2.1.2.3 Rot

Figure 2-24: Soft rot (darker area) on veneer from spruce.

Fungal infestation is the reason for a brownish/reddish decolouration which is quite common in softwoods. Two kinds of fungi are mainly causal, brown rot fungi and soft rot fungi, both breaking down the cellulose in the wood *[Ritschkoff 1996]*. Besides the influence on the optical appearance the structure of the wood is weakened which degrades the wood for technical purposes like for lumber, but not necessarily for the production of flooring, furniture or cladding purposes.

2.2.1.2.4 Reaction wood (compression wood)

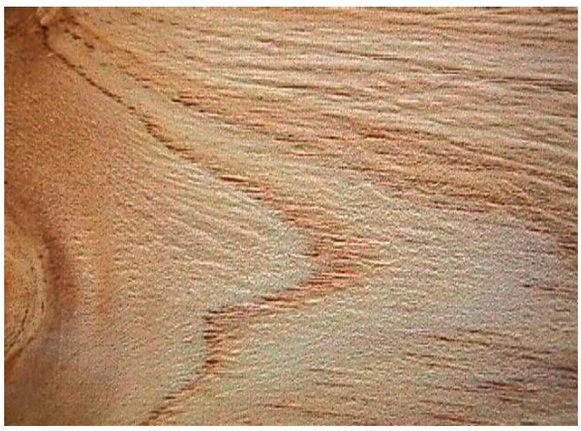

Figure 2-25: Compression wood on plywood panel of Pine Radiata. Abnormal growth of the wood fibres due to presence of tensile respectively compression on the tree (wind, grown crooked, grown on a slope, etc.).

When mechanical stress caused by wind, soil movement and alike is acting upon a tree continuously, the plant reacts by forming reaction wood to support its optimal alignment. The different tree species thereby incorporate different strategies. While angiosperms form so-called tension wood on the affected side of the trunk which pulls it contrary to the affecting force, the conifers form so-called compression wood supporting the side opposite to where the force applies to the trunk. The tension wood is almost completely consisting of cellulose while compression wood is rich of lignin *[Richter 2014]*. Visually noticeable often by a stronger reddish colour in the case of compression wood, the influence of both types of reaction wood is much more important as it concerns the mechanical properties of the wood and as it responds differently to changes in moisture and therefore its tendency to bend. As can also be seen from Figure 2-25 the cell structure of compression wood and therefore the surface itself appears much more roughly structured than normal wood.

2.2.1.2.5 Pressed-in particle

Besides the indentation, usually in form of knot holes, three-dimensional measurable defects occur when particles get pressed into the top layer veneer. Besides the appearance criteria of such an irregularity the problem is the possibility that the particle detaches again during the further processing of the panel, for example during sanding, leaving an indentation in the range of several tenths of a millimetre. The sanding normally does not take away enough overall material to compensate this slight indentation which results in a problem when foil-coating the panels for example.

Figure 2-26: Particle pressed into the surface of a spruce plywood panel.

Figure 2-27: Pressed-in particle, when removed by sanding, the indentation will remain.

2.2.2 Pure aesthetic defects

In contrast to the physical defect definition from the previous paragraph, aesthetic defects in this context are defects that cannot be discriminated from their surroundings by simple natural measurements as it is their appearance to the human visual system that makes them "looking defective" or "undesirable". Therefore instead of applying common measurement units, verbal descriptions with the intense use of adjectives are incorporated to distinguish between sound and defective/undesirable. This introduces vagueness leading to interpretation problems when mapping the defect description to logical decisions of a computer-driven automated inspection system.

2.2.2.1 Discoloration

Figure 2-28: Discoloration (red) of plywood veneer from Pine Radiata (close-up view).

Figure 2-29: Discoloration (red) of plywood veneer panel from Pine Radiata (panel view). Although defect-free in terms of knots and similar, the unusual appearance may be a severe issue in industrial production.

Wood decolourization may have a severe impact on the appreciation of a customer although it is mainly a cosmetic issue and seldom is due to a structural issue with the wood. Individual manufactured products might exploit the special appearance, but with the rising demand of added-value wood products in industrial production and thereto adapted product quality specifications, discolorations have become an important, economic problem being less tolerable.

2.2.2.2 Grain structure

Figure 2-30: Examples of different grain structures. Grain structure influences the perception of the wood colour.

The grain structure, together with the colour shade of a wooden surface plays the major role in the appearance and perception. In fact the texture generated by the grain structure influences the perception of the colour in that way that the mean percept colour is a product of background colour and texture *[Massen 2009]*. The grain structure around knots is significantly percept showing that detection of knots as well as their repair must incorporate the neighbourhood.

2.2.2.3 Blue stain

Blue stain is caused by a fungal infestation which causes a bluish to greyish discolouration, refer to Figure 2-31. The blue stain fungi only infects the sapwood as it consumes the lignin with is present in high concentration in the sapwood *[Forest Products Laboratory 2010]*.

Figure 2-31: Blue stain on sawn lamella of spruce, the crosswise cut shows the infestation of the outer sapwood.

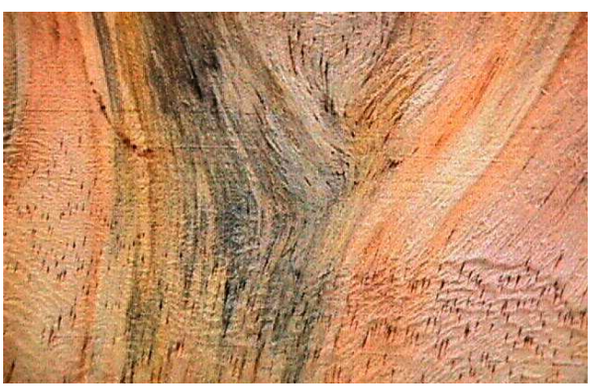

Figure 2-32: Blue stain on plywood panel of Pine Radiata.

Blue stain does not cause decay and therefore does not have influence on the strength of the wood, although some lumber rules limit the amount of blue stain on lumber for structural purposes. Under decorative aspects the appearance of blue stain is sometimes welcomed to a certain amount, but is most often perceived as a disturbance which makes it belong to the class of aesthetic defects.

2.2.2.4 Needleflex / Needleinfusion

Figure 2-33: Needleflex on Pine Radiata.

The wood working industry makes huge efforts to produce high-quality plywood boards by using knot-free veneers. These can be obtained from trees that have regularly cut off their branches so that the outer tree-rings are knot-free and give the best quality wood under appearance criteria. But trees treated like this start to grow their cones directly at the stem near to the cut off branch which results in irregularities similar to dark knots. Further, the tree without branches starts to grow its needles directly at the stem. When not removed in the silvicultural process, the needle roots disrupt the structure of the wood in the outer tree rings giving the resulting veneer a spotted texture (refer to Figure 2-33) called Needleflex or Needleinfusion which may be desired or undesired.

2.2.2.5 Knots

2.2.2.5.1 Sound knots

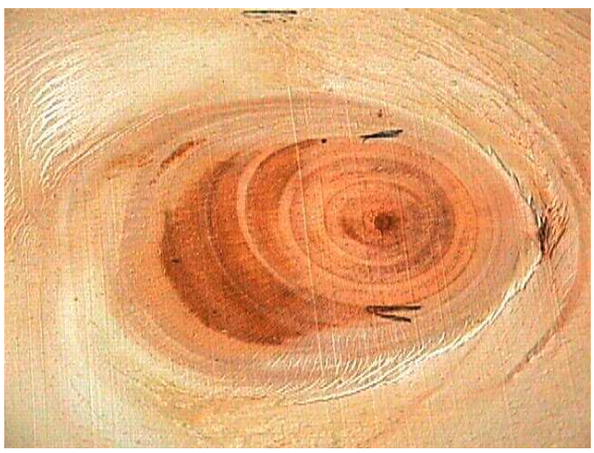

Figure 2-34: Sound grown knot on panel of Pine Radiata, fully bonded to the fibres of the surrounding wood, showing a reddish colour.

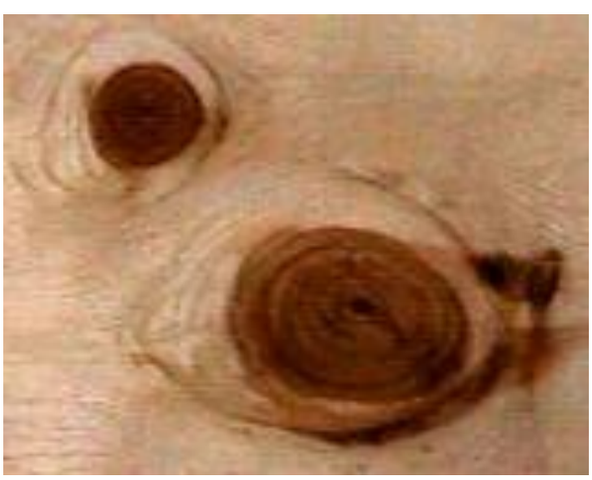

Figure 2-35: Sound grown knots on panel of Pine Radiata, tightly bonded to the surrounding wood, showing brownish colour.

Knots, although sound grown are not tolerated in principle by the various quality specifications for wooden panels. Besides the structural issues when clusters of sound knots appear, the top-quality plywood panels do not show any knots at all. Other quality definitions allow knots up to a certain diameter and/or a certain amount of knots per panel. Appearance of sound knots is also mainly influenced by their colour, refer to Figure 2-34 and Figure 2-35.

2.2.2.6 Clusters of knots

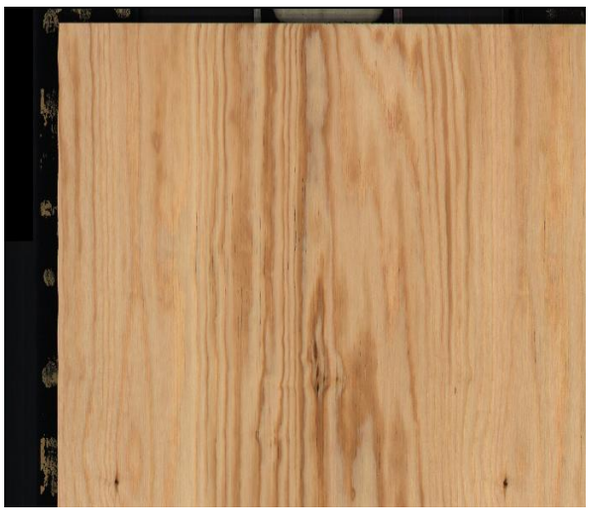

Figure 2-36: Knot-free surface preferred by South-American market.

Figure 2-37: Regular sound knots preferred in Scandinavian and Austrian market.

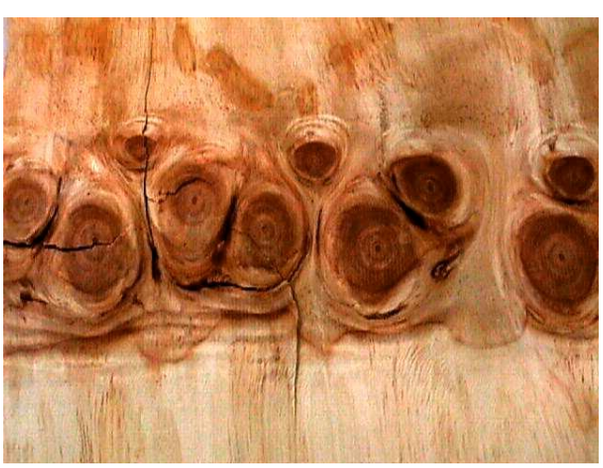

Figure 2-38: Clusters of sound knots, aesthetically undesired, being also a structural issue.

In top quality plywood panels, typically quality 'A', the most obvious quality criteria is the amount of (sound) knots. While South American plywood of pine demands no knots at all for

quality-‘A’-surfaces (Figure 2-36), Scandinavian and Austrian plywood of spruce allows regular, sound knots also in the highest quality grade (Figure 2-37). Knot-free veneer can solely be gained by using top layer veneer from the lower part of the tree (for example lower 7-8 meters of Pine Radiata) which is free from branches or by using the veneer gained from the inner parts of the trunk. Clusters of knots as shown in extreme in Figure 2-38 are nevertheless undesired.

2.2.3 Quality standards

A variety of standards and norms for the production and assessment under various aspects for wood-based panels exists. These norms are issued either by national or international standardization organizations or by the major panel manufactures.

2.2.3.1 Standards and norms

Besides the norms related to strength, bending capability, moisture resistance and other structural parameters (e.g. International Standards Organisation (ISO) norm 18775 *[ISO 18775:2008]*) the ISO norm 2426 addresses also the appearance of plywood panels *[ISO 2426-1:2000]* made from hardwoods *[ISO 2426-2:2000]* and softwoods *[ISO 2426-3:2000]*. Several appearance categories exist that specify the allowed number of certain defects but also of sound knots and further address discoloration for example. Table 2-1 shows an excerpt of the ISO norm for appearance of plywood panels made from softwood.

Category of characteristics	Appearance class		
	E	I	II
Pin knots	Practically absent	3/m^2 permitted	permitted
Sound integration knots		Permitted up to an individual diameter of:	
		15mm provided their cumulative diameter does not exceed 30mm/m^2.	50mm
		Such knots may have splits, provided they are:	
		Very slight	Slight
Unsound or non-adhering knots and knot holes		Permitted up to an individual diameter of:	
		6mm if filled and up to a number of 2/m^2.	5mm if unrepaired. 25mm if filled and up to a number of 6/m^2.
Splits open		Permitted if less than:	
		1/10	1/3
		of panel length up to an individual with of:	
		3mm	10mm
		and up to a number of:	
		3/m	3/m
		of panel width	
		If properly filled	All splits greater than 2mm in width to be filled.
Splits closed		Permitted	
Abnormalities due to insects, marine borers and parasitic plants	Not permitted	Not permitted	Marks of parasitic plants not permitted. Insects and marine borer holes permitted up to a diameter of 3mm vertically to the plane of the panel. Up to a number of 10/m^2.
Resin packets and Inbark	Not permitted	Not permitted	Permitted up to a width of 6mm if properly filled.
Resin Streaks	Not permitted	Not permitted	Permited if slight
Irregularities in the structure of the wood	Practically absent	Permitted if very slight	Permitted if slight
Discoloration which is not wood-destroying		Permitted if low contrast	
Fungal decay, wood destroying	Not permitted		

Table 2-1: Excerpt from norm ISO 2426-3:2000 defining three appearance classes (E, I, II) for plywood from softwood by limiting amount of defects, knots and other common defects *[ISO 2426-3:2000]*.

Company specific standards

The following description of surface appearance related to appearance norm EN 13017-1 can be found in the product sheet of a three-layer solid wood panel (refer to Figure 2-39) from Tilly GmbH, an Austrian panel manufacturer which cooperated in the setup of the first prototype system for automated patching of wooden panels:

" (…) For exterior applications (e.g. facades, roof undersides) the one-side visual grade AB/C is recommended. The AB grade class combines a lower susceptibility to cracking, finer wood structure and an attractive visual appearance."

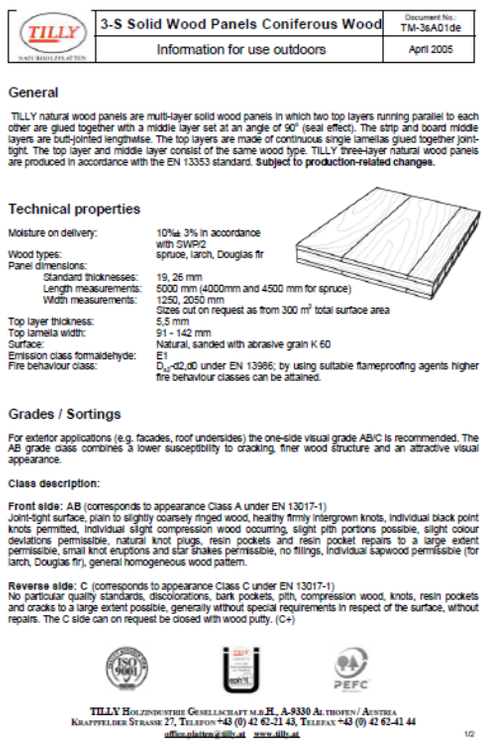

TILLY — 3-S Solid Wood Panels Coniferous Wood | Document No.: TM-36A01de
Information for use outdoors | April 2005

General

TILLY natural wood panels are multi-layer solid wood panels in which two top layers running parallel to each other are glued together with a middle layer set at an angle of 90° (seal effect). The strip and board middle layers are butt-jointed lengthwise. The top layers are made of continuous single lamellas glued together joint-tight. The top layer and middle layer consist of the same wood type. TILLY three-layer natural wood panels are produced in accordance with the EN 13353 standard. **Subject to production-related changes.**

Technical properties

Moisture on delivery:	10%± 3% in accordance with SWP/2
Wood types:	spruce, larch, Douglas fir
Panel dimensions:	
Standard thicknesses:	19, 26 mm
Length measurements:	5000 mm (4000mm and 4500 mm for spruce)
Width measurements:	1250, 2050 mm
	Sizes cut on request as from 300 m² total surface area
Top layer thickness:	5,5 mm
Top lamella width:	91 - 142 mm
Surface:	Natural, sanded with abrasive grain K 60
Emission class formaldehyde:	E1
Fire behaviour class:	D_{fl}-d2,d0 under EN 13986; by using suitable flameproofing agents higher fire behaviour classes can be attained.

Grades / Sortings

For exterior applications (e.g. facades, roof undersides) the one-side visual grade AB/C is recommended. The AB grade class combines a lower susceptibility to cracking, finer wood structure and an attractive visual appearance.

Class description:

Front side: AB (corresponds to appearance Class A under EN 13017-1)
Joint-tight surface, plain to slightly coarsely ringed wood, healthy firmly intergrown knots, individual black point knots permitted, individual slight compression wood occurring, slight pith portions possible, slight colour deviations permissible, natural knot plugs, resin pockets and resin pocket repairs to a large extent permissible, small knot eruptions and star shakes permissible, no fillings, individual sapwood permissible (for larch, Douglas fir), general homogeneous wood pattern.

Reverse side: C (corresponds to appearance Class C under EN 13017-1)
No particular quality standards, discolorations, bark pockets, pith, compression wood, knots, resin pockets and cracks to a large extent possible, generally without special requirements in respect of the surface, without repairs. The C side can on request be closed with wood putty. (C+)

TILLY Holzindustrie Gesellschaft m.b.H., A-9330 Althofen / Austria
Krappfelder Strasse 27, Telefon +43 (0) 42 62-21 43, Telefax +43 (0) 42 62-41 44
office.platten@tilly.at www.tilly.at

1/2

Figure 2-39: Company specific (related to European Norm EN 12017-1) definition of appearance characteristics for multi-layered solid wood panel *[Tilly Naturholzplatten GmbH n.d.]*

Further the company specific quality classes are defined also in terms of appearance. This description is also used by the wood workers at the manual patching lines:

"Front side: AB (corresponds to appearance Class A under EN 13017-1) Joint-tight surface, plain to slightly coarsely ringed wood, healthy firmly intergrown knots, individual black point knots permitted, individual slight compression wood occurring, slight pith portions possible, slight colour deviations permissible, natural knot plugs, resin pockets and resin pocket repairs to a large extent permissible, small knot eruptions and star shakes permissible, no fillings, individual sapwood permissible (for larch, Douglas fir), general homogeneous wood pattern.

Reverse side: C (corresponds to appearance Class C under EN 13017-1) No particular quality standards, discolorations, bark pockets, pith, compression wood, knots, resin pockets and cracks to a large extent possible, generally without special requirements in respect of the surface, without repairs. The C side can on request be closed with wood putty. (C+) "

2.2.4 Summary

The top-level classification of defects into physical defects and aesthetic defects is an appropriate method in the process of identifying suitable detection methods. The physical defects are characterized by standardised measurements while the characterization of aesthetic defects must be based on the output of more complex computations. Chapter 5, which deals with the robust defect detection, will benefit from the explanations given towards physical and optical characterization of the defects. The discrimination of physical and aesthetic defects also might point out if a low level sensorial setup like 3D-measurement can solve the specific detection task or if high-level logical operations on the sensor data have to be incorporated, for example to adapt the perception of the human visual system.

Beyond proprietary, company-specific standards addressing the structural characteristics of wood panels but also addressing their appearance, national and international accepted norms exist for plywood and solid wood panels made from either hardwood or softwood. These norms are used by the wood-workers to generate rules in either the grading or when patching is applied.

2.3 Methods of patching wooden panels

This subchapter outlines today's most commonly used types of patching wooden panels and introduces a differentiation based on the used materials. By the observations made at different panel production plants the manually carried out processes are analysed. The results are used in chapter 5 for a proper setup of the automated counterpart, also under the aspects of different optimization approaches including aesthetic aspects.

2.3.1 Types of patching on wooden panels

Figure 2-40: Box/finger joint of sound areas after cutting out crosswise the defective area on a lamella.

Patching wooden panels is a well known task in carpentry. The complete crosswise removal of a defective area together with its sound surrounding on lamellas or veneer sheets and subsequently applying stitching techniques is a common task, refer to Figure 2-40. The replacement of a defective area with appropriate fillers has also been practised already for a long time. The advantage over extensive removal, which is not applicable to all products and only at early stages of the whole production process, is the minimized amount of wasted material. For example the jointing of sound parts, after removing the defective parts, is applicable to sawn lamellas before being combined and glued or to single veneer sheets, but not to complete panels. Moreover, the jointing techniques, for example box/finger joints and dovetailing, produce clearly visible transitions as can be seen from Figure 2-40.

The scope of this research is limited to the patching by replacing the defective area locally which gives great opportunities in terms of cost-savings as well as the appearance of the final product.

To locally repair defective areas, turned off slices from branches with characteristic age rings are inserted into holes from fallen branches. Simple round pieces of solid wood with either no or an appropriate texture are inserted elsewhere. Therefore aspects of appearance and aesthetics are involved. Also common is the use of different types of pastes mixed with sawdust of different granularity for the purpose to fill cracks, to smoothen rough areas or to repair edges. With the industrial production of wooden panels also chemical fillers were introduced. The first differentiation therefore is between solid and liquid fillers.

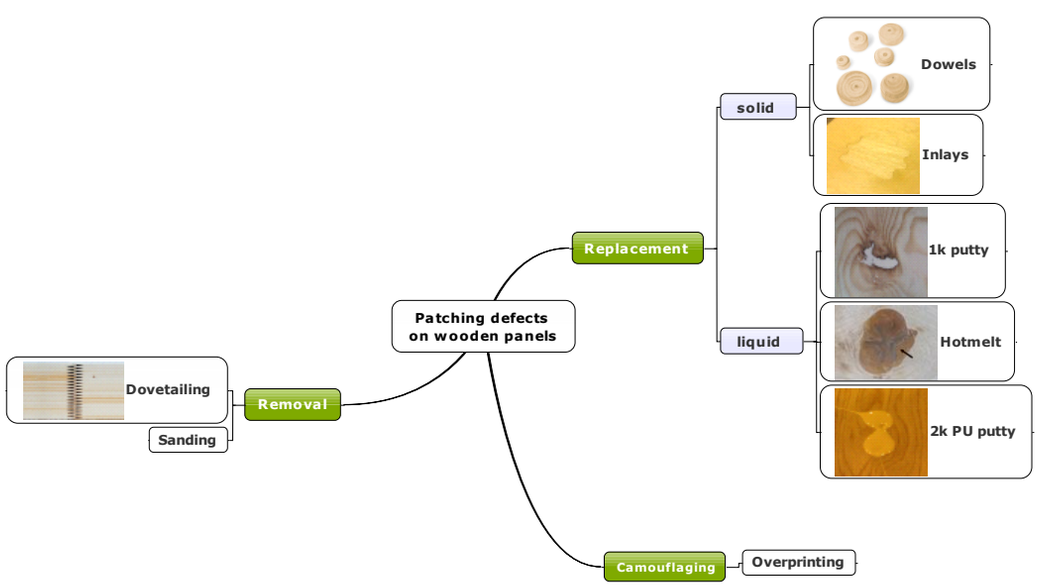

Figure 2-41: Types of patching on wooden panels: a first distinction is made between patching based on the generous removal vs. local replacement of defective areas with different types of fillers. Camouflaging is an imaginable alternative/extension.

2.3.1.1 Solid fillers

Depending on the type and composition of the wooden panel to be patched, the solid filler is manufactured from slices of branches refer to Figure 2-42 or pieces sawn from solid wood by using a holesaw like shown in Figure 2-43. Normally these patches, referred to as dowels, are applied to panels manufactured from sawn wood (multi-layered solid wood panels). Circular and elliptic dowels (Figure 2-44) in different sizes therefore exist. Plywood panels however are patched differently in the single production stages: defects on the veneer sheets are replaced before gluing by inserting inlays like shown in Figure 2-45 with the help of a punch press. The patching of the glued and pressed sandwich however is usually performed using liquid fillers.

Figure 2-42: Circular dowels (spruce) made from branches to reproduce the characteristic age-ring appearance and therefore the best choice for insertion into knotholes.

Figure 2-43: Circular dowels (spruce) made from solid sound wood. Various appearances can be produced which favours them for defective areas besides knotholes, depending on the grain structure.

Figure 2-44: Elliptic/elongated dowels (spruce) made from solid/sound wood for elongated defect areas like cracks.

Figure 2-45: Inlay (pine) produced and inserted with a punch press.

2.3.1.2 Liquid fillers

Wood putty or plastic wood has been long used to fill imperfections on the surface of wood products. While often saw dust or finer sanding dust in combination with wood glue is used in the hobby area and seldom for professional purposes, industrial putty incorporates saw/sanding dust with binders and diluting agents. With one-component (1K) putty the mixture is ready-to-use while with two-component (2K) putty the binder and diluents need to be mixed in advance to the application of the putty. This is of advantage in industrial applications because the lower viscous components can be pumped more easily when mixing takes place at the nozzle compared to the 1K-putty's high viscosity. Hotmelts are often used alternatively to liquidly applied putty.

Figure 2-46: One-component (1K), water based putty without colorant used to fill area of fallen-out bark on spruce plywood. Result after sanding.

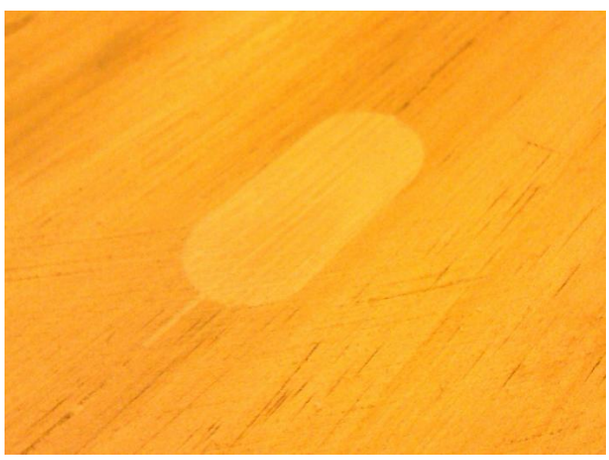

Figure 2-47: One-component (1K), water based putty with beige/light brown colouring used to fill pre-processed (routed) defective area on spruce plywood. Result after sanding.

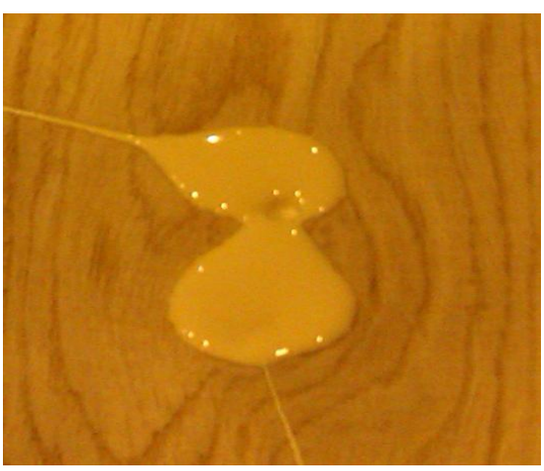

Figure 2-48: Two-component (2K) polyurethane filler with beige/light brown pigmentation used to fill knotholes on plywood panel of spruce, applied with a nozzle. Image shows result before sanding; no shrinking is recognizable but the effect of an air bubble in the low viscous filler can be seen.

Figure 2-49: Polyurethane-Reactive (PUR) transparent Hotmelt used to patch cracked knot in parquet slab of oak. The application is normally carried out using a solid metal punch to ensure backfill and fast cooling down by evacuation of heat. Image shows result before sanding.

2.3.1.2.1 One-component putty

One-component (1K) putty is a paste made up of various materials such as Calcium Carbonate, Barium Hydroxide, Barite, and Silica and, in the case of coloured paste fillers, added colorants. This filler principally consists of three basic components: a binder, a bulking agent and a solvent. There exist two different types of one-component paste fillers: Oil-based and water-based fillers. In the first case the binder is typically varnish blended with oil. In the case of water-based fillers, the binder is urethane or acrylic. The type of binder determines the type of solvent used: oil-based fillers usually use naphtha, while water-based fillers use water. Both types of filler incorporate silica as a bulking agent as it resists shrinking and stretching of the wood in response to changed temperature and changed humidity. Oil pastes have an alkyd added to the filler while water based fillers include a glycol. In industrial processes the water-based putty is preferred as it can be diluted and cleaned up with water and takes less time to dry than oil-based fillers which can only be cleaned up using naphtha.

The disadvantages of using one-component putty is its own shrinking during drying which leads to crack formations, underfilling of the defect and less adhesion to the wood compared to other liquid fillers. The application of one-component putty has to be carried out using a scraper or trowel due to its consistency. Therefore the one-component putty is best suitable for smaller defects like small holes and cracks but is incorporated to a wide range of defects when sanding can compensate the shrinkage.

2.3.1.2.2 Two-component putty

To overcome the disadvantages of filling larger defective areas with 1K-putty, two-component (2K) fillers can be used. All 2K systems show little to no shrinkage and no formation of cracks even when applied to larger areas. They stick well while being easy to sand and post-process and can also be colourised by adding pigments. The use of polyester resin based systems is decreasing due to their emission of deleterious styrene. The preference of inexpensive epoxy based systems over polyurethane based systems is a matter of the superordinated process and the product itself: Epoxy based fillers show good mechanical properties in terms of adhesion and strength but need much more time to harden compared to fast-drying polyurethane based fillers. The processing of both epoxy and polyurethane based fillers is dependent on their viscosity which can be controlled during the mixing. The usage as cast-resin with low viscosity to fill defective areas is the most

common practice in the industrial production of wooden panels as tools like scrapers or trowels become unnecessary.

2.3.1.3 Hotmelts

Hotmelts or hot glues are thermoplastic fillers that do not contain solvents. Besides very fast hardening in the range of only several minutes this is their greatest advantage over other fillers. At room temperature the thermoplastic filler is solid, by supplying heat its viscosity is lowered to a liquid state in which the filler can be applied before curing due to cooling down again. Stored in form of pellets, powder or sticks a huge variety of thermoplastic materials is available. Thereof polyurethane (PU) hotmelts are of greatest interest for the patching of wooden panels: while most hotmelts are processed at temperatures between 180°C and 200°C, the polyurethane bonding temperature can be as low as 50°C to 70°C which is in great favour for heat sensitive substrates like wood. Polyurethane Reactive (PUR) hotmelts represent advancement to the PU hotmelts as their solidification takes place even faster due to the curing incorporating moisture from the substrate or from ambient air resulting in greater mechanical strength due to stronger, cross-linked polymers.

2.3.2 Investigation into manual processes

For the development of the prototype systems for automated patching in cooperation with leading companies in the production of wooden panels in Europe, Scandinavia and in South America, comprehensive requirement analysis has been carried out. This has been done to understand the necessities and demands of the patching processes and to extract and collect the implicit knowledge of the workers who carry out the manual patching. Therefore the manual working steps were analysed and all actions and decisions during the manual patching were identified and questioned.

2.3.2.1 Patching with dowels

Patching with dowels is mainly used on solid wood panels as these panels are most valuable which justifies the high amount of manual labour. Dowels with different shapes and sizes are typically used. From a set of circular and elliptic dowels the worker chooses the appropriate dowel from two points of view:

a) appropriate shape and size to fit the defective area whereby some dowels are allowed to be combined with each other to achieve maximum coverage,

b) the appearance of the dowel in terms of colour and texture (refer to *2.3.1.1 Solid fillers*) to achieve a homogenous integration into the surrounding of the defective area.

Figure 2-50: Manual patching of solid wood panels of spruce with dowels by four workers in two teams. Picture taken in a production facility for multi-layered solid wood panels in Austria.

Figure 2-50 shows the manual patching at a panel production facility in Austria. Panels of size 2000mm in width and 5000mm in length are processed counter clockwise by two teams: Each team consists of two workers. In every team one worker decides which defect to repair and which type, amount and combination of dowels is therefore used and carries out the pre-processing with the appropriate router(s). The second worker in each team follows with a box from where the dowels are selected according to the previously made routing. The second worker makes the decision between several dowels. With the type and size defined by the pre-processing, the decision is made only concerning the best possible appearance and normally in not more than two iterations to limit the processing time. That means the first dowel taken from the box is held on the routed defect area and if not matching satisfyingly to the surrounding another one is taken. The glue is inserted into the routed hole and the dowel is tapped in with the use of a hammer.

Figure 2-51 illustrates this highly optimized process with parallelized work steps that give specific competence to each worker. That is the decision of how it is physically patched and

how it is aesthetically patched. Of course variations can exist where one single worker carries out all steps sequentially.

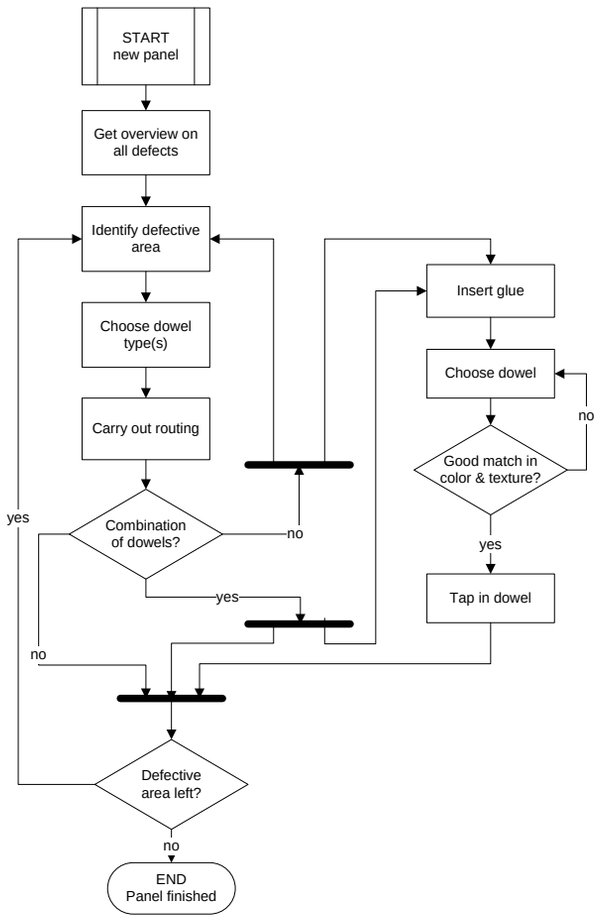

Figure 2-51: Sequence of actions and decisions when patching manually with dowels. Parallelisation of tasks at Austrian panel production facility using teams consisting of two workers responsible for routing respectively filling.

During observation one could see that there is a huge variance in these decisions: sometimes the (first) worker decided not to patch certain smaller defects to avoid concentration of dowels. Some (second) workers tried to find a good matching dowel in terms of appearance already with the first dowel taken from the box or took the chance of the second iteration to improve the result quite often while others did not care about the possible optimization.
Productivity issues of course influence this behaviour, in times where high throughput in the production line is needed the aesthetic quality seems to be lower prioritized. Chapter *2.3.3 Aesthetic aspects in physical patching* will address these observations in more detail.

2.3.2.2 Patching with putty

Patching with putty is most common on plywood panels although solid wood panels graded into lower categories are sometimes also patched with putty. In the context of a project with

a Chilean plywood panel producer a prototype system has been developed which replaces the massive manual labour illustrated below. The sequential manual process is carried out by six workers at three stations per production line. At the first station two workers from opposite side do the routing and marking. At the second station the filling of the routed areas with two-component polyurethane putty is done. At the third station the remaining defects are filled, these are mostly cracks and 1K water-based putty is used. Analogous to the previously described patching with dowels, the first worker in the process chain is responsible for the detection of the defective areas and defines how to repair them. Knot holes, bark, dark knots and resin pockets are routed. Cracks are routed only when exceeding a certain width. Otherwise cracks are marked with a pencil for repair with one-component putty for which no routing is necessary. For repairs with the 2K filler it is important to carry out the pre-processing with the router when not only defective material like bark has to be removed but also because the adhesion can be improved significantly when the bottom surface of a hole is free from glue. The same applies to the resin in large resin pockets. Therefore every defect except the cracks below a certain width where one-component putty is the better choice, are routed, this work step is shown in Figure 2-52.

Figure 2-52: Patching plywood panels of pine with two-component putty in a Chilean plywood production facility. Pre-processing: every defect area is routed to remove any glue on the underlying veneer to ensure optimal adhesion of the filler.

For the application of 2K PU putty the two components resin and hardener are transported with high pressure to a mixing device that is directly attached to the nozzle with which the filler is applied to the panel like shown in Figure 2-53. The mixing of the components at the

latest possible point of the conveyor system is necessary to reduce waste and the risk of blocked hoses due to the fast hardening of the material. The nozzle tube therefore is a wearing part. Nevertheless, while waiting for the next panel, the operator is periodically squirting to a waste bin, which makes up more than 50 percent of the overall used material. This has been identified as a subject to potential economic and ecologic optimization in an automated process.

Figure 2-53: Patching plywood panels of pine with two-component putty in a Chilean plywood production facility. Using a nozzle, the filler is applied to the previously routed defect area and if necessary smoothened with the use of a scraper. To prevent blockage of the nozzle lots of putty is wasted by flushing in idle times.

The main reason for the strict sequential execution of the pre-processing and filling in separated stations is the working safety as the two-component filler is a potential health risk especially when being squirted under high pressure. In principle parallel processing would be possible. The reason why the previously in station one marked defects are patched with one-component putty in a separate third station is to ensure that no two-component filler can be applied upon the one-component putty as this results in poor adhesion. If the proper order of applying the one-component putty after the two-component putty can always be ensured in an automated process than theses steps would not necessarily have to be separated and the third station could be economized.

Figure 2-54: Patching plywood panels of pine with one-component, water-based putty using simple scraper for application. This is the third and final step in the process, carried out after patching with the two-component filler and related routing in a Chilean plywood production.

Defects left when entering station three are therefore usually cracks and rough areas where the shrinkage of the water-based material has only a minor impact. The observations nevertheless showed that defects predestined for the repair with two-component filler, but being close to the panel border, were left open in the second stage due to the risk of leaking out and then were filled in the third stage with the higher viscous one-component putty. Figure 2-54 shows the most common repair with one-component putty: smaller cracks at the front and trailing edge of the face veneer where all large defects have already been repaired as can be seen in the upper right corner of the image. The previously described process is illustrated in Figure 2-55 showing the three stages of the processing chain.

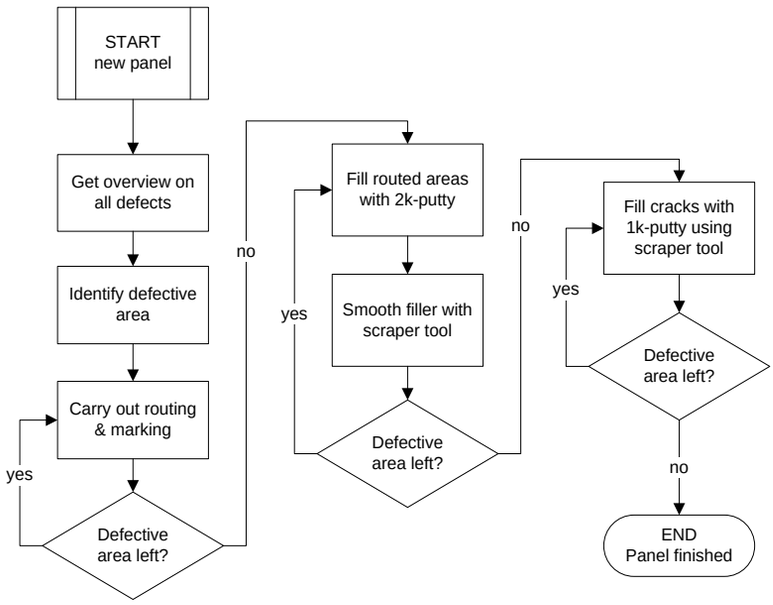

Figure 2-55: Sequence of actions and decisions for patching with different types of putty and appropriate pre-processing in a Chilean plywood production facility. The process is completely serialized for one board to avoid mixture of different putty types in wrong order.

2.3.3 Aesthetic aspects when patching

The patching with dowels is mostly for the purpose to close the surface and to ensure integrity of the material for structural reasons. Nevertheless it can be seen that at least with the choice between several dowels of the same type and size an aesthetic decision towards the final appearance of the patched panel is made by criteria like colour and texture. Also the relations of the defects with each other are incorporated by the workers, for example when deciding not to patch a less recognizable defect for the purpose of avoiding clusters of dowels. In the production of plywood there are fewer options in the choice of the filler and aesthetic aspects are addressed mainly by selecting which defect to repair and especially by the way these defects are routed when 2K-PU putty needs to be applied. The routing therefore is sometimes related to art handicraft.

2.4 Technology demands

From the industry point of view the lack of automation in the production process of panels in principle and especially in the sub-process of patching/finishing is seen most crucial. This is related to the huge amount of human labour involved. The improvements of automation are:

- Higher throughput in terms of produced panels
- Lower costs per panel
- Steady, reliable and transferable results
- Optimization capabilities
- Data collection and process monitoring capabilities

Mechanical automation offers the possibility to drive the overall production line at much faster speeds than it is possible with the patching/finishing sub-process being based on human labour. The typical transportation speed in the manual process varies around 5 meter per minute while in an automated process transportation of panels up to 30 meter per minute could be possible with patching on the move, depending on the amount of defects per panel and available tools. Higher production speed lowers the costs per panel additionally to the dropped labour costs. Besides cost effectiveness the possibility to generate repeatable, steady results over a long time period and among different production lines and even among different production facilities when using automation is important. This is due to the fact that human labour is typically influenced by physical and psychological condition and by adaption, for example are better quality panels inspected more strictly (and therefore are patched more) over time, lower quality panels are patched less over time. Optimization capabilities of an automated process can be identified under different aspects, besides aesthetic considerations (refer to 2.3 *Methods of patching wooden panels*) ecological optimization (wasting wood resources and usage of materials for patching, refer to section 2.3.2.2) economic aspects (refer section to 2.1.2 *Economical aspects - market development*) and aspects related to cost effectiveness apply as well. In modern production processes several database systems are further used to monitor, control and predict the production, therefore an automated patching system is seen as a valuable data source in the superordinated system and needs to report data continuously.

3 Literature Review

Chapter 2 built the basis to understand the economical, ecological and technical needs for intelligent automation in the wood working industry, specifically in the production of wood-based panels. This chapter gives an overview of the research work that has been carried out related to the task of automated visual inspection of wood products. A line of development is identified starting from early approaches in the 1990s incorporating single greyscale imaging sensors and limited processing capabilities to modern multi-sensor technologies incorporating state-of-the-art data mining technologies. Literature is further reviewed for research on wood appearance and aesthetics as well as concerning approaches for automating rectification tasks on wooden panels.

3.1 Machine Vision and wood based products

Machine Vision embraces all the technologies required for visual, non-contact measurements used for process monitoring, quality assurance, grading & sorting and material handling in terms of robot guidance for example. Machine vision in the wood processing industry is largely applied to the early production stages such as the grading in the saw mill and in the veneer, board and wood-based panel production. Currently an important task is the automatic, camera-based grading of wood based products into different qualities according to some standard or norm (e.g. Nordic, British, European grading rules) by classifying defects like knotholes, different kinds of knots, cracks, regions with blue stain and others. Another important task, for example, is the automated definition of cut-out regions for a subsequent sawing including the optimal use of the resources.
In the following sections the most important techniques of image data acquisition and image data processing used by machine vision systems on wood and the related research are reviewed.

3.1.1 Imaging techniques

First attempts to utilize **greyscale image sensors** together with segmentation techniques like simple thresholding *[Cho et al. 1990]*, multi-thresholding and adaptive thresholding *[Pham and Alcock 1992]*, and edge detection *[Silven et al. 1986], [Ojala et al. 1992]* showed limited industrial applicability. This is due to high false-positive rates, for example in the detection of

knots, on the one hand and high false-negative rates on the other hand. It has been realized earlier that feature-based classification incorporating texture and shape is necessary *[Szymani and McDonald 1981]* to improve the results in automated visual inspection but real-time application could not be achieved. Furthermore the detection of defects like rot and stain showed to be nearly impossible at all due to the missing informational content of the monochrome image data *[Kim and Koivo 1994]*.

Alapuranen and Westman *[Alapuranen and Westman 1992]* therefore proposed the application of **colour imaging** and the use of Hierarchical Vector Connected Components Segmentation (HVCCS), a method sensitive to local variations on wood surfaces but insensitive to global variations. With this multi-stage region-growing segmentation technique they claimed to have developed the first approach being capable of achieving better quality grading results on (softwood) plywood than human inspectors in real-time. Further work on the use of colour machine vision has been carried out *[Brunner et al. 1992], [Silven and Kauppinen 1994], [Lu et al. 1997], [Kauppinen 1999], [Kauppinen 2000], [Silven et al. 2003]*. In his dissertation work, Kauppinen *[Kauppinen 1999]* presented a system that uses previous findings and colour cameras together with techniques of unsupervised learning. A test installation in a parquet slab grading line showed promising results in comparison to an already established grey level based machine vision system.

All mentioned colour-based approaches have in common the sensitivity for variations in colour which can be diverse depending on the colour space incorporated *[Brunner et al. 1992], [Kauppinen and Silven 1996]*. Variations in colour are introduced by all involved components of an imaging system as well as from the object which is imaged itself: illumination variations and inhomogeneities due to changing temperature and due to the divergence of the light beam are common *[Kauppinen and Silven 1996]*. This is depending on the device type (fluorescent lamp, light emitting diode, etc.) and its specific characteristics *[Brunner et al. 1992]*. The image acquisition device is under great influence of the used optics. Its lenses introduce inhomogeneity in terms of non-uniformity for the intensity and, due different influence on different spectral ranges, introduce aberrations of the colour *[Meza et al. 2010a]* and *[Meza et al. 2010b]*. Finally the imaging of natural products is subjected to the natural variance of the material itself, mainly in terms of colour. While the imaging device can be calibrated and corrected and the measurement values can be normalized, the natural colour variations of the wooden surface can be problematic for

algorithms, resulting in ambiguity errors, and have great impact on the classification results. Kauppinen and Silven *[Kauppinen and Silven 1996]* who already proposed various methods for machine vision on wood realized early the importance of these influences on the classification accuracy. Brunner *[Brunner et al. 1992]* further studied the influence of illumination variations on the overall system performance using different colour spaces and colour space transformations.

Critical analysis of the previously mentioned approaches shows that one single grey level imaging channel seems not to be sufficient for robust automatic grading. Texture and shape analysis on grey levels alone are inadequate to produce reliable, stable segmentation and classification results. Incorporation of colour cameras significantly improves the results due to higher information content. Nevertheless, certain physical properties of wood (e.g. wood density) do not show up in image data that rely only on light reflectance and some defect types such as holes may be hard to differentiate from sound knots as their colour or greyscale information may not be discriminative enough. Astrand *[Astrand 1996]* addressed this problem by adding measurements of the wood density and fibre orientation gained from a laser line and related **scatter imaging** incorporating the "Tracheid Effect".

Many different arrangements of directed or diffuse illumination and cameras capturing the diffuse or specular reflection can be used for automated visual inspection of the surface properties of wood. It would be very interesting to have an imaging device able to sense the physical properties beneath the surface such as wood density, wood grain orientation etc. Such a principle was first described by Mathews *[Mathews et al. 1976]* and is based on the optical properties of the tracheids (fibrous cell channels) of wood which spread light impinging on the surface laterally within the body of wood, an effect called the Tracheid Effect:

Trees from both the group angiosperms and gymnosperms are vascular plants having lignified tissues to conduct water, minerals and the photosynthetic products through the plant *[Roth-Nebelsick 2006]*. This tissue is divided in two major types, xylem and phloem. While the phloem is responsible for carrying organic nutrients, mainly sugar (sucrose), from the photosynthesis, the xylem is responsible for the transport of water and mineral nutrients from the roots throughout the plant. In trees the phloem is the innermost layer of the bark while the xylem forms most of the inner part of the tree. The major cell type in the xylem is

the Tracheid, an elongated cell type. Like most plant cell types the tracheids have a primary and a secondary cell wall, the primary cell wall formed during the cell is growing and the secondary cell wall formed inside the primary cell wall after the cell is fully grown. The secondary cell type is regularly disrupted with so-called dapples, areas where only the primary cell wall exists and where the transportation of water from cell to cell takes place *[Roth-Nebelsick 2006].* While tracheids are the only way to transport water in gymnosperms, angiosperms additionally have vessels with larger diameter what makes the structure of their so-called hardwood much more complex. When the Tracheid cell is matured and dies, the primary cell wall is strongly thickened and lignified (by embedded lignin) which gives softwood, where tracheids are the major cell type, its strength *[Wilson and White 1986].*

The Tracheid Effect mentioned by Matthews *[Matthews 1976]* describes the spatial diffuse transmission of light through wood, whereby the light partially penetrates through the wood surface and is partially emitted at another location after having channelled through the tracheids. High lateral light propagation can be expected in structures with anisotropic, elongated fibres and hollow cells; the propagation of light in longitudinal direction (along the wood grain) is many times higher than in cross direction *[Fischer and Wendland 1999]*. As the direction of highest light propagation direction is identical to the cell/fibre orientation, thicker cell walls (heartwood) show higher absorption than thinner cell walls with less embedded lignin (sapwood); destructed cells (from fungal infestation) show abnormal low transmission compared to areas with normal fibre cell orientation. Resin pockets show very important light transmission along the pocket. These optical properties which are modulated by the inner structure of wood are therefore very useful in detecting defects that are poorly visible by their surface reflectance such as bad knots, cracks, resin pockets, marrow tubes etc. When spatially-resolved this scatter imaging therefore can provide valuable information for the inspections of wood surfaces.

The Tracheid Effect is highly dependent on the impinging angle of the projected light spot or line; it is lower when the light is perpendicular to the surface and maximal when directed with a razing angle along the direction of wood grain *[Fischer and Wendland 1999]*. The best imaging of the Tracheid Effect is achieved by projecting a sharp light stimulus and by observing the light exiting the wood after having propagated along the tracheids. Usually a laser is employed as a stimulus. With the use of dot lasers the effect can be measured in 360 degrees around the laser spot, with a matrix of fine lasers dots a scatter image with low

spatial resolution can be obtained which is suitable for the prediction of grain angle distribution *[Petersson 2010]*. When the dominant grain orientation of a wood piece is known and when it is aligned to the direction of transportation, the simplest stimulus is a sharp line of laser light projected across the wood allowing higher spatial resolution only in the preferred direction.

Measuring the Tracheid Effect puts high demands on the focus and depth of field of the laser light source on the one hand and on the clock frequency and processing abilities of the camera imaging the wood surface beyond and beneath the projected laser line. This is especially true when the wood has high density, has a structure not only consisting of Tracheid cells (hardwood), and/or shows high absorption (dark colour) as then the spatial distance between stimulus and measurement area reduces. In these cases the measurements can perform with such a low signal-to-noise ratio that no additional information can be obtained compared to a normal greyscale image. As a conclusion, bright softwoods are reported to give best results in the measurement of light scattering based on the Tracheid Effect.

Building upon the results from Astrand's and Astrom's *[Astrand and Astrom 1994]* approach, Nestler and Franke *[Nestler and Franke 2000]* added a **3D laser triangulation** sensor and diffuse white light as the sources of light to their optical inspection system of lumber. They investigated into the spectra of different regions on spruce softwood showing blue stain, resin, rot, etc. They showed that the data from the green channel of the RGB image carries no information and therefore can be neglected. By replacing the green channel bandpass filter in the colour camera with a visible light (VIS) blocking near infrared (NIR) bandpass filter, a new image channel is created for measuring the Tracheid Effect decoupled from the gloss effects in the remission of the white light at the surface. The visualization of the segmented and classified defects based on colour and scatter analysis is then done by matching the colour image on the reconstructed surface and highlighting areas of interest.

In addition to meanwhile well-established 3D laser triangulation and scatter image sensors further imaging sensors operating beyond the classical surface reflectance model were developed and are in use nowadays. Although the inspection tasks on wooden panels mostly address the wood surface characteristics, information about the inner or near-surface structure of the wood is worth evaluating as it gives valuable information to identify and classify surface defects. **X-ray imaging** is therefore an important technology to gain

information across a piece of wood. Scanning with X-rays gives an averaged image of the wood density throughout the objects thickness *[Fischer and Wendland 1999]*. This average density allows good discrimination between areas of high density like knots and bark and areas of low density like rot, decay and voids compared to areas with normal wood. It is very well suited to hardwood inspection where the scatter image acquisition is not applicable due to the low signal-to-noise ratio of the Tracheid Effect *[Fischer and Wendland 1999]*. Xiao *[Xiao 1998]* was the first to present a system for defect recognition on red oak hardwood lumber combining colour imaging, laser profiling and X-ray imaging. In his design for a sensor fusion system the 3D laser sensor plays the role of a detector just for global board variations like twist and thickness variations. Smaller, local, three-dimensional defects are assumed to be detected in the X-ray image data. Another working prototype based on the same design concept as the system from Xiao has been reported by Kline, Surak and Araman *[Kline et al. 2003]*.

A newly but increasingly popular imaging technique providing information about the inner structure of a wood object is **Infrared Thermography** which images heat radiation from the object. Three principles of thermographic measurements are common:

Passive Thermography incorporates infrared camera measures of the heat distribution at the surface of an object that is warm or has been heated up in the production process. A defect will act as a thermal insulator blocking the heat from the hot core, resulting in so-called cold spots in the thermographic image *[Maldague 2001]*.

In contrast **Active Thermography** requires the use of a heating technique that is able to heat the object's surface quickly and evenly, for example by moving the object beneath a heat radiator. The infrared camera then measures the heat front dissipation that depends on thermal properties like density, heat capacity, thermal conductivity of the piece of wood and which is influenced by the local internal wood structure *[Maldague 2001]*. A defect in the inner structure creates a barrier to the heat dissipation process and therefore generates a so-called hot spot in the thermographic image as the temperature above the defect will decrease more slowly.

With the use of fast-reacting spotlights or flashbulbs the object's surface can be warmed up quickly and for a short time (pulsed). With no defects in the structure beneath the surface, the heat penetrates the material evenly and the surface cools down homogeneously.

Analogous to the Active Thermography a defect acts as a barrier for the heat dissipation resulting in hot-spots in the thermographic image, but **Pulse Thermography** requires the object to be stationary.

The use of Pulse Thermography can be problematic, as one single heat pulse generates high temperatures at the object's surface. To ensure a non-destructive measurement the thermal load can be reduced by intensity modulation that allows distribution of the energy over a longer period of time. The infrared camera then monitors the temporal oscillating temperature field with contiguous images and pixel-wise Fourier analysis delivers local amplitude and moved phase information *[Maldague 2001], [Ibarra-Castanedo 2011]*. This principle is commonly known as **Lock-in Thermography.** The amplitude of the temperature field delivers information on the presence of a defect, analogous to the previous principles, while the phase allows conclusions about the depth position of the defect inside the object *[Dillenz and Busse 1999]*.

These four principles of Thermographic Imaging can be classified into two groups concerning their applicability: Passive and Active Thermography are well-suited for online inspection as they allow or require the object to be moved. Pulse and Lock-in Thermography require the object under test to be stationary and therefore are of limited use in the production line.

The application of Active Thermography for automated visual inspection of wooden panels has been successfully demonstrated by Meinlschmidt *[Meinlschmidt 2005]*. Commonly detectable defects on wooden panels using Thermographic Imaging are bad bonding in multilayer boards and laminates, fallen out knots in plywood, faulty glued veneer joints, compression wood and splitting. Hardly visible (based on the light reflection model) defects beyond the surface of plywood veneer like fallen out knots in the core veneer can easily be identified in the thermographic image. Thermographic imaging can support the visual inspection by means of a better discrimination between real wood defects (e.g. dry knot) and similar looking sound knots and is applicable in common to suppress false defect detection caused by contamination.

Active Thermography and Lock-in Thermography on wooden panels have been shown to work with a replacement of the (modulated) heat source by a high power ultrasonic source as well *[Tarin and Rotolante 2011]*. The vibration of the material yields to local heating by friction when certain defects like loose knots, black knots or cracks are present *[Meinlschmidt 2005].* Problematic here in terms of practicability in a production

environment is the need of the ultrasonic stimulus having direct contact with the panel as the air is a poor wave coupling medium.

3.1.2 Multi-channel image processing

Nowadays all high-performance industrial machine vision systems for surface inspection are using multi-channel imaging, continuously rising processor performance in combination with dropping costs for acquisition and processing hardware make this practicable. Advanced wood inspection systems, e.g. from WoodEye[3], LuxScan[4] or Raute[5] are therefore mostly multi-sensorial systems which combine several camera and illumination modules. The combination of different imaging channels demands the fusion of the data from the different imaging sensors which is a complex task as the sensor data fusion can be done on several levels *[Liggins et al. 2008],* for example on signal level (pixel fusion), on feature level (information fusion) or on decision level (symbol/object fusion). The information fusion based on corresponding features on a later stage in the processing chain is often preferred instead of geometric and photometric alignment via pixel-wise registration at an early stage which demands for proper and often complex calibrations *[Haghighat et al. 2011], [Chen 2012]* and image transformations *[Schmitt 2006].* Astrand and Astrom *[Astrand and Astrom 1994]* identified and addressed this problem early and introduced the first integrated industrial multi-sensor approach for softwood inspection. Integrated in a single imaging sensor they combined greyscale reflectance measurement, three-dimensional measurements gained from laser line triangulation and information about the wood density respectively about the fibre orientation by imaging the Tracheid Effect registered pixel-wise directly on the sensor due to a proprietary sensor design. Another concept combining colour and 3D-profiling in one single camera device on pixel level using a semi-permeable mirror has been presented by Massen *[Massen 1997].* Based on the results from Astrand's *[Astrand Astrom 1994]* approach, Nestler and his colleague *[Nestler and Franke 2000]* matched image channels (colour image, 3D profile and scatter image) using a 3D laser triangulation sensor and diffuse white light as the source of light by modifying the colour filter of an three-colour imaging sensor. Their approach used sharp-focused white light for a two-colour model as well as for 3D-profiling and the near-infrared for the scatter measurements.

[3] http://www.woodey.se/
[4] http://www.luxscan.lu
[5] http://www.raute.com

Although the software approach to register image data pixel-wise became realizable due to the rising computing power, the registration of multi-channel image data is mostly still done by proprietary, integrated sensor designs.

Independent from the type of sensor data fusion there exist a variety of methods for the evaluation of the image data. All evaluation methods have in common to extract information that can be used for some decision making in respect of the superior task. The task of defect detection for example involves the decision if a defect is present and which image elements (pixels) belong to the defect. Evaluation methods and decision making are nowadays mostly implemented in software. Information extraction incorporates operations of image and signal processing, for example filter or morphological operations. The extracted information is commonly a set of numeric features that are combined logically, either using rudimentary conditional computing or incorporating high-level classification or clustering techniques.

3.1.3 Classification techniques in defect detection

Using (numerical) features for the description of objects implies the creation of a model by algorithms either using patterns or finding patterns in the data (feature) set. Predictive modelling is used in classification "… which takes a set of data already divided into predefined groups and searches for patterns in the data that differentiate those groups" *[Encyclopaedia Britannica].* "Descriptive modelling, or clustering, also divides data into groups. With clustering, however, the proper groups are not known in advance; the patterns discovered by analyzing the data are used to determine the groups" *[Encyclopaedia Britannica].*

Clustering is often related to unsupervised learning *[Hinton et al. 1999],* accordingly supervised learning is the machine learning task of inferring a function from labelled training data *[Mohri et al. 2012].* Usually the training data are split to a training set a testing set. The inferred function derived by the supervised learning algorithm from the training set is rated mainly by its capability to generalize *[Mohri et al. 2012]*, that means mapping unseen examples from the testing set.

The following section addresses approaches found in literature, which incorporate classification techniques and involves machine learning in combination with machine vision.

Many applications of machine vision in industrial wood processing exist but not all of them show the need for classification using supervised or unsupervised learning. For simple tasks of grading or defect detection focused only on a specific characteristic of the wood surface an appropriate acquisition with subsequent filtering might be sufficient. Most of the applications nevertheless have to deal with several complex defects making conservative conditional programming based on filter operation outputs inefficient, confusing and inextensible. Therefore the application of classification techniques in combination with machine learning was introduced and grew in importance when appropriate computing hardware became available.

First attempts were made by *[Koivo and Kim 1989]* who constructed hierarchical tree classifiers and several linked Causal Auto-Regressive (CAR) models. Bustler, Funck and Brunner *[Bustler et al. 1993]* incorporated a modified Schreier-Sims algorithm to separate clear regions on wood from defects on Douglas-fir veneer. Hierarchical classifiers were applied to red oak boards by Kim and Koivo *[Kim and Koivo 1994].* Further work on classification techniques in colour wood image processing has been carried out by Silven and Kauppinen *[Silven and Kauppinen 1994]* using K-Nearest Neighbour (K-NN) classification, a representative of supervised learning. Iivarinen and Visa *[Iivarinen and Visa 1998]* classified wood defects using a Self Organizing Map (SOM) which is based on unsupervised learning. Heikkonen and Lampinen *[Heikkonen and Lampinen 1999]* experimented with a classification approach on lumber based on supervised Artificial Neural Networks (ANN). Neural networks have been incorporated in grading lumber by *[Gonzaga et al. 1999]* and also by Franca *[França 1996]* who used a neuro-fuzzy approach. Other classifying techniques were Learning Vector Quantization (LVQ) applied to cherry and maple hardwood by Ziadi *[Ziadi et al. 2007]*. Ziadi experimented with feature vectors formed by image tiles directly but faced severe problems with non-converging LVQ-ANNs. A Fuzzy Inference System (FIS) has been applied and studied in the grading of hardwood lumber by Kline *[Kline et al. 2003]* and Xaio *[Xaio 1998]*. The classification of knots on spruce plywood by colour images using a neuro-fuzzy approach based on automatic adaption incorporating backpropagation has been implemented and studied by the researcher itself *[Kuehn 2014].* The most modern classification technique of Support Vector Machines (SVM) for the application in wood processing has been studied and compared to K-NN by Mahram *[Mahram et al. 2012]*.

3.1.4 Features for wood defect classification

Besides favour for a specific classification technique, previously reviewed research on classification techniques and own experience show the crucial point of the classification in wood processing applications. This is the preparation and selection of the features, the feature engineering. Early approaches in the 1980s and 1990s (summarized by *[Szymani and McDonald 1981]*) were limited in computation capacity and lacked appropriate colour imaging devices. Later, shape features and texture features dominated the approaches trying to gain improvements through the proper selection of the features. *[Koivo and Kim 1989]* extracted features using CAR random field models focusing on real visual texture to classify defects on boards of red oak. Koivo *[Kim and Koivo 1994]* focused on rudimentary shapes like circles and lines represented by Freeman's chain code. Iivarinen and Visa *[Iivarinen and Visa 1998]* combined rotation invariant shape descriptors, descriptors of internal structure from the grey level histogram and the co-occurrence matrix (energy, contrast, entropy) of previously segmented image regions to a feature set. *[Gonzaga et al. 1999]* incorporated only two features from first and second order grey-level statistics due to processing-time and -capacity. Smolander, Lampinen and Kohonen *[Smolander et al. 1995]* experimented with a generic feature construction put on top of clustering using SOMs. *[França 1996]* used features derived from histograms of the difference of second order statistics. In a recent texture-based approach *[Mahram et al. 2012]* incorporated Grey Level Co-occurrence Matrix (GLCM) measures and LBPs for texture as well as statistical moments for shape features.

Colour features have been studied since mid/end of the 1990s: *[Alapuranen and Westman 1992]* used colour and shape features on plywood. *[Heikkonen and Lampinen 1999]* experimented with colour features from colour histogram percentiles and the colour histogram shape combined with shape features derived from the responses of a Gabor filter. Silven and Kauppinen *[Silven and Kauppinen 1994]* showed with the help of spectral analysis of wood defects on spruce lumber that colour features classified by a K-Nearest Neighbour (K-NN) classifier outperform both texture and shape features. Kauppinen *[Kauppinen 2000]* later refined the concept retaining the K-NN classifier but identified improving features from the colour image. Kauppinen, Rautio and Silven *[Kauppinen et al. 1999]* as well as Silven, Niskanen and Kauppinen *[Silven et al. 2003]* achieved good defect classification by incorporating colour features in combination with texture measures derived from LBPs.

From then the insight has been spread that colour and texture has to be incorporated for satisfactory classification results in wood processing applications.
Recent approaches are multi-sensorial and therefore mostly incorporate several additional features derived from special imaging techniques as outlined in 3.1.1 and in 3.1.2. *[Xaio 1998]* and *[Kline et al. 2003]* were among the first to incorporate range data, RGB colour and X-ray information in feature based classification.

Principally all (excluding Support Vector Machines) classifiers show performance impacts correlated to rising dimensionality of the feature space. Therefore the selection of the features must be carried out properly, not only in terms of significance and in terms of information content which is contributed by the selected features, but also in terms of a compromise between waiving further information in favour of less complexity and better performance. Ziadi, Ntawiniga and Maldague *[Ziadi et al. 2007]* for example tried to incorporate the pixels from 5x5 three-channel colour image tiles directly as a 75 element sized feature vector. This exceeded the practical limit due to a very long duration of the training of the ANN and therefore he switched to features (peak positions) derived from the colour histogram. When *[Mahram et al. 2012]* incorporated the K-NN with a huge feature space consisting of texture and shape features, they were forced to incorporate Principal Component Analysis (PCA) to transform and reduce the feature space due to the dependency of computation time and feature space dimensionality of this classifier in the training as well as in the classification phase. He found that the same problems apply to neural network approaches (Multi-Layer Perceptron, MLP) which converged very slowly in the training. Recently Mäenpää, Viertola and Pietikäinen *[Mäenpää et al. 2003]* investigated methods for the optimization of combined colour and texture features on beech wood parquet slabs with the aim of feature vector length reduction to keep the computational complexity of the K-NN classifier down. Beam search and genetic algorithms were incorporated to jointly test all features against each other in terms of the resulting classification performance.

3.2 Wood appearance and aesthetics

The research and the industrial systems dealing with automated inspection of wood which were summarized in the previous subchapters address mainly the physical surface defects on wood. This originates from the main concerns of quality assurance at the subsequent

stages of wood processing, e.g. cutting, sawing, and slicing etc. which primarily address the physical stability of the wood product and only to a smaller degree the visual appearance of the wood product. Although wooden panels graded into a high physical quality often show a more pleasant appearance, this is a non-deterministic result of the grading systems which are tuned for the detection of physical defects. Therefore the appearance of panels inside a certain class of physical quality fluctuates strongly. This is problematic when it comes up to produce wooden panels for the production of furniture which should have a consisting good physical and aesthetical quality as well.

From a present-day perspective there exist no known automatic grading systems or prototypes that deal specifically with the aesthetic appearance of wood products. Horrer *[Horrer 2005]* presented an inspection system for the automated visual inspection of the overall aesthetic appearance of natural looking surfaces on laminate flooring, carpet and similar, therefore with known, predictable patterns which he called *"random and pseudo-random surfaces"*. Schmitt *[Schmitt 2006]* addressed the automated inspection problem of local aesthetic defects on ceramic tiles having a random, non-predictable texture. Only little work can be found in the literature that addresses the aesthetic and appearance issues of wood at all. The related research work is reviewed in the following paragraph.

Typical characteristics which are assigned to the wooden material by consumers have been studied by Broman *[Broman 2000]*, Pakarinen and Asikainen *[Pakarinen and Asikainen 2001],* Bow and Bumgardner *[Bowe and Bumgardner 2004]* as wells by Scholz and Decker *[Scholz and Decker 2007]* with the aim to support the designing of wood furniture that meets consumer expectations. The dissertation of Broman *[Broman2000]* addresses the fundamental question if and how it is possible to detect aesthetic defects in an automated manner. Broman introduces the need for a better definition of customer preferences in the whole chain of wood processing from the feedstock to the final product. As an example, in sawmills well established grading rules guarantee a certain level of quality in the sense of minimum and maximum specifications but these do not necessarily meet with certain quality expectations of the customer. Broman's thesis states, that it must be possible to describe, measure and communicate the inherent aesthetic features of wood. Therefore the objective of his work is to understand the preferences of customers to different wood appearances, with the limitation on knotty wood surfaces. Based on questions from a former

qualitative study, interviews incorporating a questionnaire on the presentation of different wooden panels made from Pine were applied in Broman's research. The questionnaire asked for the relevance of a set of attributes like *fresh*, *gaudy*, *beautiful*, etc. With Principle Component Analysis (PCA) loading plots the most important and uncorrelated attributes were isolated by interpreting the impact of the first two principle components. The findings are that there is a clear separation between groups of attributes describing low and high visual "activity" of the surface and between groups standing for *harmony* and *disharmony*. Further investigation shows, that activity and harmony together can define the appreciation: for the involved interviewees high *activity* combined with *disharmony* resulted in bad acceptance while both high *activity* and *harmony* gave the best results in terms of acceptance. The author concludes that it is possible to identify measurable aesthetic features that describe preferences. A similar study has been carried out by Jansson *[Jonsson 2008]* investigating how wood as a material is perceived and characterized in relation to alternative wood-based materials such as panels and wood-based composites. Nordvik, Schütte and Broman *[Nordvik et al. 2009]* examined the relationship between visualization of appearance properties of wood flooring and people's impressions of this flooring for the reason to understand how computer visualization in the process of product design can be efficiently used.

Rice *[Rice et al. 2006]* tried to determine the types of environments appearance wood products can create and to gauge whether or not these types could have positive impacts on people's emotional states.

To clarify the level and variation of selected properties influencing the visual impression of Scots pine wood Riekkinen *[Riekkinen 2004]* investigated trees from 60 stands and from different ages generating statistics on colour variations, stem defects, knot types and knot count and generated suggestions for the best use of the specific raw wood material.

Other studies mainly dealt with colour as the most important feature for the perception of wood. Nakamura, Masuda and Inagaki *[Nakamura et al. 1993]* found that colour variations and pattern anisotropy are the most important visual factors that create the typical visual impressions of wood, but focused on the colour (variations) that influence the appearance in terms of warm and cold. Vetter, Coradin, Martino and Camargos *[Vetter et al. 1990]* studied the possibility to use a numerical colour description to compare the appearance of wood products and investigated the practicability of different colour systems based on comparison

samples (e.g. Munsell colour system) and colorimeters (DIN[6] colour system). His conclusions are that the measure is simply not precise enough and the large amount of variables (illumination type, angle of view, surface gloss) does not allow for objective comparison. In a newer attempt to use colorimetry Janin *[Janin et al. 2001]* characterized several different wood types with the *CIE-Lab* colour system but did not gain new insight compared to Vetter.

Not directly linked to the inspection of appearance properties of wood but in principle on appearance characteristics influenced by external parameters, Grekin and his colleagues *[Grekin et al. 2005]* investigated the change of perceived colour on Nordic pine in terms of colour distance metrics[7] measured in a perceptionally uniform colour space[8]. For wood from Nordic pine a remarkable increase in redness and yellowness was found when exposed to ultra-violet (UV) radiation on long-term, dependent on the origin of the wood in terms of latitude as well as height of the tree. His findings are aimed to control the homogeneity of floorings, panelling, and pieces of furniture. The effect of UV radiation on the visual colour properties of Nordic pine wood has also been investigated by Hautamäki *[Hautamäki et al. 2010]* for the reason to identify the time period of irradiation needed until no further colour change occurs and the product is "visually stable".
Kansai Engineering and Affective Engineering *[Nagamachi 2010]* aim at translating the customer's feelings and attitude towards a product's appearance into parameters in the product domain. Adopting these new disciplines *[Yali and Kui 2008]* calculated colour and texture features from wood images that can be mapped to an emotional feature space by using senses like *gorgeous*, *luxury*, *simple* and *beautiful.*

It can be summarized that since the 1980s the problem of how to describe the wood's appearance incorporating colour is not solved satisfactorily as all attempts mentioned above restrict to the extraction of one global colour from something that is a mixture of colour variations and structural elements (in terms of image processing a "colour texture"). An average colour can therefore only be viewed as a very rough estimate for perceived appearance. Other research, e.g. by Massen, Eberhardt and Asal *[Massen et al. 2008]* showed that the human visual system perceives "colour of wood" as a combination of colour

[6] Deutsche Industrie Norm (German Industry Norm)
[7] $\Delta E*$
[8] *CIE-L*a*b**

statistics (3D colour histogram) and spatial frequencies of the imaged wood with a surprising coupling of both parameters.

3.3 Automated physical rectification of wood based products

The wood processing industry is familiar with a number of different techniques to cope with defective regions in the feedstock of primary wood processing. It is common, for example, to define cross cut sections in the production of lamellas or veneer to remove the defective area and incorporate jointing techniques (e.g. Dovetail Joint, Scarf Joint or Finger Joint) to combine the non-defective parts again. Other common techniques have been summarized in chapter 2.3 *Methods of patching wooden panels* and include dowel insertion after drilling out defective knots, cracks and resin pockets in the wooden panel production and filling holes and cracks with putty[9]. The decisions which defect to cut out or to repair, which repair method to use and finally the execution of the repair work are nowadays mostly manual labour.

Automated visual inspection used for grading of raw wood lamellas is able to automatically define cross cut sections, often in conjunction with length optimization to maximize profit. This has first been proposed and been demonstrated by Rönnqvist and Astrand *[Rönnqvist and Astrand 1998]* in the production of lumber. In the meanwhile it is state of the art to have chop saws controlled by machine vision systems in real-time as offered automation solutions show, for example by ATB-Technology[10], Weinig[11], Luxscan[12] for lumber and automation solutions offered for veneer, for example by Mecano[13].

Instead of removing defective areas, which always results in a loss due to waste, the patching of defects with dowels or putty is practicable with several wood products, for instance with plywood panels, multilayer panels and solid wood boards. There exist machine vision controlled systems from Argus[14] and Mecano that automatically fill cracks, holes and manually drilled-out defective regions on plywood panels with putty or poly patch. For thin plywood veneer a solution is offered by Raute[15] and Mecano that inserts plywood patches in a single-step process by stamping-out and stamping-in. As most of the automatic visual

[9] Filler used by carpenter (wood putty, paste wood filler)
[10] atb-technology.de
[11] weinig.com
[12] luxscan.lu
[13] mecanogroup.com
[14] argossolutions.no
[15] raute.com

inspection systems are developed by industry in terms of products the number of publications with focus on the methods and algorithms used is highly limited due to confidentiality purposes. A generic interface for the transfer of patching data able to address the patching with putty including pre-processing with routing tools has been studied and developed by Michael Göttlicher *[Göttlicher 2011]* in his diploma thesis under the author's supervision. The author, respectively the employing company *[Massen, Kuehn and Eberhardt 2010]* were the first who presented the concept and preliminary results of automated patching. No system with automated dowel insertion based on automated visual inspection has been known so far.

3.4 Automated aesthetical rectification of wood based products

From a present-day perspective there exist no comprehensive automatic patching systems or prototypes that deal with the aesthetic appearance of wood products and the aesthetic properties of a possible (physical) patching solution on wood products. Kurdthongmee *[Kurdthongmee 2008]* proposed matching techniques to automatically group high-quality rubberwood boards of comparable colour and shade for homogenous looking finger joints. Seidel *[Seidel 2010]* investigated the possibilities of synthetic patch generation for the application via ink-jet printing on physically rectified defects of wood surfaces by incorporating image processing techniques to generate colour and texture patterns from the surrounding sound wood with the aim to camouflage the repaired area. The author of this thesis, respectively the employing company *[Massen, Kuehn and Eberhardt 2009], [Eberhardt, Massen and Kuehn 2011]* were the first who presented a concept for automated physical and aesthetic patching using liquid and solid fillers to the wood-working industry.

3.5 Summary of review

In this chapter it is shown that many approaches to apply machine vision systems to the inspection of wood have been proposed by researchers in the past 25 years. Most of them utilize a single sensor setup and the related research focused on the extraction of information in terms of colour, shape and texture features for the further processing. A line of development from single sensor greyscale imaging to colour imaging to multi-channel imaging can be identified and with rising processing capabilities classification methods become real-time capable and therefore become interesting for industrial wood-processing

application. Nevertheless in the task of automated inspection of wood there is obviously still unused potential with respect to the incorporation of multiple imaging sensors and in terms of the improvement of the related sensor data fusion. It has further been shown, that the most crucial part of setting up a classification system is the proper selection of the features to be used, demanding a high level of expert knowledge as well as a high level of experience with classification while finding a suitable classifier configuration through trial and error, especially when incorporating neural networks.

It can be concluded from present research and knowledge that it is advantageous to incorporate as much information from visual sensors as possible to establish a profound data basis for the subsequent processing in defect detection and evaluation. This raises demands not only to the selection of features but also to their processing as the underlying classification problems are non-linear by a majority, limiting the number of usable algorithms. Besides algorithmic aspects the controllability of an automated system for detection and further for rectification is seen to be crucial, especially when vague, ambiguous expectations, as with aesthetic issues for example, need to be fulfilled.

In the following chapters the methods and the overall concept for an automated defect detection and rectification system for wooden panels are presented bearing in mind the findings from previous research. The focus is hereby on the learning from examples and the decision-making by incorporating rules formulated preferably in human language to address the stated expectations. Having covered the overall system design, the development and the outcome of testing the overall interaction of the components is summarized and the performance of the scanner system for automated defect detection and defect rectification is analyzed.

4 Research Methods

This chapter presents the methods incorporated in the design experiments towards the optimal solution for a scanner system usable for automated patching. Design drivers are the objectives:

a) to achieve defect detection incorporating the aesthetic appearance and perception of defects (local aesthetics) as well as
b) to satisfy the identified necessity to model human wood-working expert knowledge for the generation of patching instructions also under aesthetic aspects.

Therefore two major components are addressed by the research methods. That is:

A) the classification of the defects being able to incorporate aesthetic judgements in the classification process and
B) an expert system that is able to generate patching instructions incorporating rules derived from wood-working practice which can be easily adapted under various aspects including economic, ecologic and aesthetics criteria.

Due to the industry-driven nature of the research project not all possible alternatives can be evaluated and compared. Nevertheless, in the following sections a profound assessment based on theoretical background knowledge is used in the argumentation for the choice of methods.

4.1 Classification of defects under local aesthetic aspects

The classification of defects is a demanding task as has already been shown in chapter 2 by summarizing possible defects on wooden panels and in chapter 3 by summarizing the research related to automated detection of defects on wooden panels. The huge variety of the defects on natural surfaces requires a good generalisation capability to solve the task of discrimination between different defect types, e.g. dark knots, ringed knots and knots with bark (refer to Table 4-1 and also to chapter 2 *Defect types on wooden panels*) that are often hard to separate even for human experts.

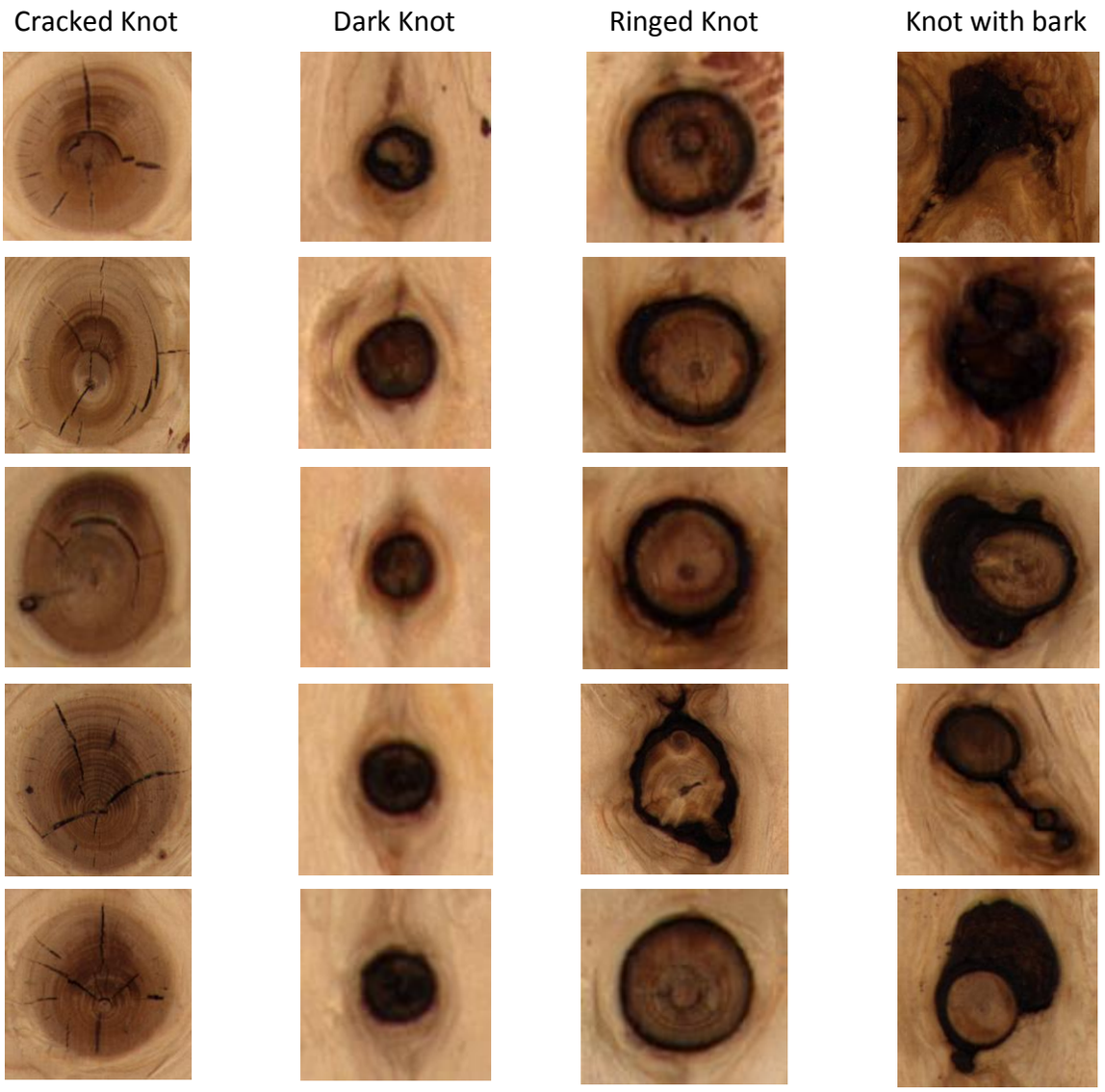

Table 4-1: Examples of four different defective knot types from plywood of spruce.

Table 4-1 gives examples for four common defect knot types on spruce plywood panels showing the quite huge variance of defects in one class (columns) on the one hand and the similarity of some of the different knot defect types on the other hand (e.g. Ringed Knot and knot with bark). Using examples of Dark Knot, Ringed Knot and knot with bark, from Figure 4-1 to Figure 4-3 one can see the complexity in discrimination between these knot defect types.

Figure 4-1: Dark knot.

Figure 4-2: Ringed knot.

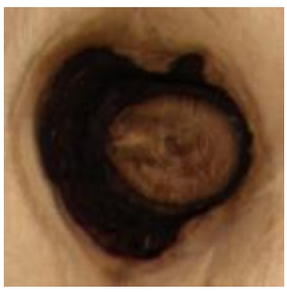

Figure 4-3: Knot with bark.

The Dark Knot (Figure 4-1) and the Ringed Knot (Figure 4-2) both show a ring-shaped boundary but the dark knot is more irregular and slightly darker in the overall area of the circular object. The intensity distribution between the object's edge and its inner area is therefore a potential characteristic (feature) for discrimination between these two defect types besides the presence of the typical ring. The ring itself is ambiguous for knots with bark (Figure 4-3) only when the amount of bark extends as can be seen from Figure 4-3.

A typical formulation of a guideline for explicit feature-based discrimination of the four knot defect types from Table 4-1 is given in Table 4-2.

Cracked Knot	**Dark Knot**	**Ringed Knot**	**Knot with bark**
1. accumulation of dark fragments is possible with radial projection 2. minor amount of dark fragments is given (cumulative, by histogram) 3. dark fragments are elongated and star-like 4. gradient image of outer contour is evenly distributed 5. outer contour is compact and elliptical 6. minimal diameter can be applied	1. homogeneously dark 2. gradient image of outer contour is evenly distributed 3. dark fragments are rounded, ring-shaped and located at the transition to sound wood 4. minimal diameter can be applied	1. inwards and outwards gradients can be found 2. dark fragments are rounded, ring-shaped and located at the transition of sound-wood to knot 3. gradient image of outer contour is evenly distributed 4. outer contour is compact and elliptical 5. minimal diameter can be applied	1. gradient image is not evenly distributed 2. dark fragments spread over complete area of interest 3. dark fragments are not rounded or elliptical

Table 4-2: Example of typical feature-based discrimination between different knot defect types.

Features like

- Colour
- Elongated shape
- Soft/sharp gradient
- Compact / elliptical
- Ring-shaped ….

can be identified which need to be substituted with a numerical representation and linked by logic operations in an automated process. This is where complexity is raised, first by calculating these numerical representations involving several sets of parameters for each algorithm and second by managing them, e.g. in terms of upper and lower limits in conditional programming (*if … else … then*).

Incorporating the need to additionally judge on the basis of appearance characteristics, e.g. “acceptable looking dark knot” vs. “unattractive looking dark knot”, as exemplarily shown in Figure 4-4 and Figure 4-5, finally requires an alternative approach. This is due to the fact that the aesthetic characteristics are hard to describe by numerical features in an approach based on selected features which need to be explicitly derived from image data.

Figure 4-4: Acceptable looking dark knot.

Figure 4-5: Unattractive looking dark knot.

In the image examples shown above (Figure 4-4 & Figure 4-5) symmetry seems to play an important role but the onion-shaped, darkened grain in Figure 4-5 may also contribute to rejection. The contributing characteristics must be carefully identified by questioning but often they are very specific to a certain example. Many other examples involving different characteristics therefore can be found so that the possible bandwidth of characteristics is evidently high and their logical combination is complex. Further the maintenance of the resulting parameter sets involved in an approach explicitly identifying and calculating these characteristics becomes nearly unmanageable.

As (colour) images of defects are sufficient for humans to make judgements concerning the aesthetics, the information content of the images is assumed to be principally sufficient[16]. Modelling the human perception as well as the (personal) aesthetic preference by an

[16] Human perception of images may additionally rely on previous experience with real wood as well as on haptics which are linked to the visual perceived information of the images.

algorithm therefore implies to find a principle for evaluating this information. If an algorithm/principle can be identified that is computationally efficient, the unreduced image data itself and therefore all available information could be used for learning from examples instead of first abstracting the information by calculating and selecting a limited set of features. The following requirements can therefore be defined for such a classification principle:

- Ability to generalize from learning examples, ideally from images
- Ability to extract relevant information (features) by itself
- Ability to deal with huge information content (feature space dimensionality) needed for aesthetic evaluation
- Ability to deal with huge sets of training samples to cover the full bandwidth of defects on natural surfaces
- Ability to handle noise in the training data
- Ability to deal with non-linear classification/separation problems
- Computational efficiency despite high feature space dimensionality and huge training sets

The use of various classification methods in defect detection on wood has already been summarized in chapter 3. Popular methods like K-Nearest Neighbour (K-NN) and Artificial Neural Networks (ANN) are not able to fulfil the above stated requirements: K-NN classification for example is a representative of lazy learning due the absence of abstraction (e.g. calculation of class centres) and does not rely on a model of the underlying data *[Dasarathy 1991]*. ANNs are able to deal with non-linear classification problems and are able to generalize by abstracting the input data but suffer from possible overfitting and ambiguous solutions in the training stage due to several possible local minima of the error function *[Smith 1997].* In the training stage of ANNs the computation of the partial differentiations is a drawback with huge training data sets. In the online application nevertheless, the simple nature of the backpropagation algorithm, incorporating only connections to the neighboured nodes predestine ANNs for the implementation on parallel computing architectures *[Friedman et al. 2003]*. The popular Self Organizing Maps (SOM) used in several applications of wood defect detection (summarized in chapter 3) are able to

generalize, are very noise tolerant and allow very good user interaction due to the reduction of the problem dimensionality but are computational inefficient with high-dimensional feature spaces and huge training sets. Furthermore SOMs do not create class boundaries but just group samples by similarity. Support Vector Machines (SVM) overcome the mentioned disadvantages of K-NN, ANN and SOM, but leave the issues with creation and handling (labelling) of the training data set unaddressed. A comparison of methods according to the initially stated requirements for the classification of defects on wooden panels incorporating aesthetics aspects is given in Table 4-3:

	Abstraction & generalization	High feature space dimensionality	Dealing with noise	Huge sets of training samples	Non-linear classification	Computational efficiency	Comment
K-NN	none	bad	good (large values of *K*)	bad (memory)	yes	proportionally decreasing with amount of training samples	easy implementation
ANN	high	problematic	problematic	bad (convergence)	yes	problematic	local minima lead to ambiguity
SOM	good	problematic	good	bad	yes	good	mapping of complex problems to planar representation
SVM	high	very good	good	good	yes	good	convex optimization problem with single, optimum solution

Table 4-3: Summary and comparison of potential classification methods according to requirements stated for defect detection on wooden panels including aesthetic aspects.

Colour coding for principle performance evaluation of classification methods:							
	good		problematic		bad		neutral/comment

Combining methods to complement each other is a logical conclusion and will be subject of the proposed cascaded classificatory system training presented in the following sections.

4.1.1 Combined unsupervised and supervised learning

Classification and clustering, respectively supervised and unsupervised learning have already been addressed in the review of classification techniques for defect detection in chapter 3. The major difference of the two machine learning models is once more illustrated in Figure 4-6 and Figure 4-7, highlighting the fact that the number as well as the prototypes of the

classes (defect types) involved are already known in supervised learning and are estimated by the algorithm itself in unsupervised learning.

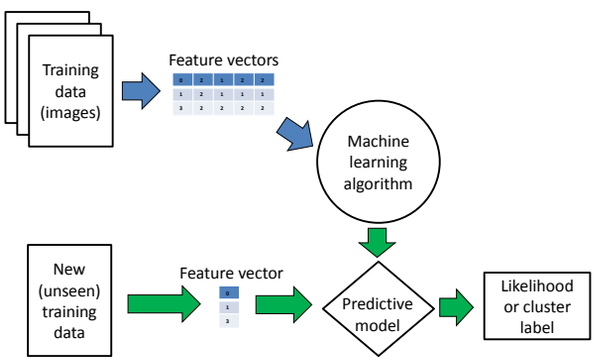

Figure 4-6: Unsupervised learning model.

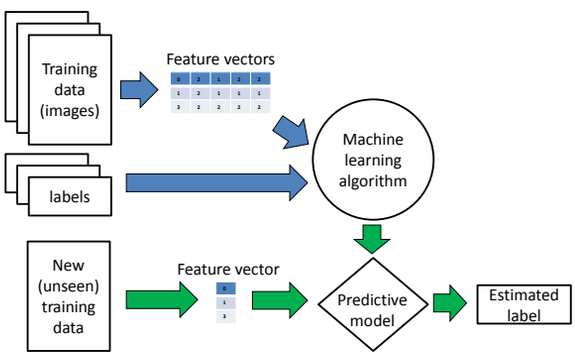

Figure 4-7: Supervised learning model.

A combination of unsupervised (e.g. SOM) and supervised learning (e.g. SVM) is proposed in a cascaded approach: The unsupervised learning is then a promising attempt to support the expert in sorting and labelling the gathered training data (images of defect types, e.g. different knots) by identifying clusters, thereby preparing the input for the supervised learning. This approach to cascaded classificatory system training will be addressed in detail when the classification system of the scanner for an automated rectification system is presented in chapter 5. In this chapter the most promising representatives from each learning principle are identified and reviewed in detail to support their choice in a cascaded training for the application on multi-dimensional image data of wood defects, based on the initially stated requirements.

4.1.2 SOM – Self Organizing Map

A representative of unsupervised learning is the Self-Organizing Map (SOM). Also called *Kohohen-Map* referring to its Finnish inventor Teuvo Kohohen *[Kohonen 2000],* this algorithm has been used and studied extensively in the area of machine vision for wood processing. This is most likely because of the relationship of the strong Finnish research group in that field at the Universities of Oulu and Turku *[Iivarinen and Visa 1998], [Kauppinen et al. 1999], [Silven et al. 2003]* but also due to its great capability of visualizing complex classification problems.

In contrast to the K-Nearest Neighbour algorithm *[Dasarathy 1991]* for example, the SOM incorporates abstraction capability in the training phase. The goal of learning is to create a map that responds with similar outputs to similar inputs. Kohonen's intention was to model

the processing of (visual) sensory data in the cerebral cortex of the human brain *[Kohonen 1989]*. The output of a SOM is a mapping of complex multi-dimensional data to a low-dimensional (usually two dimensions) representation with similar samples grouped together. The strength of the SOM is therefore its visualization capability of class distributions with underlying high-dimensional feature spaces. It is important to understand that therefore a SOM does not produce automatically a trained classifier with self-identified clusters but that user input is necessary after the adaption to define the boundaries and allocate class labels in the adapted (grouped) low-dimensional representation of the data. The grouping by similarity in a plane is very well suited to machine vision applications, as the images (tiles) from which the feature vectors have been extracted can be directly related to each other. Figure 4-8 gives an example of a trained SOM on images of knots from softwood lumber using colour and texture features including boundaries for several classes:

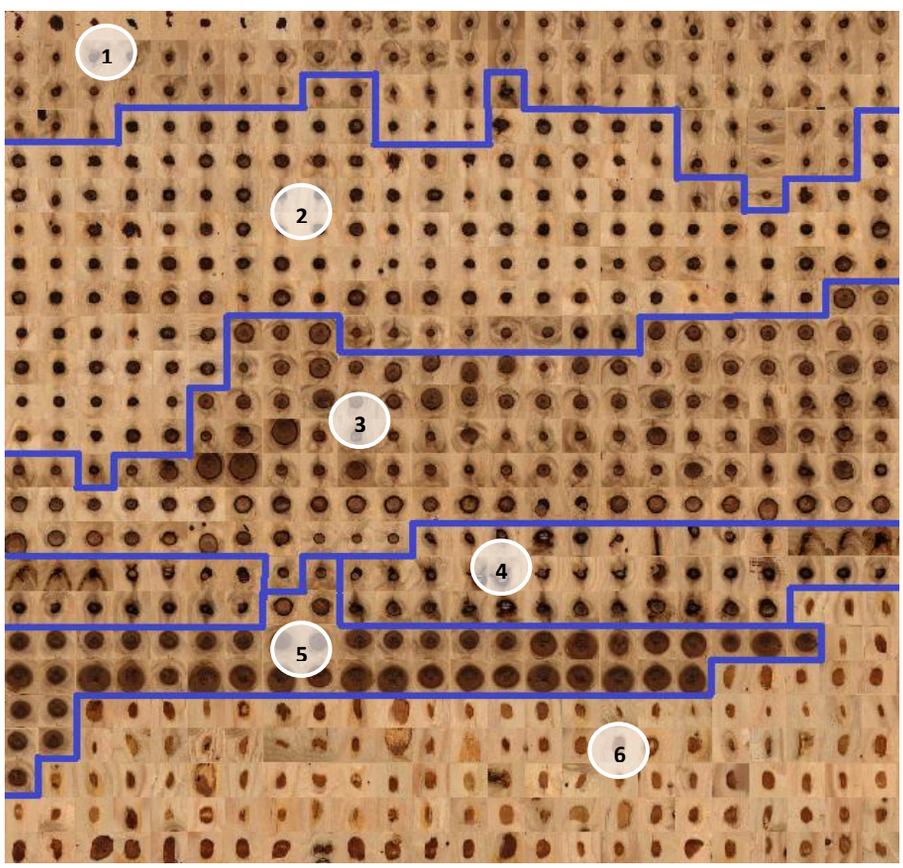

Figure 4-8: SOM clustering of image tiles. The map organizes the samples in terms of similarity. Blue lines indicate class boundaries in terms of similarity to cluster centres.

The example uses image tiles from a segmenting approach[17] and feature sets containing colour and texture features. The result is a sorted representation of the corresponding image tiles with dark knots at the top (1), knots with bark (2), ringed knots (3), bark (4), sound knots (5) and resin pockets (6) at the bottom of the map.

The function principle of the SOM is reviewed in detail in Appendix A.1. By weighting a neutral initialized map of nodes representing samples from the training, a Best Matching Unit (BMU) is found for each of the estimated classes and iteratively refined by bending the mesh, therefore achieving the grouping by similarity.

4.1.2.1 Discussion of SOM

Feature selection and reduction of feature space dimensionality are key points when incorporating this classification algorithm. Finding appropriate feature sets improves the result of the mapping to a representation with lower dimensionality. In contrary, when inappropriate data is presented in the training stage, similar prototypes might be placed in different regions of the map. Therefore the feature selection has to be carried out carefully and techniques like Singular Value Decomposition (SVD) and Principle Component Analyis (PCA) should be incorporated to evaluate and prepare the feature space. SOMs incorporating adequate neighbourhoods are very noise-tolerant as the neighbourhood function acts as a model for the noise distribution *[Yin 2008]* with the SOM itself modelling the distribution of the (noisy) samples. Unfortunately every SOM is different and finds different similarities in the data. Therefore several maps have to be trained, compared and evaluated by an expert in order to get one good final map. The good visualization capabilities of the SOM incorporating Unified Distance Matrices (U-Matrices) showing the distances of the weight vectors of adjacent nodes make it easy to identify distorted maps. Kohonen *[Kohonen 1989]* proposed the utilization of error metrics like the Quantization Error computing the average distance of input feature vectors to the BMU's vector or the Topographic Error checking for all input vectors if the BMU and second BMU are adjacent in the lattice. Computational complexity is a drawback since as the dimension of the data increases the processing time increases (refer to Formula A-1). The more neighbours are used, the better is the similarity of the resulting map to the input data, but the number of distances to be calculated increases exponentially (refer to Formula A-2). Nevertheless real-

[17] Segmenting approach: The input image is not equally subdivided into tiles (possibly fragmenting objects) but areas of interest are defined around objects

time capability has been proven by Kauppinen *[Kauppinen 1999]* and Niskanen *[Niskanen et al. 2002]*.

The necessity to use selected, limited feature sets does not allow to satisfactorily model local aesthetics incorporated in wood defect detection when using SOMs. This is on the one hand due to the difficulty of extracting aesthetics to single numerical values and on the other hand due to the limited computational performance with higher dimensional feature spaces containing sufficient information to model local aesthetics. But self-organizing maps have been found to be very effective in the learning stage of a superimposed supervised classification task where the accuracy requirement is lower than in the actual defect detection and computational performance is not constrained to online-requirements. In the offline pre-sorting of huge amounts of sample image tiles needing assignment of class labels (e.g. knot types) by a wood processing expert, the SOM is perfectly suited to generate a two-dimensional sorted representation of the image tiles. This leaves only the definition of class labels and the (graphical) correction of outliers (adjustment of blue line in Figure 4-8) for the expert.

4.1.3 SVM- Support Vector Machine

Support Vector Machines define systems for training linear learning machines on non-linear classification problems, incorporating kernel-induced feature spaces and generalisation theory as well as optimisation theory. The derived algorithms as well as their possible implementations are extremely efficient and with some restrictions the underlying optimization problem on the error function is convex, thus having no local minima which means that the best solution is guaranteed to be found. This is promising for the complex task of wood defect classification under aesthetic aspects as no restrictions in terms of dimensionality-limited feature spaces are imposed, neither from the computational performance point of view nor from the learning convergence point of view.

A SVM is actually a linear classification algorithm constructing a line between two sets of points for the separation of these two sets. In 1995 Cortes and Vapnik *[Cortes and Vapnik 1995]* presented an extended algorithm incorporating non-linear functions (so-called kernels) for mapping all the (linearly not separable) points from the input space into a transformed space where the SVM can then be applied (Figure 4-9). This is based on Cover's theorem *[Cover 1965]* which states that the probability of a classification problem to be

linearly solvable raises with the dimensionality of the underlying feature space and that it is therefore possible to find a mapping function that produces a higher-dimensional (even infinite dimensional) linearly separable, transformed feature space. The aim of the SVM classification is therefore to develop a computationally efficient and performant learning which allows separating a very high dimensional feature space with the use of hyperplanes providing the capability to generalise from the learning data and additionally being able to deal with training sets in the range of several hundred thousand samples. This is where advanced optimization theory and generalisation theory has successfully been incorporated.

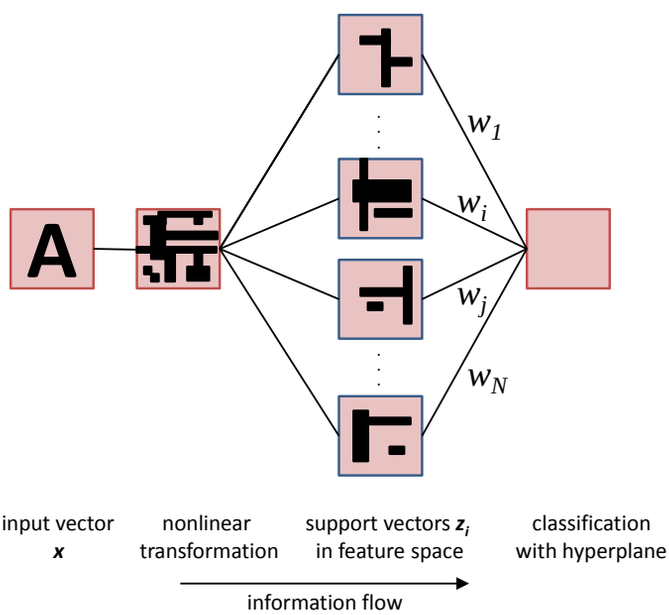

Figure 4-9: Principle of SVM-training in analogy to two-layer perceptron: Transformation of input vector (symbolized by character 'A') to a higher dimensional feature space via nonlinear function, construction of optimal hyperplane by finding support vectors, classification according to position relative to hyperplane.

Therefore the most obvious difference to other classification algorithms is the intended increase of the feature space's dimensionality in contrast to the reduction of the feature space used to control computational complexity in classical approaches. In combination with the mathematically proven existence of a single solution due to convex optimization, the need to focus the selection and reduction of features has been eliminated principally. Of course a good set of features containing all relevant information and no redundant information is still the best basis for classification and may accelerate the learning process. But as will be proposed in the following chapter, the image data itself can be sequentially seen as a feature vector in a high-dimensional feature space (rows * columns * layers) and therefore can be used for classification directly containing the maximum information

content. With SVMs this becomes practical due to their computational efficiency using the so-called Kernel-Trick *[Cristianini and Taylor 2004]*. Besides being able to deal with high-dimensional feature spaces, SVMs are optimized to handle huge sets of training data as well. By identifying and using only the strongest learning examples in the feature set, the so-called Support Vectors, the actual online computation is kept manageable.

Based on the maximum margin strategy applied on a linear learning machine the theoretical background of SVM classification is briefly reviewed in Appendix A.2. The advantageous characteristics of SVMs (good computational performance, capability of handling high-dimensional feature sets and large training sets, guaranteed unambiguous convergence) are used to supplement the decision towards this classification technique among others (K-NN[18], ANN[19], etc) in wood defect classification. For the correct parameterization of the classifier in its application in wood defect detection on wooden panels it is further important to appreciate the underlying principles and therefore the influences of the parameters.

4.1.3.1 A geometrical interpretation of SVM margins

Having the simplified definition of convexity given in Appendix A.2.1 in mind, this paragraph uses a geometrical interpretation of SVMs to support the understanding of the intention to incorporate mathematics drawn from various areas such as (mathematical) optimization theory and generalisation theory. The geometrical interpretation is advantageous over sound theory at this point as only the principle understanding of SVMs for the argumentation as the most appropriate classification algorithm being able to handle the complexity of an aesthetic judgement on wood defect types is necessary. Profound insight into the involved theories itself and into the SVM implementation principles including convex optimization based on convex problems, derivation of the Support Vectors and application of noise-tolerance using soft-margins, is given in Appendices A.2.1 – A.2.3.

A geometric interpretation of a convex problem is a set where every point in the set can be seen by every other point from the set, that is a virtual line exists between these points fully lying in the set which is given for the points on the convex hull.

[18] K-Nearest Neighbour algorithm
[19] Artificial Neural Network

The convex hull for a given set X in l-dimensional space

$$X = \{x_i, i = 1,2, \dots, N, x_i \in R^l\}$$

is defined as:

$$\boldsymbol{conv}X = \left\{ \begin{array}{c} y: y \sum_{i=1}^{N} \lambda_i x_i, x \in X \\ \sum_{i=1}^{N} \lambda_i = 1, \quad 0 \leq \lambda_i \leq 1 \\ i = 1,2, \dots, N \end{array} \right\}$$

Formula 4-1: Definition of convex hull on set of points (e.g. training data set).

having therefore as elements all the convex combinations of the elements in X.

Assuming a two-class, linearly separable distribution in X, consisting of the classes ω_1 and ω_2 and corresponding subsets X^+ and X^-, the (training) set X is the union $X = X^+ \cup X^-$. The following optimization problem can be formulated on the basis that a point in the convex hull of a subset is a convex combination of all the points in the subset and therefore the closest point/distance between the two convex hulls $\boldsymbol{conv}X^+$ and $\boldsymbol{conv}X^-$ has to be found:

minimise$_\lambda$	$\left\| \sum_{i:y=1} \lambda_i x_i - \sum_{i:y=-1} \lambda_i x_i \right\|^2$	objective function
subject to	$\sum_{i=1} \lambda_i = 1, \sum_{i=-1} \lambda_i = 1, \quad \lambda_i \geq 0$ $i = 1,2, \dots, N$	constraints for convexity

Formula 4-2: Geometrical interpretation of margin optimization problem based on convex hulls of two data sets.

By reshaping *[Theodoridis and Mavroforakis 2007]* Formula 4-2 and the associated constraints, one can achieve the following equivalent formulation of the optimization problem stated:

minimise	$\sum_{i,j} y_i y_j \lambda_i \lambda_j x_i^T \, x_j$	objective function
subject to	$\sum_{i=1}^{N} y_i \lambda_i = 0, \sum_{i=-1}^{N} \lambda_i = 2, \quad \lambda_i \geq 0$ $i, j = 1,2, \dots, N$	constraints

Formula 4-3: Formulation of margin optimization problem based on convex hulls of two data sets.

A solution to this problem (Formula 4-3) is equivalent to finding the nearest points between the convex hulls of two data sets. The formulation given by Formula 4-3 is identical to the formulation derived by pure optimization theory (refer to Appendix A.1) and serves at this point as a mathematical formulation of the geometrical interpretation of the SVM-hyperplane which is illustrated in graphical illustration in Figure 4-10:

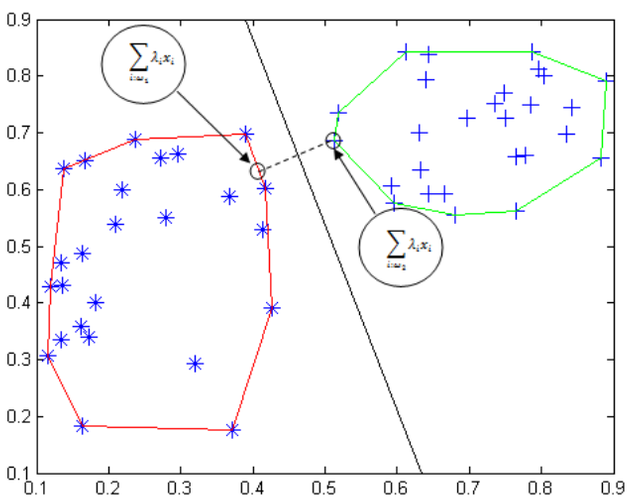

Figure 4-10: Geometrical interpretation of SVM classifier. Example of training set with linear separable classes ω_1 and ω_2. For each class the convex hull is shown. The hyperplane classifier is perpendicular to the line between the closest points of the two convex hulls.

Interpreting Figure 4-10 and having in mind that a point on the convex hull of a (training) set is a convex combination of all the points in the set, it can be understood that is necessary to only incorporate the points lying on the convex hull, which are the so-called Support Vectors. Using this principle allows to deal with huge (training) data sets as the amount of training samples does not explicitly influence the computational complexity of classification with only the Support Vectors.

The concept of a kernel induced feature space to address non-linear classification problems and the concept of soft margins to achieve generalisation and tolerance of outliers in training are discussed in detail in the appendices 1.1A.2.2 and 1.1A.2.3.

4.1.3.2 Discussion of Support Vector Machines

Support Vector Machines overcome most of the problems identified with other classification techniques and theoretically fulfil the requirements stated initially in this chapter for the intended application to defect classification on wooden panels including judgement on local aesthetics. The development of SVMs has been opposite to their most interesting counterpart, the Artificial Neural Network (ANN) (comparing only model-based supervised learning techniques so far). While the ANN has been developed by implementation and experimentation over quite a long time and theoretical studying has guided this work, the SVM evolved from sound theories and has then been brought to practical implementation. Unlike the other classification techniques the usage of SVMs is not required to control the model complexity via keeping the feature space dimensionality low. This eliminates the needs for feature selection and feature space transformation aiming at redundancy elimination and dimension reduction which is seen to be crucial for the needed information content in the judgement on local aesthetics of wood defects. As the kernel induced feature space can theoretically (due to implicit mapping) get infinite in dimension, no restriction on the number of features exist, therefore eliminating the process of feature extraction, which is fundamental in all conventional approaches, allowing theoretically the input of raw pixel data as input itself instead of deriving features from it. The parameterisation of SVMs, compared to ANNs is much simplified as no network architecture (number of hidden layers, number of neurons in the hidden layer(s)) has to be evaluated due to the fact, that the SVM selects its model size automatically in terms of the support vectors.

The soft-margin extension introduces a regularization parameter *C* (toleration of noise, generalisation capability) that has to be found empirically. The capability to tolerate noisy samples due to wrong labelling and due to the involved uncertainty is seen very valuable as faultless labelling cannot be guaranteed. Often finding the boundaries between the classes is challenging for the human expert as well, refer to examples initially given with the different knot defect types in Table 4-1 as well as to the pre-sorted planar representation of knot images in Figure 4-8. Finding the best value for C via testing and cross validation is a straight forward task not necessarily asking for expert knowledge and being automatable, also in

terms of future extension and adaption of the classifying system (e.g. adaption to other wood types, additional defect types, etc.). Finally the limitation of the hyperplane-based classifier to be able to separate only two classes can be efficiently solved by incorporating an appropriate number of SVMs in hierarchical order. Multiclass classification with SVMs has been outlined by Mayoraz and Alpaydin *[Mayoraz and Alpaydin 1999]* and Patt *[Platt et al. 2000]* for example. Standard kernels are based on either polynomial or radial basis (Gaussian kernel) functions. The use of more sophisticated kernels tailored to the structure of the underlying (training) data is largely unexplored and likely to deliver further improved results. The design of such kernels opens another field of research by itself.

4.2 Decision making for patching under appearance aspects

Based on the results of defect detection and defect classification, systems automating the rectification of panels respectively their defects must be able to generate instructions for the tools carrying out the actual patching. Generating these instruction must be done according to the patching rules incorporated within either the company (refer to chapter 2.2.3 *Quality standards*) or with the product (refer to chapter 2.3.2 *Investigation into manual processes*)

The patching instructions therefore are depending on

- A certain proprietary interface to available machinery and tools for certain patching technologies
- The guidelines, norms and instructions valid in a wood working facility
- The implicit knowledge of a wood worker carrying out the repair in a manual process

Therefore a decision-making process can be identified which requires reasoning and knowledge. This is per se the definition of an Expert System *[Jackson 1998]*.

The incorporated rules may rely on findings summarized in chapter 3.1 *Wood appearance and aesthetics* when aesthetic aspects are involved. With reference to Table 2-1 a formulation of the rules addressing the aesthetics of the overall panel can be exemplarily stated according to norm ISO 2426-3-2000 defining the appearance classes **E, I & II** for plywood made from softwood by using *if…then…else* formulations (conditional language):

Exemplary formulation of rule for ISO appearance class E:

IF amount of pin knots[20] *AND* amount of sound knots *AND* amount of unsound knots *AND* amount of loose knots *AND* amount of knot holes *AND* amount of cracks (open & closed) is near to zero *AND* there exist no resin pockets *AND* there exists no bark *AND* there is very little irregularity in wood structure *AND* there is very little discoloration *AND* there is no fungal decoy *THEN* the appearance class of the panel is **E**.

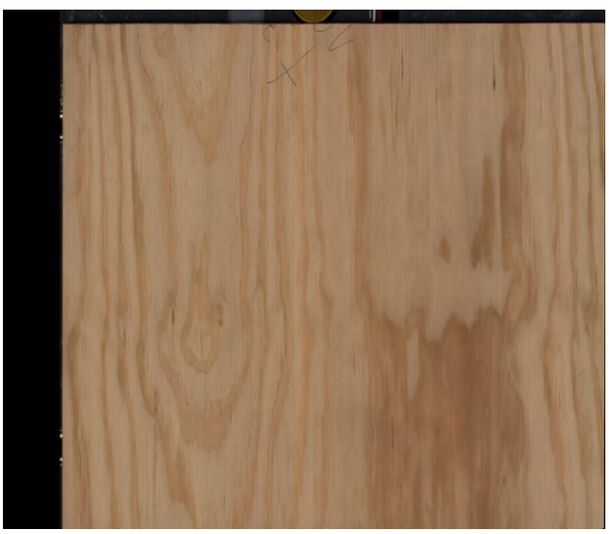

Figure 4-11: Example of plywood panel (spruce) satisfying ISO 2426-3-2000 appearance class E. (image represents approx. 1m^2).

Pin Knots	0
Sound knots	0
Unsound knots	0
Loose knots / knotholes	0
Cracks	0
Resin pockets	0
Irregular wood structure	none
Discoloration	none
Fungal decay	none

Exemplary formulation of rule for ISO appearance class I:

IF amount of pin knots is below 3/m^2 *AND* there are no sound knots with diameter exceeding 15mm OR 30mm/m^2 cumulated *AND* amount of loose knots, unsound knots or knot holes with 6mm in diameter maximum is not exceeding 2/m^2 *AND* amount of cracks (open & closed) having up to 3mm length maximum is not exceeding 3 per meter *AND* there exist no resin pockets *AND* there exists no bark *AND* there is very slight irregularity in wood structure *AND* there is only low-contrast discoloration *AND* there is no fungal decoy *THEN* the appearance class of the panel is **I**.

[20] Knot holes with diameter < 5mm

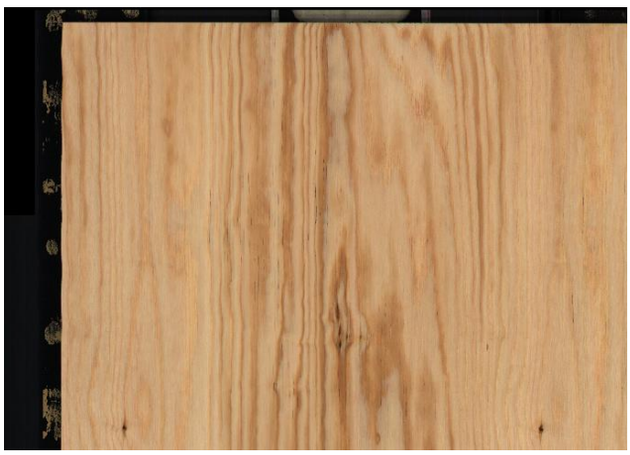

Figure 4-12: Example of plywood panel (spruce) satisfying ISO 2426-3-2000 appearance class I. (image represents approx. 1m^2).

Pin Knots	0
Sound knots	0
Unsound knots	2
Loose knots / knotholes	0
Cracks	0
Resin pockets	0
Irregular wood structure	none
Discoloration	Low contrast
Fungal decay	none

Exemplary formulation of rule for ISO appearance class II:

IF there are no sound knots with diameter exceeding 50mm *AND* amount of loose knots, unsound knots or knot holes with 25mm in diameter maximum is not exceeding 6/m^2 *AND* amount of cracks (open & closed) having up to 10mm length maximum is not exceeding 3 per meter *AND* there exist less than 6 resin pockets or bark *AND* there is only slight irregularity in wood structure *AND* there is only low-contrast discoloration *AND* there is no fungal decay *THEN* the appearance class of the panel is **II**.

Figure 4-13: Example of plywood panel (spruce) satisfying ISO 2426-3-2000 appearance class II. Class II due to unsound knots (image represents approx. 1m^2).

Pin Knots	3
Sound knots	1 (<50mm)
Unsound knots	8
Loose knots / knotholes	3
Cracks	0
Resin pockets	0
Irregular wood structure	none
Discoloration	none
Fungal decay	none

Pin Knots	20
Sound knots	0
Unsound knots	27 (<15mm)
Loose knots / knotholes	6(<6mm)
Cracks	0
Resin pockets	0
Irregular wood structure	none
Discoloration	none
Fungal decay	none

Figure 4-14: Example of plywood panel (spruce) satisfying ISO 2426-3-2000 appearance class II. Class II due to huge amount of knots (image represents approx. 1m^2).

Pin Knots	5
Sound knots	21 (<50mm)
Unsound knots	8
Loose knots / knotholes	2
Cracks	0
Resin pockets	0
Irregular wood structure	none
Discoloration	none
Fungal decay	none

Figure 4-15: Example of plywood panel (spruce) satisfying ISO 2426-3-2000 appearance class II. Class II due to size of sound knots (image represents approx. 1m^2).

From Figure 4-13, Figure 4-15, Figure 4-14 it can be seen that the lowest quality appearance class **II** spans over a quite huge bandwidth of appearance. This might be different with other (company proprietary) guidelines.

One can easily understand that long conditional sentences transformed to conditional programming result in confusing structures[21] which are error–prone and hard to maintain as the numbers (main knowledge) and their logical linking are not separated. Additionally the use of adjectives like "*little*", "*slight*", "*near to zero*" introduce uncertainty as they can hardly be represented by crisp numerical limits.

[21] Textual programming as well as graphical (data flow) programming

4.2.1 Expert Systems

In parallel to the identification of certain appropriate techniques for classification in the first half of this chapter, the second half first identifies some important requirements linked to the specific application of an automated system for rectification of wooden panels before (a specific) expert system technology is introduced and its choice is supported by reviewing the related theory.

From the viewpoint of systems design and with the complexity of patching wooden panels as well as the need for easy adaption to different products and processes in mind, the following requirements can be identified:

- Separation of knowledge from application/execution of rules (explicit knowledge)
- Best possible adaption and maintenance of the knowledge
- Incorporation of domain-experts (wood working experts) rather than computer experts for adaption and maintenance of the knowledge
- Ability to model vague formulated knowledge related with the aesthetic aspects that lack a distinct numerical representation

The stated requirements support the insight that an expert system, typically consisting of an inference engine and a knowledge base *[Jackson 1998]* for separating logic from knowledge, needs to be incorporated. In contrast to the classification methods, an assessment of different expert systems and the related optimal choice cannot be based on previous applications in wood-working processes as no such application is known to exist nor could be found in literature.

Due to the industry-driven nature of the research project not all variants of Expert Systems and possible alternatives can be evaluated. The own experience from research work *[Kuehn 2014]* with Fuzzy Inference Systems (FIS, a special type of Expert Systems incorporating Fuzzy Logic) in applications on wood leads to the decision to incorporate this specific technology. A strong argument for Fuzzy Inference Systems is the fact that they have been designed to model vagueness and uncertainty as is the task of generating patching instructions, especially under aesthetic aspects. This capability of fuzzy inference has been utilized in recent Kansei Engineering approaches *[Hotta and Hagiwara 2007], [Li and Zhu 2010]* for the same reason. While multivariate analysis has been the conventional technique for the analysis of human feelings towards product design and setting up Kansei models,

FISs seem to be predestined and work well in the mapping of features from the product domain into the customer's emotional feature space and vice-versa. This is seen as a strong argument in the decision for this specific Expert System technology.

4.2.2 FIS – Fuzzy Inference System

Fuzzy inference is actually the process of formulating the mapping from a given input space to an output using Fuzzy Logic *[Arshdeep et al. 2012]*. The process involves: membership functions (reviewed in detail in Appendix A.3.1) for fuzzification as well as for defuzzification, fuzzy logic operators (reviewed in detail in Appendix A.3.2) and *if-then* rules (reviewed in detail in Appendix A.3.3):

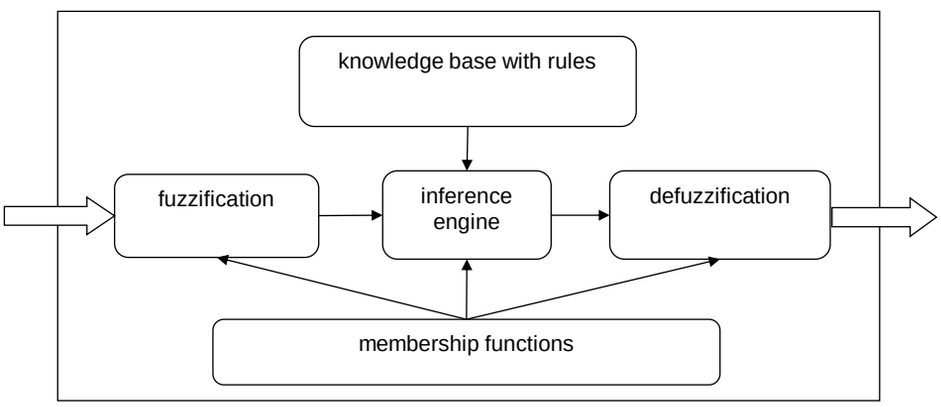

Figure 4-16: Schematic diagram of Fuzzy Inference System (FIS).

Figure 4-16 illustrates this context; the execution of the fuzzy inference system involves three main procedures in sequential order:

1. *Fuzzification*: transform a crisp input value to a degree of membership in terms of a fuzzy set using the assigned membership function.
2. *Aggregation* of the fuzzy sets with the help of fuzzy operators to an output fuzzy set or variable according to the rules from the knowledge base.
3. *Defuzzification*: transform the fuzzy output to a crisp output

The rule engine is the central element of the fuzzy inference system with fuzzy sets for the inputs and outputs as well. It carries out all the tests that are done incorporating the rules in parallel, including the application of the fuzzy operators that are used to apply the logical connectives in the rules ({if ... AND ...} OR {if ... AND...} then ...), refer to Appendix A.3 for a detailed description.

4.2.3 Discussion of FIS

Incorporating Fuzzy Logic and a Fuzzy Inference System for the purpose to setup an expert system to model human expert knowledge in the area of wood working where vagueness and uncertainty is involved seems to be the most elegant and most promising approach. Especially for the intended purpose of generating patching data instruction derived from explicit but also from implicit rules, the modifiability of the rules formulated using adjectives in human readable sentences by graphical adjustments of the membership functions seems to be sensible. This allows adaption, modification and maintenance of the system by domain experts rather than computer science experts as initially stated in the requirements.

4.3 Summary of research methods

In this chapter the methods were introduced to be used for modelling human expert knowledge in the area of wood-working. Focus has been given on the abilities to imitate capabilities related to human perception (high amount of involved features, planar representation of complex problems like in the cortex) and way of thinking (modelling noise and incorporating uncertainty). A machine learning algorithm which can handle the elaborate and complex task of defect detection incorporating aesthetic aspects is identified and its choice is supported by theoretical background knowledge. This theoretical background proofs the principal capability of Support Vector Machines (SVMs) among other techniques to handle huge data sets. This is related to feature space dimensionality, the amount of samples, non-linear classification problems and noisy training sets. Introduction to a cascaded training approach for the simplification of the training data selection carried out by a human expert by mapping and grouping image tiles in a planar representation using the advantages of SOMs has further been given. The cascaded classificatory system training including the user interaction is detailed in the following chapter. Besides the wood working expert knowledge involved in defect detection, respectively defect classification, which will be covered by an approach of learning from examples in the detection part of the next chapter, an Expert System concept based on Fuzzy Logic (FIS) has been introduced. This Expert System satisfies principally the stated requirements and is seen to be the most promising approach to model wood-working expert knowledge for the generation of patching data. Generation of patching data is subject of the second part of the following chapter.

5 System Design

In the previous chapter the research methods related to the aesthetic aspects in detection and the knowledge-based patching data generation have been introduced. In the context of a scanner system for the automated rectification of defects on wooden panels and the related design experiments, this chapter introduces the framework in which the proposed methods are used. The developed scanner system (Baumer *ColourBrain® for patching*) is shown in Figure 5-1 as part of the first prototype system for patching plywood panels using liquid fillers and in Figure 5-5 as part of the first prototype system for patching solid wood panels with dowels. The patching machinery has been built by collaborating Austrian partner company Fill. The corresponding tools are shown in Figure 5-2 - Figure 5-4 and Figure 5-6.

Figure 5-1: Backward view along automated patching line for plywood panels. From rear to front: Scanner system, routing tool portal, 2K-putty tool portal and 1K-putty tool portal in the foreground. Each portal consists of x/y axes with two tools of same type (left/right). Maximum panel size is 2.5m x 5m.

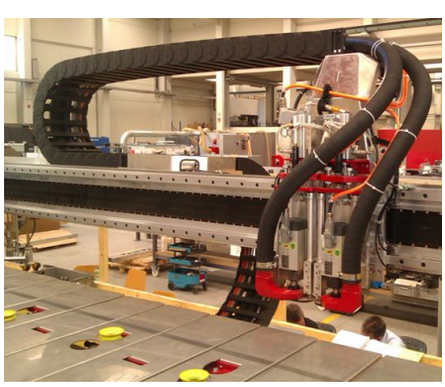

Figure 5-2: Routing tools and suction for pre-processing in automated patching using putty.

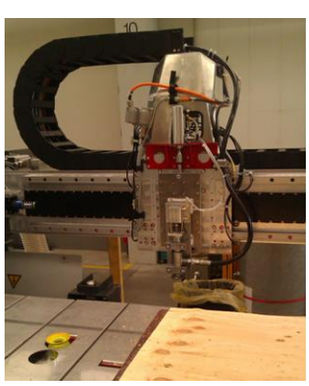

Figure 5-3: 1K putty insertion tool: stamp with nozzle.

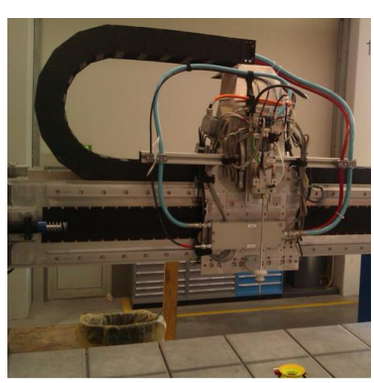

Figure 5-4: 2K putty insertion tool with nozzle and waste bin for flushing.

The *ColourBrain® for patching* scanner system used for automated patching of solid wood panels with dowels is shown in Figure 5-5. One of the four aggregates with the dowel insertion tools is shown in Figure 5-6.

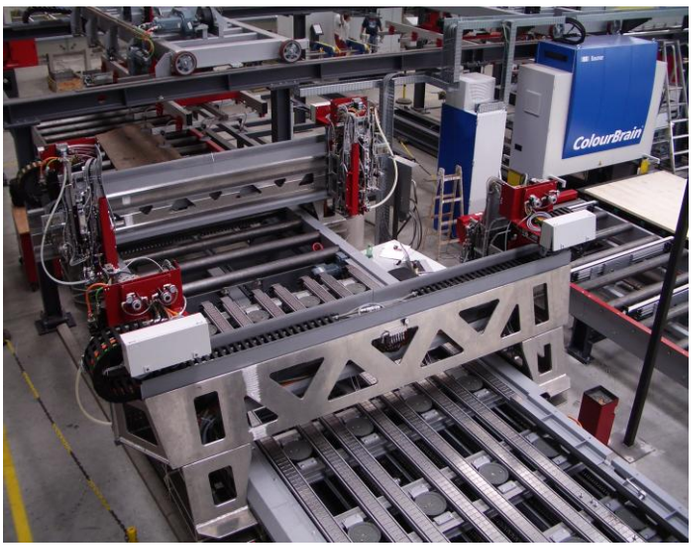

Figure 5-5: View on automated patching line for solid wood panels. In the foreground the portal with four aggregates with tools for different sized and shaped dowels can be seen. The panel is scanned forward (from rear to front in image) and is then turned to scan the backside in backward movement. Then the panel is moved to left onto the transportation through the portals.

Figure 5-6: Aggregate with tools for insertion of circular dowels. The view from below shows router (left) and punch (centre), both using a stencil mounted on a slide. The transparent hose on the right side is used to feed the dowel.

A framework has been chosen based on the scanner system *ColourBrain® for grading* used in furniture and flooring inspection. The monolithic design of these systems and their data processing linked to proprietary grading and inspection does not address the requirements of automated patching. Scanner housing, cooling, standard illumination and acquisition hardware as well as software modules for basic calibration, standard image acquisition and common Graphical User Interfaces (GUI) could be re-used. The new scanner needs to be enhanced by tailored imaging techniques, related image sensor data fusion as well as specific image data processing in the defect detection prior to the new methods for defect classification and decision making related to patching as proposed in chapter 4.

Therefore the overall system architecture of the scanner is developed first. This is followed by a refined investigation of the main components and modules added. Focus is thereby on the *optimized detection techniques* as sources of data for the new, patching-specific components *segmentation*, *classification, decision making* and subsequent *patching data generation*. Only the principles of the chosen *sensor data fusion* are explained in the following.

5.1 A dedicated cluster architecture for automated patching

The system architecture for an image processing system tailored to the requirements for a scanner used in an automated patching line is presented in this subchapter. Research and development done with respect to the prototype development of such a scanner result in a unique system which combines state-of-the-art techniques and components to a new concept of sensor fusion and multichannel image processing for the use in automated visual defect detection on wooden panels.

Common non-integrated image processing systems used for the inspection of wooden panels (excluding smart cameras, proprietary integrated sensors and similar) have to deal which huge amounts of image data and are usually based on personal computer (PC) technology like the systems from Baumer Inspection[22], Argos[23], Mecano[24], Raute[25], Luxscan[26] or Weinig[27]. A common system layout is shown in Figure 5-7. This type of setup is a hierarchical organisation of one master computer connected to several slave devices whereby each slave consists of an imaging device, a frame grabber device and a data processing unit that is usually also an industrial computer. The relationship between imaging device and processing unit is historically usually 1:1 as relationships including several imaging devices to one processing unit are limited by the data transfer from the frame grabber device and by the processing capacity of the processing device. The most common setup furthermore is to have the image processing done on the same computer to which the imaging devices are connected and to do the transformation from the image level to an abstracted level using a symbolic description of the image content as soon as possible for the purpose of data reduction. In PC based solutions there is usually (Baumer Inspection, Argos, Luxscan) one instance of signal processing software for evaluation associated to each camera, following the 1:1 relationship already mentioned. With increasing processing capacity of modern hardware, the relationship of one imaging device attached to one computer and the need to condense the information contained in the image data to a symbolic representation as soon as possible in the processing chain is no longer necessary. This is valid although the imaging device evolution itself also led to higher amounts of data

[22] baumerinspection.com
[23] *argossolutions.no*
[24] *mecanogroup.com*
[25] *raute.fi*
[26] *luxscan.lu*
[27] *weinig.com*

due to higher data rates, more pixels, greater bit depth, etc. *[Tomoyuki 2010]*. Modern multi-core processors allow the execution of several instances of software as separate tasks with adequate performance which already led to setups with up to four imaging devices connected to one processing unit (Baumer Inspection, Raute, and Mecano). Most system designs nevertheless still follow the philosophy of early image processing for the reasons of data reduction but with significant loss of information at an early stage.

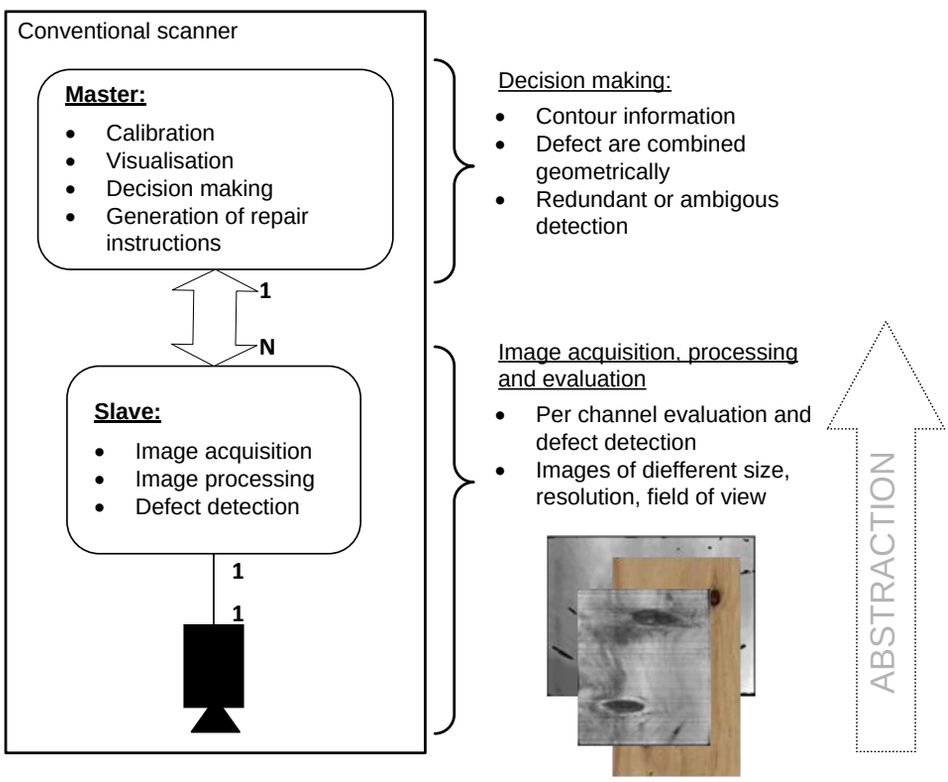

Figure 5-7: Block diagram of conventional system architecture for image processing

The conventional design dictates the execution of image processing on the different images from the different imaging devices separately and needs to combine the derived information on a higher level by a superordinated instance (master computer, refer to Figure 5-7). This might be an advantage in terms of the amount of data that has to be processed by the master computer, but the disadvantage is clearly the loss of information that is valuable in combination with the data from other imaging devices and sensors. For instance, there is no direct possibility to further evaluate image data from a specific channel if it should be necessary for the decision making. The decision making has therefore to get along with the abstracted information (contour information, symbolic representation) on the single channel's object level. Another example is object segmentation: usually the area of interest

(knot, possible defect) is not fully visible in just one channel but has to be combined from different channels. As already outlined in chapter 3.1.2 *Multi-channel image processing, [Nestler and Franke 2000]* for example addressed this disadvantage and proposed the pixel-wise combination of the radiometric data from a modified colour (Red, IR, Blue) camera and the range data from a triangulation sensor in advance of the execution of the detection algorithms. Their proposed concept incorporated only a limited number of cameras allowing only two sensors with altogether three channels (red and blue (RB)-colour, Scatter, 3D) to be attached to a single processing unit not to exceeding data rate and processing capacity of the sole computer used. Being faced with the problems of high amount of data, Xiao *[Xiao 1998]* realized a multi-sensorial image processing system with the help of dedicated, but proprietary hardware (Field Programmable Gate Array, FPGA) to integrate the different image channels and to overcome the limitations of software based approaches. The disadvantages of this concept are the missing scalability and extendibility of this hardware.

A more scalable and more flexible approach needs to be used in the scanner system for automated repair to be able to adapt the system to varying requirements (e.g. different or additional sensors for different types of wood, additional sensors for enhanced spatial resolution, etc.). Such an approach is shown in Figure 5-8. When comparing the system diagram of the two cluster architectures from Figure 5-7 and Figure 5-8 one can see a newly introduced layer for processing in the proposed cluster architecture shown in Figure 5-8. The acquisition layer therefore does not contain the image processing and evaluation anymore as it is the case in the conventional cluster architecture. Rather, the acquisition layer is optimized for high speed acquisition from all imaging devices involved and is equipped with dedicated hardware that is able to do coordinate system transformations and radiometric transformations on pixel level which requires fast memory and high computation capacity. That means the images are combined to one global image with as much image channels as there are different types of imaging sensors (e.g. Colour, Scatter, 3D, UV fluorescence, UV remission, UV absorption, IR, etc.) in advance of the evaluation and detection. The image acquisition layer therefore executes the low level tasks of sensor data fusion to provide a calibrated and registered overall image data basis. With the possibility to be easily extended with additional sensors, this approach is based on a clear structure of data processing responsibility. Additional sensors may be added either for the reason to increase resolution (adding camera of same type to existing channel) or for the reason to introduce another

imaging technique (spectral adjusted sensor addressing special physical/optical phenomena) to address special defect types. With a strict separation of the tasks *data fusion*, *data evaluation* and *decision making* by the different layers, a consequent increase of abstraction from bottom to top is achieved (Figure 5-8). With abstraction to a symbolic representation only after classification, the information content is preserved to the latest possible stage compared to the classical approach.

.

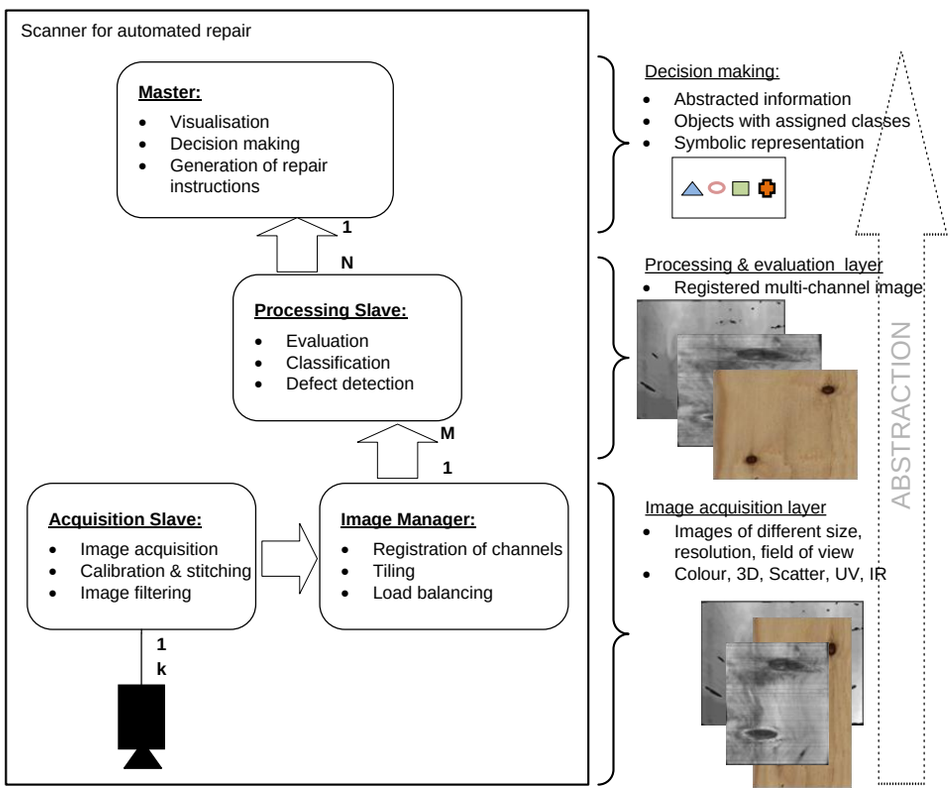

Figure 5-8: Block diagram of new system architecture for image processing

Table 5-1 lists a typical setup for a multi-sensorial scanner identifying the data rates based on spatial resolution and bit depth of the sensors. Resolutions vary greatly due to different pixel sizes and different technologies incorporated. Low-intensity, long-integrating sensors as used in UV-detection for example cannot achieve the same resolutions as high-speed colour cameras. This issue in multi-channel imaging will be covered with the sensor data fusion in the next section.

Channel	Number of cameras	Pixels in virtual scanline	Resolution (horizontal), pixels/mm	Resolution (vertical), pixels/mm	Bit depth per pixel	Data rate in acquisition MB/s	Data rate in evaluation MB/s
Colour	4	16384	7.4	10	24	273	273
3D	4	9408	4.3	5	16	52	105
Scatter	4	9408	4.3	5	16	52	105
IR	4	9408	4.3	5	16	52	105
UV Remission	2	4096	1.9	3	8	7	23
UV fluorescence	2	4096	1.9	3	8	7	23
					total:	**444**	**633**

Table 5-1: Image resolutions of the different sensors used in a dedicated scanner for automated repair and resulting data rates to be handled (acquisition) and processed (after registration). Values at production speed of 35m/min.

The incorporated imaging techniques to fully cover the detection of possible defects are described in 5.2 *Defect detection techniques* and are briefly illustrated in Figure 5-9. The multi-sensorial approach covers the human visible part of the light spectrum (wavelengths from 380 to 780nm) as well as the invisible parts beyond (UV, wavelengths smaller than 380nm) and above (Near Infra-Red (NIR), wavelengths bigger than 780nm). The cluster architecture is illustrated from the view of processing responsibility and processing capacity as well as of data transfer bandwidth. An image manager instance is responsible to provide the overall image and is therefore in the role of a proxy abstracting the specific composition of the acquisition layer to the detection & evaluation layer. The instances in the detection & evaluation layer communicate directly with the master instance after registration of their service. The image manager can then subdivide the global image accordingly to the overall processing capacity which provides the necessary flexibility in terms of scalability.

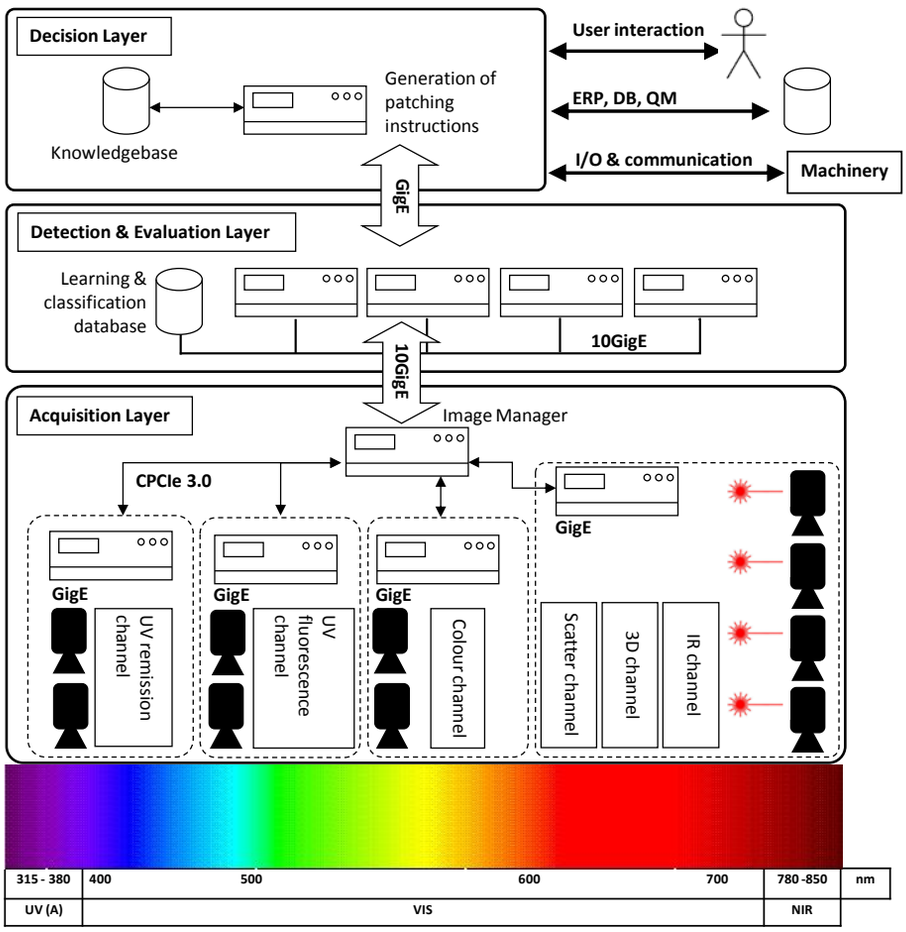

Figure 5-9: Schematic diagram of the new scanner's modular processing cluster.

The approach described has several advantages (e.g. scalability, balancing computing power, etc.) over conventional and commonly used monolithic cluster architectures. The following sections briefly cover the technologies and techniques involved for the purpose to create an overview and ensure the further understanding of the chosen concept.

5.1.1 Layer 1: Sensor data fusion - creating the global image

The task of combining image data from different sensors is known as sensor fusion. Murphy *[Murphy 1996]* derived principle methods from biological and cognitive sciences and defined sensor fusion as the conversion of sensor-specific senses to common representation, also filtering noise. Nakamura *[Nakamura et al. 1998]* adapted these findings and introduced statistical fusion methods for cybernetics. While sensor fusion in principle is not limited to combine image sensors, several principal techniques have been developed to fuse spatially-resolved sensor data. Crowly *[Crowly et al. 1993]* identified two principles of sensor data fusion, the *Common Coordinate System* and the *Common Vocabulary*. Pohl and colleagues

[Pohl et al. 1998] extended this partitioning to fusion of image sensors on *symbol*/*decision level*, *feature level* and *pixel level*.

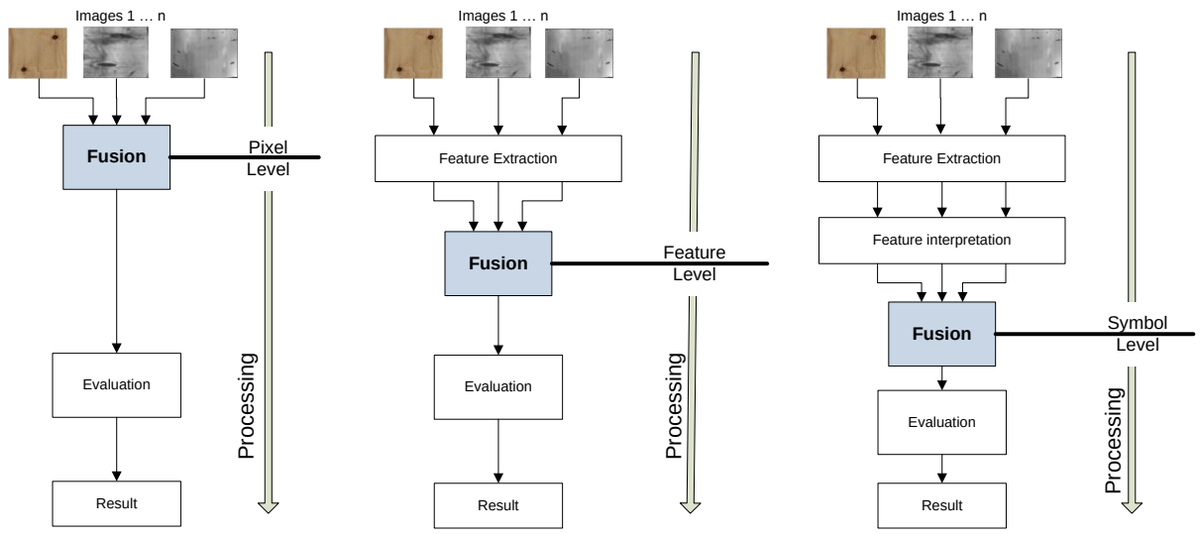

Figure 5-10: Partitioning of image sensor fusion principles into fusion on pixel level, feature level or symbol level.

Figure 5-10 adopts this breakdown and illustrates the implications on the processing. Referring to the conventional system design, the fusion on symbolic level (left principle in Figure 5-10) with much of the processing (e.g. for defect detection) on the single images is contrary to the proposed sensor fusion of registered images on pixel level (right principle in Figure 5-10). Registration on pixel level is incorporated in the new system architecture (Figure 5-8 and Figure 5-9).

A variety of solutions to fusion on pixel level exists, e.g. Li and colleagues *[Li et al. 1995]* used Wavelet transformation with composition coefficients, Burt and colleagues *[Burt et al. 1993]* used the pyramid transform domain for the fusion of images. While most applications are in the field of satellite images, remote sensing data and medical imaging, little work can be found for the purpose of machine vision in industrial wood working applications. In the following sections the approach for image sensor fusion for the scanner for automated rectification of wooden panels is introduced. This approach differs from the approaches found in literature in that not a single transformation equation is developed but well-known image processing techniques are combined and applied as illustrated in Figure 5-11. The incorporated image processing algorithms and calibrations for image sensor data fusion are reviewed in detail in Appendix A.4

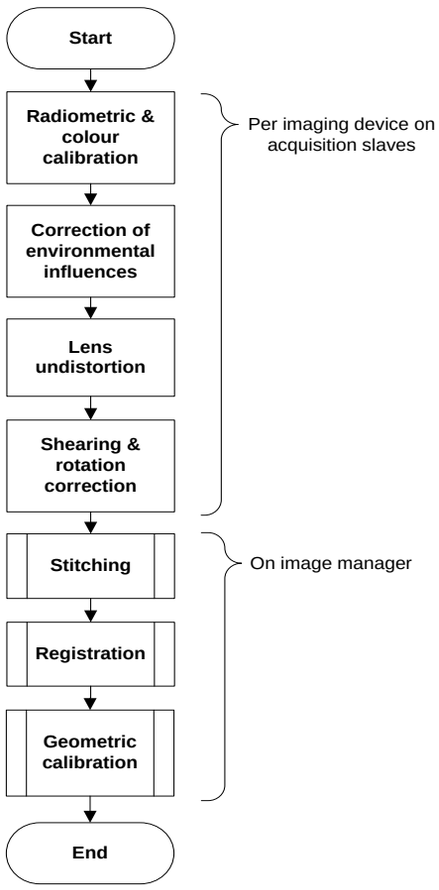

Figure 5-11: Basic image data processing chain in proposed image sensor data fusion.

The basic principle is therefore to completely integrate all the image data which is done first on camera level (stitching per channel) and then on channel level (registration of channels). In fact there are many similarities between the processes of image stitching and image registration. In the context of this research project and its application, the stitching is a special case of registration as only the overlap regions of the adjacent images are used. The images from one channel are always of the same type and, due to identical hardware, are of nearly the same resolution. As the field of view and working distance are similar to a high degree only translation, shearing correction and rotation need to be applied in stitching. The registration of (stitched) images from the different channels then only needs to incorporate scaling but additionally interpolation has to be applied. The prerequisite is therefore that previously executed image calibration routines remove radial distortion as well as shading effects (vignetting) introduced by the lenses. Radiometric calibrations[28] are needed as well as colour calibrations as proposed by Kuehn *[Kuehn 2004]* for harmonized colour values between the colour imaging devices.

With respect to unwanted influences from the industrial environment (vibration and similar) and from challenging properties of the wooden panels (warping, bending) several additional pre-processing routines and arrangements need to be incorporated to guarantee the best possible undistortion of the image sensor data in advance to stitching and registration. Warping, bending and similar cannot always be compensated by a mechanical or constructional solution. The descriptions of appropriate methods addressing distortion from the industrial environment (external influences) can be found in detail in Appendix A.5.1 and methods to eliminate disturbing effects of the panels itself (internal influences) can be found in Appendix A.5.2. A summary of the incorporated calibrations is given in Appendix A.4.1.

[28] Dark current calibration, bright and dead pixel elimination

5.1.2 Layer 2: Detection & evaluation

Having created the overall multi-channel image, the image manager can supply the single instances in the processing & evaluation layer with tiles of this global image, refer to Figure 5-9. One of the first tasks to be accomplished then in terms of detection is the segmentation of areas of interest (AOI) before the segmented defect candidates can be evaluated by the defect classification system.

5.1.2.1 Segmentation

The aim of the segmentation is therefore to decide which pixels in the registered multi-channel image belong to sound wood (which can be seen as background in the scene analysis) and which pixels are potential defects (defect candidates).

Analysing typical image processing chains in machine vision applications, two common concepts can be identified. While the image acquisition is usually always followed by some pre-processing the subsequent steps differ significantly in terms of the process for separating objects (foreground) from the background. Pre-processing incorporates filter operations and tailored image processing algorithms for image enhancement, noise reduction or calibration. The common approach is the non-segmenting approach which does not incorporate image processing algorithms for (pre-) segmentation but simply subdivides the complete image to tiles. These tiles are fed directly to the classifier which therefore has to be trained additionally with the background class, refer to Figure 5-12. As the size of the tiles is usually small and fixed, it becomes clear that the portion of the image representing the object, e.g. a defect, is spread over several tiles. Therefore tiles which are holding only pixels of the defect and tiles holding background pixels as well as pixels belonging to the defect exist. The alternative approach is to classify previously and completely segmented objects, respectively the pixels in the segmented area, and only then to assign labels either for different types of defects or false alarms. This is called the segmenting approach whose output is illustrated in Figure 5-13 exemplarily.

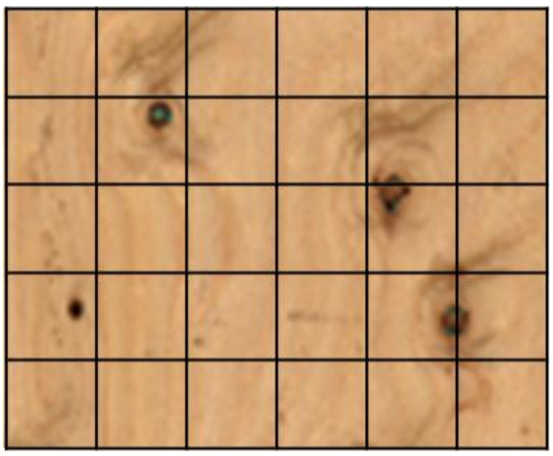

Figure 5-12: Non-segmenting approach based on classification of image tiles from the uniformly sub-divided overall image including background (sound wood).

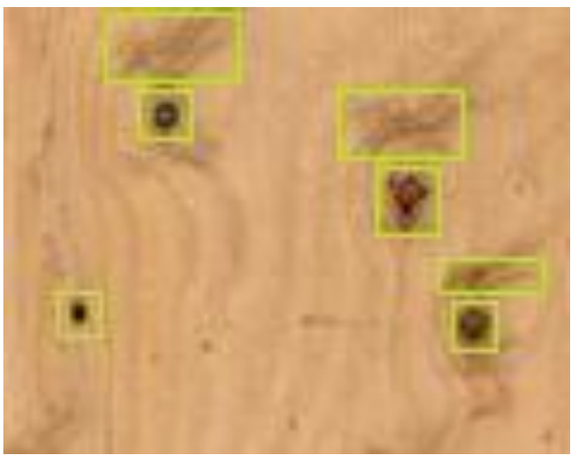

Figure 5-13: Segmenting approach generating image tiles of different size only for defect candidates that are then classified.

Advantage of the non-segmenting approach is that there is no necessity for special segmentation algorithms usually from the area of thresholding, region growing or morphological operations. Those algorithms are error-prone as they rely highly on the underlying (single channel) image data quality and information content. Also most types of algorithms (especially morphology) consume significant amounts of time in the Central Processing Unit (CPU). Depending on the classification technique, a simpler and faster approach can therefore be realized with the non-segmenting approach. Problems caused are the already mentioned fact that tiles classified as belonging to a defect eventually must be (re)connected to complete defragmented object regions, refer to Figure 5-14. Further, the resulting defect region is then a multitude of a single tile area surrounding the defect unnecessarily with sound wood. Further the defect regions often get connected to each other as can also be seen in Figure 5-14 which requires a separation by segmentation at a later stage anyway.

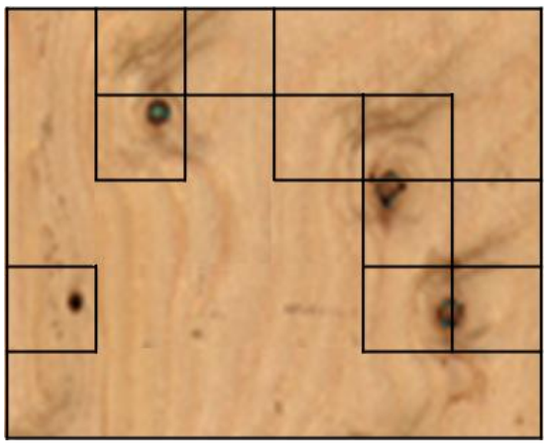

Figure 5-14: Connection of tiles/object fragments is necessary to complete defect regions in the non-segmenting approach. Problems arise with thereby connected defects for the further processing for patching.

In contrast, the advantage of the segmenting approach is a better separation from the background, ideally in terms of a pixel-wise border or a tight bounding rectangle which is a requirement anyway for the calculation of the patching instructions as will be shown later. The output of the segmentation is the so-called Defect Candidate Map (DCM). It is on the one hand advantageous in terms of CPU time consumption that only a limited number of segmented objects needs to be classified. On the other hand the segmentation might produce non-deterministic huge lists of objects if misconfigured or if the image data is not stable (e.g. shading effects when using simple thresholding techniques, noisy data, etc.). Calibration and undistortion techniques as previously mentioned in section 5.1.1 nevertheless can compensate this.

The mentioned advantages lead to the decision to use the segmenting approach in the scanner for automated patching of wooden panels. This is also because the detection process incorporating segmentation pretty much follows the approach of the Human Visual System[29] (HVS): Being able to identify objects in terms of contrasting areas even on previously unseen surfaces is a fundamental property of human visual perception. Closer examination and analysis show that the identification of the object is only done in a second step in the HVS and identification of objects in terms of irregularities (areas of interest) in a scene are a fundamental capability of the HVS *[Thorpe et al. 1996]*. The chosen image segmentation approach on a data basis built from various sensors (addressed in detail in the following section 5.2 *Defect detection techniques*) together with the subsequent defect classification addressed in section 5.3 *Defect classification system* is therefore seen as a

[29] HVS including eyes, pathway to/through visual cortex and other areas of the brain

computational model of the HVS. The fundamental idea hereby is to define sensors that easily allow the segmentation of areas of interest by exploiting the physical properties of the defects on wooden panels for the creation of the DCM.

5.1.2.2 Classification

Based on the DCM defining the areas of interest in the registered multi-channel image data, the detection & evaluation slaves execute classification procedures for groups of pixels to further decide between several possible classes like different knot types, resin pocket, crack, etc. (refer to section 2.2), but also to suppress false alarms from the segmentation caused for example by contaminations. The classification of defects is carried out by a SVM operating on the multi-dimensional image data directly. Section 5.3 *Defect classification system* approaches the defect classification in detail. The abstraction of the defects for the subsequent patching data generation is finally carried out by completing each defect's description, including shape descriptors, intensity, colour and texture information as well as depth information and spatial measurements which are absolutely needed for the patching data generation.

5.1.3 Layer 3: Decision making & patching data generation

With the abstracted information from image data in the form of defect descriptions gained from the segmentation (e.g. defect contours, mean colour, etc.) associated to the class labels gained from the defect classification, the master instance of the computing cluster finally gets involved. Incorporating the knowledge base for patching wooden panels, which is discussed in detail in section 5.4 *Decision making*, rules are applied that define *if* and *how* to repair a certain defect to achieve the best possible overall repair result in terms of aesthetics, ecological sensibility and cost effectiveness as defined in 2.4 *Technology demands*. Having applied these rules, the patching of the single defects is achieved by calculating repair instructions for the patching tool and related machinery. These instructions include the tool type for pre-processing (routing for example, if necessary), type of repair (liquid or solid fillers), volume or size information, colour and appearance characteristics and positional information for the tools. The instruction generation is discussed in detail in section 5.5 *Patching data generation*. Optionally the processing strategy of all defects on a panel can be calculated and optimized. The patching itself in terms of detailed descriptions and discussion of the tools and related aspects is out of the

scope of this thesis; however the final results based on photography for example are presented and discussed in chapter 6.

5.1.3.1 User interface and interface to machinery

To complete the system description based on Figure 5-9, a scanner system must communicate with its environment, which is first of all the machinery carrying out the actual repair process. As the proposed scanner for an automated repair system is based on expert knowledge (refer to section 5.4 *Decision making*) and user interaction for the supervised machine learning (refer to section 5.3 *Defect classification system*), the user interface of the scanner system is equally important, which will be addressed in the upcoming sections. The third interface such a system needs to provide to its highly automated environment is a data interface for the access to an Enterprise Resource Planning system (ERP), Production Planning System (PPS) and similar database systems (refer to 2.4 *Technology demands*) which is also provided by the top layer of the scanner cluster's architecture.

Except for the user interface, these interfaces will not be further addressed in the scope of this thesis. References are made at this point to the work in the scope of a diploma thesis carried out by Göttlicher *[Göttlicher 2011]* to extend the prototype development with a generic data exchange interface to the tools and which has been supervised by the author as part of the underlying research project.

5.1.4 Summary

The system design of the scanner has been introduced. Serving as a framework for the research methods introduced in chapter 4 with focus on defect detection under aesthetic aspects, automated patching data generation and incorporation of a knowledge driven approach based on expert system technology, the hierarchical structure of the cluster architecture consisting of acquisition layer, detection & evaluation layer and decision making layer has been introduced. This approach is seen to optimally address the issues of complexity in the information flow and information processing. The overall processing chain has been explained highlighting the sensor data fusion to registered multi-channel images and the computational model of the Human Visual System using a segmenting approach. Based on this general understanding the following sub-chapters will address in detail the approaches to defect detection/segmentation, defect evaluation/classification, decision making and finally the patching data generation.

5.2 Defect detection techniques

This chapter identifies techniques for the detection of defects on wooden panels. Defect detection hereby addresses the capability to define areas of interest in image data by a segmentation algorithm (refer to 5.1.2.1) which can then be input to the evaluation by a classification algorithm (refer to 5.1.2.2). In the context of the design of the scanner system applied to wooden panels, the defect detection techniques focus on appropriate imaging techniques giving adequate contrasts gained from the properties of the defects. The aim is to reduce algorithmic and computational complexity in the segmentation (e.g. using simple thresholding and adaptive contour algorithms, refer to 5.1.2.1). Besides standard techniques newly defined, specifically tailored techniques are identified.

5.2.1 Standard detection techniques

In section 3.1.1 common imaging/detection techniques used in established systems for machine vision on wood have been summarized. Besides colour imaging and simple greyscale imaging where appropriate (only limited and less complex sets of defects), triangulation and scatter measurements using projected laser lines are standard. Table 5-2 and Table 5-3 summarize the possibilities to detect (segment) and evaluate (classify) typical defects on solid wood panels respectively on plywood panels by these standard imaging/detection techniques (colour coding and legend given in Table 5-4 and Table 5-5).

	Colour	Scatter	3D
Sound knot	++	+	-
Cracked Knot	++	+	+
Dark Knot	++	++	-
Loose Knot	+	+	-
Ringed Knot	+++	++	-
Knot with bark	++	++	-
Knothole	-	-	+++
Knothole with glue (Kauramin)	+	-	-
Crack	++	+	+
Resin Pocket	+	-	-
Pressed-in particles	-	-	-
Discoloration	++	-	-
Fungal decay	+	+	-
Glue (Kauramin)	+	-	-

Table 5-2: Verification matrix for a typical detection of defects on solid wood panels using colour, 3D and scatter imaging.

	Colour	Scatter	3D
Sound knot	++	+	-
Cracked Knot	++	+	+
Dark Knot	++	++	-
Loose Knot	+	+	-
Ringed Knot	+++	++	-
Knot with bark	++	++	-
Knothole	-	-	+++
Crack	++	+	+
Resin Pocket	+	-	-
Roughness	-	-	+
Shells	-	-	-
Pressed-in particles	-	-	-
Discoloration	++	-	-
Fungal decay	+	+	-
Glue (urea-formaldehyde)	+	-	-

Table 5-3: Verification matrix for a typical detection of defects on plywood panels using colour, 3D and scatter imaging.

Contribution to segmentation	
	no detection if used alone
	unstable detection if used alone
	stable detection if used alone

Table 5-4: Colour coding for verification matrix of standard defect detection techniques.

Contribution to evaluation	
-	little to none
+	some
++	good
+++	very good

Table 5-5: Legend tor verification matrix of standard defect detection techniques.

It can be summarized that only a few obvious defect types can be detected reliably by colour imaging techniques (cracks in knots, ringed knot, cracks) respectively by spatially resolved triangulation measurements (knothole, cracks, roughness). As already stated in section 3.1.2 it can be further summarized that a combination of channels is the key to improve unstable detections based on only a single channel by supporting the information content in the data base. For example the detection of sound knots is not reliable when based on colour imaging alone due to the variance in the colour of the knots, especially when contaminations are present or when the knots appear very bright. By additionally incorporating scatter measurements, indicating the structure and direction of the grain, the detection can be stabilized. Depth information from triangulation can further strengthen the decision towards a sound knot instead towards a perfectly fallen out knot on although triangulation not being able to identify sound knots by itself.

In Table 5-2 the defect types *knothole with glue, resin pocket and pressed-in particle* can be identified to be critical in detection on solid wood panels. Fungal decay is statistically rare and should not occur at this stage of panel processing (inspection of veneers should have sorted out this defect as it is commonly hard to repair due to its large area). In principle these defects are also critical to detect with standard techniques on plywood panels (Table 5-3), although *resin pockets* are slightly more cooperative due to their large-area appearance on peeled veneer in contrast to sawn veneer (refer to 5.2.2.2). Before the development of optimized detection techniques is carried out, these demanding defect types are investigated in more detail for a better understanding.

5.2.2 Demanding defect types

5.2.2.1 Glue-filled knothole

Referring to section 2.2.1.1.2, in the production of solid wood panels a common defect type is the glued-filled knothole which is a hole in the veneer or lamella filled by glue that leaked through this hole during pressing, refer to Figure 5-15. It is obvious that this kind of defect cannot be detected reliably with a triangulation measurement as is the case with the unfilled knothole.

Figure 5-15: Glue-filled knothole on three-layered solid wood panel of spruce.

Urea-based adhesives like Kauramin® and Kaurit® are mainly used in the production of multi-layered solid wood panels and edge-glued solid wood panels. Due to different shades of colour of the glue caused by contamination with saw dust for example, the contrasts and signal stability for a colour-based detection are insufficient. Although having a crystalline structure no light conductivity can be determined in these types of glue, which means that also the scatter signal evaluation is inappropriate for detection.

5.2.2.2 Resin pocket

Another typical surface defect on wooden panels is the resin pocket, refer to section 2.2.1.1.8, either forming a flat but wide indentation, refer to Figure 5-17, or a narrow but deep crack, refer to Figure 5-16. Depending on the top or bottom side of the panel the liquid resin (liquified by the heat in pressing) from the vertically cut resin pocket may flow out (bottom side) and forms so-called resin lakes around the resin pockets as shown in Figure 5-16.

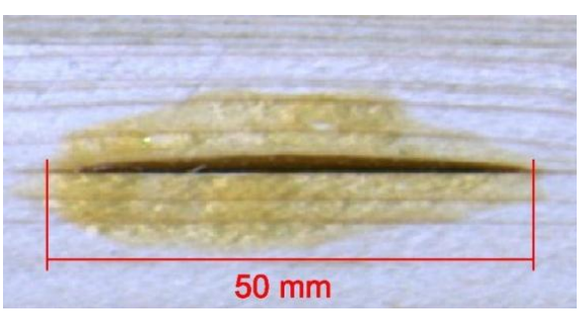

Figure 5-16: Resin pocket on solid wood panel (sawn lamella). Bottom side of panel showing lake of leaked resin.

Figure 5-17: Resin pocket on plywood panel (peeled veneer) showing crystallized resin. Left part showing nearly no indentation.

Horizontally cut (peeled) resin pockets often show a more crystalline structure (Figure 5-17) of the resin due to greater thickness of the resin. This is because the indention preserves contact with the hot surface of the press. The detection of both the leaked (bottom side of

panel) and the still filled (top side) resin crack as well as the detection of the horizontally cut resin pocket are demanding. Being filled, there is often no indentation to be detected by triangulation measurement for example and even when leaked the detection is often not complete in terms of a complete defect contour as only subareas showing a certain indentation can be detected reliably.

5.2.2.3 Pressed-in particle

Figure 5-18: Pressed-in particle on plywood panel of spruce.

Referring to section *2.2.1.2.5* thrash particles may be pressed into the face veneer destroying the surface respectively leaving an indentation when getting loose again. Due to the pressing there is hardly any difference in height measurable at the particle as most often the particle remains until a later step and is removed only during sanding for example. As indicated in Table 5-2 & Table 5-3 the colour information is useful only in rare cases where the thrash particle shows contrast to the face veneer in terms of colour or texture although in most cases the particle is clearly noticeable for the human eye. This defect is a good example for the complex and adaptable capabilities of the human visual system that are hard to model and imitate by technology in its entirety.

Some disruption in the grain structure may be indicated in the scatter measurement, but the signal is commonly not strong enough to setup a stable detection. It has been found that only Thermographic Imaging (refer to *3.1.1*) is capable to detect pressed particles reliably.

5.2.3 Specifically optimized detection techniques

The previously described detection techniques (colour, 3D measurement and scatter evaluation) cover a wide range of the given defect spectrum. Nevertheless the automated production processes require full and reliable coverage of the defect spectrum. For the demanding defect of pressed-in particles the Thermographic Imaging could be identified to solve the detection, therefore a specifically optimized detection technique based on special physical characteristics (thermal flow) that compensates the inability to perform with the capability of the HVS to detect this defect has been found. Additional detection techniques tailored to the specific, problematic defect types *knothole with glue* and the *resin pocket* are still to be defined and to be integrated into the modular system architecture.

5.2.3.1 Analysis of spectral data

Simple RGB[30] imaging does not produce satisfying segmentation results as the signal from reflected (white) light at both glue-filled holes and resin pockets is ambiguous and therefore no distinction to sound wood is possible, this has been shown in previous section 5.2.2. To verify if a suitable imaging technique exists in principal and to identify an appropriate illumination, the reflected spectrum needs to be analysed in more detail, including the near ultraviolet range (315-380nm) and infrared-range (780-3000nm). By using an optical setup sensitive from 300nm to 1300nm and a halogen lamp without UV-filter covering this range of wavelengths, an initial test shows that in the lower part as well as in the upper part of the visible spectrum a promising signal to noise ratio (SNR) can be achieved, refer to Figure 5-19.

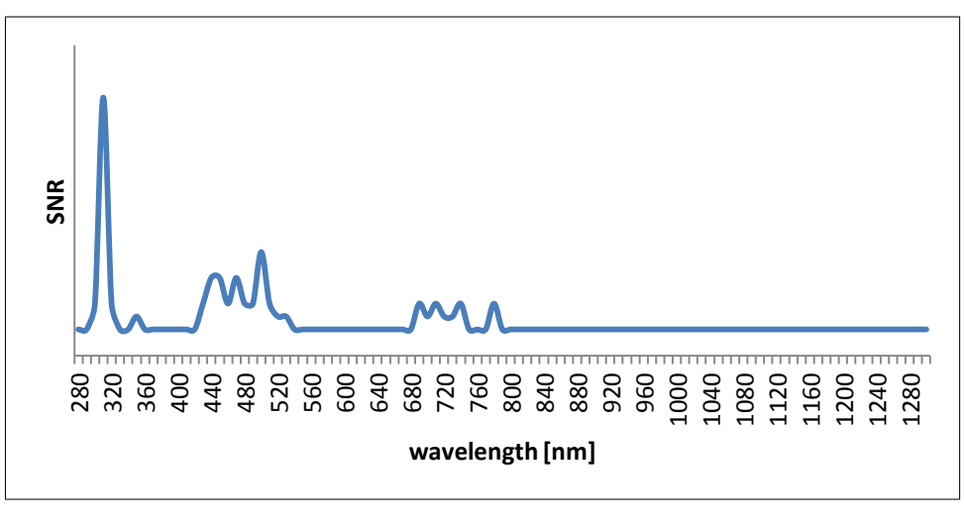

Figure 5-19: Determination of Signal-to-Noise-Ratios (SNRs) over the spectrum to identify interesting spectral bands for a specifically optimized imaging technique.

[30] Colour camera with detection elements sensitive to Red, Green and Blue parts of the spectrum

To further investigate and narrow the optimal spectral band for an optimized illumination and acquisition setup at first a UV illumination (315-380nm) is tested as (from Figure 5-19) this seems to be the most promising part of the spectrum. At first the used UV fluorescent lamp is measured using a spectrometer. Its light produces partially still visible light in the deep blue to near UV range having a spectrum with significant peaks around 436nm, 406nm and 367nm which is shown in Figure 5-20.

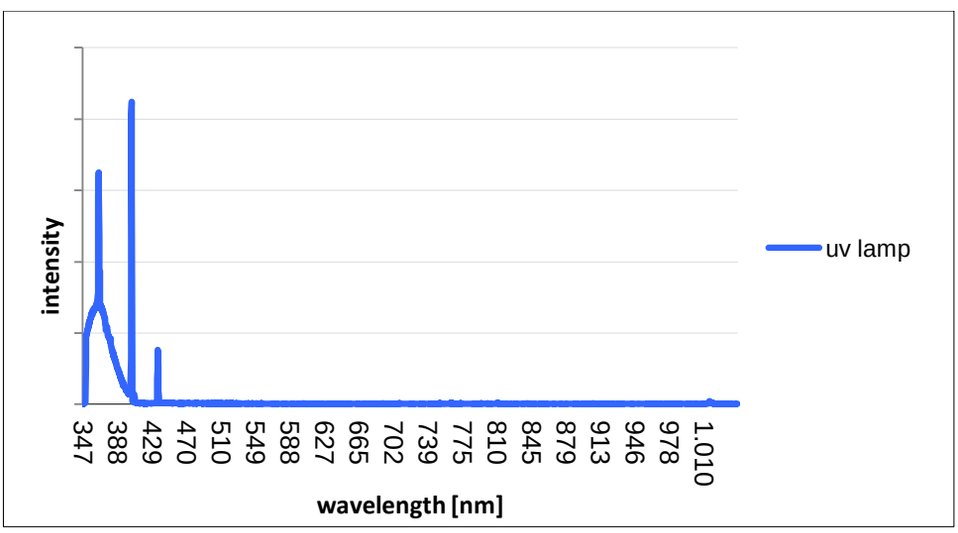

Figure 5-20: Complete spectrum of the used ultra-violet lamp with significant peaks around 367nm, 406nm and 436nm.

The analysis of recorded spectral data from the reflection of light from this lamp at glue-filled (Kauramin®) knotholes shows that there is a strong remission of light with wavelengths around the main peek in the UV range of the UV lamp's spectrum, refer to Figure 5-21. Additionally there exists a fluorescence effect in this adhesive which can also be seen from Figure 5-21. Stimulated with light only from the near UV range, an emission in the whole visible range of the spectrum from 390nm to 780nm is taking place. The maximum intensity thereby is in the band of 470-530nm, resulting in a bluish colour, refer also to the photography in Figure 5-23. Additionally, fluorescence with emission in the upper red around 710nm, 740nm and 760nm can be observed from the measured spectrum but can be seen as well in the photography from reddish colours. It can be shown by comparison with the reflecting spectra at resin pockets that this fluorescence in the red band is originating from the surrounding wood, the reddish colour can be seen in Figure 5-23.

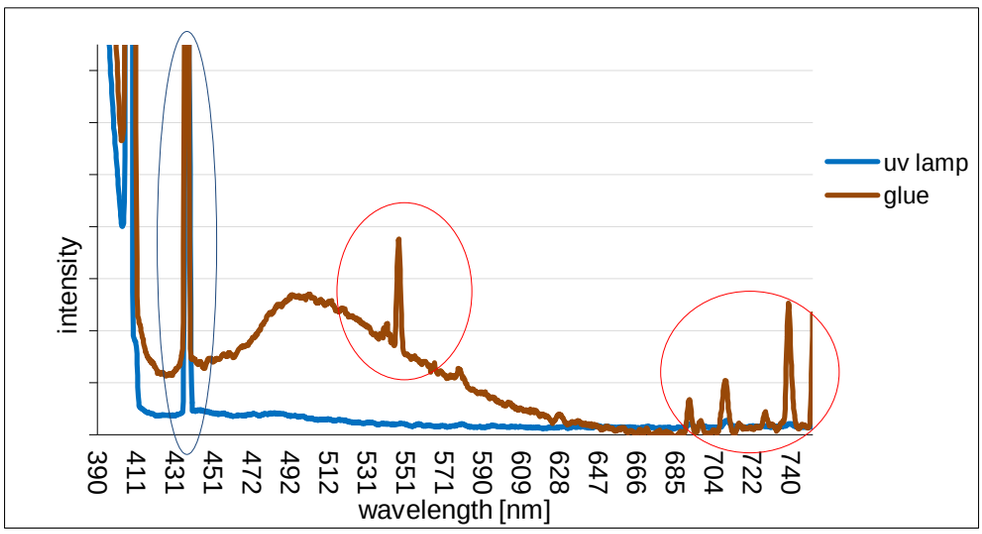

Figure 5-21: Fluorescence at glue: VIS-range of the spectrum comparing excitation and emission spectra, Red circled peaks result from fluorescence effect at surrounding wood (reddish colour). (Blue circled peak indicated remission).

Figure 5-22: Photography (VIS) of glue-filled knothole.

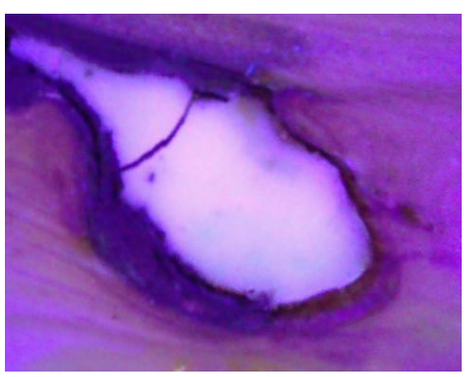

Figure 5-23: Photography (UV) of glue-filled knothole showing fluorescence at area with glue (note the light bluish, white colour) and fluorescence at the surrounding wood (reddish colour), refer to the measured emission spectrum in Figure 5-21.

Analogous to the glue-filled knothole, the analysis of spectral data taken from the reflected light at resin pockets shows significant characteristics that can be exploited for an optimized detection. The stimulation with light having wavelengths below 400nm (near UV) results in an emission of light with a different wavelength which is shown in Figure 5-24; the fluorescence mainly produces light around 550nm to 580nm in the visible range of the spectrum resulting in a yellowish colour, refer also to the photography in Figure 5-26. Unlike with the Kauramin adhesive only fluorescence can be identified, there exists no such strong remission in the near-ultra violet range.

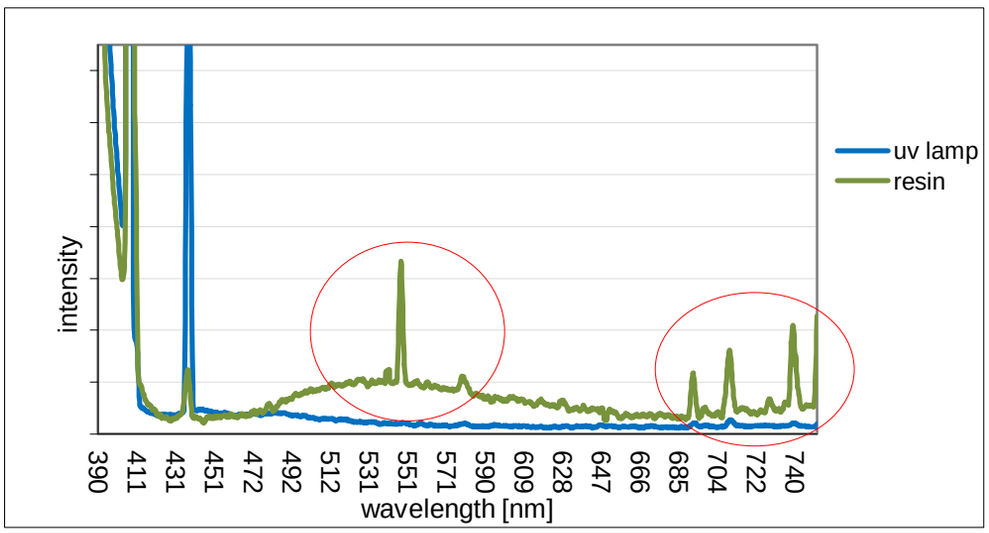

Figure 5-24: Fluorescence at resin: VIS-range of the spectrum comparing excitation and emission spectra. Red circled peaks result from fluorescence effect at surrounding wood (curve around 550nm is perceived as yellowish colour at resin and around 700m as reddish at sound wood).

Comparing the spectra (Figure 5-21, Figure 5-24) one can see that besides the presence of the different defects the fluorescence with emission of light at wavelengths 550nm, 710nm, 740nm and 760nm is taking place. Therefore this fluorescence must be caused by the surrounding wood which can also be seen in both images (Figure 5-23, Figure 5-26) by a reddish colour in the sound wood surrounding the defect.

Figure 5-25: Photography (VIS illumination) of resin pocket and leaked resin.

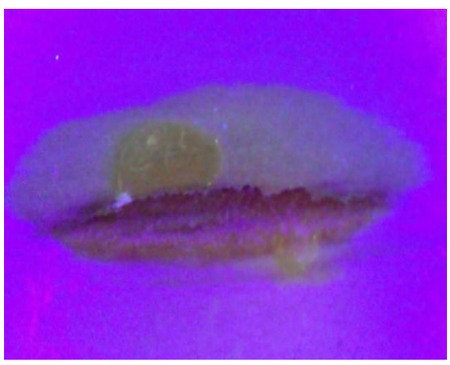

Figure 5-26: Photography (UV illumination) of resin pocket and leaked resin showing fluorescence at area with resin. Note the yellowish colour.

These findings (fluorescence at Kauramin-glue and resin, UV-remission only at glue) can now be used to setup three detection channels tailored to the detection of the common glue-filled knothole on solid wood panels and to the detection of the resin pocket on solid wood panels as well as on plywood panels. This setup is described in more detail in the following sections.

5.2.3.2 Fluorescence evaluation

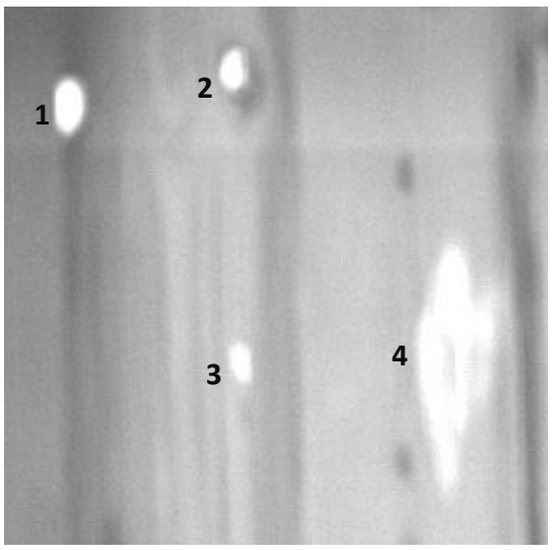

Figure 5-27: Image showing glue-filled holes (1&2), smeared glue (3) and lake of resin (4) on a wooden panel (spruce) in VIS spectrum as the result of fluorescence.

As can be seen from the spectral data acquired at both the resin and the glue there is light emitted in the visible range of the spectrum as the result of fluorescence. Figure 5-27 shows an UV-illuminated image acquired with a camera equipped with a VIS bandpass filter blocking the excitation wavelength. Therefore bright areas in the image identify areas with fluorescence. Although the signal shows high contrast and allows a stable detection and segmentation in principle, no differentiation between glue and resin is possible.

5.2.3.3 UV remission evaluation

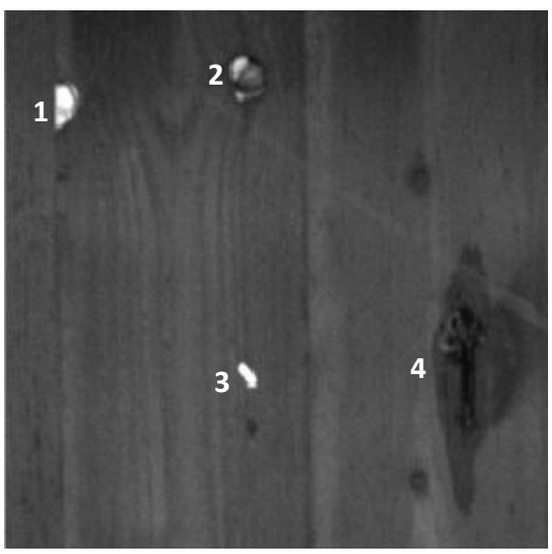

Figure 5-28: Image showing glue (1, 2 &3) as the result of remission of UV light on wooden panel (spruce). Note that the resin (4) is showing less remission.

Figure 5-28 shows an image acquired with a camera equipped with an UV-bandpass filter, blocking all light with wavelength above 400nm, therefore showing only reflected UV light. As already illustrated in the spectrum (Figure 5-21) the glue (Kauramin®) is reflecting the light with wavelength below 400nm besides fluorescing visibly. Comparing the images in Figure 5-27 and Figure 5-28 one can see from area (2) that the area of the glue-filled knothole is not complete and not homogenous in the remission image compared to the fluorescence image. This is due to (2) being a combination of a plug of glue covering only a part of the hole (brighter part) and the bottom of the knothole which is the core layer with a thin film of glue on top (darker part). Due to less intense illumination at the knothole's bottom (thickness of top layer approximately 5 mm) the response there is much weaker. The dark area (4) is identified as a leaked resin pocket.

5.2.3.4 UV absorption evaluation

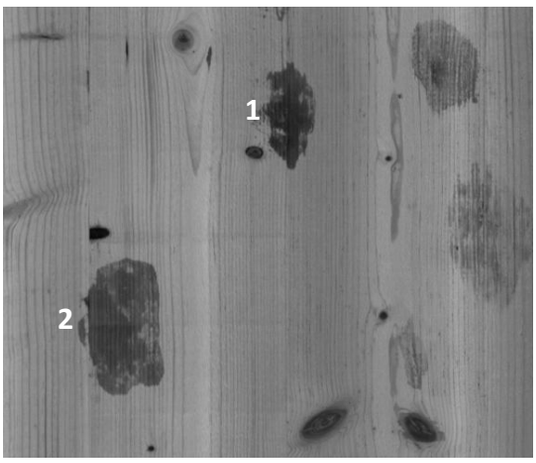

Figure 5-29: Image snippet of wooden panel (larch) showing UV absorption on resin (1 & 2).

In the UV remission image (Figure 5-28) areas with resin (4) can be identified as black areas due to strong absorption of the UV light (no UV-reflection, only fluorescence; refer to spectrum in Figure 5-24). Figure 5-29 illustrates the same effect on a solid wood panel made from larch. The use of the absorption evaluation is in an indirect detection: Starting with the fluorescence image that is suitable to segment areas of interest, the discrimination between glue and resin can be made using the absorption image showing resin as dark areas and glue (still) as bright areas. Due to varying contrasts the absorption image is not seen to be sufficient for detection solely by itself. Therefore the both images have to be registered to be able to compare the gray levels at corresponding locations

5.2.4 Summary

Initially this chapter verified the detection respectively the segmentation capabilities on image data using standard techniques like colour imaging, spatially resolved structural measurement (scatter) and depth measurement (triangulation). Several defect types were identified that can only be unsatisfactorily detected by using these standard techniques. By analysis of the extended reflection spectra including UV and IR light, the gaps in the defect catalogue concerning a reliable detection could be closed, identifying special, spectral optimized detection techniques working in the UV band of the spectrum and incorporating fluorescence, remission and absorption effects. The extended verification matrix including these new techniques is given in Table 5-6 and Table 5-8. A more simplified symbolic coding and assessment (Table 5-7) is thereby used indicating which channel is suitable for segmentation (S) and which channels contribute with features (F) while the colour coding is indicating the importance respectively the contribution.

	Colour	Scatter	3D	UV Fluorescence	UV Remission	UV Absorption	IR	Thermo-graphy
Sound knot	F,S	F,S	F		F		F	F
Cracked Knot	F,S	F	F		F		F	F
Dark Knot	F,S	F,S	F		F		F	F
Loose Knot	F,S	F	F		F		F	F,S
Ringed Knot	F,S	F	F		F		F	F
Knot with bark	F,S	F,S	F		F		F	F
Knothole	F	F	F,S	F	F		F	F
Knothole with glue (Kauramin)	F			F	F	F		F
Crack	F,S	F	F		F		F	F
Resin Pocket	F	F	F	F	F,S	F,S	F	
Pressed-in particles	F	F	F					F,S
Discoloration	F,S						F	
Fungal decay	F,S	F,S		F	F	F		
Glue (Kauramin)	F			F,S	F	F		

Table 5-6: Verification matrix for detection of defects on solid wood panels incorporating specifically optimized detection techniques.

	No detection if used alone
	Unstable detection if used alone
	Stable detection if used alone

- F: Contribution with features
- S: Used for segmentation

Table 5-7: Colour coding and legend for verification matrix, incorporating specifically optimized defect detection techniques.

	Colour	Scatter	3D	UV Fluorescence	UV Remission	UV Absorption	IR	Thermo-graphy
Sound knot	F,S	F,S	F		F		F	F
Cracked Knot	F,S	F	F		F		F	F
Dark Knot	F,S	F,S	F		F		F	F
Loose Knot	F,S	F	F		F		F	F,S
Ringed Knot	F,S	F	F		F		F	F
Knot with bark	F,S	F,S	F		F		F	F
Knothole	F	F	F,S	F	F		F	F
Crack	F,S	F	F		F		F	F
Resin Pocket	F,S	F	F	F	F,S	F,S	F	
Roughness	F	F	F,S		F		F	
Shells	F	F	F					F,S
Pressed-in particles	F	F	F					F,S
Discoloration	F,S						F	
Fungal decay	F,S	F,S		F	F	F		
Glue (urea-formaldehyde)	F,S	F					F	F

Table 5-8: Verification matrix for detection of defects on plywood incorporating specifically optimized detection techniques.

	No detection if used alone
	Unstable detection if used alone
	Stable detection if used alone

- F: Contribution with features
- S: Used for segmentation

Colour coding and legend for verification matrix, incorporating specifically optimized defect detection techniques.

To some defect types a perfect detection (green) cannot be assigned, in these cases the segmentation will produce much more false alarms which must then be identified by the classification that therefore incorporates all the information (features) from the other channels.

5.3 Defect classification system

So far the system architecture with its underlying modular, extendable approach identifying the responsibilities in the processing chain, the sensor data fusion and the detection and segmentation based on different imaging techniques have been presented in this chapter. This sub-chapter finally addresses the classification approach that has already been mentioned in chapter 4 and which is based on the research methods introduced in chapter 4, specifically in 4.1.2 and 4.1.3. A defect classification system is developed that utilises in the training phase a cascaded approach with unsupervised machine learning (SOM) for the preparation of the data sets (training and testing) carried out interactively by a wood-working expert. These data sets are then used for supervised learning with SVMs. This covers the identified requirement to base the learning approach on examples given by defect images describing not only the different defect types but also aesthetic properties (refer to 4.1).

Based on the multi-sensorial approach which has been described in section 5.1, registered image data from the incorporated sensors (colour, ultra-violet, infrared, range, scatter, etc.) is present and from section 4.1 a method is available allowing feature engineering to be waived. Therefore no compromise must be made with loss of information for the purpose of reducing computational complexity. It is therefore possible to use the raw image data itself containing maximum information content. This is in principle the approach tested by Ziadi *[Ziadi et al. 2007]* using a non-segmenting approach with tiles of 5x5 pixels from colour images to be fed directly to the classifier, but which showed to be impractical due to very slow convergence of the used neural network classifier. Modern classification algorithms like the SVM have overcome this delimitation and even perform better with rising feature space dimensionality; this has been already supported by theory in section 4.1.3.

5.3.1 Principle of cascaded training

The basis for classification is formed by independent training, testing and validation data sets which are taken from a comprehensive image snippet data base. At least several thousand image snippets must be presented to the classifier in the training stage to cover the bandwidth of appearance of natural defects especially when incorporating aesthetic aspects. While defect image snippet extraction is the result of the segmentation process (Defect Candidate Map, refer to 5.1.2.1), labelling the snippets involves manual labour from an expert. To be able to manage the huge data sets and to carry out fast overall re-training with newly added image snippets, this labelling process must be supported by automation. For this purpose the cascaded approach for the training of defect classification on wooden panels on the basis of multi-dimensional image is used. This principle is illustrated in Figure 5-30:

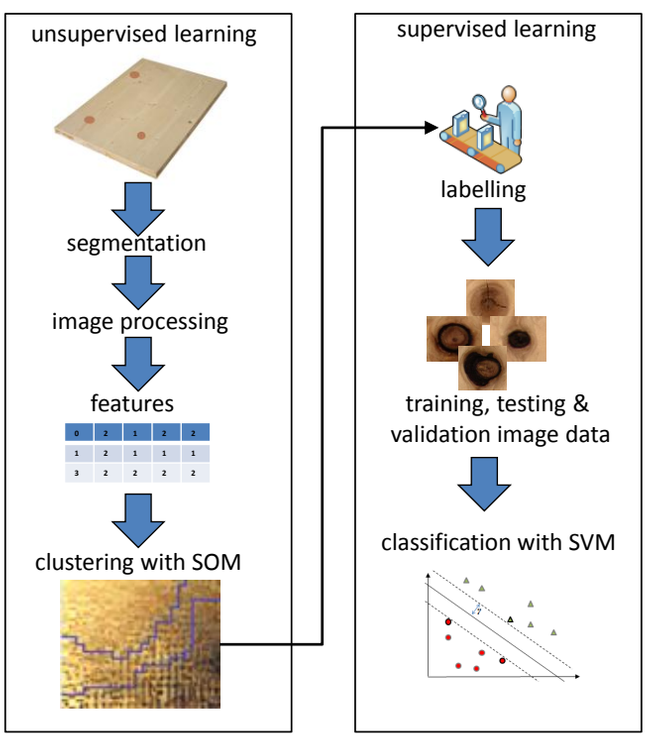

Figure 5-30; Principle of cascaded training.

For pre-sorting the huge amount of sample image snippets in advance to assignment of class labels the SOM is perfectly suited as it generates a two-dimensional sorted representation of the registered multi-dimensional image tiles represented by the colour image snippet; refer to 4.1.2 and to Figure 5-30. The time saving when class labels need only to be assigned by hand to the outliers of a previously executed grouping by similarity is obvious. Therefore the

limited accuracy of the SOM based only on some selected features containing colour, texture, shape and structural measures does not carry weight.

An exemplary training data set generation by using a SOM for grouping the training image snippets from the segmenting approach is shown in Figure 5-31. The user (usually a wood working expert) can adjust or newly define the boundaries between the clusters, move single samples among the distribution and is able to set or change class labels. In the case of multi-channel image snippets the colour channel serves for visualization.

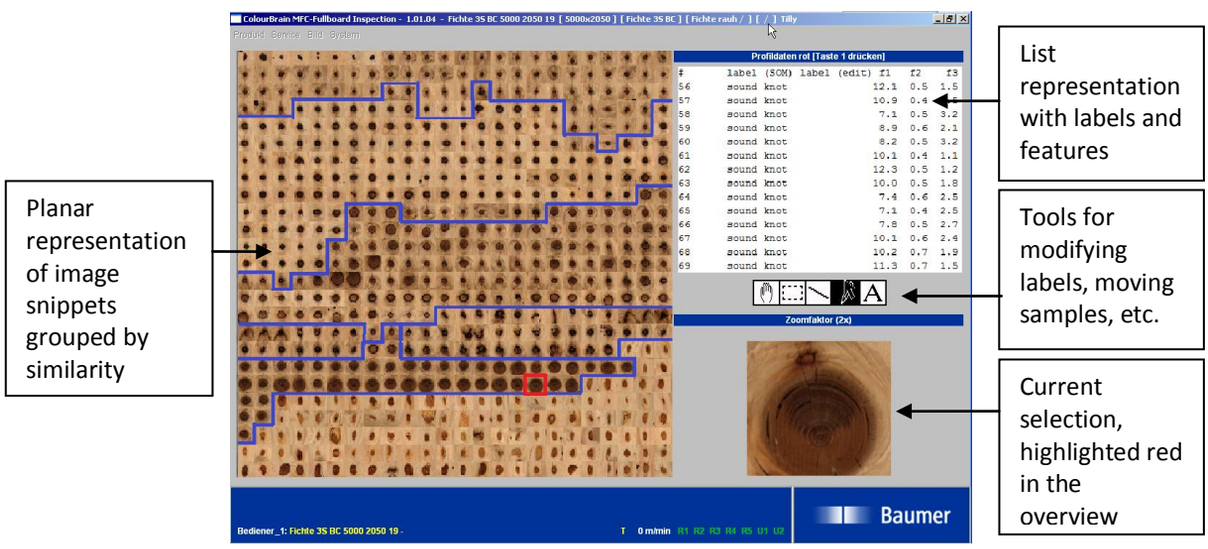

Figure 5-31: Pre-sorting of training data (images) using *ColourBrain® SOM* user interface.

The output of the tool is a folder structure containing the training images in separate folders labelled with the defined class label, so that it can be easily imported to the training of the supervised learning.

5.3.2 Classification of raw pixel data

The Support Vector Machine has been identified as being capable of handling theoretically infinite-dimensioned feature spaces and actually is exploiting high feature space dimensionality for the advantages of linear learning machines (Cover's theorem) as has been reviewed in chapter 4.1.3. The classification of raw pixel data in contrast to explicitly calculated and selected features is therefore possible, leaving the extraction of valuable features to the classifier. The input to the SVM in the training stage as well as in the online classification is therefore the serialized pixel data from the registered multi-channel image snippets (refer to 5.1.1) extracted by the segmentation (refer to 5.1.2.1). This principle is shown in Figure 5-32:

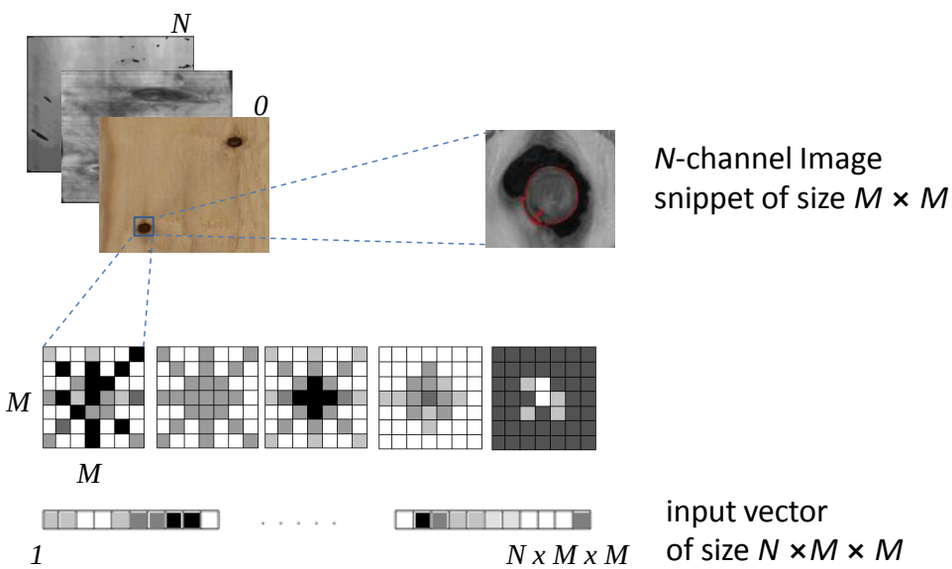

Figure 5-32: Principle of multi-channel raw pixel data serialized to feature vector.

With reference to 4.1.3, Figure 4-9, the SVM is then built literally by multi-channel image snippets serving as support vectors as illustrated in Figure 5-33. Every input vector containing the serialized pixel data that represents a defect candidate to be classified in the online procedure is then compared with the support vectors. Non-linear transformation and calculation of the inner product which is carried out implicitly by the kernel function is thereby incorporated. The position relative to the stored hyperplanes defines the class label.

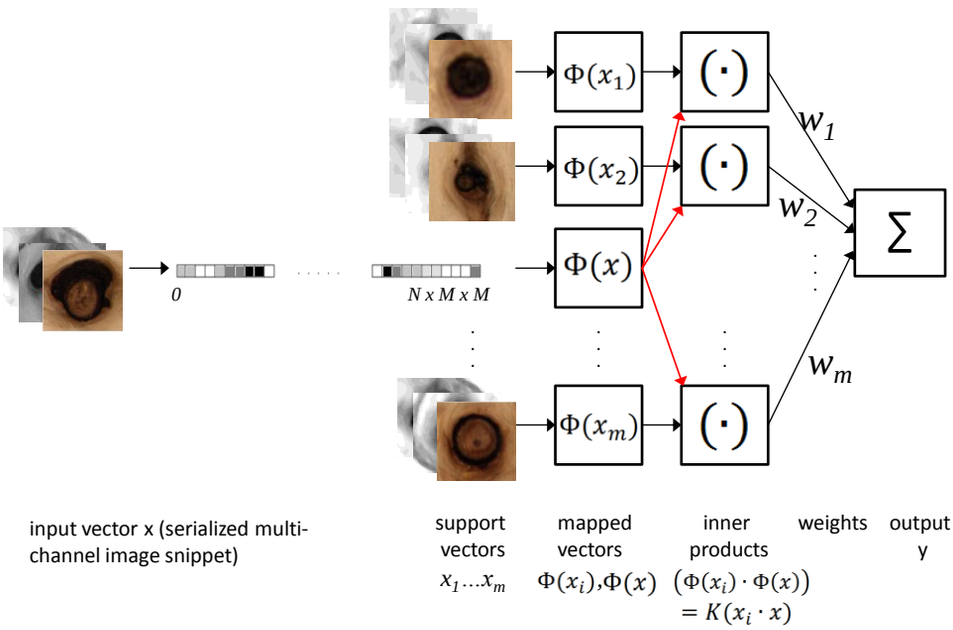

Figure 5-33: Illustration of raw pixel data used for SVM-classification. The input pattern is compared to the support vectors (red arrows) by mapping and calculating the inner product in one step using kernel function.

As the segmentation approach is producing areas of interest of variable size around the possible defect candidates, the N-dimensional image snippets must be resized to a standard size to be fed to the classifier. The standard size used in the prototype setup is set to 85 x 85 pixels, resulting in a feature vector of 65025 elements in length ([85 x 85] x [R-colour + G-colour + B-colour + Scatter + Range + UV-fluor. + UV-rem. + UV-abs. + IR]) for a fully equipped multi-sensor setup (refer to 5.2.4). Due to the different value ranges of the channels normalization of the feature vector is incorporated.

5.3.3 Incorporating a priori knowledge

The resizing of the *N*-dimensional image snippets in advance to serialization into a feature vector results in a certain loss of information about the actual defect size. The defect size nevertheless is relevant and valuable information (e.g. the similar looking dark knot and loose knot actually differ mainly in size, having the same cause, refer to chapter 2, specifically to 2.2.1.2.1). Therefore this size information must be incorporated again appropriately in the feature vector. This is done by extending the serialized image data (refer to 5.3.2 respectively to Figure 5-32) by a so-called *A Priori Knowledge Feature Vector Extension* (APKFVE). This extension is shown in Figure 5-34.

By using this approach, further valuable information that is obtainable from the *Defect Candidate Map* (refer to 5.1.2.1) can be incorporated, for example:

- Symmetry information: e.g. defect is individually placed or defect is in a row (plywood only, due to peeling)
- Neighbourhood information: class affiliation of already classified defects in the direct vicinity, valuable for aesthetic evaluation (defect cluster criteria, refer to quality standards in 2.2.3)

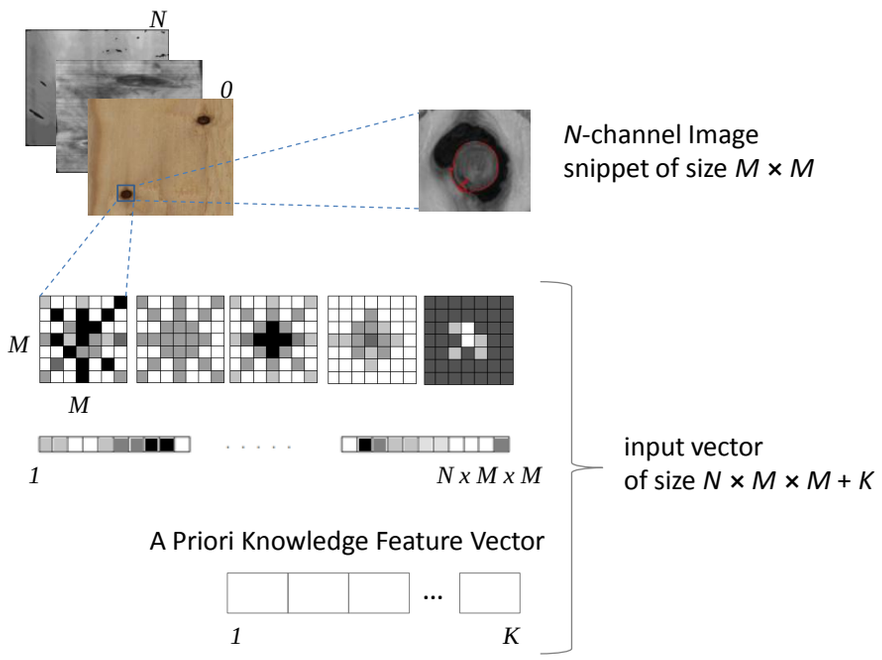

Figure 5-34: Principle of feature vector extended by a priori knowledge.

5.3.4 Summary

The setup of the final classification system of the scanner for automated detection of defects on wooden panels has been explained in detail. The issue of learning from examples is addressed by a database containing several ten thousand image snippets of wood defects gained from the segmentation on which the training of the classifier is carried out. Knowledge from wood working is thus necessary to label the training data set. To support this highly manual labour process, the clustering capability of SOMs is incorporated. The proposed system is thereby capable of fast overall re-training and only a limited amount of image snippets (outliers, noisy samples) usually needs to be labelled manually. Minimized effort in the adaption (for example to a different kind of wood or to new classification guidelines) but also in the installation phase of the system is therefore achieved. Raw pixel data from the segmenting approach extended by a priori knowledge is used to train a SVM-classifier capable of handling the huge sets of high-dimensional feature vectors to address local aesthetics without using feature engineering.

5.4 Decision making

With reference to 5.1, Figure 5-9, the third layer of the cluster architecture is addressed by this section. The related decision making has already been briefly introduced in 5.1.3. In terms of information flow the defects on the currently inspected wooden panel have been segmented from the image data, descriptions (for example defect contour information, mean colour and texture) have been generated and stored in the Defect Candidate Map and the specific defect type has been classified by the defect classification system as discussed in the previous section.

5.4.1 Information flow

In the decision layer the information contained in the defect descriptions is now combined with knowledge related to the rectification process for the specific defect types to be able to define *if* and *how* the detected defects are patched, this principle is illustrated in Figure 5-35:

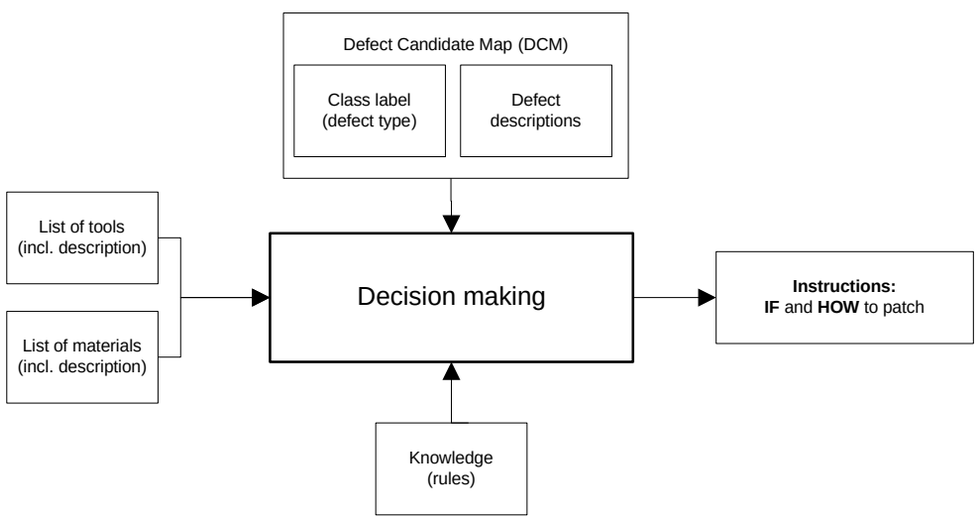

Figure 5-35: Information flow in the decision layer: decision making.

For the decision *if* a rectification of the defect is carried out, the rules which contain the limits of the specific defect types (diameter, depth, etc.) must be incorporated. This first decision then also already determines if pre-processing is necessary as in most cases the rules define specific procedures for specific defects. Dark Knots for example must always be routed to remove the defective wood. These unconditional decisions can easily be based on a look-up table as illustrated in Figure 5-36. The same mechanism (look-up table) can be used when the decision making is free to decide between several types of filling material for the specific defect type (rules often allow different types of filling).

Knotholes in contrary need to be routed only if there is bark involved or when 2K putty is used on the upper side of the panel where bad adhesion is possible due to the glue on the core layer, refer to Figure 5-37 - Figure 5-39. Therefore a sub-process as illustrated in Figure 5-40 must be incorporated in the decision. The list of available tools, for example to make a choice for the most appropriate router diameter and the list of available material, for example in terms of colour options, is then incorporated.

Figure 5-36 illustrates the issue that the rules may either only specify if pre-processing or a certain material needs to be used for the patching of a specific defect type, the corresponding ambiguity must therefore be resolved first in the decision making by identifying valid combinations which can be achieved by an approach using a look-up table.

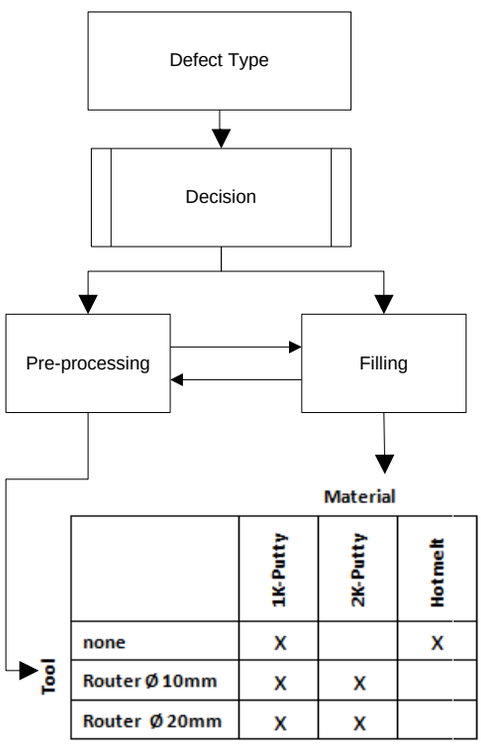

Figure 5-36: Resolving assignment of pre-processing and filling material.

Valuable and necessary information about the defect is gained from the Defect Candidate Map that is generated during segmentation (refer to 5.1.2.1). The rules rely on the descriptions from the DCM about the specific defect but also about its neighbourhood. Figure 5-37 - Figure 5-39 illustrate the previously mentioned example of a knothole that needs to be pre-processed when either bark is present at the border of the knothole or due to adhesion problems with 2K putty when glue is present on the bottom of the knothole (refer to Figure 5-38), or both (refer to Figure 5-39).

Figure 5-37: Knothole with bark (no glue on knothole bottom/core veneer due to bottom side of the panel). Needs routing due to soft/loose bark.

Figure 5-38: Knothole with glue on knothole bottom/core veneer (due to top side of panel). Needs routing due to adhesion when filling with 2K putty.

Figure 5-39: Knothole on top side of panel, therefore showing glue on core veneer and having additionally bark. Needs routing in any case.

Figure 5-40 exemplarily illustrates the corresponding sub-process that needs to be incorporated in the decision making for the knothole that may have bark or glue and which therefore may need pre-processing by routing.

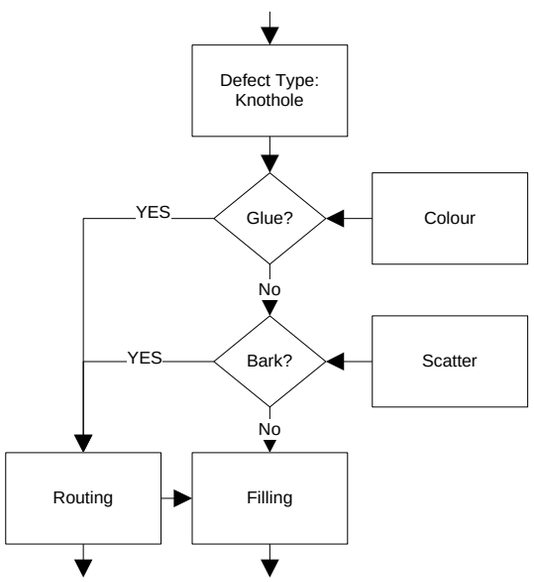

Figure 5-40: Decision process for routing knotholes incorporating neighbourhood evaluation.

The related decision is facing uncertainty in the rule specifying the neighbourhood relationship, for example a typical formulation is *"..knotholes are allowed to show some bark..."*, refer also to 2.2.3.1 and 0. The Fuzzy Inference System (FIS, refer to research methods chapter, 4.2.3) is incorporated here as it can handle such uncertainty and additionally provides a user interface with adjustment possibilities for the membership functions which are related to the adjectives introducing the uncertainty in the rules, refer to A.3.1 and Table 5-12.

5.4.2 Definition of fuzzy rules at the example of Knothole with bark

In the following the Expert System for patching defects on wooden panels based on a Fuzzy Inference System is designed and set up. First the rules in *if...then* – notation are formulated. The input and output variables can therefrom then be defined. A FIS is setup and the segmentation of the n-dimensional input space by the rules, respectively the parameterization of the membership functions associated to the input values, is illustrated. The rules are grouped in relation to the three main aspects of patching for each defect:

- Group 1.x: Main decision IF and HOW to patch principally
- Group 2.x: Addressing local aesthetics, e.g. neighbourhood appearance
- Group 3.x: Incorporation of overall panel appearance

At the example of the *Knothole with bark* on a solid wood panel of **appearance quality II** (Table 2-1 in 2.2.3.1) it is illustrated in the following how the Expert System is setup. At first the rules of group 1 address patching in principle, in this example based on the presence of bark and the diameter of the hole:

rule no.	*If-then* formulation	*Comment*
rule 1.1	IF (*bark* is some) OR (*glue* is some) AND (*diameter* is big) THEN (*pre-processing* is **routing**)	Bark bigger than a certain size and glue, both need to be routed at bigger holes
rule 1.2	IF (*bark* is little) AND (*diameter* is small) THEN (*pre-processing* is **none**)	Small holes shall stay small when there is not much bark, therefore no routing
rule 1.3	IF (*bark* is little) AND (*diameter* is too small) THEN (*pre-processing* is **none**)	Do not rectify, diameter below threshold (5mm)
rule 1.4	IF (*bark* is little) AND (*diameter* is too small) THEN (*filling* is **none**)	Do not rectify, diameter below threshold (5mm)

Table 5-9: Rule set group 1.x on *if* and *how* to patch knothole with bark in principle.

Applying the rules from group 1 results in a first segmentation of the input space by a decision surface indicating in principle if patching will take place. By additionally incorporating the rules from group 2 and group 3, which focus the choice of the filler, the appearance is taken into account and the decision surface will be biased:

rule no.	*If-then* formulation	*Comment*
rule 2.1	IF (*diameter* is medium) AND (*shape* is unround) THEN (*pre-processing* is **routing**)	Small to medium holes which are not round-shaped shall be routed to appear smooth
rule 2.2	IF (*diameter* is medium) AND (*grain* is strong) AND (*clustering* is low) THEN (*filling* is **circular-textured dowel**)	Try to adapt the patch to surrounding texture by choosing textured dowel
rule 2.3	IF (*diameter* is medium) AND (*grain* is weak) AND (*clustering* is low) THEN (*filling is* **homogenous-coloured dowel**)	Try to hide the patch by avoiding contrast in texture using untextured dowel
rule 2.4	IF (*diameter* is big) OR (*clustering* is high) THEN (*filling is* **2K-putty**)	Prevent clusters of dowels and unintended overlaps but use 2K because of shrinkage
rule 2.5	IF (*diameter* is small) OR (*clustering* is high) THEN (*filling is* **1K-putty**)	Prevent clusters of dowels and unintended overlaps as well as excessive routing (smear the area with 1K)

Table 5-10: Rule set group 2.x on appearance (decision between dowels, putty and options).

Incorporating additional rules that address the preference(s) concerning the overall appearance of the panel will bias the input space segmentation additionally by aesthetic aspects:

rule no.	*If-then* formulation	*Comment*
rule 3.1	IF (*target appearance* is knotty) THEN (*filling* is **circular-textured dowel**)	Produce tendentially knotty-looking surfaces using textured dowel
rule 3.2	IF (*target appearance* is calm) THEN (*filling* is **homogenous-coloured dowel**)	Produce tendentially homogenous-looking surfaces
rule 3.2	IF (*target appearance* is calm) THEN (*filling* is **1K-putty**)	Produce tendentially-homogenous-looking surfaces
rule 3.3	IF (*target appearance* is calm) THEN (*filling* is **2K-putty**)	Produce tendentially homogenous-looking surfaces

Table 5-11: Rule set group 3.x incorporating overall panel appearance.

To every adjective (some, weak, calm, etc.) related to the input variables (bark, diameter, grain, etc.) contained in the rules, a set of membership functions is linked which models the uncertainty. Table 5-12 lists all membership function involved with the rules above:

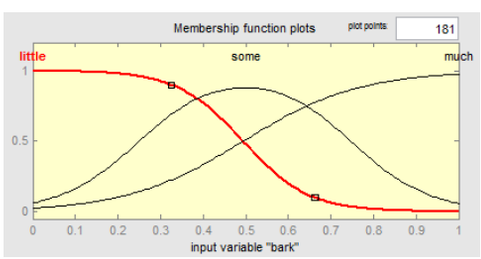

Figure 5-41: Membership functions for “bark”.

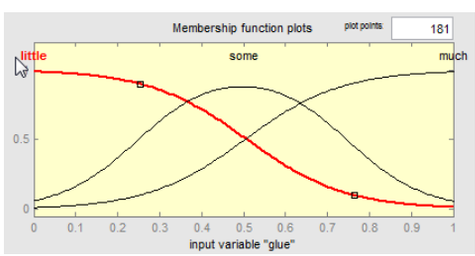

Figure 5-42: Membership functions for “glue”.

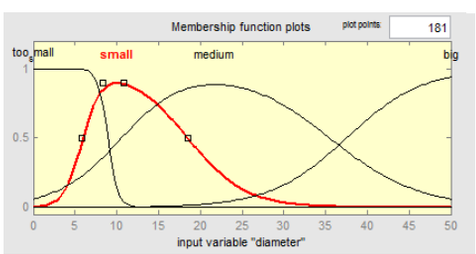

Figure 5-43: Membership functions for “diameter”.

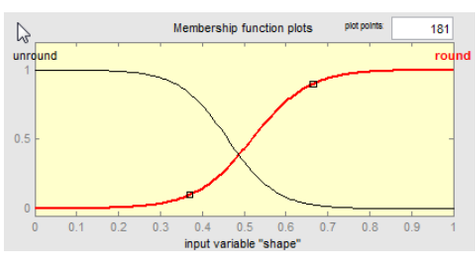

Figure 5-44: Membership functions for "shape".

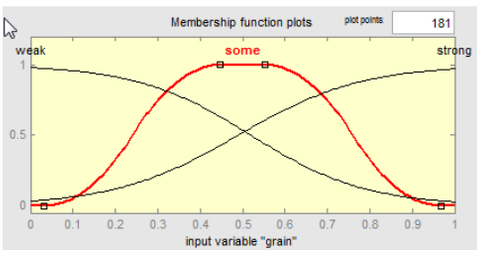

Figure 5-45: Membership functions for "grain".

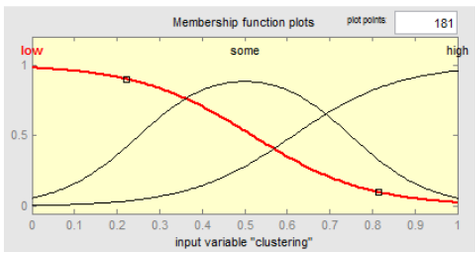

Figure 5-46: Membership functions for "clustering".

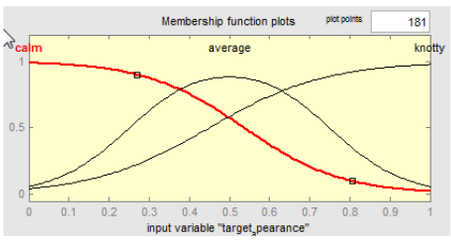

Figure 5-47: Membership functions for "target appearance" (overall panel appearance).

Table 5-12: Membership function used for modelling rules concerning Knothole with bark.

Note the steep function modelling “too small” for input variable *diameter*, which actually represents a threshold. The fuzzification with “too small” and “small” addresses the issue of uncertainty with the diameter of not perfectly round knotholes. Apart from that, the illustrated setup in Figure 5-25 segments the input space quite homogenously. Adjustment of the membership functions can be done graphically, therefore Figure 5-18 to Figure 5-24 represent the graphical user interface to the decision making system for the defect type *Knothole with bark*.

5.4.3 Spanning the decision surface

The above defined rules and related membership functions span a 7-dimensional input space that is segmented according to the output variables *pre-processing* (with possible values *routing* and *no routing*) and *filling* (with possible values *1K-putty, 2K-putty, circular-textured dowel, homogenous-coloured dowel, no filling*). Table 5-13 lists the two-dimensional combinations of the inputs to illustrate the input-space segmentation towards the output *pre-processing* related to the decision *if* routing is necessary for a specific defect. Red colours indicate no pre-processing while blue colours indicate that pre-processing is needed (for a binary, defuzzified decision output appropriate thresholds still need to be applied). With reference to the membership functions given in Table 5-12 some interpretations are further given to illustrate the concept:

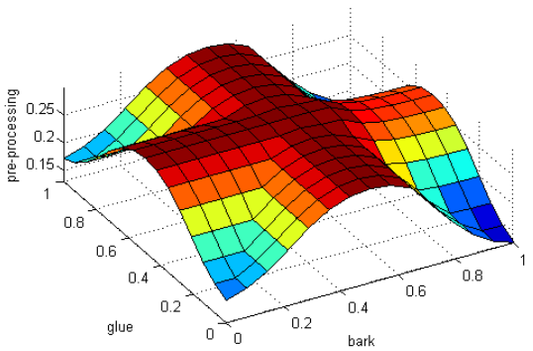

Figure 5-48: Decision surface (pre-processing) bark – glue.

Interpretation: *Some* bark combined with *some* glue indicates potential false detection of bark (actually glue) and the ouput of *no routing* is supported.

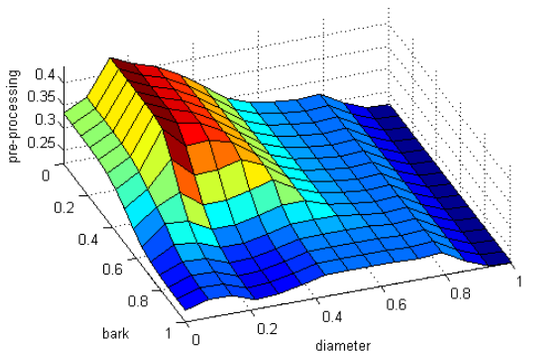

Figure 5-49: Decision surface (pre-processing) bark – diameter.

Interpretation: with rising certainty (*much*) for bark as well as rising diameter (*small* → *medium*) the routing becomes necessary and likely.

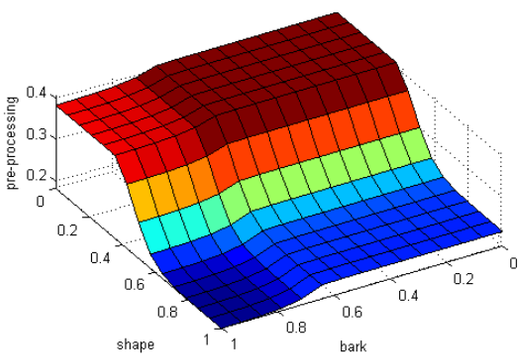

Figure 5-50: Decision surface (pre-processing) bark – shape.

Interpretation: With increasing roundness 'barky' candidates will be routed more likely.

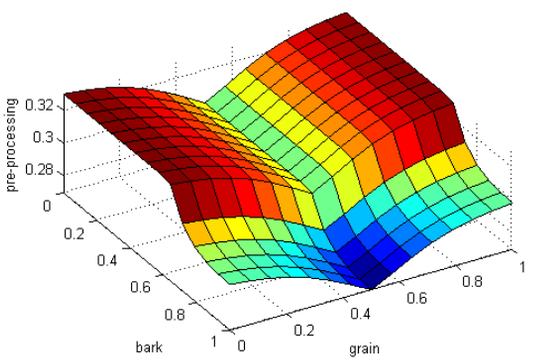

Figure 5-51: Decision surface (pre-processing) bark – grain.

Interpretation: This combination of the two dimensions from the decision space is more relevant for the second output variable *filling* where appropriate textured dowels are prefereed for specific grain surroundings (therefore routing needs to be applied for pre-processing).

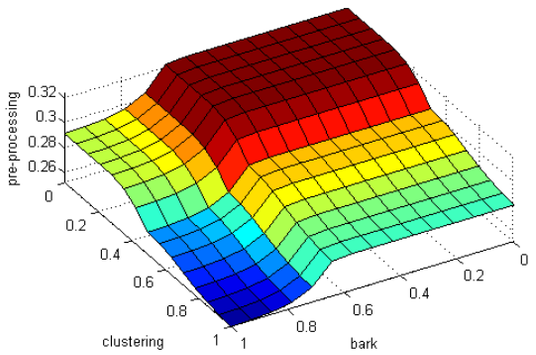

Figure 5-52: Decision surface (pre-processing) bark – clustering.

Interpretation: Part of the rule to avoid clusters of dowels for clustered knot defects and use 2K putty with appropriate routing instead.

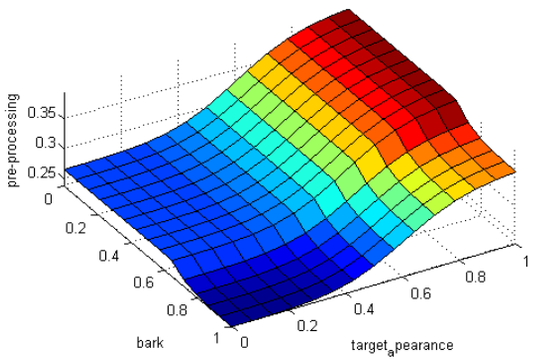

Figure 5-53: Decision surface (pre-processing) bark – panel appearance (overall).

Interpretation: Depending on the intended overall appearance (*calm* ↔ *knotty*) the removal of knot defects including knots with bark is prevented (red) or emphasized (blue).

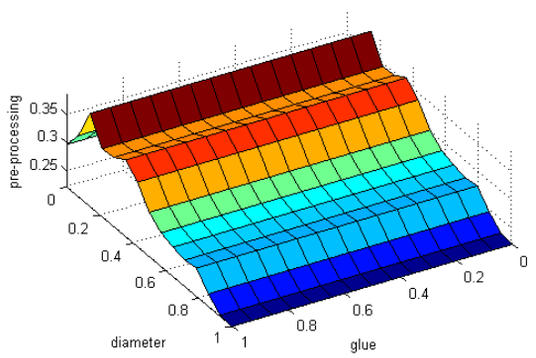

Figure 5-54: Decision surface (pre-processing) glue – diameter.

Interpretation: Removal of glue depending on size.

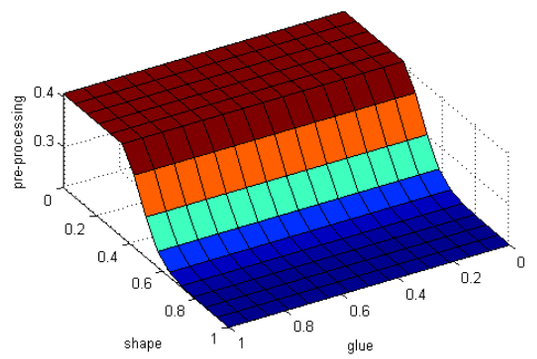

Figure 5-55: Decision surface (pre-processing) glue – shape.

Interpretation: Removal of glue depending on roundness, more round candidates with glue will be routed.

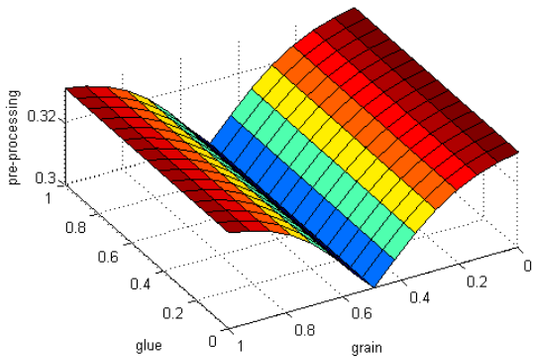

Figure 5-56: Decision surface (pre-processing) glue – grain.

Interpretation: This combination of the two dimensions from the decision space is more relevant for the second output variable *filling* where appropriate textured dowels are prefereed for specific grain surroundings (therefore routing needs to be applied for pre-processing).

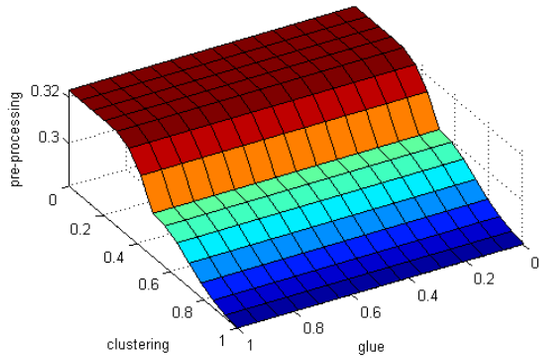

Figure 5-57: Decision surface (pre-processing) glue – clustering.

Interpretation: Part of the rule to avoid clusters of dowels for clustered knot defects and to use 2K putty with appropriate routing instead.

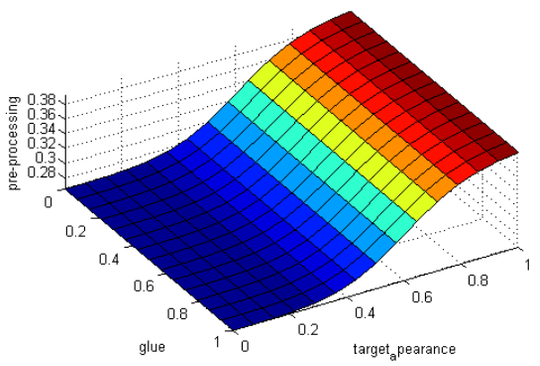

Figure 5-58: Decision surface (pre-processing) glue - panel appearance (overall).

Interpretation: Depending on the intended overall appearance (*calm* ↔ *knotty*) the removal of knot defects is prevented (red) or emphasized (blue). Note: decision to repair/remove knotholes with glue is mainly influenced by type and diameter, with less influence from this combination.

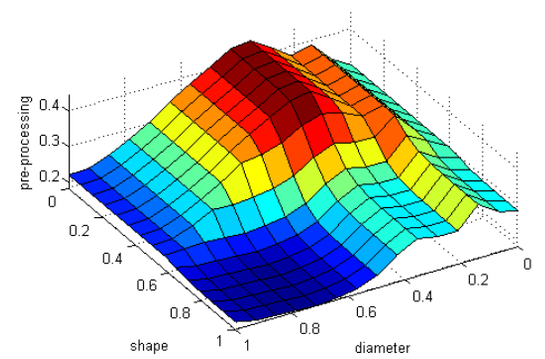

Figure 5-59: Decision surface (pre-processing) diameter – shape.

Interpretation: The combination of roundness and diameter is important for the repair of pinholes and gradually bigger knot defects. Knots with bark are to be routed for better adhesion of 2K putty (necessary due to shrinkage with 1K putty on bigger defects) on glue while pinholes may be filled with 1K putty without routing.

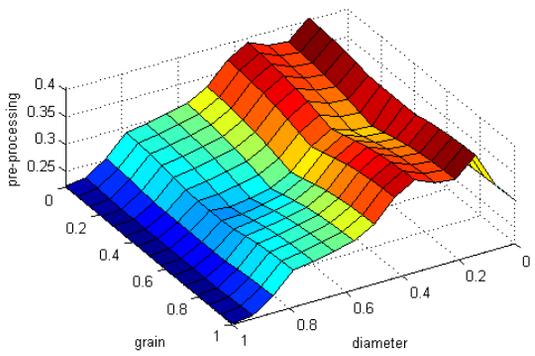

Figure 5-60: Decision surface (pre-processing) diameter - grain.

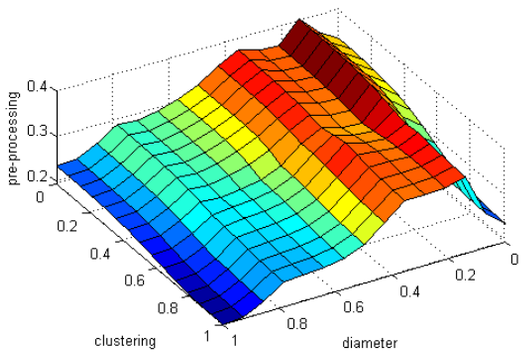

Figure 5-61: Decision surface (pre-processing) diameter – clustering.

Interpretation: The diameter overrules the influence of the information about the surrounding grain (this is more important for the second output *filling*)..

.. also, the clustering is less important on the decision if pre-processing is necessary than it is the diameter information.

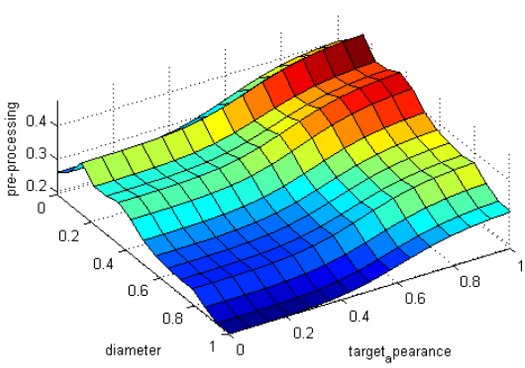

Figure 5-62: Decision surface (pre-processing) diameter – panel appearance (overall).

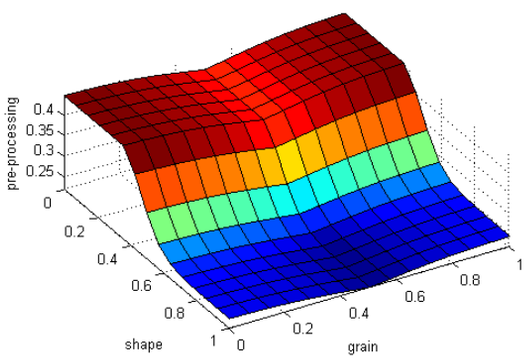

Figure 5-63: Decision surface (pre-processing) shape – grain.

Interpretation: For a calm overall appearance of the panel the bigger defect (knots and knotholes are more important to be removed than smaller ones (of course this is biased additionally by clustering).

Interpretation: Roundness (characteristical for knotholes and knots) mainly influences the decision to preprocess, with only a slight influenceof the surrounding grain (this is more important for the second output *filling*).

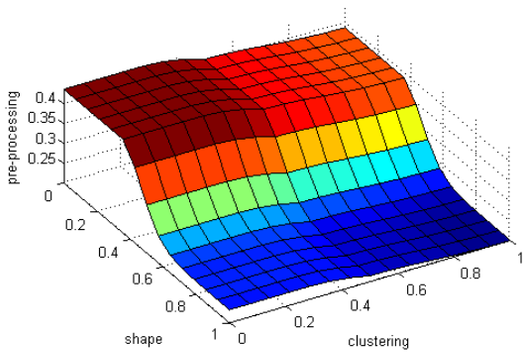

Figure 5-64: Decision surface (pre-processing) shape – clustering.

Interpretation: Knotholes and knots (characterized by roundness) are to be routed for better adhesion of 2K putty (necessary due to shrinkage with 1K putty on bigger defects) on glue.

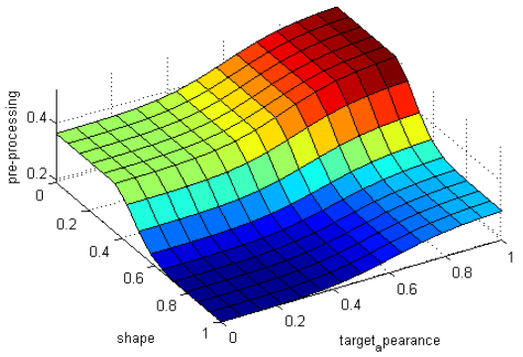

Figure 5-65: Decision surface (pre-processing) shape – panel appearance (overall).

Interpretation: Removal of knots and knotholes is most important to achieve a calm appearance of the final panel.

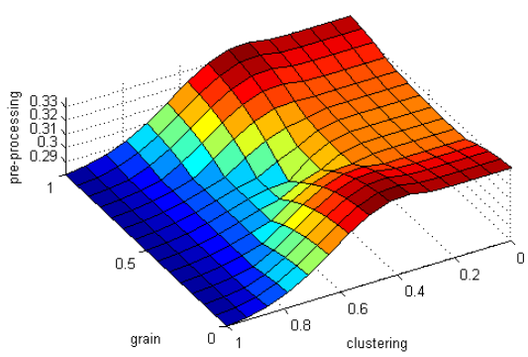

Figure 5-66: Decision surface (pre-processing) grain – clustering.

Interpretation: The rule to prevent clusters of repairs overrules any influence of the grain surrounding in the decision.

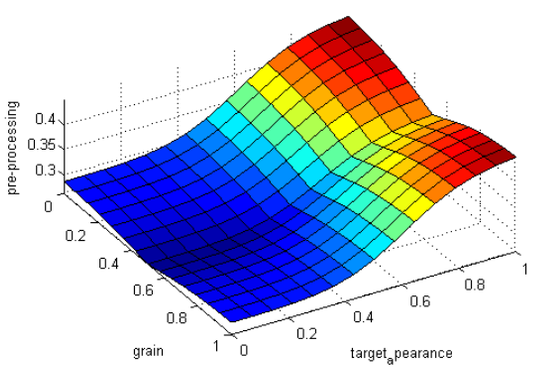

Figure 5-67: Decision surface (pre-processing) grain – panel appearance (overall).

Interpretation: The rule to adapt to the intended final appearance of the panel (*calm* ↔ *knotty*) overrules any influence of the grain surrounding in the decision.

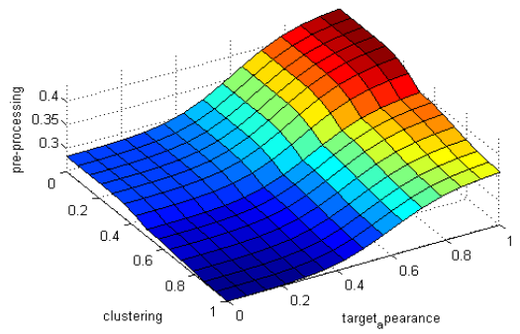

Figure 5-68: Decision surface (pre-processing) clustering – panel appearance (overall).

Interpretation: The rule to adapt to the intended final appearance of the panel (*calm* ↔ *knotty*) overrules any influence of clustered knot defects in the decision.

Table 5-13: Segmentation of decision space towards output "pre-processing"

Analogous, Table 5-14 lists the two-dimensional combinations of the inputs to illustrate the input-space segmentation towards the output *filling* related to the decision *if* and *how* a specific defect is to be patched. (Deep) blue indicates no filling while lghter shades up to red colour indicate gradually (no threshold to produce a crisp, defuzzified output is applied yet) that filling with *1K-putty, 2K-putty, circular-textured dowel, homogenous-coloured dowel,*is needed.

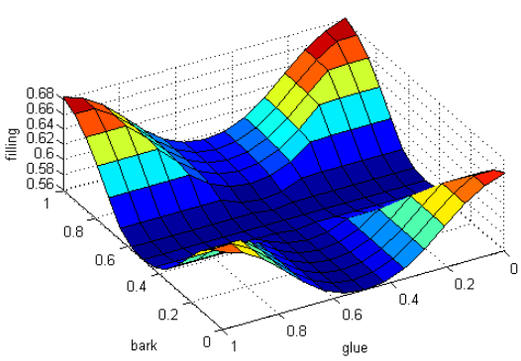

Figure 5-69: Decision surface (filling) bark –glue.

Interpretation: Equivalent to the output *pre-processing*, but inverted in terms of colour.

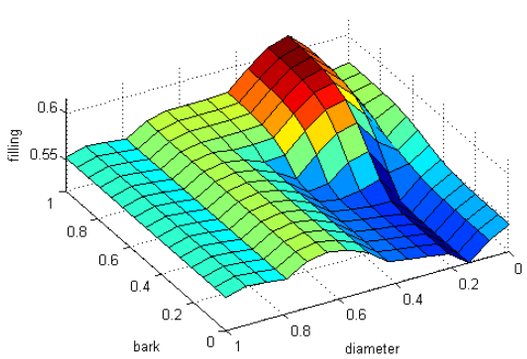

Figure 5-70: Decision surface (filling) bark –diameter.

Interpretation: Rising likelyness for bark as well as rising dimater gradually imply appropriate filling.

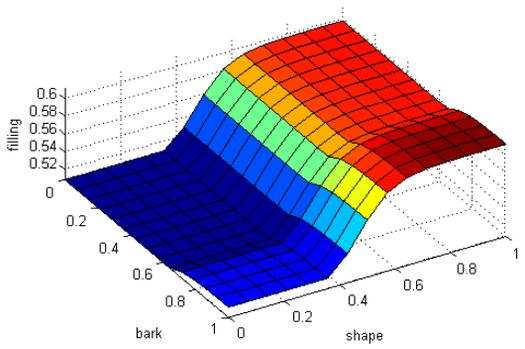

Figure 5-71: Decision surface (filling) bark –shape.

Interpretation: With increasing roundness 'barky' candidates need appropriate filling, equivalent to output *pre-processing*.

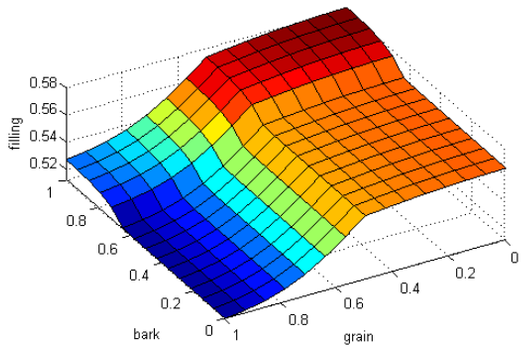

Figure 5-72: Decision surface (filling) bark – grain.

Interpretation: The preservation of a grainy surrounding is taken into account, making a filling unlikely when strong grain is present biased additionally with uncertainty for bark. Filling with putty in contrast is ensured in homogenous areas when bark is most likely.

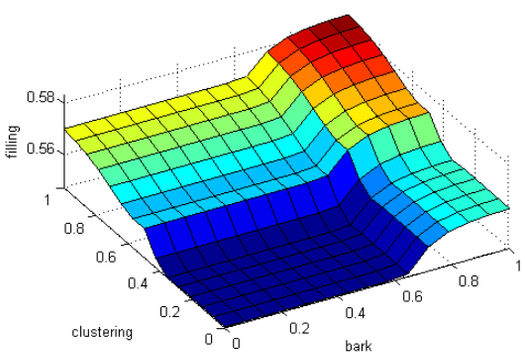

Figure 5-73: Decision surface (filling) bark – clustering.

Interpretation: the use of putty for filling is gradually preferred for clusters of candidates..

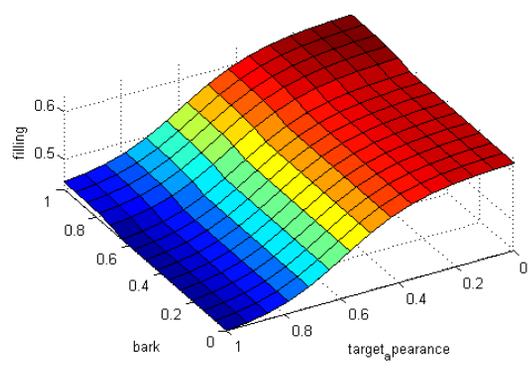

Figure 5-74: Decision surface (filling) bark - panel appearance (overall).

..but must be combined with the superordinated preference for either a *calm* or *knotty* overall appearance.

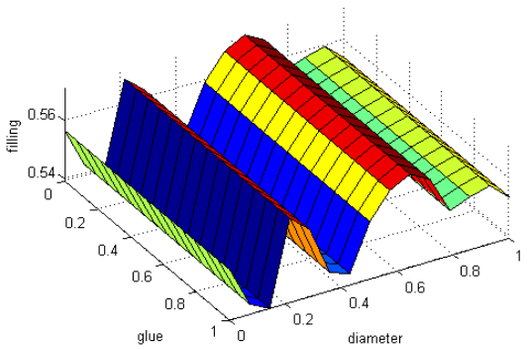

Figure 5-75: Decision surface (filling) glue – diameter.

Interpretation is not realy feasible as there is no real dependency between glue and diameter in terms of the output *filling*. The decision surface is biased by the other combinations mainly.

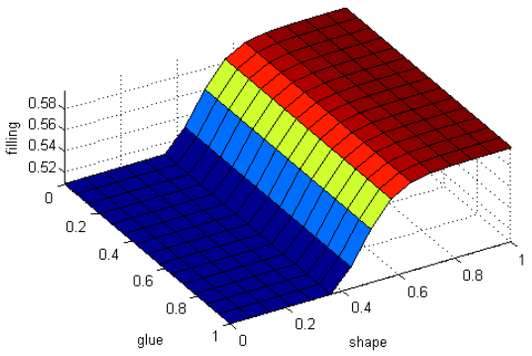

Figure 5-76: Decision surface (filling) glue – shape.

Interpretation: Equivalent to the output *pre-processing* the removal of glue is depending on the roundness, more round candidates will be filled.

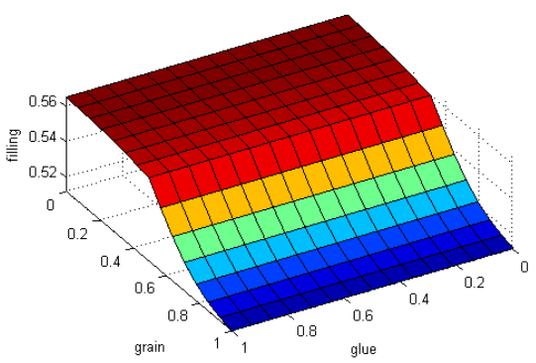

Figure 5-77: Decision surface (filling) glue – grain.

Interpretation: In contrast to the output *pre-processing* the output for *filling* is clearly biased by the presence of a grainy surround which is aimed to be preserved and therefore only homogenous surroundings should be (excessively) filled with putty.

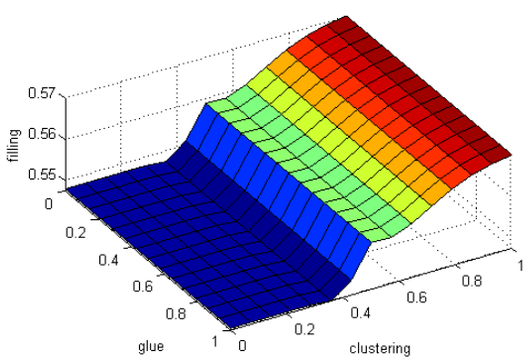

Figure 5-78: Decision surface (filling) glue – clustering.

Interpretation: Equivalent to the output for *pre-processing* this combination is part of the rule to avoid clusters of dowels for clustered knot defects und to used 2K putty instead.

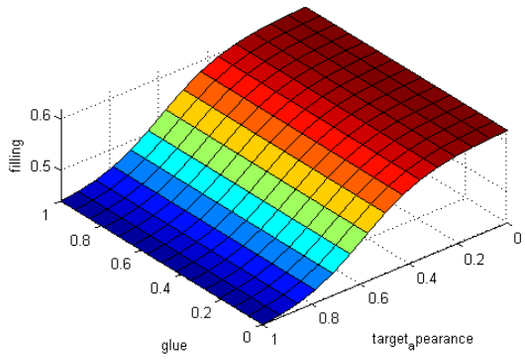

Figure 5-79: Decision surface (filling) glue - panel appearance (overall).

Interpretation: Equivalent to the output *pre-processing* and depending on the overall appearance (*calm* ↔ *knotty*) the removal of knot defects is prevented (blue) or emphasized (red).

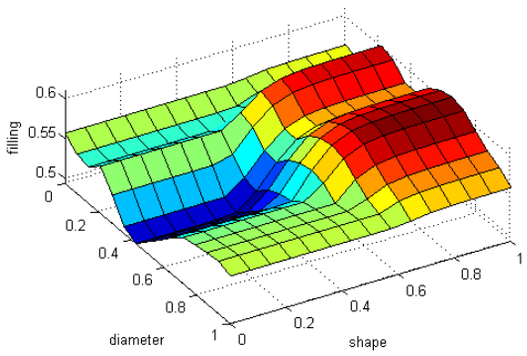

Figure 5-80: Decision (filling) surface diameter – shape.

Interpretation: The doundness and diameter are important characteristics for the repair of pinholes and gradually bigger knot defects. The tendency to to repair/fill bigger defects with 2K putty for the reason to prevent problems with shrinkage is modelled equivalent to the output *pre-processing*.

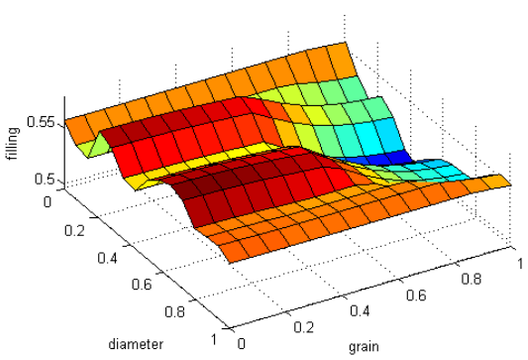

Figure 5-81: Decision surface (filling) diameter – grain.

Interpretation: not really related with each other, this combination shows the overruling property of the input from the surrounding grain, contrary to the influence on the output pre-processing.

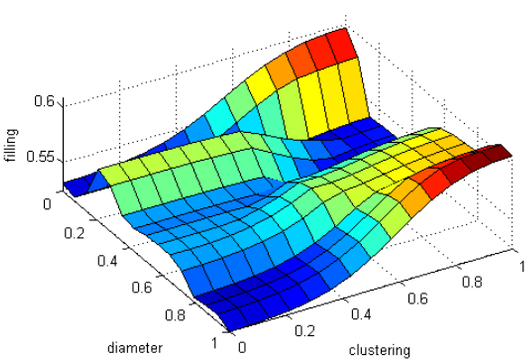

Figure 5-82: Decision surface (filling) diameter – clustering.

Interpretation: Only small and large diameters of Knotholes with bark in combination with high clustering bias the decision towards the filling with putty.

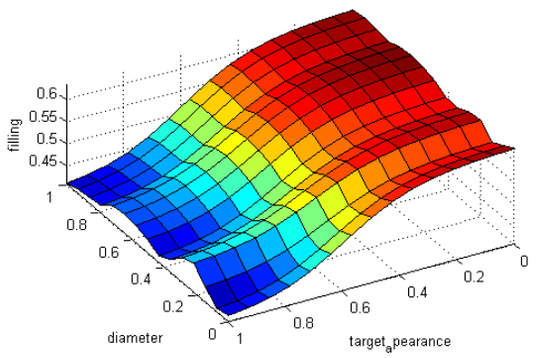

Figure 5-83: Decision surface (filling) diameter - panel appearance (overall).

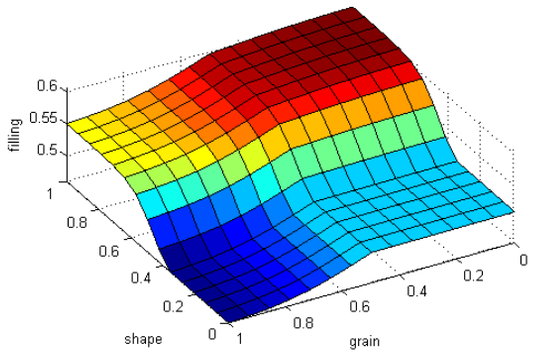

Figure 5-84: Decision surface (filling) shape – grain.

Interpretaion: Analogous to the output pre-processing, for a calm overall appearance of the panel the bigger defects the removal of the candidates is getting more important, additionally biased with increasing size.

Interpretation: The surrounding grain influences the type of filling, with leaving smaller defects in a grainy environment unrepaired and using putty in homogenous surroundings.

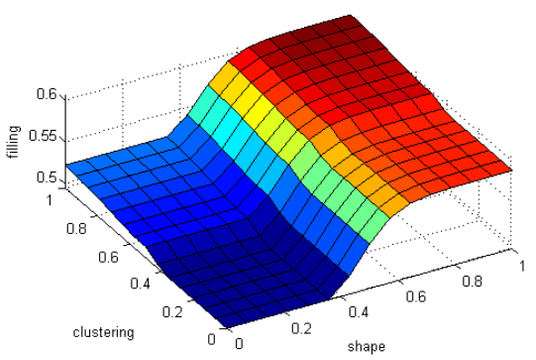

Figure 5-85: Decision surface (filling) shape – clustering.

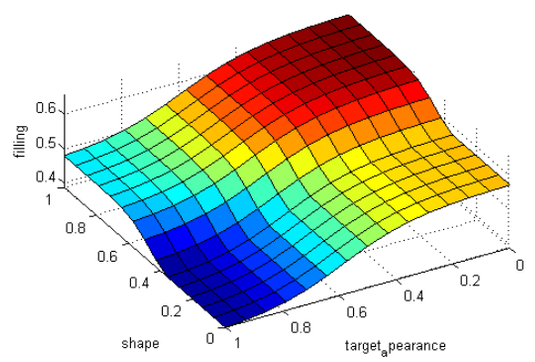

Figure 5-86: Decision surface (filling) shape - panel appearance (overall).

Interpretation is not realy feasible as there is no real dependency between clustering and shape in terms of the output *filling*. The decision surface is biased by the other combinations mainly.

Interpretation: The removal of knot defects is most important to achieve a calm appearance of the final panel, therefore bigger defect need to be repaird for a *calm* appearance while for a *knotty* appearance especially the smaller defects are left unpatched.

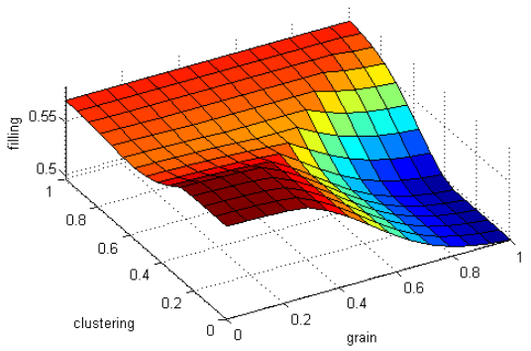

Figure 5-87: Decision surface (filling) grain – clustering.

Interpretation: Equivalent to the output *pre-processing*, the *filling* is influenced mainly by the surrounding grain, in a homogenous surrounding there is a strong decision towards patching, but also in a heavily clustered, knotty surrounding patching must/will occur.

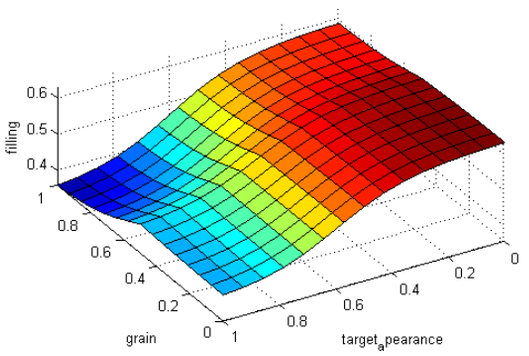

Figure 5-88; Decision surface (filling) grain - panel appearance (overall).

Interpretaiton: Analogous to the output *pre-processing*, the targeted final, overall appearance of the panls (*calm* ↔ *knotty*) overrules any influence of the grain surrounding in the decision, with putty used for homogenous appearance.

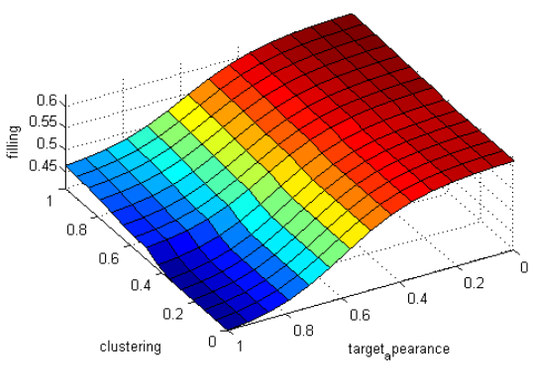

Figure 5-89: Decision surface (filling) clustering - panel appearance (overall).

Interpretation: The rule to adapt to the intended final appearance of the panel (*calm* ↔ *knotty*) overrules any influence of clustered knot defects in the decision with putty used for homogenous appearance.

Table 5-14: Segmentation of decision space towards output "filling".

The decision not to patch a defect (e.g. knothole with bark is too small, refer to rule 1.3 and rule 1.4 in Table 5-9, is therefore always defined by a combination of the outputs *pre-processing=no routing* and *filling=none.*

It seems natural to define and incorporate further rules possibly addressing the preference to avoid routing for economic reasons, biasing the decision surface accordingly. Saving filling material, especially when patching with putty, is nevertheless influenced most efficiently in the patching data generation itself (this will be addressed in the following section). The simulations, respectively the calculations and comparisons of different solutions which need to be incorporated for the decisions related to savings should therefore be handled separately from the decision process on *how* to patch principally.

5.4.4 Summary

The decision making principle by modelling human wood-worker knowledge in rules grouped to *principal patching, local aesthetics* and *overall panel appearance* has been set up and configured exemplarily for the defect type *Knothole with bark*. What is challenging in conditional programming can be solved in an elegant manner by the Fuzzy Inference System which incorporates rules in *if...then* notation with fuzzy membership functions connected to the contained input variables for segmenting the n-dimensional input space according to the desired output of *if* and *how* to patch. Additional rules can easily be incorporated (e.g. ecological, economical aspects) to further bias the decision surface.

5.5 Patching data generation

This section approaches the fourth step in the automated patching process after the defect detection which is the defect classification and the decision making using the knowledge base. The differentiation of patching methods for wooden panels based on the used materials and the resulting classification by solid and liquid fillers has been introduced in chapter 0. From the observations made at different panel production plants, automated processes were defined in chapter 2.3.2, also under aesthetic aspects in chapter 2.3.3. Finally, the main concepts behind patching data generation are introduced in this chapter based on the early findings from patching solid wood panels with dowels and the processing of defects for patching with liquid fillers (putty). This includes pre-processing by routing in most plywood applications. A generic framework that allows the flexible creation of patching

instructions and their transmission to patching robots has been implemented and studied by Göttlicher *[Goettlicher 2011]* in his diploma thesis under supervised by the author.

Having detected a defect and defined an area of interest for segmentation, having segmented an image snippet to be used for the classification of the corresponding defect type and having finally made a decision on *if* and *how* to patch this specific defect, the patching data generation can be carried out. Analogous to the illustration of the information flow for the decision making and its outcome in terms of *if* and *how* instructions in the last section, the information flow for the patching data generation is shown in Figure 5-90.

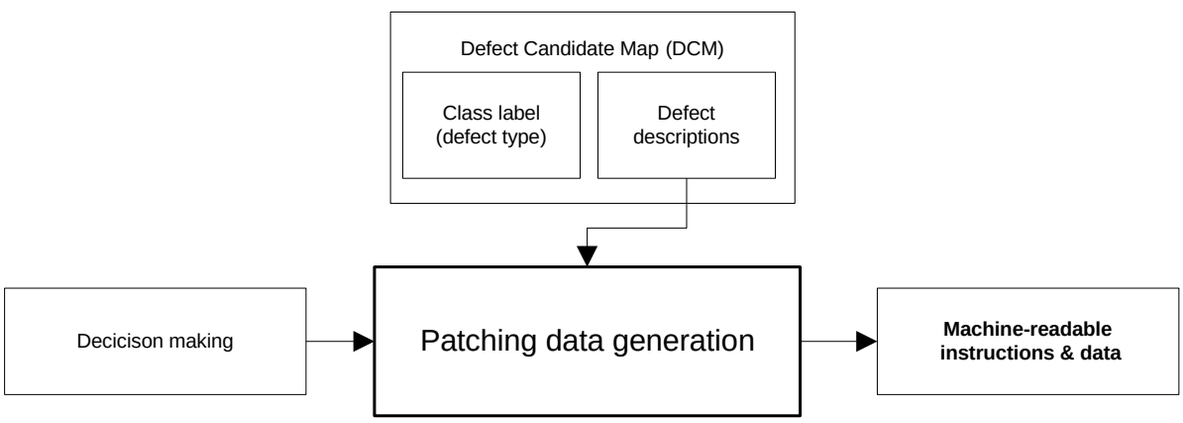

Figure 5-90: Information flow in the decision layer: generation of patching instructions and data.

Based on the input how to patch (filler type, colour/appearance variants, pre-processing) the defect description, mainly the defect contour is used to create machine-readable instructions.

5.5.1 Patching with dowels

In the case of patching with dowels, the patching data simple consists of a list indicating dowel types (circular, elliptical and different sizes each, refer to 2.3.1.1), position information in x-/y-coordinates with reference to the panel edges in the correct order and the orientation (for elliptical dowels). Optional variant information can be used to define a certain colour or texture, refer also to 2.3.1.1.

#ID	Type	Pos_x	Pos_Y	Orientation	Variant1	Variant2
193	1	695,4	3901,5	0	dark	circular
194	3	586,6	3014,1	0	dark	stripy

Table 5-15: Exemplary patching data set for patching with dowels on solid wood panels including dowel type (circular, elliptical), position with reference to panel edges, orientation and information containing preferred colour and/or texture.

Based on the contour information of the defect which is gained from the segmentation the possible dowels are tested for the best fit in terms of coverage of the defect contour in an iterative approach. Starting with centres of gravity from both the defect contour and the dowel contour, the figures in Table 5-16 illustrate the corresponding procedure:

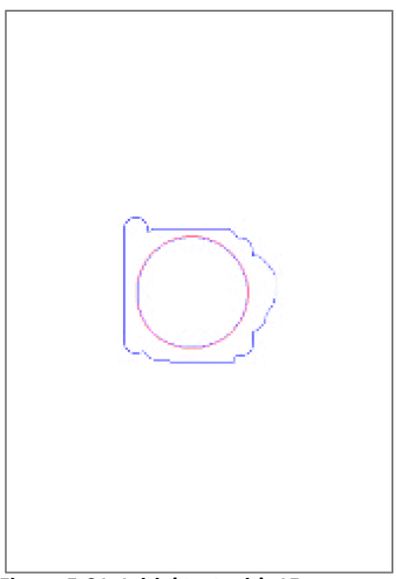

Figure 5-91: Initial test with 15mm circular dowel: coverage not reached.

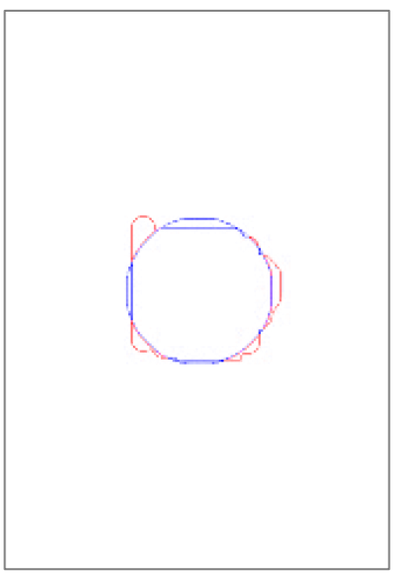

Figure 5-92: Test: 20mm dowel is sufficient / promising to start position optimization.

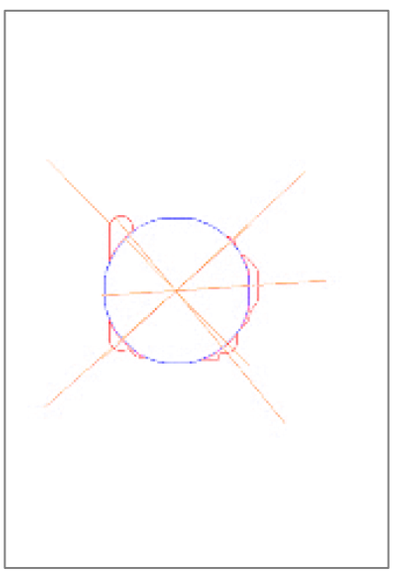

Figure 5-93: Calculation of shift vectors based on uncovered areas.

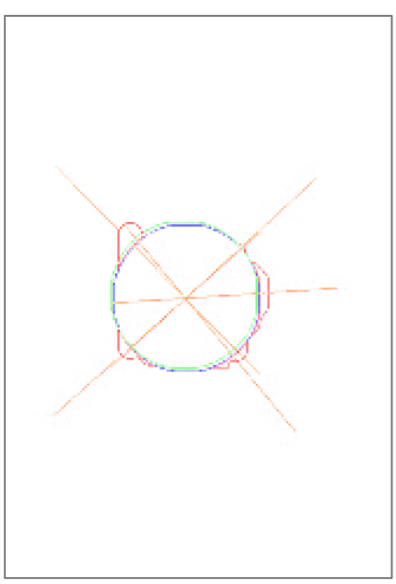

Figure 5-94: Movement of dowel according to added shift vectors and re-testing the coverage (result: insufficient at multiple positions).

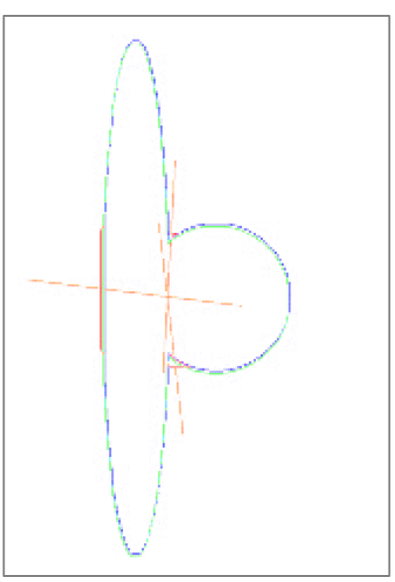

Figure 5-95: Testing & shifting a combination of one circular and one elliptical dowel (result: insufficient at the left).

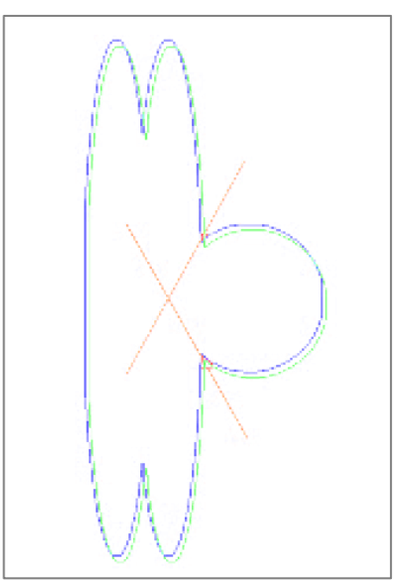

Figure 5-96: Testing and shifting a combination of one circular and two elliptical dowels results in sufficient coverage of the defect.

Table 5-16: Sequence of finding appropriate dowel size/ dowel combination including position optimization.

Starting with the defect's contour (blue contour in Figure 5-91 the possible dowels respectively the possible combinations as defined in the patching rules are tested in terms of

coverage. Exemplary the following dowel types are available in the sequence illustrated in Table 5-16:

- Type 1: 15mm circular dowel
- Type 2: 20mm circular dowel
- Type 3: 50mm elliptical dowel
- Combination of 1 x 20mm circular and 1 x 50mm elliptical dowel allowed
- Combination of 1 x 20mm circular and 2 x 50mm elliptical dowels allowed

Commonly there exist further variants in the combinations with different horizontal offsets between the dowels for the reason to optimize the coverage of either horizontally or vertically extended defect contours (usually the rotation of elliptical dowels is mechanically not possible or unwanted). From Figure 5-91 one can see that in the first iteration the 15mm circular dowel is not sufficient at all in terms of coverage (uncovered area is indicated by red colour). In the next iteration the 20mm dowel is tested for coverage satisfying a certain percental coverage criteria indicating that it is worth to carry out position optimization. This in turn is done by first defining direction and length of shift vectors (white parts of orange lines in Figure 5-93) according to the uncovered parts of the defect contour (red areas in Figure 5-93), subsequent shift vector addition and finally repositioning of the dowel on the defect contour for testing the coverage again (Figure 5-94). In this example the coverage criteria satisfying the final choice for the dowel is not reached (Figure 5-94) and the next bigger dowel is tested which is the combination of one circular dowel and one elliptical dowel, refer to Figure 5-95. Due to an exemplary strict final coverage the coverage is finally satisfying with a combination of one circular and two elliptical dowels (Figure 5-96) after a slight shift to the right (initial position by blue contour, final position by green contour).

A cost-benefit analysis can be carried out by comparing the additional dowel necessary to achieve full/preferred coverage and slight non-coverage when saving this dowel, related to the given example this would be a decision between the solutions found in Figure 5-95 and Figure 5-96.

5.5.2 Patching with putty

In contrast to the patching with dowels, single position information for the placement is mostly insufficient when patching with putty as the corresponding tools need to incorporate paths defined by a sequence of at least two x-/y-coordinates. Only in rare cases (small diameter knotholes for example) a single coordinate may be sufficient for filling the defect with putty respectively for routing the area with the predefined router (so-called “short dip” approach). Therefore the patching data ideally consists of a list of positions defining the optimal path across the defect contour for both the so-called routing-path and filling-path and additionally defining volumes of putty assigned to the segments of the filling-path.

It is necessary to realize that when incorporating routing in the pre-processing of the defect (for the reason to remove defective wood like bark, dark knots, etc. but also to remove material showing bad adhesion as it is the case with resin and glue, refer to 2.3.2.2) the original defect contour is destroyed and a synthetic defect contour is created. This must then be incorporated in the calculation of the path for the filling tool (so-called filling path) as well as in the volume calculation. The advantage of the synthetic defect contour is the well-defined depth that can be incorporated in the calculation of the putty volume. Figure 5-97 and Figure 5-98 illustrate this fact by the example of two differently sized routing tools (orange circles) applied to the original defect contour (black contour):

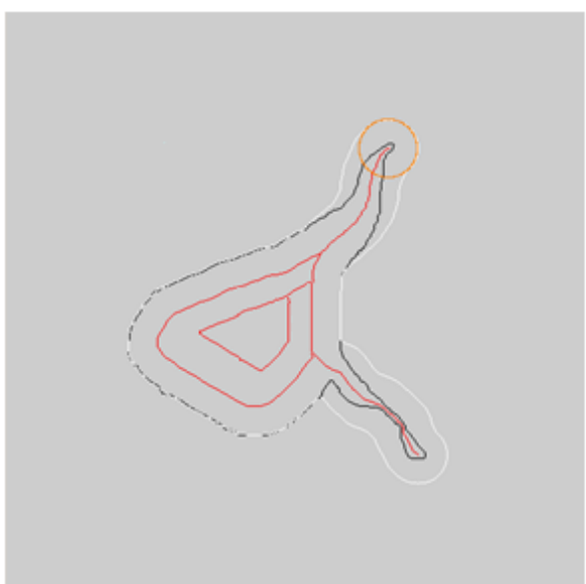

Figure 5-97: Small diameter router applied to defect contour. Red path is needed to fully cover/mill the defect contour. White contour is the resulting synthetic defect contour.

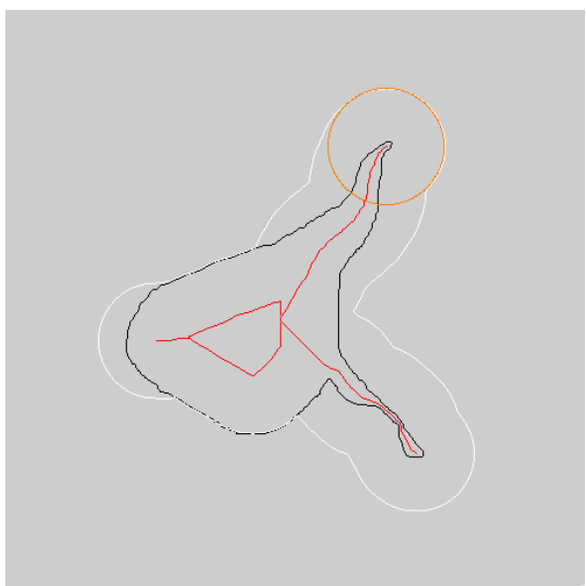

Figure 5-98: Large diameter router applied to defect contour. Red path is needed to fully cover/mill the defect contour. White contour is the resulting synthetic defect contour.

The difference in the results is obvious from the white contour which is the resulting synthetic contour. While a router with small diameter is able to follow the original defect contour more precisely (Figure 5-97), meaning that less sound wood from the surrounding is unnecessarily removed as in comparison to the larger diameter router in Figure 5-98, this is at the cost of an extended path length and therefore processing time. Also the appearance of the resulting defect contour is affected by the router diameter as larger diameters (in relation to the size of the defect contour) produce more artificial looking shapes (Figure 5-98). This is an important issue as a compromise between favoured aesthetic appearance and costs in terms of processing time has thus always to be found. This issue will get extra attention in the evaluation of performance in chapter 6.

From a mathematical perspective the calculation of the routing path is easily accomplished by incorporating morphological operations: when the router is defined as a circular kernel, simple morphological erosion is carried out iteratively, decomposing the defect contour like an onion with the kernel's centre moving along the path of the router.

Based on either the original defect contour or the synthetic contour an appropriate filling path has to be calculated for the final filling with putty. Unlike the routing path, the filling path is not relying on a certain diameter but on the viscosity of the liquid material in the case of 2K-PU putty (refer to 2.3.1.2.2) or the aperture and operating pressure of the 1K-putty (refer to 2.3.1.2.1) nozzle. As identified by Göttlicher *[Goettlicher 2011]* these parameters can be transformed and reduced to volume and motion speed. The aim is nevertheless to abstract the incorporated machinery as much as possible. Acceleration ramps and associated limits of the available drives for example need therefore not to be configured on the scanner system. This means that ideally only path segments with associated volumes are contained in the generated patching instructions and data. The filling path calculation is therefore trying to find the optimal path across the defect in terms of homogenous distribution of putty. This is exemplary illustrated in Figure 5-99 - Figure 5-101:

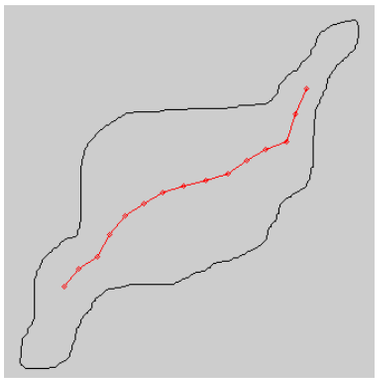

Figure 5-99: Low viscosity guarantees homogenous filling of the narrowings.

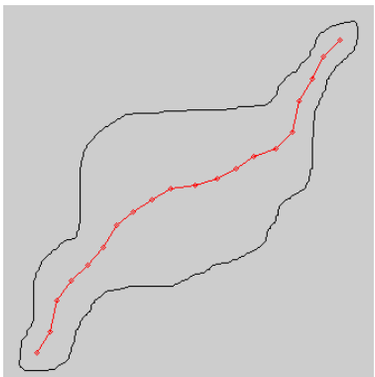

Figure 5-100: Higher viscosity requires nozzle to move into the narrowings.

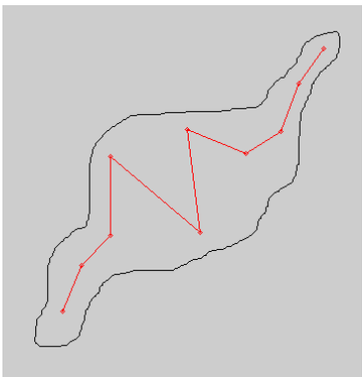

Figure 5-101: Depending on expanse of the defect and the viscosity of the putty the filling path needs extension.

In the above figures an unprocessed original defect contour is shown (black contour). Two major parameters influence the final result of the patching with putty, both related to the viscosity of the liquid filler. These are the ability of the putty to flow into narrowings of the defect contour (Figure 5-99) or if the tool has to follow into these narrowings (Figure 5-100) and the ability of the putty to distribute evenly by itself within the boundaries of the defect contour. Depending on the expanse of the contour the tool needs to follow a path offside the shortest path across the defect to ensure homogenous distribution of the putty (Figure 5-101).

From a mathematical perspective the calculation of the filling path is based on the operation of morphological skeletisation and subsequent adjustment of the skeleton points according to an optimal distribution of putty.

5.6 Summary

With reference to the dedicated cluster architecture presented in 5.1 (refer to Figure 5-9), the different processing layers of the scanner system for automated defect detection and defect rectification have been introduced and refined in this chapter. Layer 1 has been designed to be responsible for the data acquisition and sensor data fusion of various sensors with great differences in spatial resolution. The resulting overall multi-channel image is then split again according to the processing capabilities and configuration level of layer 2. This is responsible for defect detection by segmentation and defect evaluation incorporating the classification research methods introduced in chapter 4 being able to judge on local aesthetics. The classification system that has been introduced is based on the learning from examples in terms of image tiles to address the complexity of describing defects. The

creation of the related training data sets (image snippets) is supported by SOM-clustering which is optimal suited to support the manual task of labelling the training data due to its capability to group the images by similarity. Incorporating the detection and classification results, abstracted defect descriptions and information gained from the Defect Candidate Map a knowledge-based approach has been defined to be used in layer 3 that is able to make decisions whether and how to repair a certain defect also under aesthetic aspects and based on the rules defined by a wood-working expert. Finally, the principles and implementation concepts of patching data generation for both patching with dowels and liquid fillers (putty) have been illustrated.

Having covered the overall system design, the following chapter summarizes the development and the outcome of testing the overall interaction of the components and analyses the performance of the scanner system for automated defect detection and defect rectification.

6 System development & performance

This chapter deals with the possibilities to control and measure the performance of a system for the automated rectification of wooden panels. The automated patching system incorporates image acquisition devices, image processing units, common sensors and several patching tools and therefore performance evaluations from several points of view have to be incorporated. The overall performance is mainly derived from the visible result, which means assessment of the final repaired panel. To understand and define the capabilities as well as the limits causing possible errors perceived as imperfect repairs, the processing chain needs to be differentiated. The most obvious failure of a repair is an incomplete repair either due to

- incomplete/wrong detection,
- a wrong repair instruction (inappropriate filler and/or pre-processing) or due to
- misplacement resulting in insufficient coverage of the defective area.

The first and the second scenario are mainly seen in the area of signal and data processing related to the research methods as it is assumed that a proper sensor setup is used. The third scenario is severe because it combines the insufficient repair with the destruction of sound material, eventually calling for manual rework and resulting in a downgrade of the final product, and may be related to system/hardware design. Nevertheless, all scenarios are related to accuracy and precision but under different aspects which will be addressed separately in this chapter.

Slight over-detection in the segmentation is deliberately adjusted as this must be handled conceptually by the classification system. Therefore the focus is first on the classification rates in terms of accuracy and precision of the classification system. This will be addressed in section 6.1 *Detection performance*.

Assuming correct defect detection, the repair itself is always characterized by the proper choice of the repair kit[31] related to the amount of unnecessarily affected (removed) sound material and the coverage of the defective area. The proper choice of the repair kit underlies physical and aesthetical requirements as has been described in section 2.3 and is furthermore dependent on the capability of the Expert System to model human knowledge.

[31] Repair kit: Either solid (dowel) or liquid (putty) filler including optional pre-processing.

The assessment of unnecessary destruction of sound wood (and correlated to this the waste of filler material) together with the perceived appropriateness of the rectified defect are therefore the only measures which can be applied. This aspect of performance will be addressed in 6.2 *Patching performance.*

Accuracy in the classical sense and related to the positioning is the bias from the true value *[Dunn 2005]* that can be compensated by calibration *[Foster 1982]*. What remains after calibration is the error in precision which is in the best case distributed around the true value *[ANSI Y14.5M]*. There is usually no single responsibility in the processing chain for the errors in terms of precision. Positioning errors are more likely a product of lens aberration, limited resolution of the image acquisition devices and calibration errors, rounding errors in the data processing units and in the conversion between different coordinate systems. Rounding errors also occur in the control software of the actuators and finally the actuators (x-y-z axis, tools and conveyor belt) as well as their sensors (shaft encoders, etc.) are all limited in precision. The aspect of positioning accuracy will not further be addressed in the scope of this study.

6.1 Detection performance

6.1.1 Training of the classification system

The following section covers the actual development of the classification system and the related testing of the performance by carrying out training experiments. During these training experiments it was noticed that besides the huge potential of SVMs with non-linear kernels (refer to 4.1.3 and A.2) the computation of the kernel values in the training and testing is very time consuming (approx. 14 hours per class on the database containing 60.000 samples with 6 classes). Therefore cross-validation by varying several parameters would become inefficient with the available hardware (Pentium i7, 8GB of Random Access Memory, RAM). The objective to show the capability of learning from (image) examples therefore is addressed by the fact that large-scale non-linear SVMs can be approximated by linear ones using explicitly computed feature maps *[Vedaldi et al. 2010]* that approximate the kernel function and their generated, theoretically infinite feature spaces. This approach results in much lower training and testing times (in the setup used for this evaluation below 1 hour per class) while still producing comparable results.

The multi-class classification problem (4.1.3.2) is addressed by an one-versus-all (OVA) approach, resulting in actually one binary SVM-classifier per class being trained and tested with the positive samples of that class and all samples of the other classes as the negatives. The class with the highest score is then used in the final multi-stage classification. The model testing involves per-class performance evaluation by using Precision-Recall Curves (RPCs) which are favoured over ROC[32]-curves due to unbalanced data sets[33] and to address the loss of precision if moving to sparser data. Besides the principle capability to distinguish between the different defect types the capability to judge on local aesthetics is evaluated separately also using RPCs for comparison with the standard defect classification.

6.1.1.1 Training experiment setup

The classification system as proposed in 5.3 incorporating semi-automated generation of training and testing data sets is used. A database consisting of 60.000 multi-channel image snippets from lengthwise scanned plywood panels of spruce is hereby generated that contains the defect types *Dark Knot, Ringed Knot, Bark, Sound Knot, Cracked Knot* and *Resin Pocket.* Originally 15.000 image snippets were extracted by the segmentation approach proposed in 5.1, but every image snippet is rotated by 180° and additionally mirrored horizontally as well as vertically to extend the database by factor 4 and to cover rotation invariance while preserving the grain structure orientation (lengthwise scanned panels). The 6 data sets are quite balanced with initial 2000 – 2500 (extended to 8000 – 10.000) snippets per class while using 50% of the snippets from each set for training and 50% for testing. To the corresponding negatives (the remaining 5 classes) of each class 3000 additional image snippets of glue are added to address the false detection issue.

[32] Receiver-Operator-Characteristics, a popular method used for characterising binary classificatory system by comparing true positive rates against false positive rates at various thresholds.
[33] Ratio of positives and negatives approximately 1:26

Among several parameters the following options are used to optimize the training result. These parameters are not explicitly analysed, varied and compared for each defect type/class due to the still high training and testing times:

- Ratio to split data sets for gaining training and testing data:
  - 50% training, 50% testing for cross-validation
- *K*-fold cross-validation:
  - 2-fold cross-validation[34], switching training and testing data randomly assigned from the overall set
- Sub-sampling / scaling of the multi-channel image snippets:
  - 85 x 85 pixels, 9 channels, 10 possible a priori features: 65035-dimensional input feature space, refer to 5.3.2
- A priori features used:
  - symmetry (row), 4 nearest neighbour estimates
- Linear SVMs and feature maps:
  - Hellinger Kernel[35] generated feature map

Matlab R2014a and LIBLINEAR[36] are used to implement the training experiment. The linear SVM classifier used has just one parameter *C* which controls the regularization and misclassification penalties (refer to 4.1.3.2 and A.2.3). *C* is either set to 10 (low level of generalisation), 100 (medium level of generalisation) or 1000 (high level of generalisation) differently for each SVM respectively for each class to achieve best performance.

6.1.1.2 Training and testing

In the following sections the trained binary SVM classifiers are evaluated on the independent testing sets. This is done by quantitative evaluation using the precision (in the binary case this is the proportion of returns that are positives) and the recall (in the binary case this is the proportion of positives returned) at various thresholds, illustrated by the precision-recall curve. Further, every 15th support vector is illustrated in a 6x6 image snippet representation including its score (distance to the hyperplane: $w' * x + b$, refer to Formula A-6). Thereby an impression of the class boundaries (defined by the support vectors) and the decision

[34] Advantage of 2-fold cross validation: training and testing set are both large and each data point is used for both training and validation on each fold.

[35] $K(x, y) = \sum_{i=1}^{N} \sqrt{xy}$

[36] A library for large-scale linear classification *[LIBLINEAR n.d]*

boundary (hyperplane stylised by red line) can be gained. From the RPC the Average Precision (AP) is gained as the area under the curve in order to assess the performance by a single number. Further the RPCs indicate the corresponding random classifier by a red, dotted horizontal line for comparison purpose. Due to the unbalanced data sets (ratio of positives and negatives) the random classifiers may have a precision different from 0.5.

6.1.1.2.1 Bark

Best result achieved with regularization parameter *C* = 100 (medium level of generalisation):

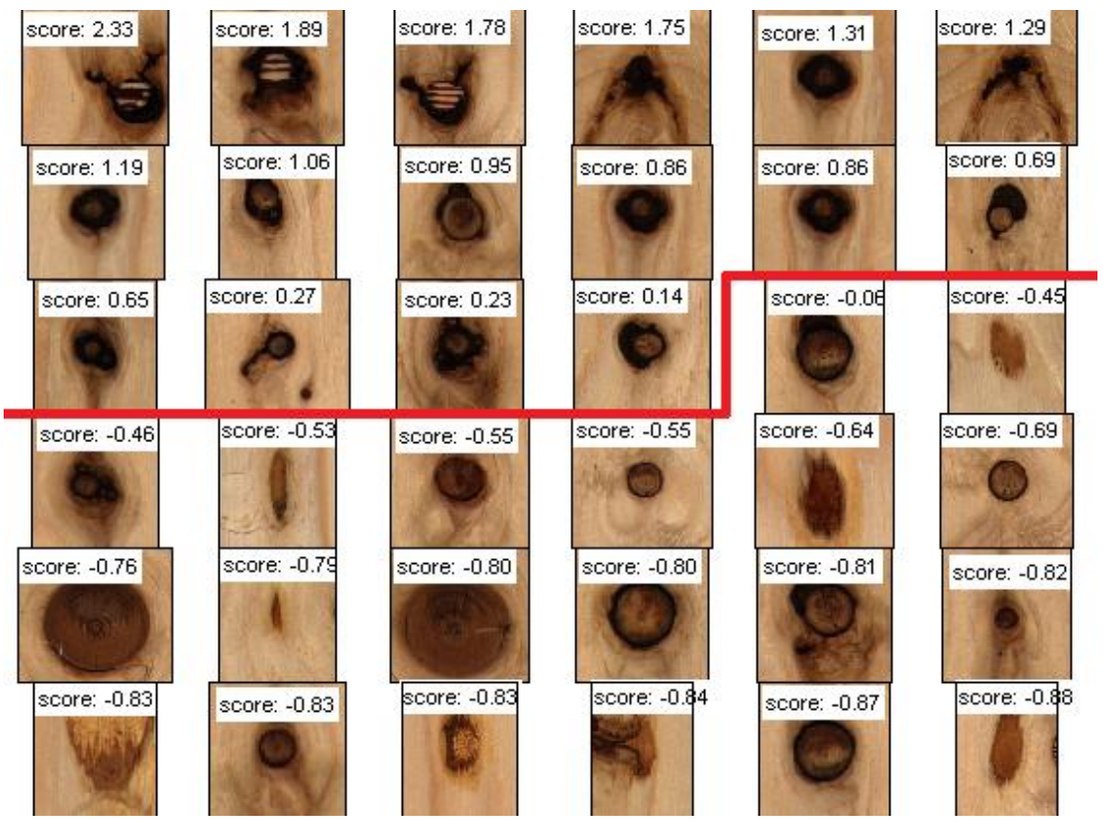

Figure 6-1: Support Vectors of SVM for defect type "Bark". Every 15th SV is shown including its scoring by the hyperplane, red line indicating decision boundary.

When viewing the decision boundary between the samples representing the two classes, it is striking that in third row, second from right a support vector of the negative class is obviously Bark which is also underlined by the very low score to the decision boundary. This is presumably a training sample wrongly assigned in the semi-automated generation of the training and testing data sets, contaminating the training data of the negatives and therefore reducing the accuracy to a certain extent. In the same way the testing set is likely to be affected and therefore the Average Precision also. This is accepted to be a natural error in the proposed process which of course opens room for optimization. Presumably this issue

will never be totally eliminated due to the huge amount of samples, due to uncertainty and finally due the subjective manner the expert is assigning the class labels. Higher values for the regularization parameter *C* improve the soft margin capabilities of the SVM as outlined in Appendix A.2.3 and certainly can compensate this error influence.

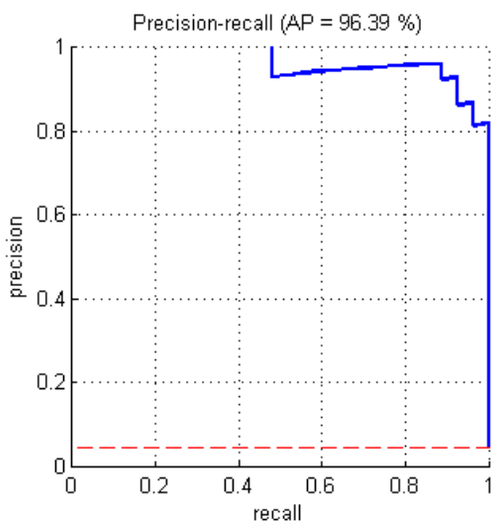

Figure 6-2: RPC for defect type "Bark", Average Precision (AP) is 96.39%. Red dotted line represents random classifier.

From Figure 6-1 one can further see that the decision boundary is most likely very tight to samples from ringed knots among the negatives. The knotholes with bark in the upper row (part of bark in this experiment) are clearly distinguished, presumably due to the unambiguous depth information contained in the 3D channel of the image snippets. The representation, although being just a very small subset, indicates visually quite strong support vectors. 96.39% is achieved as overall accuracy (AP), refer to Figure 6-2.

6.1.1.2.2 Dark Knot

Best result achieved with regularization parameter *C* = 1000 (high level of generalisation):

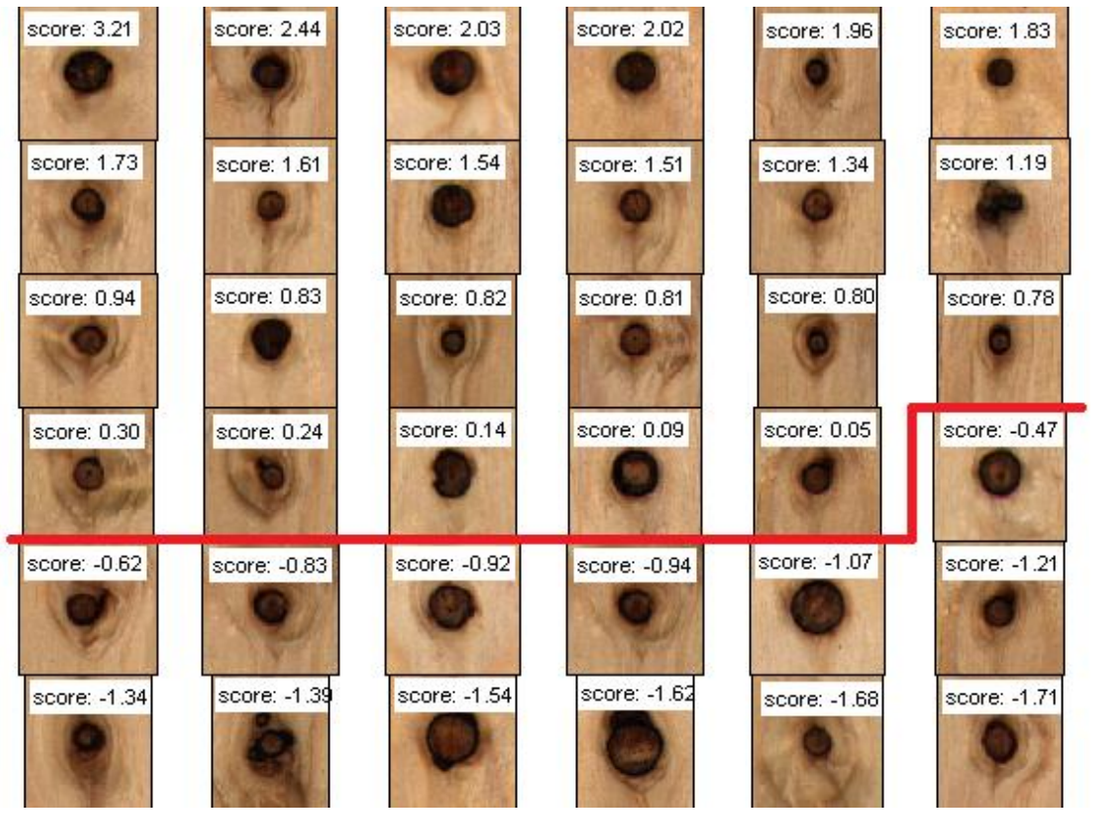

Figure 6-3: Support Vectors of SVM for defect type "Dark Knot". Every 15th SV is shown including its scoring by the hyperplane, red line indicating decision boundary.

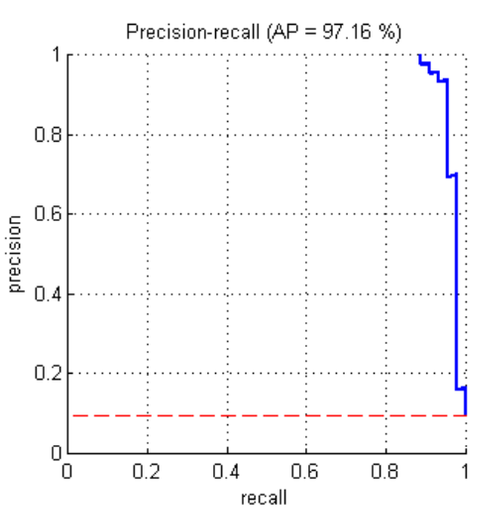

Figure 6-4: RPC for defect type "Dark Knot", Average Precision (AP) is 97.16%. Red dotted line represents random classifier.

To distinguish between Dark Knots and Ringed knots is presumably one of the most critical issues in knot classification, also for human experts, as the transition is floating especially with the main characteristics of homogeneity in the dark area versus the ring-shaped boundary. The support vectors seem visually to be less strong than previously with the classification of bark. Therefore an Average Precision of 97.16% is quite satisfying when the uncertainty in the labelling process is considered. As with the Bark a certain contamination of the training data influencing the achievable Average Precision must also be assumed.

6.1.1.2.3 Ringed Knot

Best result achieved with regularization parameter *C* = 100 (medium level of generalisation):

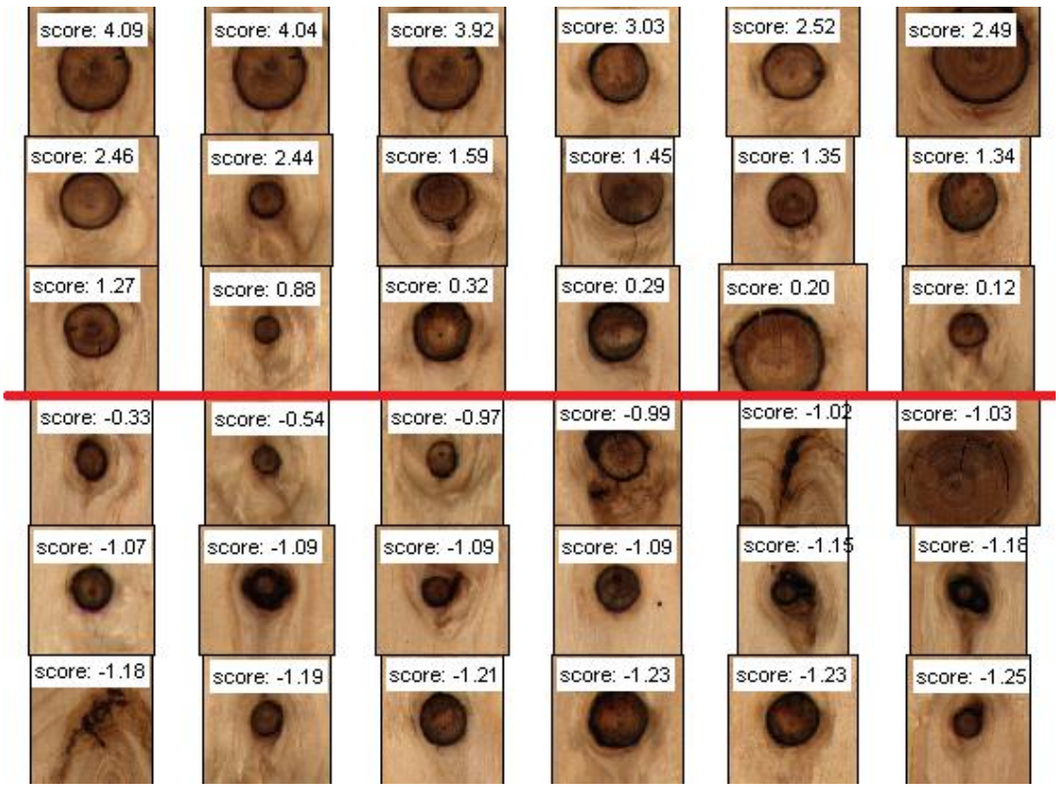

Figure 6-5: Support Vectors of SVM for defect type "Ringed Knot". Every 15th SV is shown including its scoring by the hyperplane, red line indicating decision boundary.

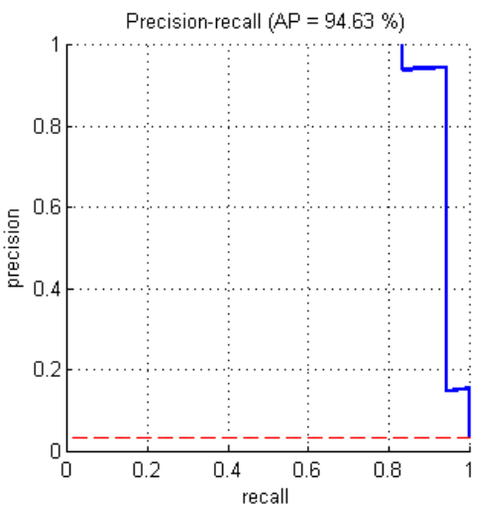

Figure 6-6: RPC for defect type "Ringed Knot", Average Precision (AP) is 94.63%. Red dotted line represents random classifier.

Also challenging is therefore the discrimination between Ringed Knots and Dark Knots due to the same reasons as mentioned previously for the Dark Knot classification. Visually the support vectors seem to rely on the diameter to some extent which is correct, as the Ringed Knot is physically the larger grown branch, refer to 2.2.1.2.1 and 2.2.1.2.2. Nevertheless the AP is lower (94.63%) in the classification of Ringed Knots than with the Dark Knots although the classes seem to share their boundaries. Uncertainty in the training and/or testing data set might be responsible.

1.1.1.1.1 Sound Knot

Best result achieved with regularization parameter *C* = 100 (medium level of generalisation):

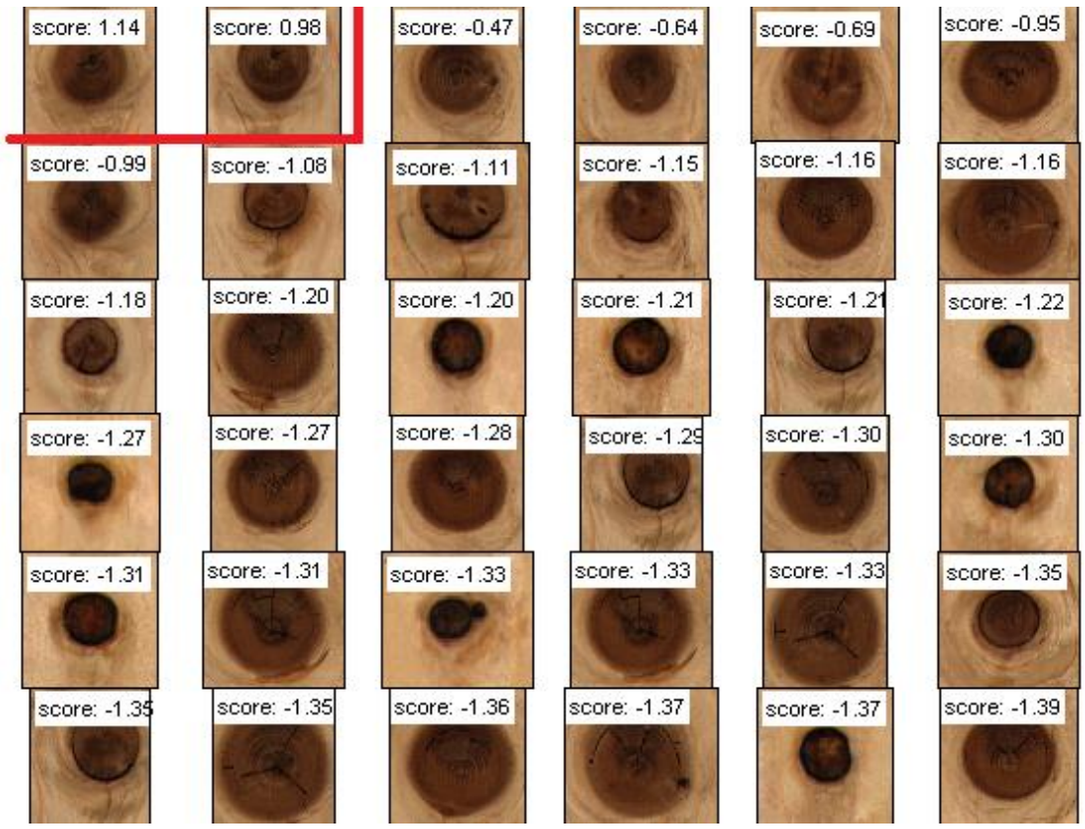

Figure 6-7: Support Vectors of SVM for defect type "Sound Knot". Every 15th SV is shown including its scoring by the hyperplane, red line indicating decision boundary.

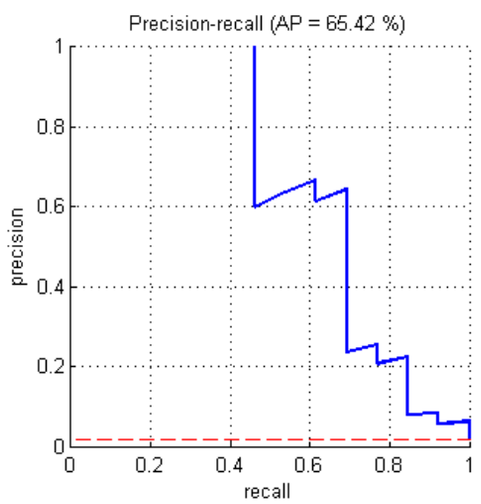

Figure 6-8: RPC for defect type "Sound Knot", Average Precision (AP) is 65.42%. Red dotted line represents random classifier.

The limits of the raw-pixel data approach are reached when it comes to the discrimination between Sound Knots and Cracked Knots. As the major distinguishing characteristic is actually the quantization of the crack's width (refer to 2.2.1.1.8), there are possibly much more samples needed to represent this in the training data implicitly. Further, to a certain extent the training data of Sound Knots has been found to be contaminated with Cracked Knots and vice versa (see support vectors in Figure 6-7), this is most likely due to a pure visual sorting incorporating more a "feeling" and the appearance than

quantitative measurements, ideally the measurements of the crack widths. Therefore the a priori knowledge extension introduced in 5.3.3 is additionally populated with the explicit calculation of a feature representing the crack width.

The challenge hereby is the finding that no single sensor is providing a signal to solely base on a stable measurement of the crack width, refer to Table 5-3 in 5.2. Therefore the multi-channel concept is used to support the crack segmentation and its subsequent evaluation: While the colour image (Figure 6-9) provides high-resolution, the knot colour varies greatly. The segmentation is therefore supported by incorporating the Scatter signal providing information based on the light scattered in the crack (Figure 6-10) and, at larger indentations (illuminated and less visible in the colour image), the depth information from the triangulation sensor (Figure 6-11). A fused single channel image is shown in Figure 6-12.

Figure 6-9: Colour image snippet of Cracked Knot.

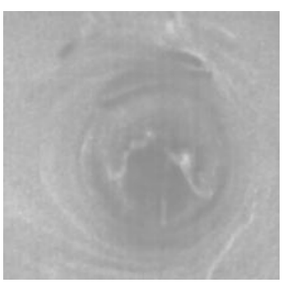

Figure 6-10: Scatter image snippet of the same Cracked Knot.

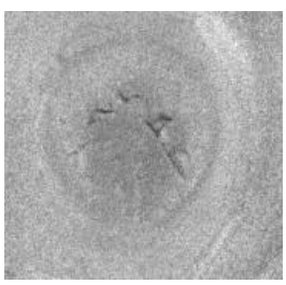

Figure 6-11: 3D image snippet of the same Cracked Knot.

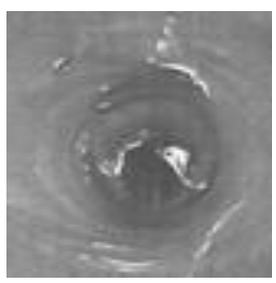

Figure 6-12: Fused image snippet of Cracked Knot for crack width estimation.

Based on radial projection, the star-like components are segmented and can then be measured for generating the a priori information containing the crack's width. Subsequently re-training and testing is carried out.

As can be seen already from the new representation of the decision boundary and related support vectors in Figure 6-13 when comparing to Figure 6-7, the support vectors are much stronger. Although the class distribution of Sound Knots is presumably close or even overlapping the class distribution of Cracked Knots, the decision boundary is clearly separating the samples with the presence of the crack width. This is also reflected by the much improved Average Precision which is enhanced from 65.42% to 95.75% (refer to Figure 6-14).

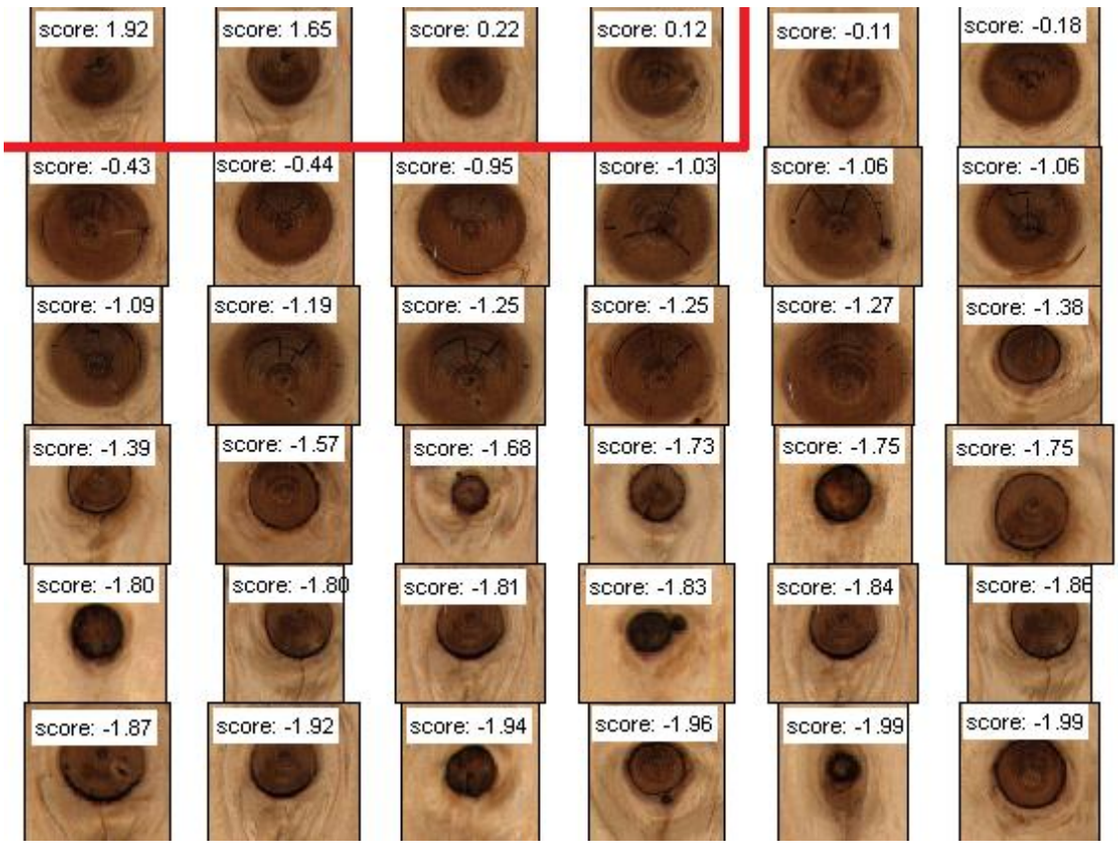

Figure 6-13: Support Vectors of SVM for defect type "Sound Knot" based on improvement with crack width incorporated in the a priori knowledge extension.

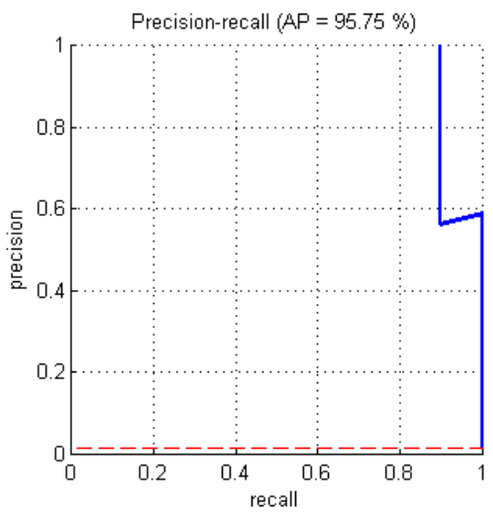

Figure 6-14: RPC for defect type "Sound Knot", based on improvement with crack width incorporated in the a priori knowledge extension. Average Precision (AP) is improved to 95.75%. Red dotted line represents random classifier.

6.1.1.2.4 Cracked Knot

Best result achieved with regularization parameter *C* = 100 (medium level of generalisation):

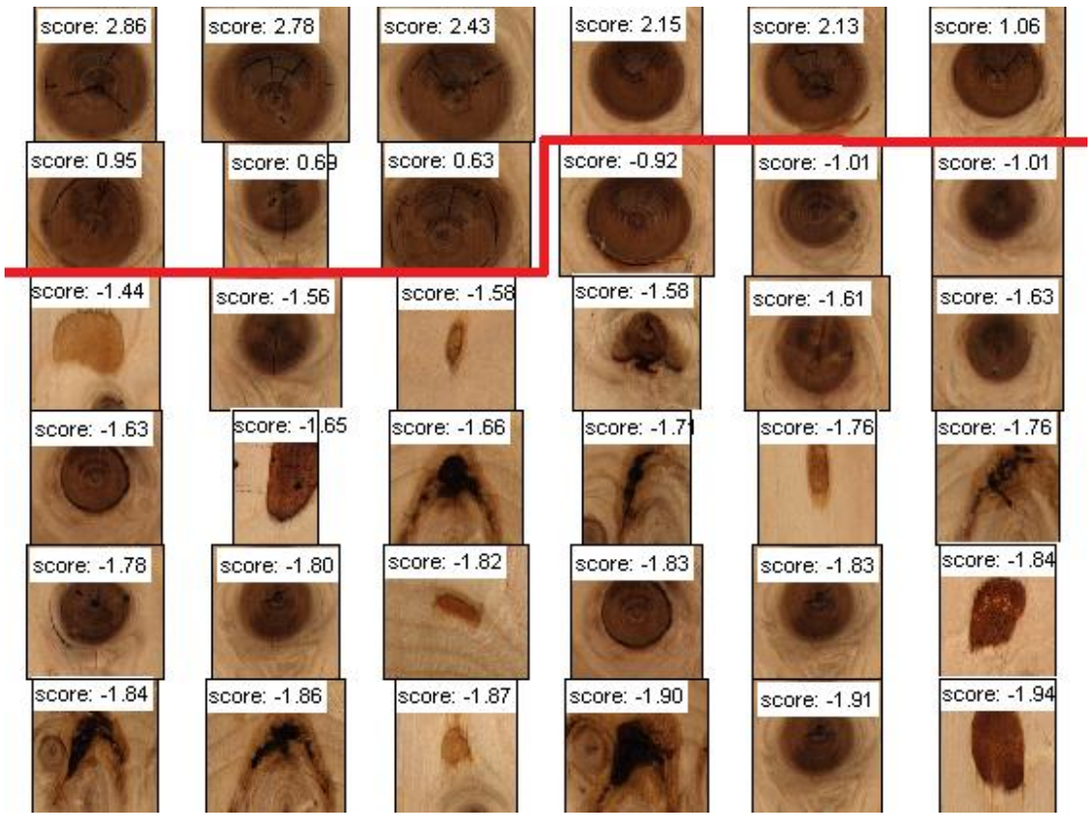

Figure 6-15: Support Vectors of SVM for defect type "Cracked Knot". Every 15th SV is shown including its scoring by the hyperplane, red line indicating decision boundary.

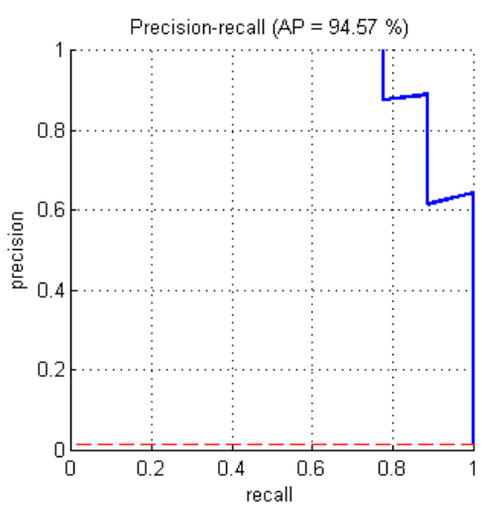

Figure 6-16: RPC for defect type "Cracked Knot", Average Precision (AP) is 94.57%. Red dotted line represents random classifier.

The improvement based on the a priori knowledge related to the crack width applies to the classification of the Cracked Knot itself too of course. Interestingly the support vectors of the negatives are relatively wide spread among the different classes showing samples of Sound Knots in direct immediate vicinity as expected but also (very dissimilar) Resin Pockets and Bark with quite large scores indicating a good separability incorporating the width feature.

6.1.1.2.5 Resin Pocket

Best result achieved with regularization parameter *C* = 100 (medium level of generalisation):

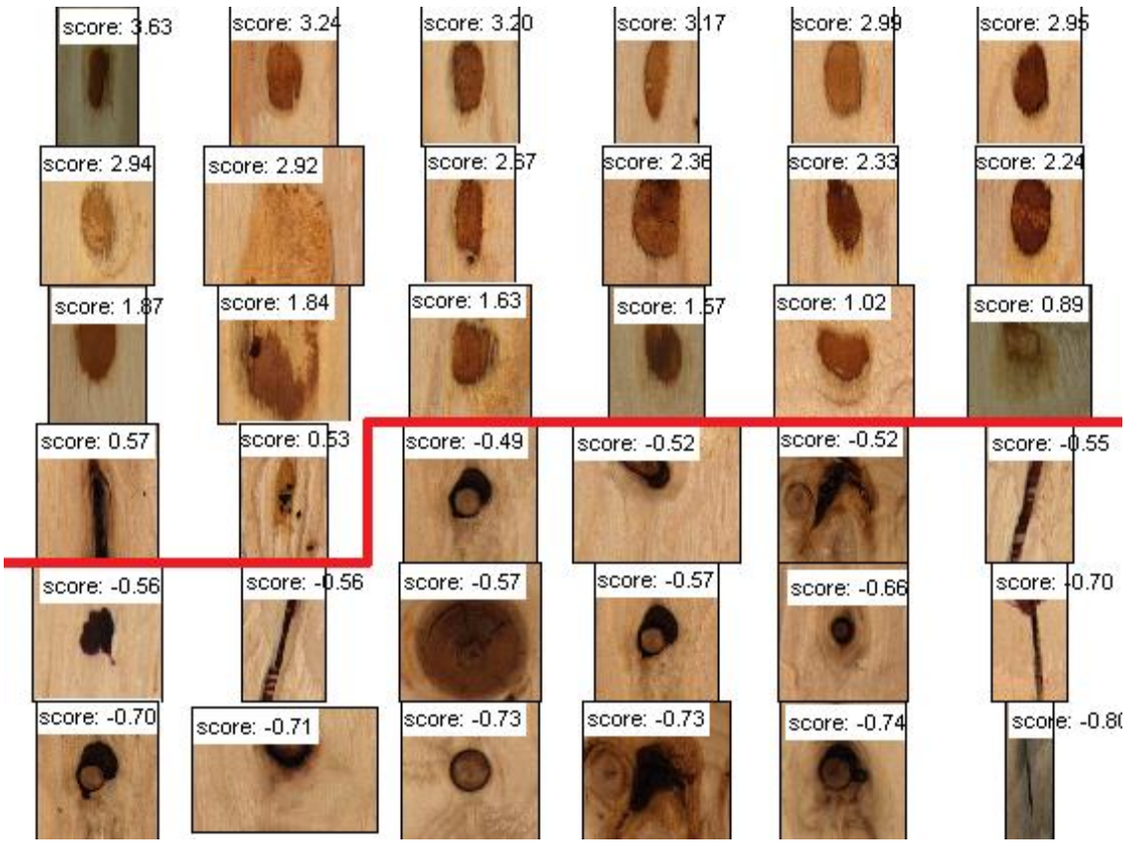

Figure 6-17: Support Vectors of SVM for defect type "Resin Pocket". Every 15th SV is shown including its scoring by the hyperplane, red line indicating decision boundary.

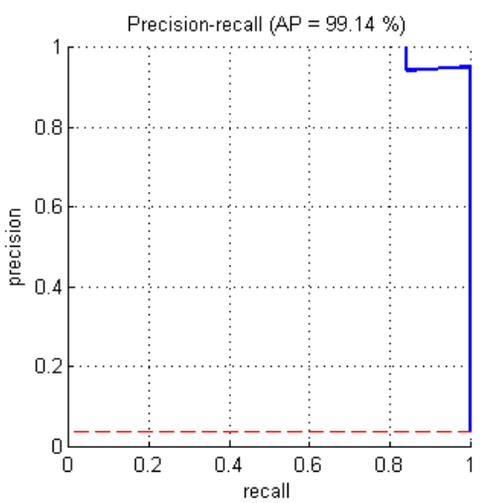

Figure 6-18: RPC for defect type "Resin Pocket", Average Precision (AP) is 99.14%. Red dotted line represents random classifier.

The classification of Resin Pockets is fairly stable due to strong support vectors as can be seen in Figure 6-17. It can be assumed that the UV reflection/absorption information (refer to 5.2.2) is mainly supporting the discrimination as often the colour information seems to be ambiguous and depth information is only partly present and at the limits of depth resolution, refer also to the verification matrix Table 5-3 in 5.2. The accuracy of 99.14% is therefore satisfactorily high.

6.1.1.2.6 Judgement on local aesthetics

The capability to automatically judge local aesthetics in terms of nice-looking or ugly-looking knots for example has been stated to be feasible by training from images as it is possible for humans to differentiate on the basis of (colour) images and because a learning fully incorporating all available information is incorporated. The judgement on Dark Knots is used exemplarily to assess this capability. In parallel to the other defect types previously trained and tested, images of Dark Knots were rated as “unobtrusive” or “looking unpleasant”. The set with examples of the unpleasant looking Dark Knots is taken as the positives and the acceptable, unobtrusive Dark Knots are trained as the negatives. Only several hundred image snippets could be incorporated in this experiment as the automated pre-sorting using a SOM does not perform well in this task, most likely due to wrong features.

No closer examination of the criteria in the manual sorting has been incorporated. The decision making applied to this sorting is further assumed to be subjective. From The training/example image sets one can nevertheless recognize a preference to symmetry, roundness and an undisturbed surrounding of the Dark Knot in terms of less discoloration.

The achievable average precision of 91.93% in the training experiments carried out with samples of aesthetic and unaesthetic Dark Knots is less high than the precision achieved in the differentiation between Dark Knots in common and the other involved defect types. The class distributions are recognized to be much tighter, presumably due to weaker features. Nevertheless the sub-sampled representation of the support vectors in Figure 6-19 reflects the already mentioned impression of shape and homogeneity having been the basis of judgement in the sorting of images for the training data set creation. The fact that less samples are included than with the previous experiments certainly influences the results in a negative way.

Best result achieved with regularization parameter C = 100 (medium level of generalisation):

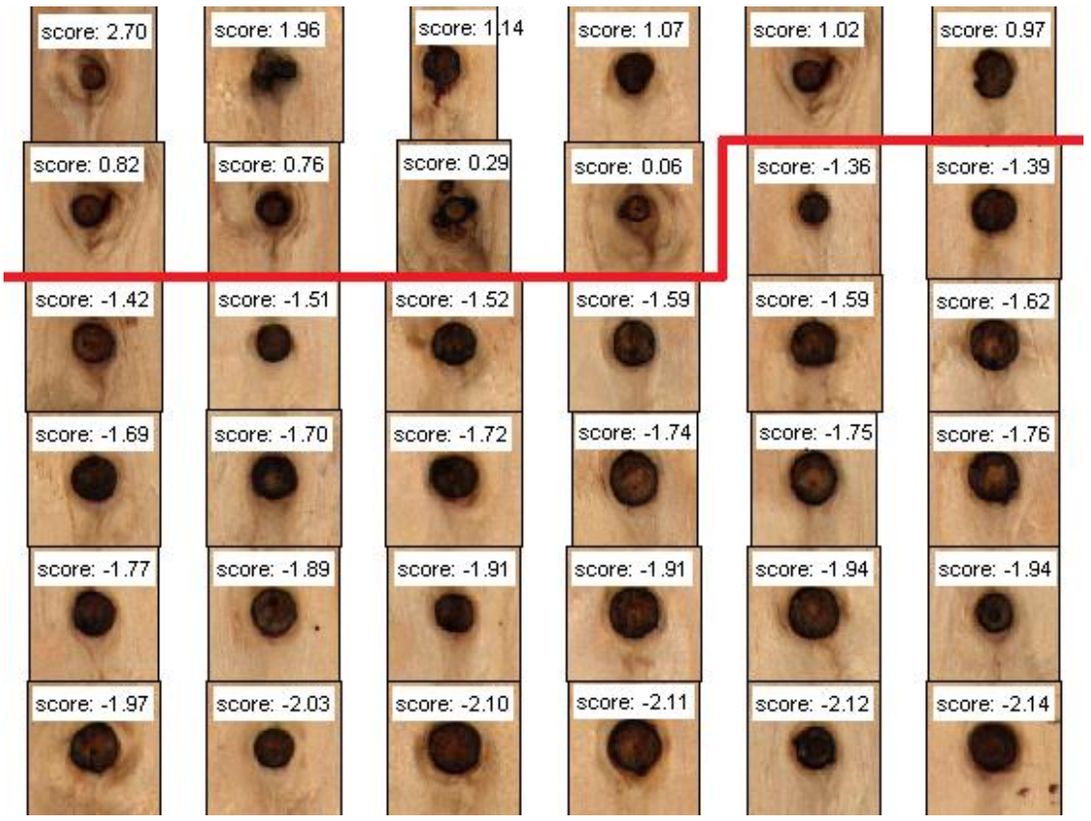

Figure 6-19: Support Vectors of SVM in aesthetic judgement on Dark Knots. Every 15th SV is shown including its scoring by the hyperplane, red line indicating decision boundary.

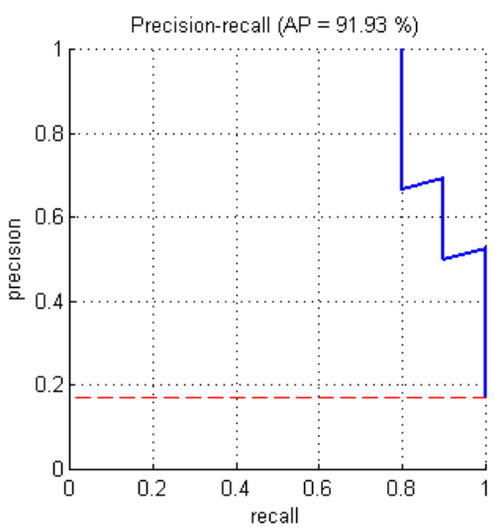

Figure 6-20: RPC for local aesthetics judgement yielding in an AP of 91.93%. Red dotted line represents random classifier.

6.2 Patching performance

6.2.1 Decision making

Evaluating the performance of the Decision Making is rather a validation (check if the right things are done) of the choice for a specific pre-processing, filler type and possible related options (size, combination, colour, etc.) and therefore the assurance to meet the customer's needs rather than numeric verification (check if things are done right) of requirements. This is due to room for interpretation and uncertainty in the rules (refer to 5.4). Therefore the performance evaluation under the aspect of decision making is the result of suitability and acceptance tests carried out with cooperating panel manufacturers using prototype installations of the automated patching system.

Due to the fact that panels are unique and a repair can be carried out only once per panel, the test procedure is as follows:

1. Scan the panel and execute the process of detection, classification, decision making and patching data generation.
2. Verify the defect detection again roughly (corresponds to detection performance, previous section), identify the defects unambiguously (e.g. by numbering).
3. On the user interface of the scanner system the generated patch is visualized, either on-screen (refer to Figure 6-21 & Figure 6-22) or using a print-out.
4. The appropriateness of the patch is therefrom assessed qualitatively.
5. Adjustments in the rules (refer to section 5.4) or to the patching data generation (refer to section 5.5) are made on statistical basis and based on general observations, e.g. *majority of dowel-combinations too excessive*, *routing on majority of small Dark Knots unnecessary*, etc. to incorporate a certain variety.

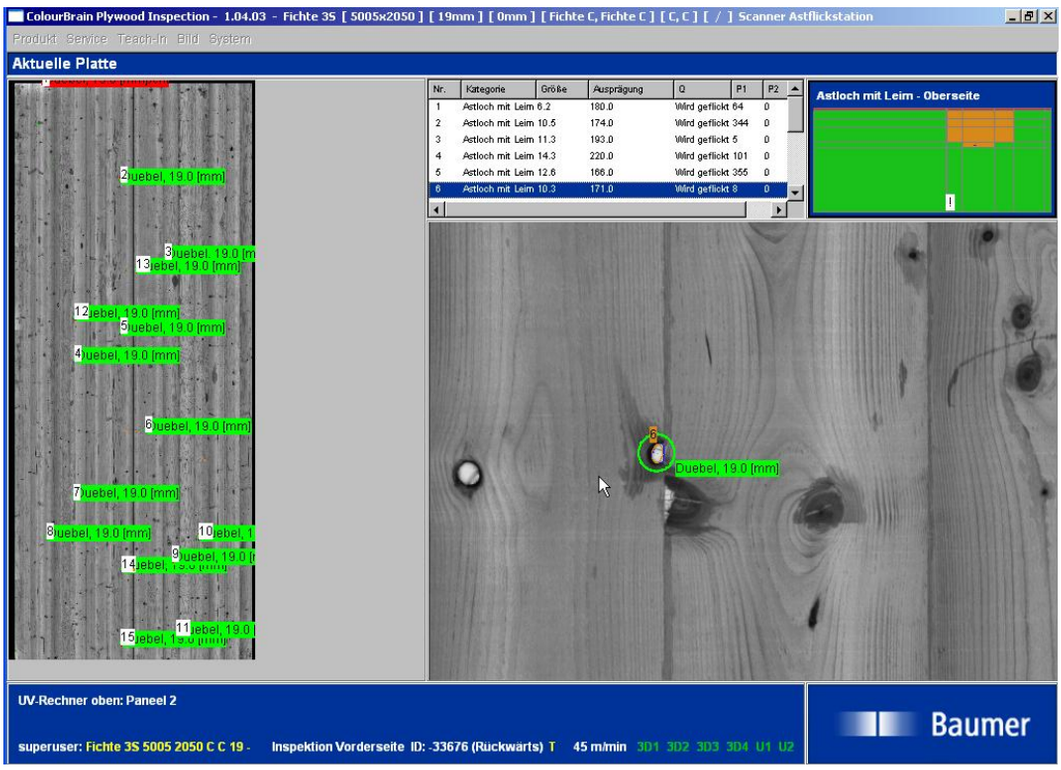

Figure 6-21: User interface visualizing the result of the decision making and patch data generation for validation. UV channel image of solid wood panel undergoing patching (knothole with glue) using a dowel is shown. Green circle represents circular dowel true to scale.

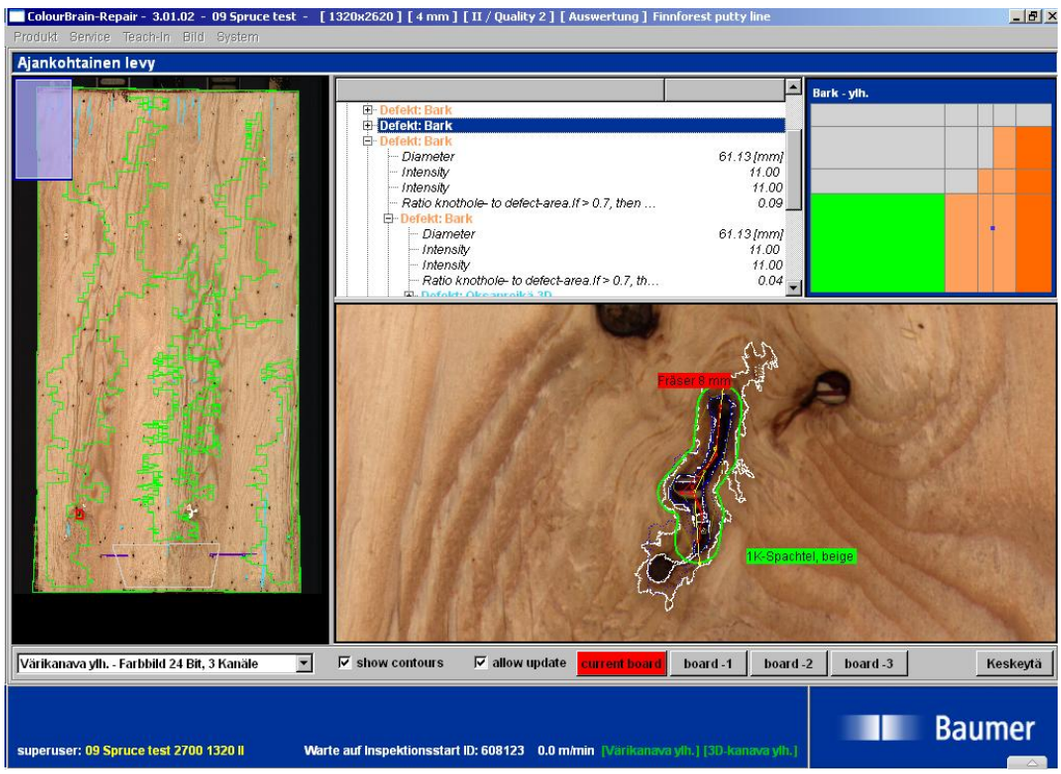

Figure 6-22: User interface visualizing the result of decision making and patch data generation for validating the patching on a plywood panel. Colour image channel is shown with overlays indicating routing path, resulting synthetic defect contour and filling path true to scale.

6.2.1.1 Patching with dowels

Figure 6-23 gives an example from the production of solid wood panels made of spruce respectively their automated patching with dowels according to the iterative approach outlined in 5.5.1. Generating patching instructions is thereby done by finding the most appropriate dowel(s) from an allowed set of dowels and optimizing the position(s) in terms of coverage:

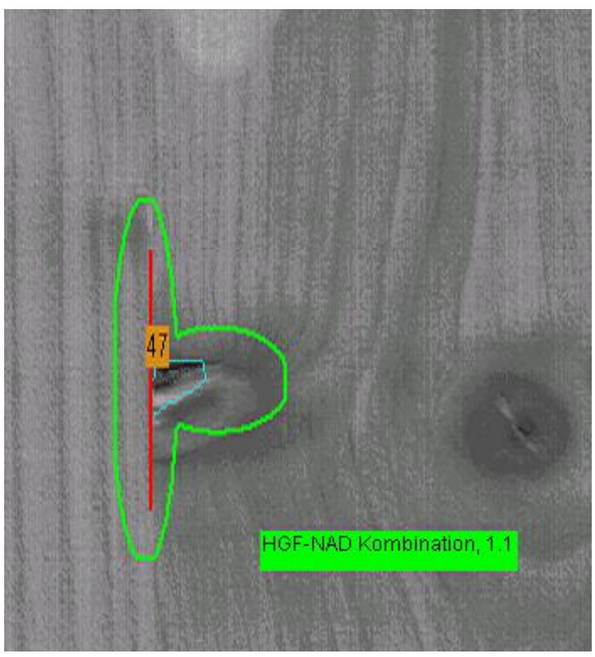

Figure 6-23: Screenshot of combination of circular and elliptic dowel placed on a knothole addressing the requirement to align the elliptical dowel to the lamella border (indicated by red line). Cyan contour is indicating a defect in 3D channel.

With reference to 2.2.3 *Quality standards* and 5.4 *Decision making* one can see from Figure 6-23 that certain rules are incorporated in the underlying decision process: The requirement to align elliptical dowels to the lamella border (if present) for better appearance is satisfied in Figure 6-23 indicating the lamella border by the red line.

The corresponding result from Figure 6-23 is further illustrated in the photography in Figure 6-24 showing the patched area right after dowel insertion. Remains from gluing the dowels can be seen as well as the fact that the patched panel has not yet undergone sanding to finish the surface entirely, further obfuscating the patch.

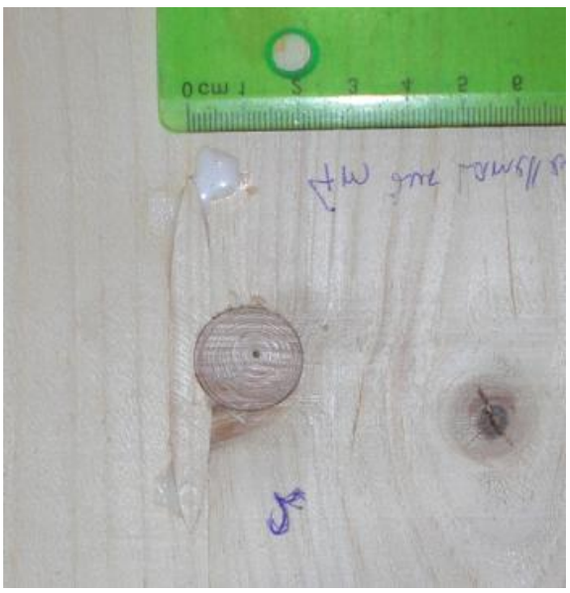

Figure 6-24: Photography of result from patching with combination of circular and elliptical dowels, refer to Figure 6-23.

The fulfilment of the requirement to preserve sound wood when patching at the lamella border can be seen from a similar defect in Figure 6-25 by the closest possible placement of the right elliptic dowel to the defect contour shown in cyan. Further the segmentation of the defect respectively the defect contour based on the multi-sensor approach can be seen in Figure 6-25 indicating the combination of the defect contours from UV-channel (blue contour) and 3D-channel (black area) to the contour highlighted in cyan.

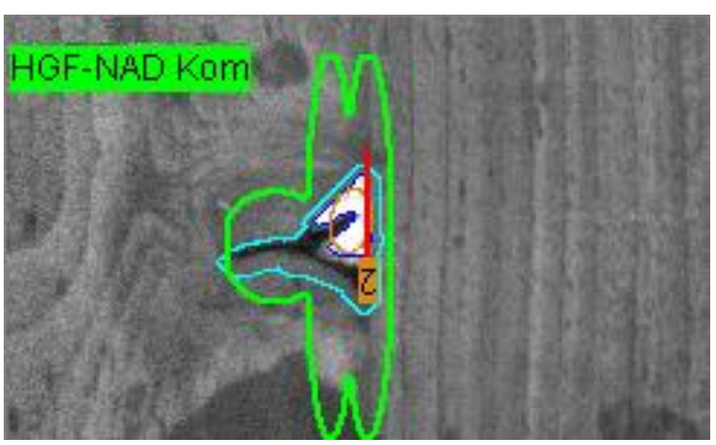

Figure 6-25: Screenshot of combination of circular and two elliptic dowels placed on a glue-filled knothole addressing the requirement to align the elliptical dowel to the lamella border (indicated by red line). Cyan contour is indicating a combination of defect segmentation partially in UV channel (dark blue contour) and partially in 3D channel, being merged.

Figure 6-26 and Figure 6-27 show an before and after example of patching a resin pocket on a solid wood panel of spruce (before sanding). The dowel is correctly placed but shows a low-frequency texture which does not perfectly match to high-frequency texture around the resin pocket.

Figure 6-26: Resin pocket on solid wood panel of spruce with leaked resin forming resin lake.

Figure 6-27: Same resin pocket on panel of spruce patched correctly with one elliptic dowel.

For repeatable validation tests in the development and setup of the system a standard solid wood panel of spruce is used which contains 13 defects from all relevant defect types (*Knothole* / *Knothole with Glue*, *Bark*, *Ringed Knot*, *Resin Pocket*). With the already verified Classification System the focus is thereby on the principle appropriateness of the output of the Decision Making and further on the patching instructions related to the appropriate dowel or combination of dowels. The results are judged accordingly to the main processing steps Detection, Classification, Decision Making and Patching and lead to an overall result in terms of (customers) acceptance as shown in Table 6-1:

ID	Detection		Classification		Decision Making		Patching		Accepted
	complete	incomplete	correct	incorrect	Repair instruction by expert	Repair instruction by system	Position & coverage ok	Position & coverage not ok	
1	x		x		1xCD + 1xED	1x CD + 1x ED	x		yes
2	x		x		1xED	1xED	x		yes
3		x	x		1xED	1xED	x		yes
4	x		x		1xCD	1xCD	x		yes
5	x			x	1xCD	1CD+1xED	x		yes
6		x		x	1xCD+1xED	1xCD+2ED	x		yes
7	x		x		1xCD	1xCD	x		yes
8	x			x	1xCD	1xED	x		yes
9	x		x		1xCD	1xCD	x		yes
10	x		x		1xED	1xED	x		yes
11	x		x		1xED	1xED	x		yes
12		x	x		1xCD+2ED	1xDD+3xED	x		yes
13	x		x		1xED	1xED	x		yes
								Panel acceptable:	**yes**

Table 6-1: Evaluation of standard panel for validation of patching performance. Each defect is compared according to detection, classification, decision making (system vs. expert) and patching. CD=circular dowel, ED=elliptic dowel.

The system is tuned until an optimal result is achieved on this standard panel and actually patched only in the final run. For the purpose of a realistic evaluation including variance in the (scanning) process, the panel is scanned each time although a simulated evaluation on once acquired image data is thinkable. Acceptance of patching is mainly rated by sufficient coverage. From Table 6-1 it can be seen that to achieve acceptance of the result from automated patching with dowels the bigger defects which show slightly incomplete detection and some wrong classifications (which in all the cases can be disregarded, e.g. medium sized hole with bark classified to Bark) obviously need larger combinations of dowels (orange highlighted patching instruction) than the expert would have chosen. This is related to the fact that bigger defects are more often a compound, therefore getting more complicated due to components such as hole, bark, contamination, etc.

For statistical measures a bigger number of panels needs to be evaluated to gain a sound data basis. Based on the evaluation of 50 solid wood panels of spruce of quality A/C (upper side quality A, lower side quality C) 624 defects overall (refer to Figure 6-28) were evaluated for appropriateness of the automated patching according to the previously mentioned

procedure (scanning, comparison of patching instructions from system and expert, execution of patching and subsequent evaluation of patched panel).

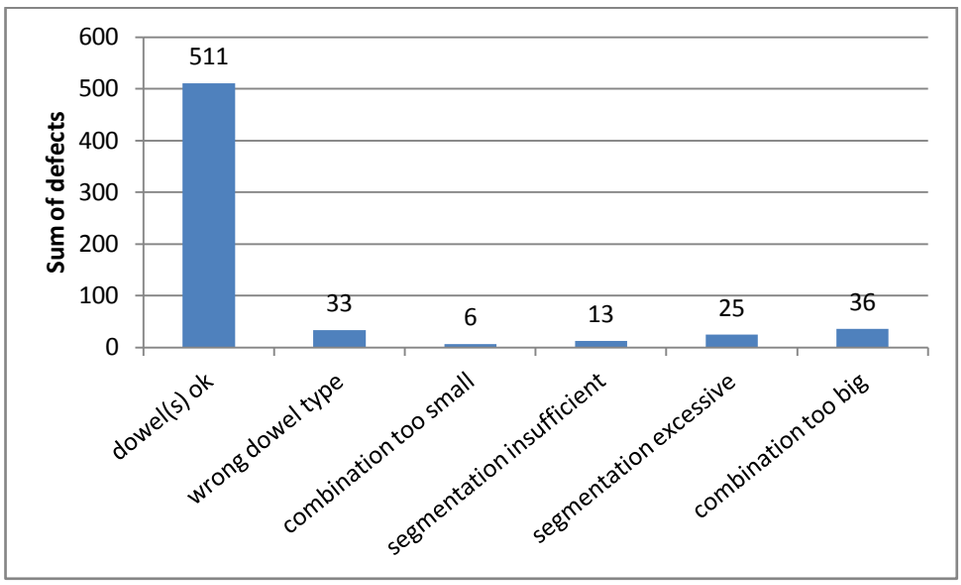

Figure 6-28: Statistical validation of decision making and patching instruction generation on a solid wood panel patched with dowels only (48 panels with 624 defective areas).

From these 50 panels 2 panels were discarded by the scanner without patching due to not allowed defects (panels obviously not satisfying either quality A or C, system setting is not to patch excessive defects). 3 panels were not accepted in the final evaluation due to several occurrences of wrong dowel types and thus either bad appearance (27 times) or insufficient coverage (6 times). Wrong dowel types are chosen either due to wrong classification or due to wrong segmentation (segmentation incomplete and resulting in too small dowel combinations, over-segmentation resulting in unnecessarily big dowel combinations).

6.2.1.2 Patching with putty

In Figure 6-30 and Figure 6-31 examples of defects filled with putty on the basis of the patching data generation introduced in chapter 5.5.2 are shown. In contrast to patching with dowels an evaluation of the appropriateness of the patch is possible only after sanding as can be seen from Figure 6-29.

Figure 6-29: Combined patching with 1K and 2K putty on plywood panel of spruce (note strong Needleflex that is tolerated in this setting. Panel not sanded, therefore no evaluation is possible yet.

Figure 6-30: Example of putty (1K) filled defect without pre-processing, after sanding.

Figure 6-31: Example of putty (2K) filled defect with pre-processing by routing, after sanding.

The difference in appearance between a previously routed synthetic contour (Figure 6-31) and a natural defect contour (Figure 6-30) can clearly be seen, especially when the surrounding texture is considered. Therefore the choice to incorporate pre-processing and its parameterization needs to be based not only on the defect type and technical considerations (adhesion, etc.) but also on the surrounding texture which has been successfully achieved in the given examples in Figure 6-30 and Figure 6-31 with respect to the available options (putty with only one colour).

In contrast to the patching with dowels a comparative assessment using the patch visualized on a screen or printout is found to be impossible. Dowels can be placed manually or measurements using a calliper can be used for evaluation of the patching with specific dowels after scanning but before the actual patching. The patching with putty, especially the pre-processing, is quite complex to assess virtually. Furthermore, the putty fully covers the patched area (refer to Figure 6-29). Therefore the validation tests must incorporate multiple panels and actual patching as well as subsequent sanding.

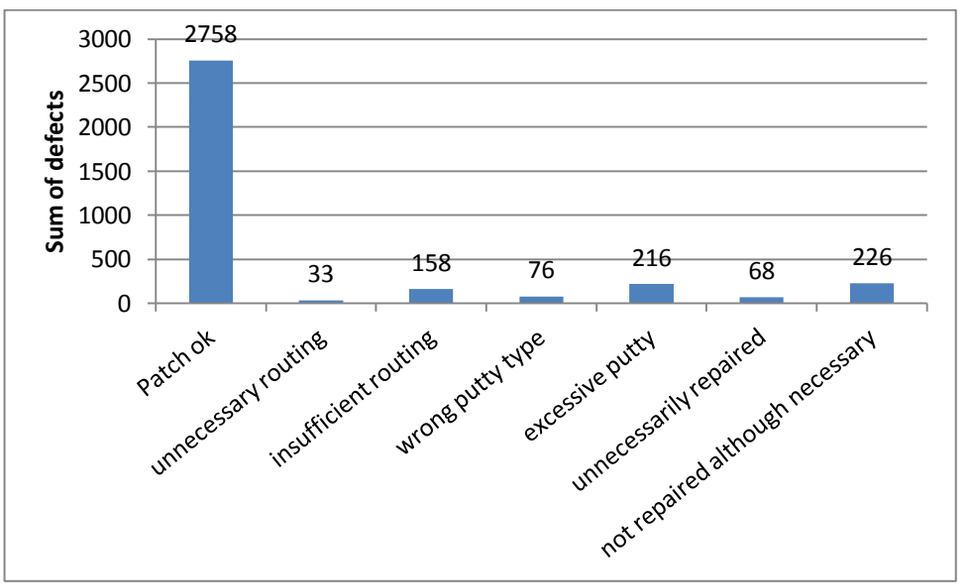

Figure 6-32: Statistical validation of decision making and patching instruction generation on plywood panels of spruce (50 panels with 3535 defects).

Again one packaging unit consisting of 50 panels was used for the validation test. Plywood panels of spruce in quality C/C (only topside with quality C is repaired) were used which is demanding due to the quite bad quality, also in terms of appearance. From Figure 6-32 it can be seen that 6% of the amount of defective areas are not repaired at all. If the amount of insufficient routed areas (either due to segmentation errors or positioning errors) is added (depending on the purpose of the panel, e.g. panels for laminating/coating must not show soft bark at all), approximately up to 10% of the defects need manual re-work or lead to a downgrade of the panel. With higher quality panels showing only some defects with less complexity (e.g. less than 10 per face in quality A in contrast to 30 defects and more on quality C panels) the patching result is improving dramatically.

To highlight the challenge of automated patching on low-quality plywood panels Figure 6-33 illustrates a quality C panel after automated patching and sanding.

Figure 6-33: Example of low-quality (C-quality) plywood panel (spruce) posing high demands especially on segmentation, classification and decision making. Red circles highlight selection of patched defects shown below (from left to right).

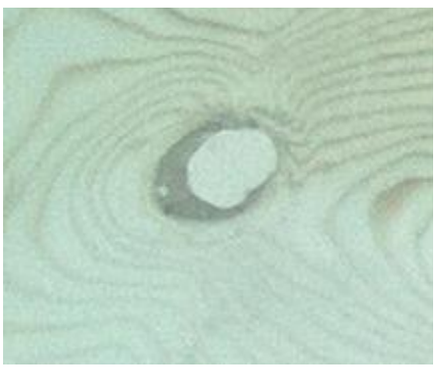

Figure 6-34: Patch ok, although insufficient routing results in poor appearance. (Left highlighting circle in Figure 6-33).

Figure 6-35: Path intentionally not carried out completely at the panel's edge, combined with crack.

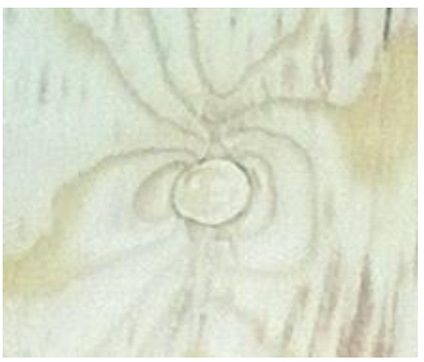

Figure 6-36: Proper patched defect without pre-processing. (Right highlighted circle in Figure 6-33).

One can see the potential of false detection on the various coloured texture and the issues along the panel border which are shown yet untrimmed. Therefore a certain ratio of unnecessarily repaired to not repaired defects needs always to be accepted. The decision if the resulting compromise is towards excessive or insufficient patching is therefore a fundamental configuration of the system.

6.2.1.2.1 Optimization approaches

As already identified in the beginning of the previous section, optimization in the (automated) patching of wooden panels can be summarized under three main aspects:

- Economic optimization mainly addresses throughput of panels in the production line and to a subordinated extent the usage of material.
- Ecological optimization favours less usage of chemicals (putty) and preservation of as much wood as possible.
- Appearance optimization focuses the aesthetics of the final result in terms of selection from colour and/or texture options of the filler (if available) and minimization of artificial-looking contours as a result from routing.

Optimization under economic aspects in terms of throughput and reduced processing time is highly related to the complexity of the individual patching operations. An example is given for the patching with putty: complex shapes that force the routing and filling tools to execute complicated movements (sudden changes in direction in the context of discrete curves, forcing accelerations and de-accelerations) may preserve sound material and may need less filling material but are most time-consuming. On the other hand, especially with x/y-axis based patching tools, smooth curves can be executed with high acceleration, but the limitation to shapes that fulfil this criterion is at the cost of removing sound material (and therefore the need to use more filling material).

Figure 6-37 shows an image of a resin pocket on a panel of spruce plywood that needs to be repaired by pre-processing with a router and subsequent filling with two-component putty. An example for an associated repair instruction generated by the algorithm introduced in 5.5 is shown in Figure 6-38. The red lines and vertices show the path for the routing tool while blue lines and vertices correspond to the path for the filling tool. Additional information about area (A, mm^2) is given.

Figure 6-37: Resin pocket that has to be repaired by routing first and then filling with 2K putty.

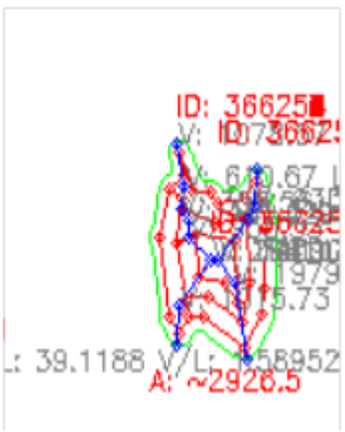

Figure 6-38: Example for a corresponding repair instruction (red track: router, blue track: filling tool) where the preference is set to the preservation of sound wood and less usage of putty, resulting in complex, time-consuming movements. Area is 2926.5mm^2.

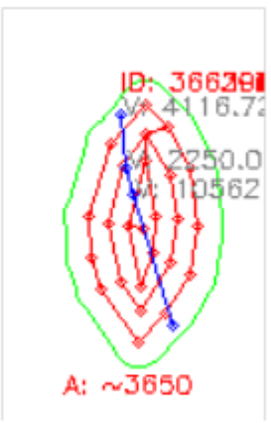

Figure 6-39 Example for a corresponding repair instruction (red track: router, blue track: filling tool) where the preference is set to the least time-consuming execution of both tools which is achieved by smoothed and straight movements. Area to process increases to 3650mm^2.

The way the repair is carried out in Figure 6-38 is preserving the sound wood but consists of complicated movements of the tools with unsteady curves for the router (red) and four impasses for the filling tool (blue) which require unfavourable inward and outward movements. Figure 6-39 shows an alternative repair instruction where the settings are adjusted to produce smooth curves with the avoidance of abrupt reverse movements. The nozzle can thereby operate with high flow. With rising viscosity a slightly S-shaped movement would be more favourable. In the example given, the area that is routed and therefore has to be filled is raised from approximately 2927mm^2 to 3650mm^2 by therefore nearly 25% (volume is depending on the thickness of the face veneer to be routed which is in certain limits a machinery parameter). In parallel the overall execution time is reduced by more than 50% (depending on various parameters at the machinery which are out of the scope of the scanner). With reference to low-quality panels showing 30 - 50 defective areas to be repaired (refer to Figure 6-29 and Figure 6-33 the saving potential in terms of throughput as well as in putty consumption is enormous but a compromise needs to be found.

Optimization under economic and also ecological aspects (in terms of less usage of chemicals) means therefore a preference to either high performance of the machinery or less consumption of filling material or vice versa. In practice the higher quality panels are

automatically patched with adjustments preferring slower but more precise processing while lower quality panels are patched at high throughput. This is because a compromise between process throughput and saving material respectively, creating less artificial looking patches, needs to be found. Finally, the correlation of the two optimization possibilities with the quality of the panels supports the finding that appearance aspects are tightly linked to ecological optimization.

6.3 Summary

The possibilities to control and measure the overall performance of the proposed system respectively of the implemented research methods have been shown by testing.

By setting up a training experiment, the learning from image examples has been accomplished and the proposed classification system has been verified. Six common defect types on plywood panels (Bark, Dark Knot, Ringed Knot, Sound Knot, Cracked Knot and Resin Pocket) have therefore been evaluated in terms of the achievable Average Precision of the classificatory system and by varying the generalisation capability. Further the improvement of the a priori knowledge extension to the pixel feature vector has been tested and compared. To address the claimed capability of judgement on aesthetic appearance (local aesthetics) additionally to these six common defect types the training and classification of *unobtrusive* and *unpleasant looking* Dark Knots has been carried out. With the knowledge base for detection of defects built up, the main component in the detection & evaluation layer of the new scanner architecture has been addressed.

The Expert System component in the decision making layer of the scanner has been evaluated for the patching with dowels as well as with putty, using the rule base established in chapter 5 based on the *appearance quality II* defined in ISO 2426-3:2000. With data from realistic, industrial environments the decision making component has been validated by customer satisfaction. Finally the identified optimization approach under economical, ecological and appearance-related aspects has been evaluated.

In the following chapter the results of the research are briefly reviewed. Results and findings are discussed and interpreted also with regard to relevant applications found in literature. Besides the generalisation and the impacts of the study, the limits of the study are subject to the discussion and outlook to future applications is given.

7 Discussion and Conclusions

7.1 Review

It is understood that the availability of an automated visual inspection system being able to deal with tasks of aesthetics and being usable in the context of an automated, industrial patching is highly desirable in the wood working industry from an ecological view as well as from an economical view. A rethinking from scrapping defective wooden panels to upgrading them for the reason of added value raises the labour costs in this currently still mainly manual process. In highly automated woodworking production environments, inspection systems incorporating machine vision technologies are already successfully used mainly for the purpose of grading with respect to the various natural defects. So it seems sensible to use similar systems in the important process of upgrading by patching those defects. The review of literature summarized the findings of previous research in the area of automated visual inspection on wood products which led to the insight that multi-sensorial setups are essential to overcome the identified deficiencies and limitations of current systems. An overview on the production–sub-processes of patching solid wood panels and plywood panels has been gained as well as an overview on the defects on wood. The variety of a natural product like wood poses high demands on both machine vision systems and humans. The huge bandwidth of appearance, mainly influenced by the presence of acceptable knots and unacceptable surface defects is manageable by trained human workers, but issues with reproducibility and reliability arise, especially when aesthetic aspects are included. Methods were identified that address the two main tasks in the rectification process; these are the detection and the decision making. Both tasks are carried out easily by humans through incorporation of their abstraction capability, flexibility, creativity and fast decision-making ability. Having understood that colour and texture are equally important and that further supporting measurements of defect-specific characteristics should be incorporated in an automatic pendant of the wood worker, the system design of a multi-sensorial scanner system has been accomplished. The design on system level as well as on processing level has thereby adopted the principles of the human way of working as a model. The aesthetic issues are found to be necessarily addressed separately as local and global aesthetics in different processing stages. While local aesthetics

are found to be modelled best by teaching image examples in a supervised machine learning approach for the use in the detection and evaluation, the global across-the-board aesthetics follow certain rules which can be formulated well in human language to be incorporated in the decision making for patching.

The overall concept towards automated patching can therefore be summarized on a top-level view with a:

- *System architecture*, abstracting the information flow based on modules related to hardware and logical building blocks/units in hierarchical order and providing sensor data fusion.

- *Segmentation approach* as the first instance in the image processing chain based on registered image data following the human approach to this task identifying common irregularities first before classifying them.

- *Classification* capable to address the complexity of industry standards as well as human perception-related product requirements (local aesthetics) with the concept of using the maximum available information.

- *Decision making* using an Expert System based on fuzziness in the rules and to be able to deal with the creation, modification and adjustment of the overall favoured panel appearance (overall aesthetics).

- *Patching data generation* being able to provide instructions to machinery on *where* and *how* to perform the actual patching using different filling materials and pre-processing tools. Optimization capabilities are provided in this final processing step related to costs as well as to appearance.

- *User interface* for interaction with the wood working expert for the purpose of adjustment, teaching, monitoring and process control, incorporating rather wood worker expert knowledge than machine vision expert knowledge.

From the tests related to customer satisfaction and acceptance it can be stated that the complexity of the rectification rises with decreasing quality of the panel as this is closely related to an inferior appearance which is dominated by bigger defects. Often these bigger defects are a compound of several defects (e.g. knothole with bark showing also glue and

cracks) which is the main cause for the rising complexity. Depending on the panels' purpose a rejection rate of 6-10% of the defects has currently to be accepted on low-quality panels. With 30 defects on average on C-quality plywood panels this implies statistically 1 – 3 unsatisfactorily patched defect(s) on each panel. Therefore a subsequent manual process for re-working seems be unavoidable at least for low-quality panels, still offering huge potential for cost savings and throughput enhancement compared to the overall manual process.

7.2 Discussion

7.2.1 Interpretation of findings

A novel system has been designed, implemented and studied in real-production environments showing partially the capabilities of human workers when it comes to incorporate specific aesthetic issues in the decision of what and how to patch. The system can therefore be used for the adjustment for different levels of perceived acceptable aesthetic appearance. As aesthetic appearance is a subjective notion, standards like ISO 2426-x and company-specific specifications try to establish certain parameters and related values for acceptable appearance classes of wooden panels. The system provides capability to define and adjust detection and repair rules according to these specifications including the level of intervention (patching type including pre-processing) for a certain production batch. It is hereby possible to achieve satisfying results with automated rectification in comparison to manually carried out patching under certain constraints. The Human Visual System (HVS) is greatly optimized to judge new scenes, to identify previously unseen objects and is able to identify irregularities often on a basis of like and dislike. The great abstraction capability is seen to be the HVS's key of success. Learning is understood to be thereby an important component as abstraction relies on a certain amount and variety of observations. The common characteristics are assumed to be learned from such a variety, enabling generalisation capability. Besides that, some simple principles can be identified in the iteratively repeated completion of the manual tasks involved in defect detection as a first step to defect rectification. These principles can be used to improve the result of the automated counterpart, once adopted. The approach to extract irregularities on previously unseen data before an actual assessment is one of them. Learning from examples is another, very important one: A child learns what a cat looks like by direct experience and being

shown many visual images of cats. If asked to draw a cat the child will produce a very abstracted line drawing but will recognizable as an abstraction.

The human perception and especially the HVS are much too complicated to be fully understood, but these clearly identifiable principles can be adopted to model the HVS in specific tasks, for example the human wood worker in defect detection. With the studied approach of automated defect detection on wooden panels the main principles "segmentation prior to classification" and "learning based on image examples" have been demonstrated to be adaptable and to be feasible also for a machine.

The concept of learning from raw data, waiving feature engineering is adopted from Deep Learning *[Deng and Yu 2014]* which is a branch of machine learning and whose research has spawn several algorithms specifically for large-scale complex data structures like images, recorded speech and similar. The decision to incorporate the well-known classification techniques (SOM, SVM) in this research is due to their proof in industrial applications, related to the aim to install prototype systems in real-production environments. Great capabilities are seen when following the path of development of Deep Learning as the underlying principle has been shown to work in the context of an industrial application.

Having shown the feasibility of replacing manual labour in the defect detection by dedicated machines, a quite huge field of similar applications is opened. The automated quality control incorporating visual sensors is currently facing its limits with the huge bandwidth in the appearance of natural products. The principles of recognition identified and adapted for defect detection in this research might help to improve defect detection on other natural surfaces as well, more generalized the localization of objects in terms of irregularities and their identification in previously unseen natural scenes can thereby be addressed. Thinkable applications are therefore sub-tasks in face-recognition, for example the segmentation of the major elements like mouth, eyes, nose and their correct classification prior to further processing. In parallel to the implicit and complex aesthetic information contained in images of knots, visual data of eyes contains information (male/female, happy/sad, tired, etc.) which is quite easily interpretable by humans, but currently is limited interpretable by machines. This issue could be promisingly addressed with the proposed approach of raw features and large-scale non-linear classification. The limitation of this approach is thereby on single objects as elements of a scene rather than on complete scenes, e.g. knots on a

wooden panel have been shown to be classifiable well, also in terms of local aesthetics, but not full images of complete panels. A prerequisite for adopting this approach is the availability of huge training data sets.

The appearance assessment of complete wooden panels and related global aesthetics is incorporating several relationships among the objects (e.g. knots) in the scene. Besides the fact that complete images of panels are represented by many times the amount of pixels than it is the case for a knot image snippet for example, the approach of raw features in the training from examples is impracticable for an automated approach on panel-level. Decomposition of the scene is done by the human counterpart and has been adopted in the approach to decision making in the automated rectification. The relationships of elements in a scene are part of implicit and explicit knowledge of the wood worker and reflect also in the implicit preference of a customer of the wood product. To model this incorporated knowledge uncertainty has to be addressed in the formulation of rules that are used to represent such knowledge. From a technical point of view such complex decisions can be represented by a high-dimensional decision space spanned by a certain number of parameterized rules which thereby define a decision surface in that space. Adding a rule simply helps to refine the decision making in terms of decision space segmentation while the parameters add weight along the axis belonging to the specific rule. Using rules formulated in human language but interpretable by a system as used in the decision making for automated patching is seen to be the key to a variety of complex decisions related to human perception in automation technology. In combination with the previously discussed classification of objects in a scene, the interpretation of the scene analogous to the overall appearance of a wooden panel could be adapted to the evaluation of camera-acquired scenes in autonomous driving vehicles for example. Especially the concept of incorporating rules formulated in human language, linking the segmented and classified objects, might fit well to the interpretation of traffic signs and the related decision making. Coming back to wood products the development of a wood grading system could be accomplished to ensure the visually acceptable combination of wood-based components. For example in the production of kitchens and furniture having a wood look certain homogeneity is desired by the end customer and all cabinet carcasses of a kitchen should have similar looking faces related to the visual texture, which is defined by the mean colour and frequency of the grain structure, but also by the amount and frequency of knots.

The actual patching of wooden panels has been identified partially as art handicraft, especially when it comes to the proper selection of dowels by means of colour and texture or when routing needs to be executed prior to filling with putty as several options exist on how to achieve a pleasing result. While manual labour will always incorporate human creativity which hardly can be modelled by algorithms, automatically generated patching instructions run the risk of producing more artificial looking patches as well as of producing repeatedly, similar looking patches which might be appreciated in some cases and might be annoying in others. The judgement capability incorporated in this matter remains reserved to humans at the present time. Nevertheless optimization parameters have been indentified that allow adjustments towards either precise - therefore more complex - carried out patching or more efficient patching favouring throughput and therefore addressing economic aspects. In large-scale industrial productions like for wooden panels, this lack of creativity and related judgement is less a disadvantage than in the manufacture of more or less unique products where manual labour is favoured over cost saving and increase of throughput, as highly automated processes favour reproducibility and reliability.

The bottleneck in automated patching seems to depend on the amount of defects per panel. For the studied prototype systems it can be seen that with only a couple of defects (higher quality boards) the transportation speed and processing by the tools is quite high and the scanner system is the limiting component. With rising amount of defects both the software computation time of the scanner and the processing time of the patching tools increased, but more drastically for the machinery, whereby the path optimization (between the defects) for the tools is currently out of the scope of the scanner and is seen as an area of improvement. The detection and patching data quality decreases on more complex and therefore more demanding panels of low-quality and with more defects. When incorporating these two findings it can be concluded that it is more efficient to use automated patching on medium and high quality panels.

Besides the automation of the actual patching process a system for automated patching offers secondary benefits as a source of data related to the process. With its data interfaces, not only to the patching machinery, but also to Enterprise Resource Planning systems (ERP), Production Planning Systems (PPS) and similar databases, an automated patching system is able to deliver valuable information. This includes statistics about the occurrence of certain

defects, amount of used materials, achieved qualities as well as a possible feedback-loop to the preceding veneer sorting, addressing overseen, not repairable defects. It can be stated that superior production processes thereby may become more effective, to a certain extent more intelligent.

7.2.2 Interpretation in context of literature

Earlier research and present known systems addressing the similar, but less demanding, task of grading wooden panels evolved from single image channel to multi-channel imaging systems, incrementally incorporating colour imaging, structural and three-dimensional measurements. The ever-growing computational power enables the further development of multi-channel imaging systems. Imaging in spectral bands like UV, tailored to specific effects on wood, has been incorporated additionally and with benefit in this study. With a rising number of sensors the importance of a well-structured concept concerning the sensor data fusion comes to the fore to handle the algorithmic complexity. Unlinked evaluation of the single channels is found to be still common in current system designs, only linking the results on the highest level of information processing (sensor fusion on symbol level). Ideally a multi-imaging sensor system acquires pixel-wise registered multi-channel images, independently from varying spatial resolutions, number of sensor elements (pixels) and sampling rates (sensor fusion on pixel level). This allows the linkage of the channels on the earliest possible stage of evaluation when using appropriate algorithms. Known present and comparable systems have further been found to be designed in a monolithic approach from the aspect of information processing. The studied system design differs to these systems in terms of its clearly structured, modular system architecture for both software and hardware. This incorporates different layers for image data acquisition, pre-processing and data fusion, evaluation and classification and finally content-interpretation to derive patching instructions. This design follows the paradigm of increasing abstraction of the underlying image data.

The majority of comparable systems are found to be based on the non-segmenting approach, which means that the captured image data of a wooden panel is processed entirely in equal-sized tiles. Problems arise from this tiled processing approach in terms of the tile size being inappropriate to the various defect sizes. In automated patching, it has been found to be more intuitive to use the segmenting approach: Strong characteristics of

surface and aesthetic defects gathered with optimized sensors in combination with a priori knowledge, for example derived from symmetry and repetition of the defects, are proposed to be used to create a so-called Defect Candidate Map. This map is then used for a reliable delimitation of areas of interest from the background. These defect candidates are then fed solely to the defect classification system. This approach imitates the manner in which humans solve the task by first identifying irregularities in an adaptive manner and only then categorizing them. Thereby, in the very beginning of the image processing chain, the adaption to human visual perception is achieved. The design experiments and related testing show mainly satisfactory results which are seen to be superior over the non-segmenting approach that often fragments the defect candidates. A worsening in terms of segmentation results getting incomplete with rising complexity of the defects is however observed.

Based on the segmenting approach a processing chain has been developed with respect to the comparative human approach to the task of defect detection and defect classification. The processing is thereby executed on the complete defect. This completeness allows a much more effective classification (average precision significantly above 90% constantly among the different defect types). Table 7-1 shows the average precisions achieved for the defect types incorporated in the training experiments, including a pure aesthetic judgement of unpleasant Dark Knots.

	Bark	Dark Knot	Ringed Knot	Sound Knot	Cracked Knot	Resin Pocket	Unpleasant Dark Knot
Average Precision (AP)	96.39%	97.16%	94.63%	95.75%	94.57%	99.14%	91.93%

Table 7-1: Summary of average precisions achieved in the classification of defect types.

Other, earlier research on machine vision applications for grading wooden panels (either solid wood or plywood) reports classification accuracies in the range of 75% – 98%. The different defect types thereby perform with great variance; easy to classify defects as holes and cracks can be classified in the range of 90 - 98% due to strong (3D) features. Other defects are reported to perform less reliable, independent from the classification technique used. For example, Alapuranen and Westman *[Alapuranen and Westman 1992]* showed that only using colour features with a K-NN classifier can result in correct classification rates of 92% for rotten knots, 88% for sound knots, 85% for colour strokes, 98% for clear wood and

only 75% for pressed-in thrash particles on plywood panels of spruce. More complex defect types like finer discriminated knot types (dark knots, rotten knots, knots with bark, sound knots and cracked knots) addressing implicitly local aesthetic issues, which are sometimes even hard to discriminate correctly by human experts, are commonly reported to perform only in the 75% - 85% range of correct classification. Lampinen and Kauppinen *[Lampinen et al. 1994]* showed a performance increase from 77.0% to 81.3% when extending solely texture feature-based classification on solid spruce boards using a K-NN classifier with colour features, respectively a multi-layer perceptron neural network from 76.0% to 82.7% mean correct classification rate. In particular their setup distinguished between seven different knot types (sound knot, decayed knot, dry knot, encased knot, leaf knot, horn knot, edge knot). It is necessary to understand, that in the scope of automated patching much higher demands are posed on classification accuracy than in grading tasks. This is due to the fact that false positives destroy sound material unnecessarily. This may result in a quality downgrade for the whole panel. False negatives leave defective areas unrepaired. This is unacceptable in certain subsequent processing steps like foil-coating the panel.

The underlying research has identified that improvement of the classification accuracies, especially under local aesthetic aspects, is gained from maximizing the involved information content. This is achieved in terms of new sensors gathering additional information, but also by waiving explicit feature preparation and selection in favour of using raw image data directly and incorporating huge amounts of training samples. This clearly distinguishes the studied approach from the approaches based on feature engineering commonly used. To deal with the related huge amount of data, respectively with the thereof resulting high-dimensional feature spaces, novel classification techniques like Support Vector Machines (SVM) must be incorporated. The concept of the support vectors representing the relevant training samples on the optimal decision boundary guarantees a good computational performance (O(n) in testing) compared to the popular K-NN algorithm (O(log(n)) for example, as K-NN needs to store all the training samples and needs to carry out an excessive search. SVMs show therefore to be suitable for large-scale online classification in industrial applications. Improvement of the classification accuracy nevertheless remains substantial due to the huge quantities of defect candidates. With thousands of repairs per hour, only some tenths of a percent of either higher true positive rate or lower false positive rate imply higher creation of value, respectively some tenths of a percent of lower false negative rate

save money due to unnecessary manual re-work. In the worst case an already coated panel needs to be scrapped solely due to a single undetected and therefore unpatched defect.

The main requirements to the patching instruction generation are the preservation and the adjustment of the global aesthetics of a wooden panel. Patching instructions must be compiled incorporating explicit as well as implicit rules which are part of the wood-working expert's knowledge. This knowledge can be formulated well in human language and has been extracted by observations of manually carried out repairs in real production facilities. The approach to use an Expert System in form of a Fuzzy Inference System processing these formulations including linguistic variables (adjectives) whose meaning can be fuzzy (*little, some, strong, weak, knotty, plain, unsettled, calm,* etc.) represents expert knowledge in a more intuitive way than sets of hard to interpret thresholds in conditional programming. This approach has to the best of one's knowledge never before been applied in the production of (wood) products, especially not in the automated generation of patching data which is seen to be accomplished on wooden panels for the first time by the prototype systems developed and studied in the scope of this research. Expert Systems and neuro-fuzzy methods have recently become popular for mapping product parameters to customer feelings towards the product. This is of interest in product design incorporating Affective (Kansei) Engineering. This parallel development strengthens the chosen approach.

The extension with additional rules can be used to further bias the decision surfaces under several aspects, e.g. economic, ecological or aesthetic optimization. In addition, fundamental parameters in the patching with liquid fillers have been identified that allow the optimization of the patching process based on the necessary compromise between panel throughput and material consumption and appearance.

For the system to be easily adaptable, explicit feature selection which would require a machine vision expert's work of analysis and testing has been waived. This means the wood working expert now has to correctly label huge sets of example image snippets for the supervised learning. The advantage of SOMs to project high-dimensional problems to a two-dimensional grid is exploited hereby for an automated pre-sorting of the image snippets used for the final training. This concept of grouping similar images from defects on wooden panels has been proposed initially by Kauppinen *[Kauppinen 1999]* for the actual classification in his research. Kauppinen achieved comparatively good results, but faced the

limitations caused by feature selection which he needed to incorporate due to issues with the computational complexity of SOMs. In the setup of the prototype systems used in this research, the SOM is used offline only to pre-group the images by similarity based also on handcrafted features. This considerably supports the wood working expert in the tasks of defining and labelling training sets and training set harmonization. The number of training images which must be explicitly labelled is thereby reduced drastically to only the visually noticeable outliers. Fast retraining from scratch as well as learning something new is therefore possible based on an easy to understand pictorial representation. Appropriate (radiometric) image calibration techniques further allow the exchange and re-use of the image database representing fundamental knowledge between different systems. This in turn allows more homogenous results among different production lines and even among production plants.

7.2.3 Generalisation and implications

In the discussion of the research methods for detection and decision making, several fields of application were already outlined where the proposed methods might be of beneficial use. The generalisation from wood to other natural surfaces, especially with coloured and textured appearance and huge portions of visually perceived quality, seems logical and feasible. The large-scale classification using raw features is seen to be able to replace conventional methods whenever image data can serve for learning from examples directly, enabling much more complex inspection tasks to be automated. This is especially valuable when aesthetic judgements are requested as these are hard to describe numerically in a feature engineering approach. It is definitely useful to incorporate registered colour images in any case due to the good interpretability and to establish a connection to the perception and knowledge of the human(s) creating the training data sets. Furthermore quite huge training data sets should exist. The concept of the A Priori Knowledge Feature Vector Extension may be used to additionally incorporate data from acoustic sensors and/or haptics sensors to improve automated product quality inspection for example.

As identified previously, the rule-based Expert System incorporating fuzziness is actually analysing a scene which is set up by the various apparent defective and non-defective elements in the case of the surface of a wooden panel. This concept of combining object-identification with scene-interpretation could be adapted to various applications

incorporating (multiple) spatially resolving sensors, from vision-based autonomous driving to earth-imaging for geo-information.

Automated rectification can be understood as the automated drawing of specific consequences from the scene analysis and can be imagined on a variety of products. Although non-flat surfaces introduce an extra challenge, for the sensors as well as for the actuators, the automated production of wooden goods beyond the limitation to panels could profit from the technology developed in this research. The application to panels of stone is more a question of adapting the sensor setup than the decision making, patching data generation and patch application, as higher-valued stone panels are currently patched in a very similar way to plywood panels by using liquid fillers. The modular approach of the system design and the fact that importance has been placed on the traceability of the information processing, involving images whenever possible is seen as the key to adaption of automated patching to other natural surfaces in principle.

Large-scale automated patching on natural materials like wood and stone, used as feedstock for therefrom assembled goods, might have impact on the availability and therefore the price of these goods. While real-wood flooring, for example, has had, for several years, an exclusive character due to much higher costs than laminate flooring or of course linoleum covered floors, the modern production of ultra-thin face veneers for parquet flooring has already dropped the price significantly. With large-scale automated patching not only the yield from the currently used wood species is significantly increased, but other, faster growing wood species like Eucalyptus and Caribbean Pine with therefore more and bigger defects might become usable and worthwhile. While ecological benefits can easily be derived from such a theoretical progression of an increased use of renewable raw materials, questions arise on the possibilities and needs of recycling large quantities of natural materials patched with artificial compounds ranging from water-based putty to polymers like polyurethane and epoxy resin.

7.2.4 Limitations of the study

This thesis and the underlying study of prototype systems for automated patching of wooden panels is solely based on panels (solid wood panels and plywood panels) made of softwood, mainly Nordic Spruce and to some extent on panels of Pine Radiata (plywood

only). Due to the industry-driven nature of the research project the prototype systems were linked and therefore limited to the needs of potential customers. The availability of panels made from other types of softwood like Larch and Fir could have proven the concept in more detail especially under appearance and aesthetic aspects. Further, the degree of flexibility of the information processing components could have been shown, concerning detection as well as the actual patching, as different defects and different appearances imply different rules for the generation of repair instructions.

Panels made from hardwood, for example birch, needed to be excluded from this research for the same reason as for Larch and Fir. The scatter effect on hardwood is expected to be much less intense due to the different cell structure compared to softwood. This presumably raises several issues on the segmentation concept and the Defect Candidate Map in the application on hardwoods.

The validation tests using real-production panels are extremely time-consuming. Only a packaging unit of 50 panels can realistically be scanned, marked, evaluated, patched and assessed per day, which represents a certain constraint on the validity of the gained statistics. Besides a limited number of panels the fact that a natural product like wood incorporates an almost infinite bandwidth of appearances, both locally per defect and concerning the overall panel, renders it practically impossible to provide the proof that such a system for automated patching works correctly in all cases. Measures like accuracy in detection and decision making used as a statistical measure on the basis of a representative sample of panels therefore must be accepted as sufficient. Only by proving the adaptability of such a system to changes on the raw material by efficient configuration and training capabilities can the acceptance be achieved.

While wooden panels patched solely with dowels can be verified in detail before sanding, this is impractical for panels patched with plywood, refer to Figure 7-1. Marking the defects manually before scanning has been incorporated on solid wood panels as shown in Figure 7-2.

Figure 7-1: Plywood panel patched with putty does not allow assessment and replicability using markings made previous to scanning.

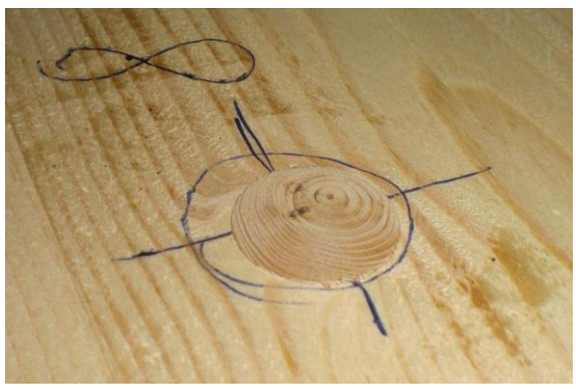

Figure 7-2: Defect marked previous to scanning and patching with dowels for replicability purposes and evaluation before sanding.

The assessment of patched plywood panels after sanding has therefore been carried out on the basis of acceptance of the final result. No unique traceability of the panels from scanning to sanding was available. This could have been achieved by the use of Radio-Frequency Identification (RFID) technology with RFID chips laminated into the panel for example but was not adopted due to cost. More simple and cheaper methods like printed barcodes, stickers and similar are destroyed during sanding and edge trimming. Therefore no link from the appearance and the condition of the panel before patching to the visible result of patching after sanding, by viewing the corresponding images for example, could be established. Further, no reconstruction of the patching data generation including decision making could be made for the same reason. This has several implications:

- The existence of a better solution could not be assessed in the case of an accepted patch.
- A certain unknown amount of false detections and subsequent unnecessary repairs may be assumed among the accepted patches.

The limitations and constraints of the industry-driven research, especially in terms of available time, also did not allow investigating into all possible alternatives concerning the research methods and related algorithms. The methods therefore needed to be pre-selected by theoretical assessment and by specified requirements, e.g. a classifier able to handle huge sample sizes, high dimensionality, showing good convergence and a unique solution in training, and an expert system to incorporate fuzziness in the rules. Furthermore, the industrial applicability of the methods stood in the foreground.

Due to the quite time-consuming training and testing on the available hardware, linear SVMs approximating the proposed non-linear counterparts had to be used. By showing acceptable results, this technology in principle has been shown to be appropriate and gives a promising outlook.

Certainly the cultural background influences the rules derived. The restriction on panel products produced for the European market introduces limitations concerning the cultural differences in the perception and appreciation of wood surfaces including aesthetics preferences which most likely pose further, yet unknown requirements.

7.3 Conclusions

Human labour in the production of wooden panels, specifically in the task of finishing the wooden surface by patching, can now be replaced by machines. It is therefore now possible to detect and rectify surface and aesthetic defects in an automated manner such that the output is satisfying compared to the results of the human counterpart.

Specifically, it is now possible to automatically discriminate defects on wood surfaces by physical and aesthetic properties through a newly built system using machine vision, knowledge-based decision making and intelligent automation. This answerers the research question on “how it is possible to detect and repair surface and aesthetic defects on natural surfaces like wooden panels in an automated manner such that it can replace human labour?”. It has been demonstrated that for this purpose human perception can be modelled by training from huge sets of multi-channel images. Further, human expert knowledge formulated in natural language has shown to be usable in machine-interpretable rules by a specifically adapted Expert System. When compared to the results of the wood workers’

labour, in certain limits it is possible to achieve aesthetically satisfying results with this novel automated patching,

The underlying research successfully addressed the thesis that an industrial-suited automated system can be designed, built and integrated, satisfying the requirements for rectification of natural surfaces. The therefrom derived aim “to develop a solution to automatically generate patching instructions which are to be applied on natural surfaces by automated tools” has been met by attaining all the five initially stated objectives:

- The first objective was to identify defect detection techniques and to assess their adaptability for the specified task of automated patching. This has been met by gaining an overview on potential methods from a comprehensive literature review first. A selection of appropriate methods has then been made academically by contrasting them against previously identified requirements.
- The second objective was to establish research methods for the purpose of defect detection for decision making, including the requirement of aesthetic assessment. This has been met by developing a unique combination of a segmenting approach on the input images and Support Vector Machines with direct image classification, following the principle of the Human Visual System.
- The third objective was to indentify suitable common patching techniques for different types of defects on different types of wooden panels. The patching with solid fillers (dowels), mainly on high-valued solid wood panels, and the filling of optionally previously routed defects on both solid wood panels and plywood panels with different types of liquid fillers (putty) have been identified as the most required, reasonable and promising techniques to be automated for industrial productions.
- The fourth objective was to implement and integrate the corresponding generation of patching instructions. By development of a specifically tailored Expert System this objective has been completed. This Expert System is holding the rules for patching with different types of putty and dowels including appropriate pre-processing. The concept has been demonstrated working in an industrial production.
- The fifth objective was to devise possibilities for adjusting quality, also in terms of the final appearance of the panels. This has been met by incorporating wood working expert knowledge in both main data processing stages of defect detection and

patching data generation. This has been achieved first by combining unsupervised and supervised learning to a unique method preventing loss of information. This novel method is able to model and generalise also aesthetic properties of potential defects. Second, this objective has been met by incorporating adjustable rule sets in the Expert System for modelling the customers' preferences towards the overall product appearance.

Prototype installations show that replacing the manual labour in this diverse and demanding task by a machine is now possible. Patching wooden panels has previously been conducted by trained operatives. Despite certain limitations automated patching can therefore achieve economic benefits due to:

- A much higher production throughput because of reduced need for manual workplaces.
- Sensor data fusion from multiple imaging sensors at low level to combine colour, texture, structural and defect-specific measurements to gain maximized information content in detection and evaluation. This opens new possibilities for intelligent automation.
- A defect-segmenting approach followed by classification to better model the human visual system for the improvement of intelligent automation.

The main findings of studying the proposed methods and the contribution to knowledge are:

- Training with image examples directly in supervised machine learning is the best way to tell a machine what is visually acceptable and what is not. This could not be achieved in former attempts and is now possible.
- Feature engineering must therefore be replaced by methods similar to deep learning in machine vision tasks addressing aesthetics. This is seen as the best way to deal with the related complexity.
- Multi-sensorial images holding information (features) from different spectral bands like UV and IR as well as from Scatter Imaging can and need to be incorporated. This is related to wooden properties not being visually perceptible from the colour image but being perceived by human experts through a-priori knowledge.

The result from development, integration and testing in an industrial environment is:

- Modern machines are not yet able to outperform human workers when creativity and decision making is necessary to address natural variety. But specific and clearly delineated automated tasks of patching on wooden panels of pre-sorted quality outperform human labour in terms of speed, throughput and reproducibility.
- A working parametric model incorporating high degrees of uncertainty to represent the woodworker's explicit and implicit knowledge related to the actual patching and the final appearance of wooden panels. This could also be used in similar tasks like grading.

Automated visual inspection of panels is significantly enhanced by the findings related to the previously unsolved, complex task of aesthetic judgement. Having demonstrated that patching can be carried out autonomously to a huge extent by machines, a gap in the automation of wooden panel production is closed. Costs of manual labour can therefore be substantially reduced. For the panel producing sector of the wood-working industry facing competition from dumped imports, the automated patching technology is prospectively vital. For this reason it is important to establish the generalisation of the methods to hardwoods and also to other cultural backgrounds which influence the appreciated appearance. This generalized approach to surfaces of other types of wood is rated positively and may be extended to natural surfaces such as stone.

The algorithms developed significantly take control over the sub-process where added value is attained and represent a further advancement in intelligent automated production. Another future aspect is the coupling with modern and future product design techniques incorporating for example customer psychology for the creation of customized product appearances.

The classification and decision making component could further be applied in other areas where automated scene-analysis based on classified objects and complex rules relating these objects is demanded.

7.4 Further research

The research presented in this thesis resulted in the first (prototype) system for automated patching available to the wood working industry and introduced several further questions which could not be answered in the scope of this thesis. Further possibilities of research are seen with the following topics:

The investigation into and development of optimized kernels for the use with non-linear Support Vector Machines in the classification of raw multi-channel pixel-data, tailored to improve the classification accuracy as well as the runtime performance both in training and testing. This is seen necessary due to the ever-growing demands concerning production capacity and overall performance mainly rated by the achievable throughput. Computation time could further be saved with parallel computing and the use of General Purpose Computation on Graphics Processing Units (GPGPU).

The application of the patching instructions generated by an automated system is irreversible. Additionally there exist no two identical panels made from real wood. Especially in the setup-phase of the prototype system it has been found difficult to test several different settings as no real comparison could be made due to these facts. Furthermore, the test panels are in the best case downgraded or need to be scrapped in the worst case. Computer simulations of the results from different patching strategies and related options would help improving the capabilities, adjusting efficacy, shorten setup times and reduce costs. Theoretically, auto-adjusting rules incorporating learning from the characteristics of a production batch by extending the FIS - Expert System to an Adaptive Neuro-Fuzzy Inference System (ANFIS) could be used with simulated patching results.

Perception of appearance and aesthetics of wood in other, non-European cultures needs to be studied to understand the requirements for adaption and extension of the rule-sets used in the knowledge base for patching.

A purely aesthetic repair is a wide but nearly unexplored area in the field of automated patching on natural surfaces. Retouching as the process of photo/image manipulation can be carried out on digital images quite effectively. Although mainly carried out manually by experts using professional image processing applications, a variety of algorithms already exists that allows semi-automated retouching. Retouching includes the deletion of parts or

objects in an image as well as their creation, either by assembling from several images (photomontage) or by creating artificial parts and objects. The artificial creation of image data by algorithms is called *inpainting.* Inpainting could be used to generate synthetic patches applicable also to wooden panels. The application could include the overprinting of already physically patched defective areas for the reason to fully camouflage the repaired area. Ink-jet printing is already successfully applied in large-area digital printing on wood, for example in the production of real wood floorings showing so-called “Wood-Design” surfaces (e.g. *Kaindl TWO real wood design, [Kaindl-TWO n.d.]*) which are clear-varnished additionally. For the generation of locally printed patches a variety of issues needs to be addressed: Besides optimized inpainting algorithms for the image patch generation, the colour calibration and colour adaption to the surrounding wood is seen crucial to make the patch visually imperceptible. Presumably issues related to the printability of putty and other filling materials used for the physical patching will arise in this context and specifically optimized filling materials may necessarily need to be developed. The automated decision making could thereby draw on much more possibilities in terms of “knot generation”, generation of “camouflage textures” and similar. This in turn could open the possibility to radically change the aesthetic appearance of a wooden panel. While the current approach is able to modify the appearance only in certain limits, for example sound knots are currently most often accepted, the panel is therefore being inappropriate for top-quality ‘A’ (no knots allowed). Panels which are visually free from any irregularity like shown in Figure 7-3 could be produced using overprinting.

Figure 7-3: Defect free surface of plywood panel quality ‘A’. This result would be achievable also with large-scale overprinting on lower quality panels while local patching is able to remove only some defects and cannot radically change the appearance.

The appropriateness of such camouflaged panels would of course be limited to only certain purposes as the overprinting most likely will not withstand outside influences in the same way as the real surrounding wood and further cannot be processed arbitrarily (e.g. sanding). Clear varnish coating might be appropriate nevertheless for several end products like furniture and floorings. The fact that most of nowadays produced parquet is no longer sandable anyway due to ultra-thin face veneers is a strong argument for this purpose.

A coupling of large-scale overprinting and the already mentioned Affective (Kansei) Engineering could open new possibilities in automated, customized produced furniture, floorings and similar wood-based products. With full freedom in the creation of visual wood textures by printing, the approach to “Wood-Design Surfaces” described by Kansei features linked back to a common Expert System might allow the creation of an unique and customer-specific appearance which is seen as an important property in the more exclusive range of products. In the example of floorings, besides the acoustics and haptics, the overprinted wood would thereby be much more ‘natural’ than laminates for example.

The overall concept of the proposed automated patching might be transferred to other natural and natural looking surfaces. This might be panels of hardwoods as well as from stone. E.g. marble which is today patched manually with resin in a similar way compared to plywood, refer to Figure 7-4 which shows panels of *Spanish Dark Emperador Marble* being manually patched with brown epoxy resin to close surface defects.

Figure 7-4: Panel of marble patched with epoxy resin (not yet sanded) in a similar manual way like plywood. *[GHGGroup 2010],* image used with kind permission.

Single approaches and components like the classification under local aesthetic aspects by training examples of what is nice and what is ugly could be adapted to the referenced grading systems for wooden panels, lumber and veneer to improve their detection capabilities.

Further unconventional patching techniques respectively patching materials could be incorporated. There exist several approaches to use materials for patching that do not attempt to hide the repaired area but in contrary emphasize them in an artistic manner as shown in Figure 7-5, Figure 7-6 and Figure 7-7:

Figure 7-5: Oak board with tin used for filling cracked knots with the purpose to emphasize aesthetically. *[LUNA-DESIGN n.d.], i*mage used with kind permission.

Figure 7-6: Walnut board with tin used for filling knot holes with the purpose to emphasize aesthetically. *[Buck 2015*], image used with kind permission.

For example liquid metals like tin or aluminium can be used for patching and to intentionally create an aesthetically pleasing contrast at the defective area, refer to Figure 7-5 & Figure 7-6 which show hardwood panels of oak and maple whose indentations at knots were filled with hot tin. Another interesting synthetic/artificial appearance with an intended contrast between the wood and the filling material is achievable by incorporating coloured resins. Figure 7-7 shows fluorescent resin used to fill natural and intentionally produced indentations on a wood board of Pecky Cypress.

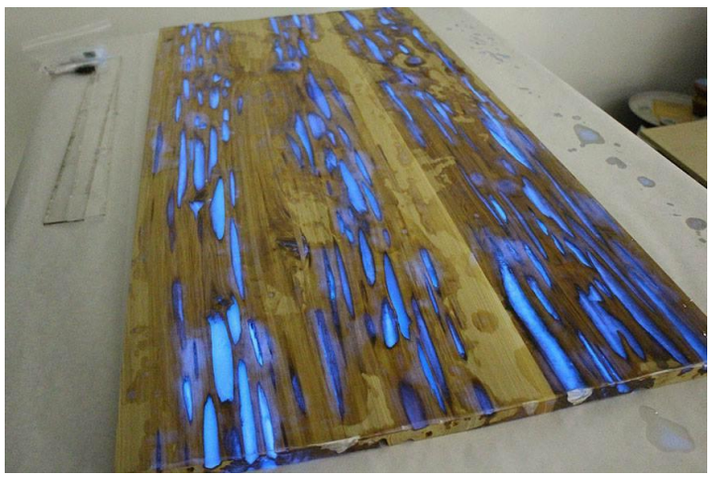

Figure 7-7: Fluorescent resin used for filling immersions on a panel of Pecky Cypress. Pecky Cypress shows pockets that reside from heartwood which is destroyed by a fungus [Saurus 2014]. Image used with kind permission.

Aesthetic patching does therefore not necessarily mean to disguise defective areas but might follow the contrary approach of enhancing them, creating intentionally artificial looking surface. This opens another field of future work reaching into the field of arts and arts created by machines.

References

Aizerman, M., Braverman, E., Rozonoer, L. (1964) 'Theoretical foundations of the potential function method in pattern recognition learning'. *Automation and Remote Control*, Vol. 25, p. 821–837

Alapuranen, P. and Westman, T. (1992) 'Automatic visual inspection of wood surfaces'. *Proceedings of 11th IAPR International Conference on Pattern Recognition, Conference A: Computer Vision and Applications*, Vol. 1, p. 371-374

American National Standard Institute (1983), *ANSI Standard for Dimensioning and Tolerancing*. Y14.5M:10983. The American Society of Mechanical Engineers, United Engineering Center

Arshdeep, K., Amrit, K. (2012) 'Comparison of Mamdani - Type and Sugeno - Type Fuzzy Inference Systems'. *International Journal of Soft Computing and Engineering (IJSCE)*, Vol. 2, Issue 2, ISSN: 2231 -2307

Astrand, E. (1996) *Automatic Inspection of Sawn Wood*. Linköping: Disseration No.: 424. Linköping: Departement of Electrical Engineering Linköping University, Sweden, ISSN: 0345-7524

Astrand, E. and Astrom, A. (1994*)* 'A single chip multi-function sensor system for wood inspection'. *Proceedings of the 12th IAPR International Conference onPattern Recognition, Conference C: Signal Processing,* Vol. 3, p. 300-304

Baldwin, R. F. (1981) *Plywood manufacturing practices*. 2nd edition, San Francisco: M. Freeman Publications, ISBN: 978-0879300302

Belhumeur, P. N., Mumford, D. (1992) 'A Bayesian Treatment of the Stereo Correspondence Problem Using Half-Occluded Regions'. *Proceedings 1992 IEEE Computer Society Conference on Computer Vision and Pattern Recognition*, p. 506–512

Bowe, S. and Bumgardner, M. (2004) 'Species selection in secondary wood products: Perspectives from different consumers'. *Wood Fiber Science,* Vol. 36, p. 319–328

Boyd, S. P. and Vandenberghe, L. (2004) *Convex Optimization.* Cambridge*:* Cambridge University Press, ISBN 978-0-521-83378-3

Broman, N.O. (2000) *Means to measure the aesthetic properties of wood*. Doctoral Thesis, Luleå: Luleå of Technology, Sweden

Broman, N. O. (2001) 'Aesthetic Properties in Knotty Wood Surfaces and their Connection with People's Preferences'. *Journal of Wood Science*, Vol. 47, Issue 3, p. 192-198

Brown, L. G., (1992) 'A survey of image registration techniques'. *ACM Computing Surveys*, Vol. 24, Issue 4, p. 325-376

Brunner, C., Maristany, A., Butler, D., Van Leeuwen, D., Funck, J. (1992) 'An evaluation of color spaces for detecting defects in Douglas-fir veneer'. *Industrial Metrology,* Vol. 2, p. 169–184

Buck, P. (2015) *Table from solid maple having knotholes filled with tin*. [online] available from <http://www.paul-buck.de/Bilder/tischahornzinndetail.jpg>

Burt, P. J., Kolczynski, R. J. (1993) 'Enhanced image capture through fusion'. *Proceedings on Fourth International Conference on Computer Vision*, p. 173-182

Butler, D. A., Funck, J. W. , Brunner, C. C. (1993) 'An Adaptive Image Pre-processing Algorithm for Defect Detection in Douglas-fir Veneer'. *Forest Products Journal*, Vol. 43, Issue 5, p. 57-60

CEI-Bois: Guy-Quint, C., Beyer, G., Defays, M., Fischer, M., Fletcher, J., de Munck, E., de Jaeger F., van Riet, C., Wijnendaele, K. (2011) *Tackle Climate Change: Use Wood*. [online], Brussels: European Confederation of woodworking industries (CEI-Bois), chapter 7- Industry facts and figures, p. 70-78, available from: <http://www.cei-bois.org/files/FINAL_-_BoA_-_EN_-_2011_text_and_cover.pdf> [31 July 2015]

Chen, C. H. (2012) *Signal and image processing for remote sensing*. Boca Raton,FL: CRC/Taylor & Francis, ISBN 9781439855966,

Cho, T. H., Conners, R. W., Araman, P. A. (1990) 'A computer vision system for analyzing images of rough hardwood lumber'. *Proceedings of 10th Int. Con. on Pattern Recognition*, Vol. 1, p. 726-728

Cortes, C. and Vapnik, V. (1995) 'Support-Vector Networks'. *Machine Learning,* Vol. 20, Issue 3, p. 273-297

Cover, T. M. (1965) 'Geometrical and statistical properties of systems of linear inequalities with application in pattern recognition'. *IEEE Transactions on Electronic Computers*, Vol. EC-14, Issue 3, p. 326-334

Cristianini, N. and Shawe-Taylor, J. (2004) *Kernel methods for pattern analysis*. Cambridge: Cambridge University Press, ISBN: 978-052181397

Cristianini, N. and Shawe-Taylor, J. (2000) *An Introduction to Support Vector Machines and Other Kernel-based Learning Methods*. Cambridge: Cambridge University Press, ISBN: 978-0521780193

Crowley, J. L. and Demazeau, Y. (1993) 'Principles and Techniques for Sensor Data Fusion'. *Multisensor Fusion for Computer Vision,* p. 15–36

Dasarathy, B. V. (1991) *Nearest Neighbor: Pattern Classification Techniques (Nn Norms : Nn Pattern Classification Techniques)*. Washington: IEEE Computer Society Press Tutorial, ISBN: 978-0818689307

Deng, L. and Yu, D. (2014) 'Deep Learning: Methods and Applications'. *Foundations and Trends in Signal Processing,* Vol. 7, p. 197–387

Dillenz, A., Busse, G. (1999) 'Monitoring of defects in laminates with lock-in thermography'. *Stuttgarter Kunststoff-Kolloquium*, Vol. 16

Donges, A., Noll, R. (1993) *Lasermesstechnik.* Heidelberg: Hüthig-Verlag, ISBN 3-7785-2216-7

Dubois, D., Prade, H., (1996) 'What are fuzzy rules and how to use them'. *Fuzzy Sets and Systems - Special issue dedicated to the memory of Professor Arnold Kaufmann*, Vol. 84, Issue 2, p. 169-185

Dunn, W. (2005) *Fundamentals of Industrial Instrumentation and Process Control*. New York: McGraw-Hill Professional, 1st edition, ISBN: 0071457356

Eberhardt, J., Massen, R. and Kuehn, M. O. (2011) 'Automatic physical and aesthetic patching of wood-based panels saves Woodstock resources'. *International Panel Products Symposium IPPS 2011, Llandudno, Wales*, p. 171-177

FAOSTAT: Food and Agriculture Organization of the United Nations (2014) [online], available from: <http://faostat3.fao.org/home/E> [31 July 2015]

Fischer, R., Wendland, G. (1999) 'Using the Tracheid Effect for automatic inspection of wood'. *Wissenschaftliche Zeitschrift der Technischen Universität Dresden*, Vol. 92, p. 82-84

Forest Products Laboratory: Bergman, R., Cai, Z., Carll, C. G., Clausen, C. A., Dietenberger, M. A., Falk, R. H., Frihart, C. R., Glass, S. V.; Hunt, C. G., Ibach, R. E., Kretschmann, D. E., Rammer, D. R., Ross, R. J.. (1999) *Wood Handbook: Wood as an Engineering Material*. [online], Madison, WI: U.S. Department of Agriculture, Forest Service, Forest Products Laboratory, available from: <http://www.fpl.fs.fed.us/documnts/fplgtr/fpl_gtr190.pdf> [31 July 2015]

Foster, L. W. (1982) *Answer Book and Instructor's Guide for Modern Geometric Dimensioning and Tolerancing*. 2nd edition. Fort Washington: National Tooling and Machining Association

França, C.A., Gonzaga, A. and Slaets, A. F. F. (1996) 'Quality Control of Wooden Plates by Neuro-Fuzzy Approch'. *International Conference on Quality Control by Artificial Vision – QCAV*, p. 173-178

Friedman, J. H., Hastie, T. and Tibshirani, R. (2003) *The Elements of Statistical Learning: Data Mining, Inference, and Prediction*. 1st edition, New York: Springer, ISBN: 978-0387848570

GHG Group (2010) *Panels of marble patched with liquid fillers (putty)*. [online] available from: <http://ghgstone.com/uploadfile/201007/20/1026333485.JPG> [31 July 2015]

Gonzaga, A., de Franca, C. A. and Frere, A. F. (1999) 'Wood texture classification by fuzzy neural networks'. *Neural Networks in Image Processing IV*, SPIE Vol. 3647, p. 134-143

Gottesfeld, L. B. (2007) 'A Survey on Image Registration Techniques'. *ACM Computing Surveys*, Vol. 24, Issue 4, p. 325-376

Göttlicher, M. (2011) *Entwurf und Implementierung einer Softwareschnitt-stelle zur optimierten Übertragung von automatisch erkannten Fehlstellen im Holz an ein automatisiertes Reparatursystem für Holzoberflächen [Design and implementation of a software interface for the transmission of automatically detected defects to an automated tooling system for the repair of wood surfaces].* Diploma Thesis. Rosenheim: University Rosenheim & Baumer Inspection GmbH

Graves, M., Batchelor, B. G., (2003) *Machine Vision for the Inspection of Natural Products*. New York: Springer-Verlag New York, ISBN 9781852335250, p. 5

Gregory, R. L. (2001) *Auge & Gehirn [Eye & Brain]*. Reinbek bei Hamburg: Rohwolt Taschenbuch Verlag, ISBN3-499-60805-7, p. 105-107

Grekin, M., Lukkarinen*, A., Verkasalo, E. (2005)* 'Colour change of Nordic Scots pine wood under UV radiation - A laboratory approach'. *IUFRO WP S5.01.04 Conference: Connection between forest resources and wood quality - modelling approaches and simulation software,* p. 21-29

Haghighat, M. B. A., Aghagolzadeh, A. and Seyedarabi, H. (2011) 'A non-reference image fusion metric based on mutual information of image features'. *Computers & Electrical Engineering*, Vol. 37, Issue 5, p. 744-756

Hapgood, F. (2007) 'Factories of the future', *CIO magazine,* Vol. 20, Issue 6, p. 46, ISSN 0894-9301,

Hautamäki, S., Kipeläinen, H. Kannisto, K., Wall, T., Verkasalo E. (2010) 'Factors and models for the grade distributions of sawn timber for Scots pine and Norway spruce in Finland and north-western Russia: appearance quality and visual strength'. *Baltic Forestry Journal*, Vol. 16, Issue 1, p. 113-125

Hinton, G., Sejnowski T. J. (1999) *Unsupervised Learning: Foundations of Neural Computation*. Cambridge, MA: MIT Press, ISBN: 978-026258168

Horrer, A. M. (2005) *Automatic visual inspection of the aesthetic appearance of surfaces.* PhD Thesis. Coventry: Coventry University & Massen Machine Vision Systems GmbH

Hotta, H. and Hagiwara, M. (2007) 'An Automatic KANSEI Fuzzy Rule Creating System Using Thesaurus', *2007 IEEE International Fuzzy Systems Conference*, p. 1-6

Ibarra-Castanedo, C., Bendada, A., and Maldague, X. (2011) 'Infrared vision applications for the non-destructive testing of materials'. *5th Conference for NDT in Cancun, Mexico*

Iivarinen, J., Visa, A. (1998) 'An Adaptive Texture and Shape Based Defect Classification'. *Fourteenth International Conference on Pattern Recognition Proceedings*, *Brisbane*, Vol. 1, p. 117-122

ISO (2011) *Veneers - Terms and definitions, determination of physical characteristics and tolerance.* ISO 18775:2008 2011, Geneva: International Organization for Standardization

ISO (2011) *Plywood - Classification by surface appearance - Part 1: General.* 2426-1:2000 2011, Geneva: International Organization for Standardization

ISO (2011) *Plywood - Classification by surface appearance - Part 2: Hardwood.* ISO 2426-2:2000 2011, Geneva: International Organization for Standardization

ISO (2011) *Plywood - Classification by surface appearance - Part 3: Softwood.* ISO 2426-3:2000 2011, Geneva: International Organization for Standardization

Jackson P. (1998) *Introduction To Expert Systems.* 3rd edition, Reading, MA: Addison-Wesley, ISBN 978-0-201-87686-4

Janin, G., Goncalez, J., Ananías, R., Charrier, B., Fernandes da Silva, G., & Dilem, A. (2001) 'Aesthetics appreciation of wood colour and patterns by colormetry: Part 1. Colorimetry theory for the CIELab system'. *Maderas, Cienca y tecnologia*, Vol. 3, Issue 1-2, p. 3-13

Jonsson, O., Lindberg, S., Roos, A. Hugosson, M., Lindström, M. (2008) 'Consumer Perceptions and preferences on solid wood, wood-based panels and composites: A repertory grid study'. *Wood and Fiber Science*, Vol. 40, Issue 4, p. 663–678

KAINDL (n.d.) *Kaindl-TWO: Every Piece Unique.* [online] available from <http://www.starman.si/uploads/slo_kaindl_two_dekorji.pdf>

Kauppinen, H. (1999) *Development of a color machine vision method for wood surface inspection*. Dissertation. Oulu: University Oulu, ISBN: 951-42-5423-6

Kauppinen, H. (2000) 'A two stage defect recognition method for parquet slab grading'. *Proceedings of the 15th International Conference on Pattern Recognition*, Barcelona, Spain, Vol. 4, p. 803–806

Kauppinen, H., Silven, O. (1996) 'The Effect of Illumination Variations on Color-Based Wood Defect Classification'. *Proceedings of 13th International Conference on Pattern Recognition*, *Vienna, Austria*, p. 828-832

Kauppinen, H., Rautio, H., and Silvén, O. (1999) 'Non-segmenting defect detection and SOM based classification for surface inspection using color vision'. *Proc. SPIE 3826, Polarization and Color Techniques in Industrial Inspection,* p. 270-280

Kim, C. W. and Koivo, A. J. (1994) 'Hierarchical Classification of Surface Defects on Dusty Wood Boards'. *Pattern Recognition Letters,* Vol. 15, Issue 7, p. 713-721

Kline, D. E., Surak, C., Araman, P. A. (2003) 'Automated Hardwood Lumber Grading Utilizing a Multiple Sensor Machine Vision Technology'. *Computers & Electronics in Agriculture*, Vol. 41, Issue 1-3, p. 139

Kohonen, T. (1989) *Self-Organisation and Associative Memory*. 3rd edition, Berlin: Springer Verlag Berlin, ISBN: 978-3-642-88163-3

Kohonen, T. (1999) 'Analysis of Processes and Large Data Sets by a Self-Organizing Method'. *IPMM'99, The Second International Conference on Intelligent Processing and Manufacturing of Materials*, Vol. 1, p. 27-36

Koivo, A. J. and Kim, C. W. (1989) 'Automatic Classification of Surface Defects on Red Oak Boards'. *Forest Products Journal*, Vol.39, Issue 9, p. 22-30

Kuehn, M. O. (2004) *LED Farb- und Intensitätsinspektion mit CCD-Matrix Kameras [Colour and intensity inspection on LEDs using CCD-matrix cameras]*. Diploma Thesis. Constance: University of Applied Sciences Constance

Kurdthongmee, W. (2008) 'Colour classification of rubberwood boards for fingerjoint manufacturing using a SOM neural network and image processing'. *Computers and Electronics in Agriculture,* Vol. 64, Issue 2, p. 85–92

Lampinen, J., Smolander, S., Silven, O., and Kauppinen, H. (1994) 'Wood Defect Recognition: A Comparative Study'. *Proceedings of Workshop on Machine Vision in advanced production*, *Oulu, Finnland*, p. 7

[Li and Zhu 2010] Li, Y. and Zhu, L. (2010) 'Research on Product Image Form Design Based on ANFIS', *2010 International Symposium on Computational Intelligence and Design*, p. 119-122

Li, H., Manjunath, B. S., Mitra, S. K. (1995) 'Multisensor Image Fusion Using the Wavelet Transform'. *Graphical Models and Image Processing*, Vol. 57, Issue 3, p. 235–245

LIBLINEAR: National Taiwan University (n.d.) *LIBLINEAR -- A Library for Large Linear Classification.* [online] available from: <http://www.csie.ntu.edu.tw/~cjlin/liblinear/> [31 July 2015]

Liggins, M., Hall, D., Llinas, J. (2008) *Handbook of Multisensor Data Fusion: Theory and Practice.* 2nd edition, Boca Raton, FL:CRC Press, ISBN 9781420053081

Lu, Q., Conners, R., Kline, D., Araman, P. (1997) 'A real-time algorithm for color sorting edge-glued panel parts'*. Proceedings of the International Conference on Image Processing*, Barcelona, Spain, Vol. 1, p. 822–825

Höfling, M. (n.d.) *saga_info-detail_nussbaum-geoelt_zinn_aluwinkel*. [online] available from <http://www.luna-design.eu/fileadmin/files/produkte/wohnmoebel/tische/saga/1_info/saga_info-detail_nussbaum-geoelt_zinn_aluwinkel.jpg> [31 July 2015]

Mäenpää, T., Viertola, J., and Pietikäainen, M. (2003) 'Optimizing color and texture features for real-time visual inspection'. *Pattern Analysis and Applications*, Vol. 6, Issue 3, p. 169-175

Mahram, A., Shayesteh, M. G., Jafarpour, S. (2012) 'Classification of wood surface defects with hybrid usage of statistical and textural features'. *35th International Conference on Telecommunications and Signal Processing (TSP)*, p. 749-752

Maldague, X. P. (2001) *Theory and practice of infrared technology for nondestructive testing*. New York: John Wiley & Sons, ISBN: 978-0-471-18190-3

Maryland's SFLA (2003) *Secondary Wood Manufacturing: Data & Indicators*. [online] available from: <http://www.dnr.state.md.us/forests/planning/sfla/indicators/secondary_wood.htm> *[31 July 2015]*

Massen, R. (1997) 'The multisensorial camera: a new approach in multi-sensory pattern recognition'. *Bildverarbeitung '97 Forschen, Entwickeln, Anwenden*, p. 51-57

Massen, R. (2009) 'Die Inspektion von Naturholz [The inspection of natural wood]'. *Enwicklerkonferenz 17. Oktober 2009 bei Baumer Inspection GmbH, Konstanz*

Massen, R., Eberhardt, J., Asal, S. (2008) 'Automatic in-line monitoring of the visual appearance in analogue direct and digital décor printing with virtual computer-based reference proofs'. *TCM European Laminate Conference*, Vol. 4, p. 75-83

Massen, R. Kuehn, M. O., Eberhardt, J. (2009) 'Automatic physical and aesthetic repair of wood panels: an intelligent alternative to automatic downgrading'. *International Panel Products Symposium, IPPS 2009*, Nantes, France, p. 191-201

Massen, R., Kühn, M. O., Eberhardt, J. (2010) 'Saving Resources by Advanced Vision-based Automatic Patching of Wood-based Panels'. *Conference on Processing Technologies for the Forest and Bio-based Products Industries 2010, PTF, BPI,* Salzburg, p. 9-15

Matthews, P. (1976) *Tracheid Effect for detection of timber defects.* US patent US 3,976,384 1976

Mayoraz, E., Alpaydin, E. (1999) 'Support Vector Machines for Multiclass Classification'. *Proceedings of the International Workshop on Artificial Neural Networks (IWANN1999)*, Part II, Vol. 1607 of *Lecture Notes in Computer Science,* p. 833-842.

Meinlschmidt, P. (2005) 'Thermographic detection of defects in wood and wood-based materials'. *4th International Symposium of nondestructive testing of wood*, Vol. 14

Merriam Webster Dictionary: Encyclopaedia Britannica (2015) *Definition of aesthetics.* [online] available from: <http://www.merriam-webster.com/dictionary/aesthetics> [31 July 2015]

[Meza et al. 2010a] Meza, P., Vera, E., Parra, F. and Torres, S. (2010) 'Applied Non-uniformity Correction for Striping Noise removal in Hyperspectral Images'. *Proceedings of Latin American Remote Sensing Week, Santiago, Chile*

[Meza et al. 2010b] Meza, P., San Martin, C., Vera, E. and Torres, S. (2010) 'A Quantitative Evaluation of Fixed-Pattern Noise Reduction Methods in Imaging Systems'. *Lecture Notes in Computer Science*, Vol. 6419/2010, p. 285-294

Mohri, M., Rostamizadeh, A., Talwalkar, A. (2012) *Foundations of Machine Learning*. Cambridge, MA: MIT Press, ISBN 9780262018258,

Murphy, P. R. (1996) 'Biological and cognitive foundations of intelligent sensor fusion'. *IEEE Transaction on Systems, Man, and Cybernetics, Part A: Systems and Humans,* Vol. 26, Issue. 1, p. 42-51

Nagamachi, M. (2010) *Kansei/Affective Engineering (Industrial Innovation)*. 1st edition,. United States: CRC Press, ISBN-13: 978-1439821336

Nakamura, Y. and Xu, Y. (1989) 'Geometrical fusion method for multi-sensor robotic systems'. *Proceedings of IEEE International Conference on Robotics, Automation and systems*, *Scottsdale, Arizona*, Vol. 2, p. 668-673

Nakamura, M, Masuda, M, Inagaki, M. (1993) 'Influences of knots and grooves on psychological images of wood wall-panels'. *Mokuzai Gakkaishi - Journal of the Japan Wood Research Society*, Vol. 39, Issue 2, p. 152-160

Nestler, R., Franke, K.-H. (2000) 'Realisierung eines multisensorischen Ansatzes zur Oberflächeninspektion von Holz *[Realisation of a multi-sensorial approach to surface inspection of wood]*'. *Proceedings of 10. Workshop Farbbildverarbeitung,* 2004, p. 10-17

Niskanen, M., Kauppinen, H., Silven, O. (2002) 'Real-time aspects of SOM-based visual surface inspection'. *Proceedings SPIE 4664, Machine Vision Applications in Industrial Inspection,* [online], available from doi: 10.1117/12.460189s [20 June 2015]

Nordvik, E., Schütte, S., Broman, S. O. (2009) 'People's Perceptions of the Visual Appearance of Wood Flooring - A Kansei Engineering Approach'. *Forest Products Journal,* Vol. 59, Issue 11/12, p. 67-74

Ogale, A. S., Yiannis, A. (2005) 'Shape and the stereo correspondence problem'. *International Journal of Computer Vision*, Vol. 65, Issue 1, p. 147-162

Ojala, T., Pietikainen, M., Silven, O. (1992) 'Edge-based texture measures for surface inspection', *11th IAPR International Conference on Pattern Recognition, Conference B: Pattern Recognition Methodology and Systems,* , Vol. 2, p. 594 - 598

Pakarinen, T., Asikainen, A. (2001) 'Consumer segments for wooden household furniture'. *Holz Rohstoff Werkstatt,* Vol. 59, p. 217–227

Peck, E. C. (1957) 'How wood shrinks and swells'. *Forest Products Journal*, Vol. 7, p. 235-244

Petersson, H. (2010) 'Use of Optical and Laser Scanning Techniques as Tools for Obtaining Improved FE-input Data for Strength and Shape Stability Analysis of Wood and Timber'. *European Conference on Computational Mechanics*, *Paris, France*, Paper No. 350

Pham, D. T. and Alcock, R. J. (1996) 'Automatic detection of defects on birch wood boards'. *Proceedings of the Institution of Mechanical Engineers, Part E: Journal of Process Mechanical Engineering 1989-1996 (vols 203-210),* Vol. 210, Issue 15, p. 45-52

Platt, J., Cristianini, N., Shawe-Taylor, J. (2000) 'Large Margin DAGS for Multiclass Classification'. *Advances in Neural Information Processing Systems,* Vol. 12, p. 547–553

Pohl, C., Van Genderen, J. L. (1998) 'Multisensor image fusion in remote sensing: Concepts, methods and applications'. *International Journal of Remote Sensing,* Vol. 19, Issue 5, p. 823-854

Relf, C. G. (2003) *Image Acquisition and Processing with LabVIEW*. London: Taylor & Francis, ISBN: 978-0849314803

Rice, J., Kozak, R. A., Meitner, M. J., Cohen, D. H. (2006) 'Appearance wood products and psychological well-being'. *Wood and Fiber Science*, Vol. 38, Issue 4, p. 645–658

Richter, C. (2014) *Wood Characteristics: Description, Causes, Prevention, Impact on Use and Technological Adaptation.* 1st edition, Cham(ZG, CH): Springer International Publishing, ISBN: 978-3319074221

Riedel, T., Stahl, J. (1999) 'Encyclopaedia of Aesthetics - Review'. *Art Documentation: Bulletin of the Art Libraries Society of North America*, Vol. 18, Issue 2, p. 48-48

Riekkinen, M., Lukkarinen, A., Lindström, H., Verkasalo, E. (2004) 'Timber assortments and selected aesthetic wood properties of Nordic Scots pine'. *The Forestry Woodchain - Quantifying and forecasting quality from forest to end product*, p. 78-79

Ritschkoff, A.-C. (1996) ‘Decay mechanisms of brown rot fungi’. *Technical Research Centre of Finland, VTT Publications 268*, p.14, ISBN: 951-38-4926-0

Rönnqvist, M., Åstrand, E. (1998) ‘Integrated defect detection and optimization for cross cutting of wooden boards’. *European Journal of Operational Research*, Vol. 108, Issue 3, p. 490-508

Roth-Nebelsick, A. (2006) ‘Nach oben gezogen: Die Prinzipien der pflanzlichen Wasserleitung *[Pulled up: the principles of botanical water conduit]*’. *Biologie in unserer Zeit*, Vol. 36, Issue 2, p. 110-118

Saurus, M. (2014) *Glow-table: Table from Pecky Cypress having indentations filled with fluorescent resin*. [online] available from: <http://www.instructables.com/id/Glow-table/> [31 July 2015]

Schmitt, C. (2006) *Automatic inspection of industrial products based on multi-dimensional image data.* PhD Thesis. Coventry: Coventry University and Massen Machine Vision Systems GmbH

Scholz, S., Decker, R. (2007) 'Measuring the impact of wood species on consumer preferences for wooden furniture by means of the Analytic Hierarchy Process'. *Forest Products Journal,* Vol. 57, p. 23–28

Seidel, S. (2010) *Farbkalibrierte Reparatur von Holzoberflächen durch lokale Texturextrapolation [Colour-calibrated repair of wood surfaces using locally extrapolated textur].* DiplomaThesis. Konstanz: University of Applied Sciences Konstanz

Shum, H.-Y. and Szeliski R. (1997) ‘Panoramic Image Mosaicing’. *Technical Report MSR-TR-97-23*, Redmond: Microsoft Research

Shum, H.-Y. and Szeliski, R. (2001) ‘Construction of panoramic mosaics with global and local alignment’. *Monographs in Computer Science*, [online], Section III, p. 227-268, available from doi: 0.1007/978-1-4757-3482-9_13 [20 June 2015]

Silven, O., Kauppinen, H. (1994) ‘Color vision based methodology for grading lumber’. *Proceedings of the 12th IAPR International Conference on Pattern Recognition 1994 - Conference A: Computer Vision & Image Processing*, Vol. 1, p. 787-790

Silvén, O., Niskanen, M. and Kauppinen, H. (2003) 'Colour and Texture Based Wood Inspection with Non-Supervised Clustering'. *Machine Vision and Applications*, Vol. 13, Issue 5-6, p. 275-285

Smith, S. W. (1997) *The Scientist and Engineer's Guide to Digital Signal Processing*. San Diego, CA, USA: California Technical Publishing, ISBN 0-9660176-3-3

Smith, M. L., Dawson, D. (2001) *Surface Inspection Techniques: Using the Integration of Innovative Machine Vision and Modelling Techniques (Engineering Research Series (REP))*. London: Professional Engineering Publishing Limited, p. 1, ISBN: 978-1860582929

Smolander, S, Lampinen, J., Korhonen, M. (1995) ‘Wood surface inspection system based on generic visual features'. *International Conference on Artificial Neural Networks ICANN'95*, *Paris*, p. 35-42

Steedly, D. (2005) 'Efficiently registering video into panoramic mosaics'. *10th International Conference on Computer Vision (ICCV 2005), Beijing, China*, p. 1300–1307

Steger, C., Ulrich, M., Wiedemann, C. (2008) *Machine Vision Algorithms and Applications*, 2nd edition, Germany: Wiley-VCH Verlag GmbH, ISBN 9783527407347, p. 1-2

Szymani, R and McDonald, K. A. (1981) 'Defect Detection in Lumber: State of the Art'. *Forest Products Journal,* Vol. 31, Issue 11, p. 34-44

Tarin, M. and Rotolante, R, (2011) 'NDT in Composite Materials with Flash, Transient, and Lock-in Thermography'. *FLIR Technical Series: Application Note for Research & Science,* [online], available from: <http://www.flir.com/workarea/downloadasset.aspx?id=50058> [31 July 2015]

Theodoridis, S., Mavroforakis, M. (2007) 'Reduced Convex Hulls: A Geometric Approach to Support Vector Machines'. *IEEE Signal Processing Magazine May 2007*, Vol. 24, Issue 3, p. 119-122

Thorpe, S., Fize, D. and Marlot, C. (1996) 'Speed of processing in the human visual system'. *Nature*, Vol. 381, Issue 6582, p. 520–522

Tilly Naturholzplatten GmbH (n.d) *Dreischicht Nadelholzplatten [Three-layered softwood panels]*. [online], available from: <http://www.tilly.at/tilly/us/produkte/drei-schichtplatte-nadel.php?navid=5>

Tomoyuki, S. (2010) 'Discussing Image Sensor Evolution and the Future of Imaging at the ISSCC 2010 Plenary Session'. *International Solid-State Circuits Conference ISSCC 2010*, San Francisco, [online], available from: <http://www.sony.net/Products/SC-HP/cx_news_archives/img/pdf/vol_60/sideview60.pdf> [31 July 2015]

Vedaldi, A. and Zisserman, A. (2010) 'Efficient Additive Kernels via Explicit Feature Maps'. *IEEE Computer Society Conference on Computer Vision and Pattern Recognition* (CVPR), Vol. 34, Issue 3, p. 480-492

Vetter, R. E., Coradin, V. R., Martino, E. C., Camargos, J. (1990) 'Wood colour - A comparison between determination methods'. *IAWA journal*, Vol. 11, Issue 4, p. 429-439,

Wilson, K., White, D. J. B. (1986) 'The Anatomy of Wood: Its Diversity and variability'. London: Stobart & Son Ltd, ISBN: 978-0854420339

Wood Explorer, The (2014) *Radiata pine (Pinus radiata)*. [online] available from: <http://www.thewoodexplorer.com/maindata/we918.html> [31 July 2015]

Xiao, X. (1998) *A Multiple Sensors Approach to Wood Defect Detection.* Dissertation. Blacksburg, VA: Virginia State University

Yali, F. and Kui, C. (2008) 'Indexing wood image for retrieval based on kansei factors'. *9th International Conference on Signal Processing*, p. 1099-1103

Yan, J., Ryan, M., Power, J. (1994) *Using fuzzy logic towards intelligent systems*. New York: Prentice-Hall, ISBN: 9780131027329

Yin, H. (2008) ‘The Self-Organizing Maps: Background, Theories, Extensions and Application*s*’. *Studies in Computational Intelligence*, Berlin: Springer, ISBN 978-3-540-78292-6, p. 715-762

Zadeh, L. (1965*)* ‘Fuzzy sets and systems’. *Information and Control,* Vol. 8, Issue 3, p. 338-353

Ziadi, A. Ntawiniga, F., Maldague, X. (2007) 'Neural Networks for color image segmentation: Application to sapwood assessment'. *20th Canadian Conference on Electrical and Computer Engineering (CCECE 2007),* p. 417-420

Appendix

A.1. Function principle of SOM

The function principle of the SOM can be briefly summarized as follows: The initial setup is a mesh with a predefined number k=$q_1 \times q_2$ of equally distanced nodes $m_j \in R^p$, each node holding a mesh-coordinate $l_j \in Q_1 \times Q_2$ with $Q_1 = \{1, 2, \dots q_1\}$, respectively $Q_2 = \{1, 2, \dots q_2\}$ and a random initialized weight vector $w_{l_j i}$ whose length equals the feature space dimension p, refer to Figure A-1.

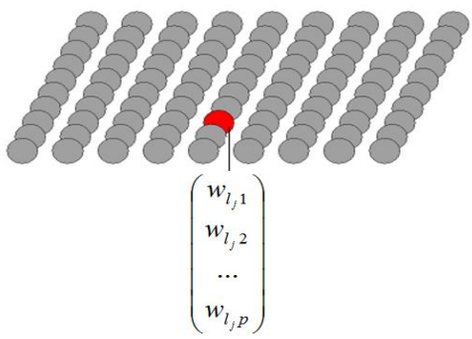

Figure A-1: SOM principle: initially equally distanced nodes in the mesh holding weight vector with length equal to the feature space's dimension.

The mesh is trained by iteratively presenting the training sample x_i to the map. The goal hereby is to find the best matching node m_j defined by minimal Euclidian distance to x_i (refer to Formula A-1) incorporating the Euclidian norm of the vectors in feature space R^p.

$$\|w\| = \sqrt{\sum_{i=0}^{p} w_i^2}$$

Formula A-1: SOM principle: Euclidian norm for identification of BMU.

$$\|x_i - m_{BMU}\| = min_i\{\|x_i - m_j\|\}$$

Formula A-2: SOM principle: identification of BMU in terms of Euclidian distance to input sample.

This best match is called Best Matching Unit (BMU). Adaption of the BMU and, referring to the lateral inhibition of the cortex in the human brain, also the neighbour nodes m_k is then carried out:

$$m_k \leftarrow m_k + \alpha(x_i - m_k)$$

Formula A-3: SOM principle: adaption of BMU and neighbours according to lateral inhibition.

The adaption according to Formula A-3 incorporates a learning rate α and influences all neighbour nodes defined by a threshold r on the distance between m_j and m_k in terms of the Euclidian distance in the two-dimensional space $Q_1 \times Q_2$ of the mesh. The adaption therefore bends the mesh to approximate the BMU and its neighbourhood to the presented training data, refer to Figure A-2.

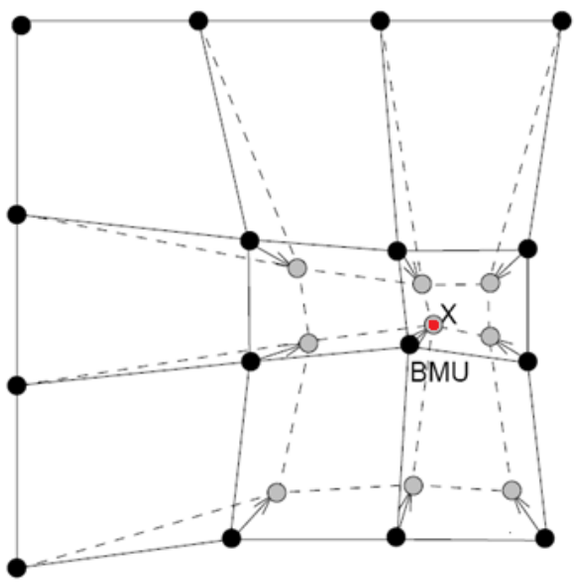

Figure A-2: SOM principle: mesh bended to best matching unit (BMU) adapting to similarity among the samples.

Starting from a state of complete disorder when using random initiated weight vectors, the training can be separated into two phases: the organisation phase and the convergence phase. Large values for the learning rate as well as for the neighbourhood radius should be used in the organisation phase to incorporate the whole mesh respectively all the weight vectors to move towards the training data so to avoid artefacts. The convergence phase can be considered as the fine-tuning of the mesh where the neighbourhood decreases as well as the learning rate becomes very small so the weight vectors converge to their correct values. While α is typically decreased linearly from 1.0 to 0.0 over the predefined number of iterations, the neighbourhood distance can be incorporated to the adaption:

$$m_k \leftarrow m_k + \alpha h(\|l_j - l_k\|)(x_i - m_k)$$

Formula A-4: SOM principle: neighbourhood kernel h and learning rate α decrease during convergence.

h is thereby the so-called neighbourhood kernel giving more weight to nodes m_k with coordinate l_k closer to coordinate l_j of BMU-nodes m_j. Much research has been done on possible functions for m_k but ideally some monotonically decreasing function is chosen *[Kohonen 1989]*, widely used is the Gaussian function.

The iterative approach to train a self organizing map is summarizing given in pseudo code as follows:

initialisation
for i=1:number of training samples
take sample x_i;
find BMU;
define neighbourhood;
adaption of BMU & neighbourhood;
end for

A.2. Function principle of SVM

A.2.1 Linear learning machines

To establish naming conventions, the linear learning machine will be briefly reviewed. Figure A-3 shows a distribution of samples in a two-dimensional feature space which is separable (linear two-class classification problem) by a linear function $f: X \in R^n \rightarrow R$, in the two-dimensional case this is a straight line, in general this is a hyperplane expressed by Formula A-5

$$f(x) = \langle w * x \rangle + b = \sum_{i=1}^{n} w_i x_i + b$$

Formula A-5: Hyperplane in n-dimensional space.

assigning each sample $x = \{x_1, \ldots, x_n\}$ a value of 1 when being above the plane and a value of -1 when being below the plane by incorporating $sgn(f(x))$. $(w, b) \in R^n * R$ are the control parameters of the function where *w* is a vector perpendicular to the hyperplane defining its orientation and *b* is an offset to zero point, Figure A-3 gives an exemplary graphical representation for the case in the two-dimensional space:

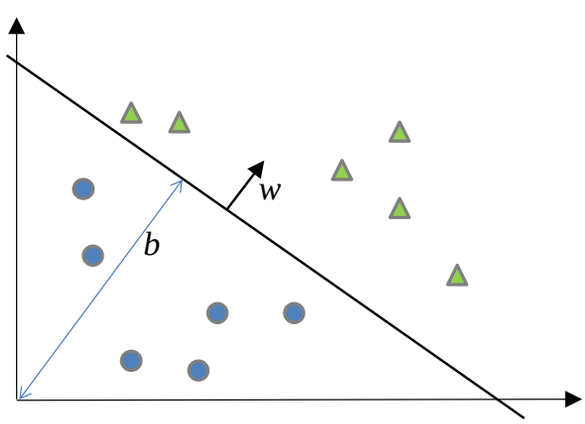

Figure A-3: Separating hyperplane (*w, b*) for a two-dimensional training set.

In literature with SVMs *[Cristianini and Taylor 2000]* the parameters *(w, b)* are often referred to *weight* and *bias/threshold*, terms that will be used accordingly in this context.

Hyperplane margin optimization

In an iterative process to find the (optimal) hyperplane for separating a linearly separable data set the most obvious approach is to update the weight vector w and bias b each time a mistake in terms of separation has been made. This is done by calculating the margin γ in terms of the distances from a sample point (x_i, y_i) of the (training) data set by:

$$\gamma_i = y_i(\langle w * x_i \rangle + b)$$

Formula A-6: Margin to hyperplane calculation for sample point (x_i, y_i).

The graphical illustration of this margin is given in Figure A-4 showing that the margin can be interpreted by the shortest Euclidian distance of the sample to the hyperplane which is a straight line in the two-dimensional case:

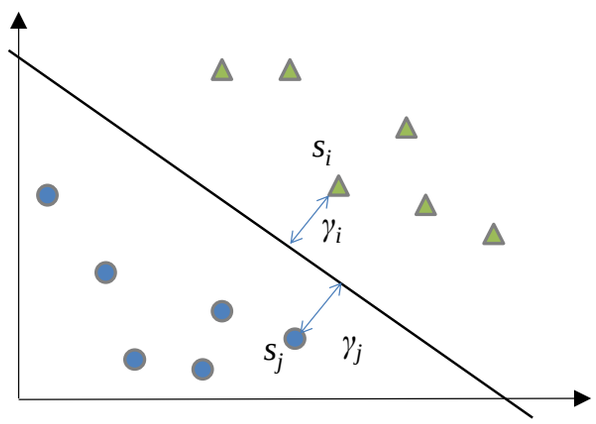

Figure A-4: Margin γ_i, γ_j of two samples s_i, s_j, each from one of the two classes, as Euclidian distance to a hyperplane.

According to the margin of a single sample point, the margin of the complete data set in terms of the maximum margin among all possible hyperplanes can be defined which is illustrated in Figure A-5:

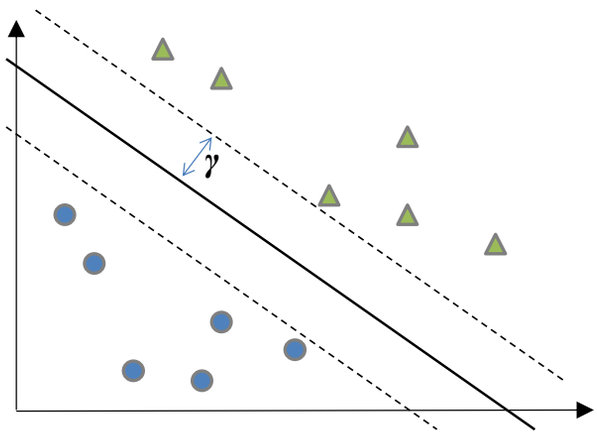

Figure A-5: Margin of training set defined by closest sample(s).

The following sections briefly review the efficient calculation concept and the mathematical formulation of the margin optimization before the already mentioned advantageous behaviour of the SVM on high-dimensional feature sets and nonlinearly separable data and noise-tolerance is addressed.

Maximum margin

To satisfy the generalisation requirement of a classifier operating on linearly separable data, the strategy of the margin-based classifier is to maximize the margin calculated according to Formula A-6 among all samples in the training data set as illustrated in Figure A-5. The *margin of the training set* in this context is therefore referred to as the maximum margin among all hyperplanes. Such a hyperplane is called *maximal margin hyperplane* and is the basis of the maximum margin classifier.

Optimization strategy

To realise this strategy from the viewpoint of optimization theory, the one separating hyperplane has to be found which minimizes or maximizes a certain functional[37]. With respect to the (linear) learning machines, this comes down to finding a vector of parameters that minimises (maximises) a cost function f bounded to certain constraints g,h which is formulated as the *primal optimization problem [Cristianini Taylor 2000]*:

[37] a function from a vector space into its underlying scalar field taking vectors as inputs and returning a scalar

minimise	$f(w), w \in \Omega, \Omega \subseteq \mathbb{R}^n$	objective function
subject to	$g(w) \leq 0$	inequality constraint
	$h(w) = 0$	equality constraint

Formula A-7: Primal optimization problem with objective function and constraints.

With the codomain *R* where the objective function is defined and where the constraints are satisfied, which is called the *feasible region*:

$$R = \{w \in \Omega : g(w) \leq 0, h(w) = 0\}$$

Formula A-8: Codomain (feasible region) of the objective function.

With the feasible region the basis for the statement of the optimization problem is given, working towards the solution in terms of the *optimal point* $w^* \in R$ with no other $w \in R$ for which $f(w) < f(w^*)$, therefore w^* being a global minimum of $f(w)$.

When the objective function and both the inequality and the equality constraints are *linear functions*, the optimization problem is referred to as a linear programme. When using a quadratic function for the objective function and linear functions for the constraints the optimisation problem is referred to as a *quadratic programme [Cristianini and Taylor 2000]*. When the set Ω, the objective function and the constraints are convex, the optimisation problem is also convex. For the use of SVMs, the constraints are chosen to be linear, the objective function is chosen to be quadratic and convex and the (training) set Ω is chosen to be a subset of $\mathbb{R}^n$ to establish a *convex quadratic programme* as a restriction from the classes of optimisation problems on which optimisation theory can be applied. The class of convex optimization problems incorporating linear inequalities has been well-studied and very effective algorithms have been implemented (Lagrange function, Lagrange multipliers and related theory) that can reliably and effectively solve large complex problems with hundreds or thousands of variables and constraints *[Boyd and Vandenberghe 2004]*, (chapter 1.1).

Convexity

An affine function $f(w)$ with $w \in \mathbb{R}^n$ is convex by definition *[Cristianini and Taylor 2000]* and is expressed by

$$f(w) = A * x + b$$

with *A* being a matrix and *b* being a vector. For a convex function f being the objective function of an optimization problem, any local minimum w^* qualifies as global minimum *[Cristianini and Taylor 2000]*, (definition 5.3).

A set Ω is convex if $\Omega \subseteq \mathbb{R}^n$, if every $w, u \in \Omega$ and if for any $\theta \in (0,1)$ the point $(\theta w + (1-\theta)u) \in \Omega$ *[Cristianini Taylor 2000].* A geometric interpretation of this convention is a set where every point in the set can be seen by every other point from the set, that is, a virtual line exists between these points fully lying in the set.

The convex hull of a set Ω, denoted with $\boldsymbol{conv}\Omega$, is then the set of all convex combinations of the points in Ω which is convex itself by definition and which is the smallest convex set that contains Ω*. [Boyd and Vandenberghe 2004]*, (chapter 2.1.4).

Application of optimization strategy

In the maximum margin classifier, the convex optimization problem to be solved can be refined to an affine classifying function (hyperplane) $f(x) = a^T x - b$ being a set of linear inequalities on the variables *a* and *b* that define *f*. If two sets in $\mathbb{R}^n, \{x_1, \dots, x_N\}$ and $\{y_1, \dots, y_N\}$ in n-dimensional feature space can be linearly separated, there exists a geometric body (polyhedron) of affine functions that separates these sets *[Boyd,Vandenberghe2004], (8.6.1, p. 428)*. In terms of the maximal margin hyperplane the goal is to find those functions that give the maximum possible gap between the positive values returned for the samples x_i and the negative values returned for the samples y_i by the hyperplane which can be formulated as a standard optimization problem:

maximise	t	
subject to	$a^T x_i - b \geq t,$ i=1,…,N	
	$a^T y_i - b \leq t,$ i=1,…,N $\|a\|_2 \leq 1$	

Formula A-9: Formulation of convex optimization problem for maximum margin classifier.

The optimal value t^* is positive only if the two sets to be separated are linearly separable, optimizing the inequality $\|a\|_2 \leq 1$ to become close to 1.

A geometric interpretation of this optimization problem is that if the convex hulls of the sets do not intersect they are therefore separable by an affine function (hyperplane). In any optimal point t^*, $\|a^*\|_2$ is equal to 1 and $a^T x_i - b$ is therefore the Euclidian distance from point x_i. Accordingly $b - a^T y_i$ is the Euclidian distance from point y_i to the separating hyperplane $H = \{z | a^T z = b\}$. The optimal value t^* is then half the distance between the convex hulls of the two sets *[Boyd,Vandenberghe2004]*, (chapter 8.6.1).

Extended optimization theory

In the previous paragraph the basic concept behind the SVM has been introduced. The concept of using linear learning machines in dual representation will be shown to be significant for the good performance of SVMs. Some further detail of Lagrangian (optimization) theory and one of its most important derivates the Kuhn-Tucker (optimization) theory will therefore be introduced briefly in this section to complete the image.

Reconsidering the optimisation problem in standard/primal form

minimise	$f_0(x),$	objective function
subject to	$f_i(x) \leq 0, \quad i = 1, \ldots, m$	inequality constraint
	$h_i(x) = 0, \quad i = 1, \ldots, p$ $x \in R^n$	equality constraint

Formula A-10: Primal optimisation problem.

Lagrangian theory introduces the idea of taking the constraints into account by magnifying the objective function with a weighted sum of the constraint functions *[Boyd,Vandenberghe2004]*, (chapter 5.1.1, p.215), *[Cristianini and Taylor 2000],* (definition 5.13)

$$L(x, \lambda, v) = f_0(x) + \sum_{i=1}^{m} \lambda_i f_i(x) + \sum_{i=1}^{p} v_i h_i(x)$$

Formula A-11: Lagrangian dual function for optimization problem statement, magnifying the objective function with weighted sum of constraint functions.

where λ_i, v_i are referred to as the *Lagrange multipliers* and λ, v to as the *Lagrange multiplier vectors* or *dual variables* of the optimization problem. With λ, v as the dual variables the *Lagrangian dual function* g is formulated as the minimum of the Lagrangian function which can in turn be expressed as the *Lagrangian dual problem*.

maximize	$\theta(\lambda, v)$	objective function
subject to	$\lambda \geq 0$	constraint
	$\theta(\lambda, v) = inf_{x \in R^n} L(w, \lambda, v)$	

Formula A-12: Lagrangian dual optimisation problem.

The dual optimization problem is much easier to solve than the primal optimization problem due to no direct inequality constraints and it allows working in high dimensional feature spaces (which will be subject in the next paragraph when introducing the kernel-trick). The value of the objective function at the optimal point is called *optimal value.* The optimal value is subject of the optimization efforts when using SVMs in terms of finding those optimization problem values that are equal for the primal and for the dual problem which is denoted as minimizing the *duality gap*. The dual problem further allows applying state of the art algorithms from the field of optimization theory like Kuhn-Tucker theory. Kuhn and Tucker extended Lagrangian theory which can be used to characterize the solution to an optimisation problem to allow inequality constraints *[Kuhn,Tucker1951]*. This allows solving a convex optimization problem related to the minimization of the duality gap in a highly efficient way without the calculation of the primal problem *[Cristianini and Taylor 2000],* (definition 5.2.1, 4.2.3).

minimise	$f_0(x)$,	objective function
subject to	$f_i(x) \leq 0, \quad \mathrm{i} = 1, \ldots, \mathrm{m}$	inequality constraint
	$h_i(x) = 0, \quad \mathrm{i} = 1, \ldots, \mathrm{p}$ $x \in R^n$	equality constraint

Given that f_0 is convex and f_i, h_i are affine, according to Kuhn-Tucker theory the conditions for an optimal point x^* with optimal λ^*, ν^* are:

$$\frac{\partial L(x^* \lambda^* \nu^*)}{\partial x} = 0$$

$$\frac{\partial L(x^* \lambda^* \nu^*)}{\partial \nu} = 0$$

$$\lambda^* f_i(x^*) = 0, \quad i = 1, \ldots, k$$

$$f_i(x^*) \leq 0, \quad i = 1, \ldots, k$$

$$\lambda^* \geq 0, \quad i = 1, \ldots, k$$

Formula A-13: Kuhn-Tucker theory: Lagrangian dual optimization problem with inequality constraints solved via Karush-Kuhn-Tucker conditions for optimal point.

The fact that the dual problem (and therefore the primal problem indirectly) is solvable very efficiently and much more efficient than the primal problem directly is one of the most important principles of Support Vector Machines *[Boyd,Vandenberghe2004]*, (chapter 5.5.3, p. 244 & chapter 5.5.5, p. 248). This is achieved by incorporating the Karush-Kuhn-Tucker (KKT) conditions and due to the fact that the KKT conditions (refer to Formula A-13) can be solved analytically via differentiation *[Murray et al 1981]* followed by resubstitution to the Lagrangian function.

Support Vectors

To close the circle, the already explained function principle together with the background (optimization) theory from the previous paragraph can now be incorporated to fully explain the functionality of the SVM.

From 1.1A.2.1 the hyperplane is defined with weight vector *w* and bias *b* by:

$$f(x) = \langle w * x \rangle + b = \sum_{i=1}^{n} w_i x_i + b$$

The optimization strategy for the hyperplane parameters is to formulate the optimization problem with a quadratic objective function under linear inequality constraints. The intention hereby is to optimize the margin in terms of the norm of the normalized weight vector on to points x^+ and x^- which is formulated as:

$$\langle w * x^+ \rangle + b = +1$$

$$\langle w * x^- \rangle + b = -1$$

And therefore the primal optimisation problem on the training set $T = ((x_1, y_1), \ldots, (x_k, y_k))$ to be solved by a separating hyperplane is formulated by:

minimise$_{w,b}$	$\langle w * w \rangle$	objective function
subject to	$y_i(\langle w * x_i \rangle + b) \geq 1, \quad \mathrm{i} = 1, \ldots, \mathrm{k}$	Linear inequality constraint

[Cristianini and Taylor 2000], (proposition 6.1)

The corresponding Lagrangian function *L* with Lagrangian multipliers λ can be obtained from this primal optimization problem as follows:

$$L(w, b, \lambda) = \frac{1}{2}\langle w * w \rangle - \sum_{i=1}^{k} \lambda_i \left[y_i(\langle w * x_i \rangle + b) - 1 \right]$$

Formula A-14: Primal Lagrangian for Support Vector Machine margin optimization.

with the dual form under KKT [38]conditions obtained by differentiation:

[38] Karush-Kuhn-Tucker conditions: allowing generalisation of method of Lagrangian multipliers (limited to equality constraints) to inequality constraints

$$\frac{\partial L(wb\lambda)}{\partial w} = w - \sum_{i=0}^{k} y_i \lambda_i x_i = 0$$

$$\frac{\partial L(wb\lambda)}{\partial b} = \sum_{i=0}^{k} y_i \lambda_i = 0$$

Applying the KKT conditions the optimal solution $\lambda^*(w^*, b^*)$ is constrained *[Cristianini and Taylor 2000]*, (remark 6.4) to:

$$\lambda_i^* [y_i(\langle w^* * x_i \rangle + b^*) - 1] = 0, \quad \mathrm{i} = 0, \ldots, \mathrm{k}$$

Formula A-15: Constraint on optimal solution - meaning of Support Vectors in the SVM optimization concept/strategy.

It can be seen from this term, that the KKT condition can only be satisfied for those x_i with a margin of 1 to the hyperplane, for all other inputs x_i the λ_i need to be zero and therefore the weight vector *w* is not influenced by these inputs. This is the origin of the term *Support Vectors* indicating those input points from the training set that contribute to the parameterization of the separating hyperplane as illustrated in Figure A-6 by bold framed symbols:

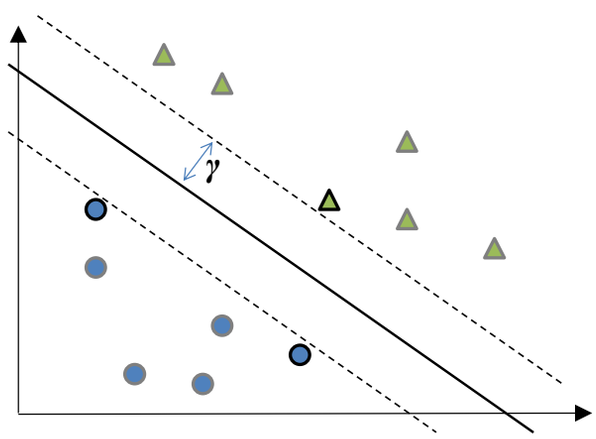

Figure A-6: Maximal margin hyperplane, support vector highlighted.

Solving the above equations (Lagrangian primal, KKT conditions applied) by differentiation

$$\frac{\partial L(wb\lambda)}{\partial w} = w - \sum_{i=0}^{k} y_i \lambda_i x_i = 0$$

$$\frac{\partial L(wb\lambda)}{\partial b} = \sum_{i=0}^{k} y_i \lambda_i = 0$$

followed by resubstitution of w, b:

$$w = \sum_{i=0}^{k} y_i \lambda_i x_i$$

$$0 = \sum_{i=0}^{k} y_i \lambda_i$$

into the primal Lagrangian (refer to Formula A-14) results in the corresponding dual Lagrangian:

$$L(w, b, \lambda) = \sum_{i=1}^{k} \lambda_i - \frac{1}{2} \sum_{i,j=1}^{k} y_i y_j \lambda_i \lambda_j \langle x_i \cdot x_j \rangle$$

Formula A-16: Dual Lagrangian for Support Vector Machine margin optimization.

The geometric interpretation of SVM maximum margin optimization referring to Formula 4-2 with the corresponding optimization problem statement, the identity of the objective function from Formula 4-3 (finding the closest distance between two convex hulls) and the dual Lagrangian function in Formula A-16 can be seen.

A.2.2 The Kernel Trick

The maximum margin SVM classifier reviewed so far can only be applied to linearly separable data as it cannot converge on data that is linear nonseparable. This is a severe limitation as most applications (including the classification of high-dimensional data from multi-channel images of wood defects) have to deal with nonlinearity and noisy (training) data (wrong labelled training examples, etc.). One of the basic ideas of SVM classification is

to find a way to use the well-understood theory and efficient implementation of the linear learning machines incorporating convex optimization which has been introduced in the previous sections and to transform the input/feature space to be usable by these linear learning machines. Cover's theorem states that the probability of a classification problem to be linearly solvable raises with the dimensionality of the underlying feature space and that it is therefore possible to find a mapping function that produces a higher-dimensional (even infinite dimensional), linearly separable, transformed feature space *[Cover1965].* This is the basis for kernel representations of the training data used by modern SVM classifiers.

The use of Mercer's theorem for interpreting kernels as inner products in a feature space was introduced into machine learning in 1964 by the work of Aizermann, Bravermann and Rozoener *[Aizerman et al. 1964].* The fact that the dual representation of learning machines allows the separating hyperplane of the SVM to be expressed as a linear combination of the training points and the fact that the decision rule can be evaluated using just the inner products between the test point and the training points lead therefore to computing the inner product in the transformed feature space directly: Mercer's theorem identifies a class of (nonlinear) function, known as kernels, that produce a mapping of the input data $x \in R^m \rightarrow \phi(x) \in R^n,\ n > m$ into a higher or even infinite space such, that the inner product in this higher dimensional space can be expressed by $f(x_i^T x_j)$ (equivalent: $\langle x_i . x_j \rangle$) where $f(\cdot)$ is the so called kernel function. Therefore, replacing the inner product in Formula A-16 by a kernel function *K* is equivalent to working in a higher dimensional feature space *[Cristianini and Taylor 2000]*, (proposition 6.6):

$$L(w, b, \lambda) = \sum_{i=1}^{k} \lambda_i - \frac{1}{2} \sum_{i=1}^{k} y_i y_j \lambda_i \lambda_j K(x_i, x_j)$$

Formula A-17: Dual Lagrangian incorporating kernel function for implicit mapping of feature space.

An important consequence of this is that the dimension of the feature space does not affect the computation. As the features are not necessarily to be represented explicitly but mapped implicitly by the kernel function, the amount of operations which are required to compute the inner product by the kernel function is independent from the number of features, allowing even infinite feature spaces.

There exists a variety of functions which can be used as kernel functions with this approach. The most common group of kernel functions are polynomial and Gaussian radial basis functions (RBFs), the latter resulting in a feature space of infinite dimension *[Cristianini and Taylor 2004]* and being used widely in all kinds of SVM-based classification setups. The design of proprietary kernels tailored to the structure of the underlying data gives further options in terms of performance and accuracy but might call for the incorporation of a domain expert.

A.2.3 Soft margin extension

In the previous paragraph the Kernel-Trick has been introduced allowing the creation of a high-dimensional, even infinite feature space, which is linearly separable, by transformation of the linearly nonseparable input feature space. The transformed feature space then can be used by a linear learning machine. Nevertheless the hard margin concept will produce a perfectly separating classifier by default, which is problematic in terms of overfitting on noisy data as can be seen from Figure A-7.

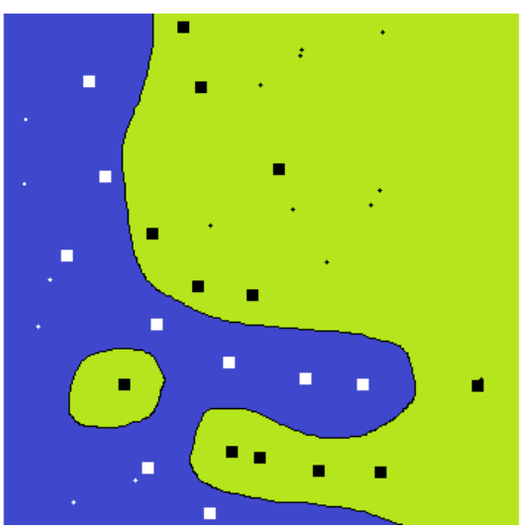

Figure A-7: Comparison of maximal margin classifier and soft margin classifier working on linearly nonseparable data:
Hard margin classifier producing complex overfitted hyperplane due to noisy data. Highlighted (square) sample points indicate support vectors.

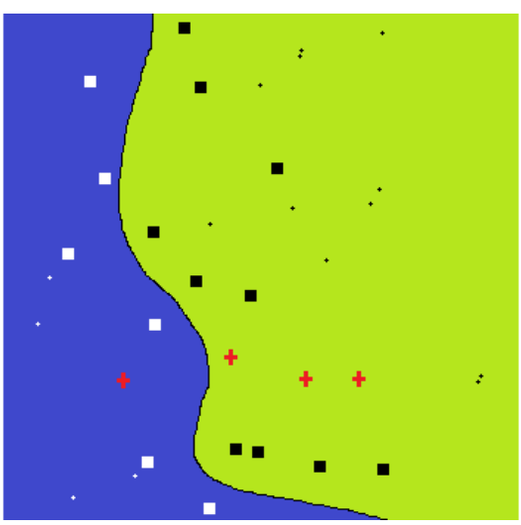

Figure A-8: Comparison of maximal margin classifier and soft margin classifier working on linearly nonseparable data:
Soft margin classifier tolerating noise (big/red crosses) in favour to generalizing capabilities. Highlighted (square) sample points indicate support vectors.

Figure A-7 and Figure A-8 show a two-dimensional (training) data set transformed with a Gaussian kernel using a hard margin (Figure A-7) as well as using a soft-margin (Figure A-8) applied on the feasibility region. The separating hyper-plane in the transformed feature

space (the untransformed, original feature space is shown in Figure A-7 & Figure A-8, representing the hyperplane as a curve) divides the data set into a positive (green/bright area, dark spots) and a negative (blue/dark area and bright spots) area according to their position in relation to the hyperplane. The involved support vectors are highlighted by bigger squares. While the hard margin classifiers produces a hyperplane perfectly separating the training data including the noisy samples, a soft margin classifier is based on a hyperplane tolerating some potentially misclassified sample points which are marked with red/bigger crosses in Figure A-8.

The soft-margin extension introduces a regularization parameter C that has to be found empirically by testing the performance of the SVM over a wider range of values *[Cristianini and Taylor 2000]*, (chapter 6.1.2), incorporating cross validation for example. In a cascaded training of a classification using huge sets of pre-sorted image tiles with wood defects labelled by an expert, the capability to tolerate noisy samples due to wrong labelling and due to the involved uncertainty is very valuable as faultless labelling cannot be guaranteed and often the boundaries between the classes are challenging for the human expert as well, refer to examples initially given with the different knot defect types in Table 4-1 as well as to the pre-sorted planar representation of knot images in Figure 4-8.

A soft margin classifier is based on a hyperplane tolerating some misclassified sample points. This is achieved by introducing slack variables ξ_i to the primal optimisation problem (refer to beginning of Appendix 1.1A.2.2):

minimise$_{w,b}$	$\langle w * w \rangle$	objective function - origin
minimise$_{\xi,w,b}$	$\langle w * w \rangle + C \sum_{i=1}^{l} \xi_i^2$	objective function - incorporating slack variable
subject to	$y_i(\langle w * x_i \rangle + b) \geq 1, \quad \mathrm{i} = 1, \ldots, \mathrm{k}$	Linear inequality constraint - origin
subject to	$y_i(\langle w * x_i \rangle + b) \geq 1 - \xi_i, \quad \mathrm{i} = 1, \ldots, \mathrm{k}$ $\xi = 1, \ldots, \mathrm{l}$	Linear inequality constraint – incorporating slack variable

Formula A-18: Primal optimization problem extended by slack variables to produce a soft margin classifier

That is leading to Lagrangian function *L*:

$$L(w, b, \lambda) = \frac{1}{2}|w * w| + \frac{C}{2}\sum_{i=1}^{l} \xi_i^2 - \sum_{i=1}^{k} \lambda_i \left[y_i(|w * x_i| + b) - 1 + \xi_i\right]$$

and the derived optimal solution $\lambda^*(w^*, b^*)$ constrained by the KKT conditions:

$$\lambda_i^*[y_i(|w^* * x_i| + b^*) - 1 + \xi_i] = 0, \quad \mathrm{i} = 0, \ldots, \mathrm{k}$$

where *C* is a constant called regularisation parameter that has to be found empirically by testing the performance of the SVM over a wider range of values *[Cristianini and Taylor 2000]*, (chapter 6.1.2), incorporating cross validation for example.

A.3. Fuzzy logic

Since Lotfi Zadeh established Fuzzy Logic in 1965 at University of California *[Zadeh 1965]*, many publications have been made in this field which in the meanwhile developed to a wide area of research. In all kinds of applications where the relationships of the system's input variables are complex and therefore the partitioning of the input space is difficult, especially if the input data contains much noise, the advantages of the unsharp/fuzzy logic in contrast to crisp logic has been proven. Expert systems, especially, could gain a lot from the methods based on the newly developed operators.

A.3.1 Membership functions

Fuzzy set theory is an extension to crisp set theory. The belonging or membership $\mu(x)$ of the value *x* to one or another class *B*, *D* in the interval [0,*threshold*] using crisp logic can be expressed as:

$$\mu(x) = 0 \; if \; x < threshold \; (x \; is \; totally \; in \; D)$$

Formula A-19: crisp threshold example, class dark

For *D*, respectively in the interval [*threshold*,255] for *B* as*:*

$$\mu(x) = 1 \; if \; x \geq threshold \; (x \; is \; totally \; in \; B)$$

Formula A-20: crisp threshold example, class bright

Figure A-9 shows the corresponding function which can be grasped as the membership function of the values belonging to class B:

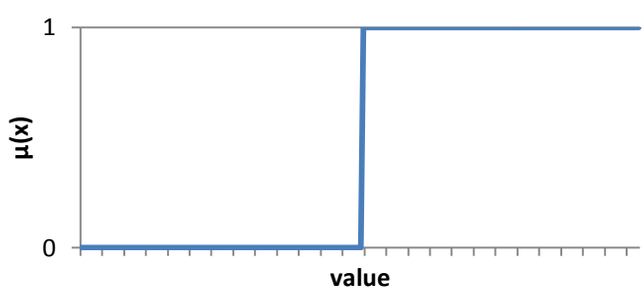

Figure A-9: Crisp value of membership to class *B* when threshold is applied.

Analogous to Figure A-9, the membership function for the values belonging to class *D* is the inverted membership function. With the extension of the crisp set theory by fuzzy sets, the belonging can be expressed alternatively by a value in the interval [0,1], with the meaning that value x belongs to *D* and *B* as well, implementing the concept of degree of membership $\mu(x)$ as illustrated by the sigmoidal function in Figure A-10:

$$(x \text{ is totally in } D) \;\; 0 < \mu(x) < 1 \; (x \text{ is totally in } B)$$

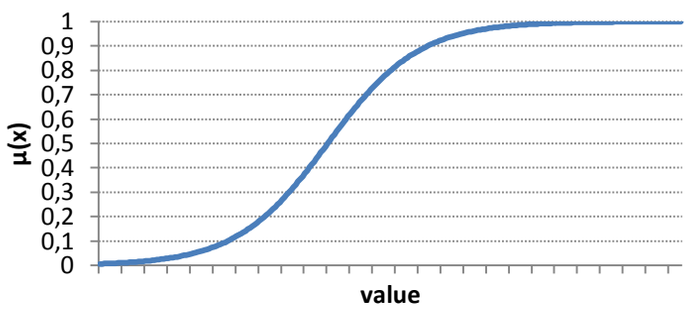

Figure A-10: Fuzzy value of membership to *B* (sigmoidal membership function).

When the sigmoidal membership function shown in Figure A-10 is utilized, the membership of a value may be 0.5 for both *B* and *D*. The membership function *μ(x)* is therefore the essence of the fuzzy inference system, mapping the input space to a fuzzy set, expressing the degree of membership beyond the two conventionally possible and therefore exclusive values 0 and 1. There exist various types of membership functions *[Hazlina2013], [Mathworks1995]*. The proper selection depends on the specific demands for simplicity, speed and accuracy of the underlying system and is in the responsibility of an expert doing proper testing and evaluation *[Yan et al. 1994].*

A.3.2 Fuzzy logic operators

Fuzzy logical reasoning is based on the fact that it is a superset of standard Boolean logic. If the fuzzy values are kept at their extremes of 0 (completely false) and 1 (completely true) the standard logical operations will remain valid *[Zadeh 1965]*. That is for example, "*a* AND *b*" operator is replaced with minimum - min (*a,b*) operator, "*a* OR *b*" with maximum - max (*a,b*) operator and "NOT *b*" with 1-*b.*

A.3.3 If-then rules

Fuzzy sets as well as fuzzy operators are the subjects and the verbs of the fuzzy logic language *[Zadeh 1965]*. Usually the knowledge involved in fuzzy reasoning is expressed as rules in the form:

If x is A then y is B

where *x* and *y* are fuzzy variables (input and output) and *A* and *B* are fuzzy values generated by the membership functions. The if-part of the rule "*x is A*" is called the antecedent or premise, while the then-part of the rule "*y is B*" is called the consequent or conclusion *[Zadeh 1965]*. Note, that in the if-then rule, the word "*is*" gets used in two entirely different ways depending on whether it appears in the antecedent or the consequent part *[Mathworks1995]*. Statements in the antecedent parts of the rules may, and usually do involve fuzzy logical connectives such as 'AND', 'OR' and 'NOT', for example a typical rule connecting two inputs has the form:

If x is A AND y is B then z is C

where *x* as well as *y* are again fuzzy input variables and *A* and *B* are the fuzzy values from the fuzzification which form together the antecedent. The right hand side of the rule, the consequent, now is the resulting fuzzy variable *z* from the fuzzy set *C*. Figure A-11 illustrates the principle of the fuzzy rule and its application to the input space exemplarily by two inputs *x* and *y* and a corresponding set of three membership functions for each input:

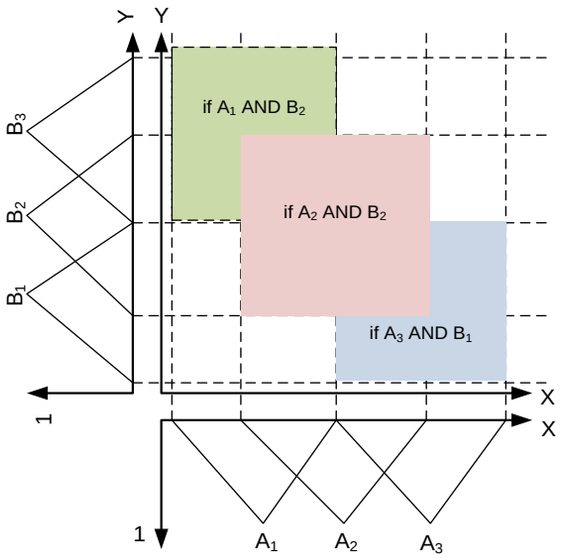

Figure A-11: Principle application of fuzzy rules to the input space, top view illustrating the segmentation of the input space by the rules.

It can be seen from Figure A-11 that applying the rules determines to which degree (output *z*) a two-dimensional input is related to the output (fuzzy set C) associated with each rule (represented as coloured fields). It is in the nature of fuzzy logic that this can result in the membership to several fields as those overlap as can also be seen in the figure. Note that for the purpose of illustration not all rules and connected fields are drawn and that the degree of membership cannot be estimated from Figure A-11 as it is the two-dimensional top view.

Figure A-12 illustrates another input space segmented by two fuzzy rules and their appropriate membership functions (not shown), but also representing the degree of membership due to the three-dimensional perspective.

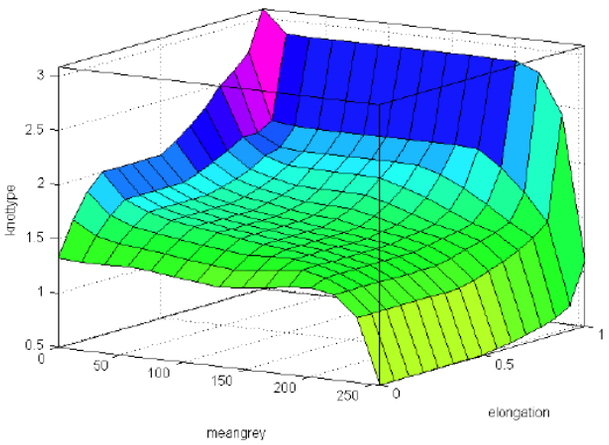

Figure A-12: Principle application of fuzzy rules to the input space spanned by three fuzzy variables, surface plot visualizing the degrees of membership.

If, for example, the input space is the n-dimensional space spanned by the rules derived from ISO 2426-3-2000 (norm for wood appearance, refer to 2.2.3), then the surface plot would represent the floating membership to either the appearance classes **E, I & II.**

Decisions are therefore gained by testing all rules, the so-called rule base or rule engine, in a fuzzy inference system. The results of all rules must then be aggregated to get to the final decision. Aggregation is therefore the process by which the fuzzy sets that represent the fuzzy outputs of the rules are combined into one single fuzzy set *[Dubois et al. 1996].* The output is one fuzzy set for the output variable which represents the final output of the rule base but which encompasses a range of output values and therefore must be de-fuzzified in order to resolve a single output value (crisp value *n*) from the set. There exist several defuzzification methods *[Zadeh 1965]* whereby the most common method is to calculate the centroid in terms of the centre of gravity under the curve of aggregation.

A.4. Algorithms and calibrations for image sensor data fusion

The output of the fusion process is the so-called global image which combines (stitches) equal sensors in a row to channels and combines channels to a global image with corresponding pixels registered.

A.4.1 Calibrations

With reference to chapter 5.1.1 addressing the sensor data fusion, this section summarizes the various calibrations needed in the fusion process. The requirements are:

- Removal of sensor-specific noise and distortion in the image sensor signals (radiometric calibration).
- Removal of lens distortion and shading effects caused by the optics (lenses) and illumination invariance.
- Normalization of intensities between monochrome imaging devices.
- Normalization of colour values between the different colour imaging devices.
- Geometric alignment of pixels to real world coordinates to be used by the patching tools.

The ColourBrain® inspection system technology of Baumer Inspection GmbH was used as a framework for the integration of a scanner for automated patching. The ColourBrain® software framework provides calibration methods satisfying the requirements stated above, this includes shading correction and removal of lens distortion as well as normalization of intensities by white balancing. Geometric calibrations are carried out using special calibrations plates as shown in Figure A-13 and are provided by the ColourBrain® framework as well.

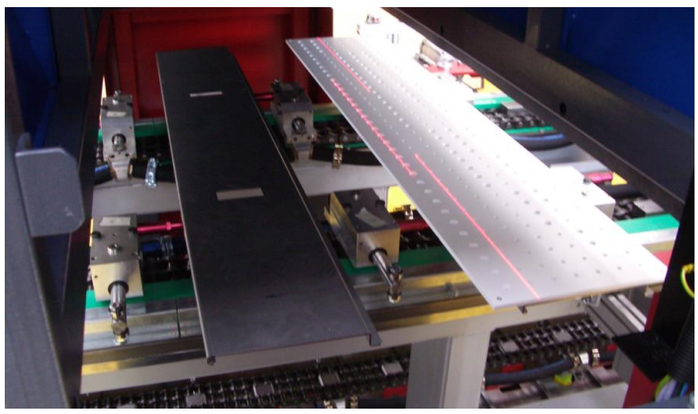

Figure A-13: Scanner calibration plates used to carry out various calibrations. Right calibration plate showing laser alignment, white balancing and geometrical calibration using column-wise binary-coded real world coordinates.

In addition to the existing calibrations the stitching and registration itself were newly implemented for the application of patching. Further, the elimination of dynamic effects (which are in the wider sense also calibrations but are carried out iteratively per panel) was newly introduced in the scope of this work and is summarized in the subsequent Appendix 5.

A.4.2 Image stitching

Image stitching is commonly found in digital consumer cameras, Smartphone cameras and similar. To generate a panorama view a certain number of images is taken in sequential order. This is done while following a certain direction of viewing (mostly in horizontal direction for the creation of landscape panoramas). Based on a movement model *[Shum et al. 1997]* the images are combined by an algorithm resulting in a new image with much more pixels in the direction of the movement than the image sensor is able to acquire in a single acquisition.

The process of image stitching usually relies on finding strong reference points in the adjacent images which therefore must define overlap zones in which the reference points have to be present *[Shum et al. 1997], [Shum et al. 2000]*. By mapping the reference points between the images next to each other, a transformation instruction can be derived to combine the images in such a way that there are ideally no transition artefacts visible. The procedure of finding the corresponding points is known as the correspondence problem *[Shum et al. 1997], [Ogale et al. 2005], [Belhumeur et al. 1992]*. Finding the most appropriate transformation has been subject of lots of research, Brown *[Brown 1992]* gives a nearly

complete list of successfully applied methods and classifies them first by the type of misregistration (translation, rotation, warping) and type of distortion which is involved, then by the complexity of the transformation (affine, polynomial, elastic).

For the use in non-stationary setups the process of finding corresponding reference points and deriving the transformation parameters from them is normally done with every image sequence taken. This is most practical because there is no need to carry out any calibrations in advance *[Steedly 2005].* For an industrial application like for the scanner for automated defect detection, the retrieval of strong reference points in the overlapping image regions by solving the correspondence problem and deriving the transformation instruction repeatedly is unnecessary and also excessively time consuming. As the scanner's setup is stationary with static fields of view, working distances, etc., the transformation parameters for one image channel (several cameras of same type lined up, refer to Figure A-14) can be determined in an offline calibration routine using a suitable calibration normal offering strong reference points in the zone of overlapping fields of view.

Having created all the global channel images, the next step in the processing chain is the creation of a registered multi-channel image which will be addressed in the next section.

A.4.3 Image registration

In image processing and machine vision, Image Registration is the term used for the process of calibrating images from different sensors in such a way, that the pixels corresponding to a physical coordinate in the object plane are linked together although the different imaging devices have different resolutions, fields of view, acquisition rates, etc *[Gottesfeld 2007]*. A mapping algorithm is used to transform the pixels respectively from their camera coordinate system to one common world coordinate system used for all involved imaging devices.

Table 5-1 already gave an overview of the different resolutions and data rates of the imaging devices incorporated in the proposed setup of the scanner for automated repair to illustrate the need and extent of the registration process. It can be seen that there are great differences between the channels in terms of amount of imaging devices and also in terms of their spatial resolution, which makes it necessary not only to apply transformations but also interpolations to the channels with lower resolution to obtain a fully populated matrix

representation of the registered multi-channel image. The output from the registration is however the result of image sensor fusion.

Based on the previously combined geometric and photometric calibrated images from one channel, the registration process can be reduced to a combination of translation, scaling and pixel value interpolation applied to the different channel images. The proposed sensor data fusion based on image registration is mainly based on the findings and implementation of Schmitt *[Schmitt 2006]* and his research on multi-channel imaging for automated visual inspection systems for ceramic tiles, but has been extended by multiple-camera channels; refer to the image stitching presented in A.4.3.

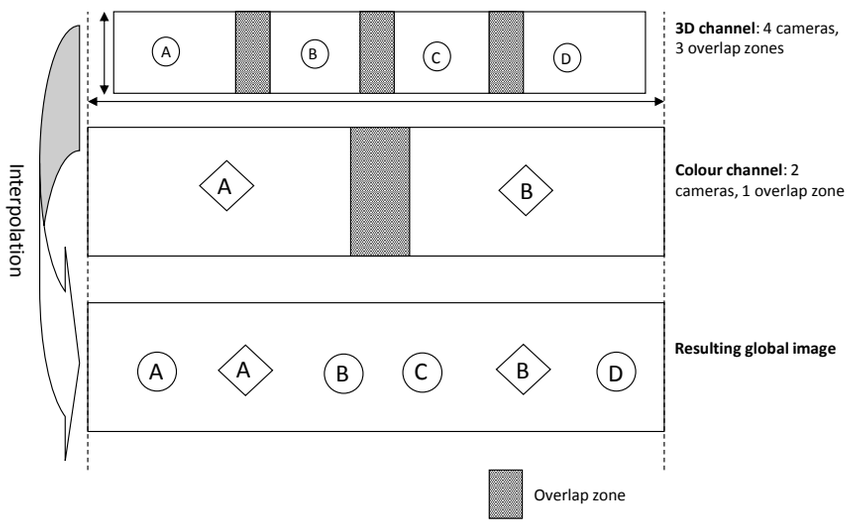

Figure A-14: Exemplary registration (translation, scaling and interpolation of lower resolution 3D channel image to high resolution colour image, channel images are the product of stitching the channel's single overlapping camera images.

Figure A-14 illustrates the combination per channel by stitching calibrated, undistorted camera images, exemplary from a colour channel (2 cameras) and a 3D channel (4 cameras) and illustrates further the combination in terms of registration of the channel images to one global multi-dimensional image with the dimensions of the higher-resolved colour image (upscaling). The labels from the four origin cameras are kept in the transformed image to illustrate the virtual boundaries.

A.5. Elimination of internal & external disturbing effects

The following sections address effects influencing the reliability and accuracy of optical inspection on wooden panels that cannot be calibrated statically.

A.5.1 Elimination of dynamic effects from vibration

Vibration is common disturbing influence in an industrial environment using heavy machinery like in wood-working production facilities. Transportation systems like roller tracks or belt tracks are never free from vibrations and always show some unsteadiness in forward movement. While the latter is in forward direction and can be compensated with the use of shaft encoders, vibrations are directed vertically. The change of height results in a distortion of the image signal. This distortion - often a superimposed periodical signal in the case of vibration or a single impulse in the case of a stroke - normally shows propagation in the direction of transportation.

In the case of a plain periodical disruption signal the identification of its frequency and the application of a band-pass filter would give an undisturbed image signal. Non-periodical shocks cannot be filtered properly in an un-shading process (refer to A.5.2 *Shaded images*) because of their signal characteristics (impulse) and therefore need special treatment. Using the a priori knowledge of the orientation of the pulse in the image signal, a row-wise calculation of a correction factor or correction offset from the mean grey value to a nominal value can be incorporated like illustrated in Figure A-15.

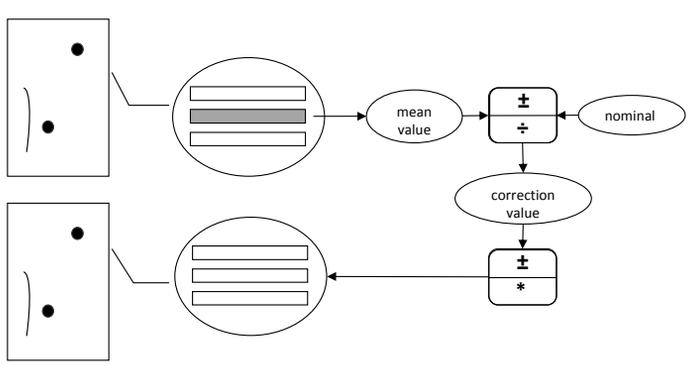

Figure A-15: Elimination of disruptive impulse disturbance.

The described pre-processing of shading correction and vibration correction can be carried out serially to compensate both influences and to provide best possible data for the subsequent detection algorithms.

A.5.2 Elimination of dynamic effects from panel warping

Wooden panels (plywood panels as well as solid wood panels) tend to bending and warping during drying as shown exemplarily in Figure A-16. Mechanical measures (vacuum belts and similar) are incorporated to flatten panels during scanning and the processing with patching tools, but the dynamic effects hereby cannot be eliminated entirely. Software algorithms and optical measures therefore need to be incorporated additionally.

Figure A-16: Warped plywood panel introducing disturbing dynamic effect

The following sections present techniques (software and hardware) to address the issues with flatness imperfection during image acquisition.

Shaded images

A triangulation camera, measuring height and representing different height levels with different grey values in a 3D-image, delivers shaded images as a result of the changing height. Change of height is introduced by twist and warping of the panel (a reflection-based setup with directed light delivers shaded images too, although the changing grey values result from a change in the reflection on the surface caused by a different reflection angle). While shading in the terminology of machine vision normally refers to a constant influence induced by the light source and/or the lens, these disruptive influences are neither constant nor regular, neither per panel nor from panel to panel and therefore demand a dynamic

compensation. Shaded images complicate the utilization of thresholding techniques in the image processing, most often a global threshold value results in severe segmentation errors. Besides the use of dynamic thresholding techniques with a floating threshold value, a pre-processing of shaded images is common in machine vision as then the full bandwidth of image processing operations is useable again. As already mentioned, the shading effect is normally constant and therefore teachable to the system, often in form of mathematically defined correction functions or look-up-tables. In the case of dynamic and irregular shading, the signal with the unwanted information (change of height due to warping) has to be separated from the signal with the useful information (holes, cracks, etc – the real defects in common). This is effectively done by applying a carefully designed low-pass filter to the shaded image, which only leaves the low-frequent component induced by the overall unevenness of the panel in the resulting image. The signal carrying the useful information is normally much more high-frequent in relation to the influence of skew and twist allowing the design of a good and stable filter. From this low-pass-filtered image representing the unevenness of the panel, correction factors or offsets (depending on the restriction on additive shading correction) to a nominal value can be computed that then are applied to the original, unfiltered image, resulting in an signal carrying almost exclusively the information of real defects. The processing chain is illustrated in Figure A-17.

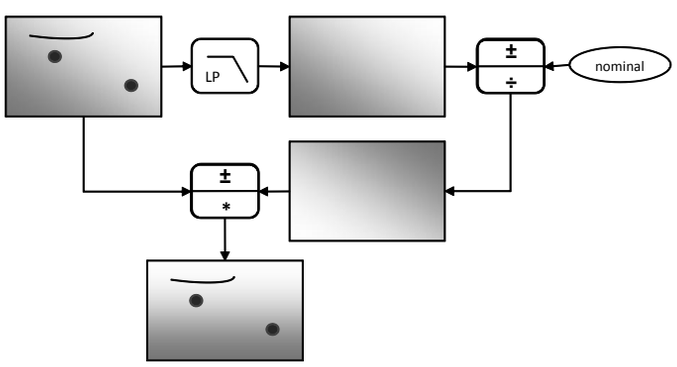

Figure A-17: Elimination of disruptive shading using low-pass (LP) filter and either an additive of multiplicative shading model. Grey values represent depth/height.

The decision if multiplicative or additive shading is appropriate depends on the physical interpretation of the image signal. In case of triangulation measurement the multiplicative variant induces a change of contrast by spreading the values which results in depth measurement errors, therefore additive shading correction must be applied in the case the shaded image signal is a triangulation signal.

Displacement of image plane in triangulation

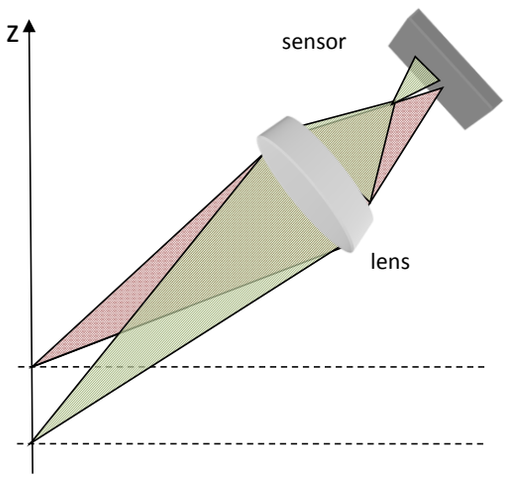

Figure A-18: Displacement of focus/image plane with variation of depth in object plane.

Figure A-18 shows the displacement on the image plane as the welcome effect of the triangulation as well as a displacement vertical to the image plane that is unwanted as it introduces blur in all but one object positions. The effect on the laser line evaluation based on the centre of gravity method for the triangulation measurement is quite small. This is due to tolerant algorithms for the estimation of the laser line (e.g. centre of gravity evaluation is unaffected by unfocused and therefore wider laser line). The effect on the scatter evaluation, for example, results in an uncertainty or error in the determination of the width of the blurred (laser) line. To correct the setup optically, it is necessary to satisfy the Scheimpflug-rule by tilting the sensor plane. This can be achieved with so called tilt/shift lenses; the derivation of the tilted image plane that satisfies the Scheimpflug-rule is described in the following section.

Derivation of tilted image plane satisfying the Scheimpflug rule

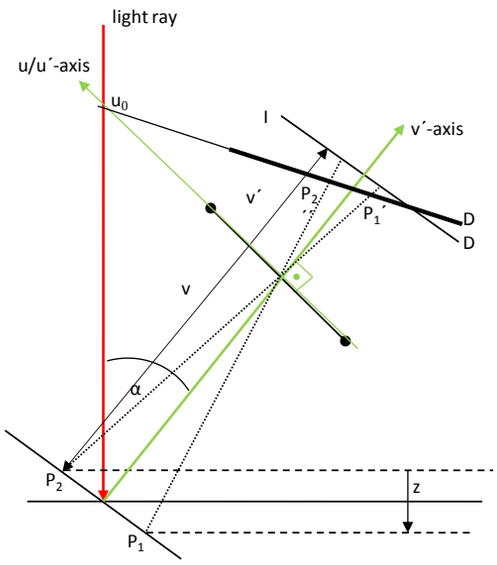

Figure A-19: Optical setup satisfying the Scheimpflug rule.

The mathematical description of a correct tilted image plane regarding the Scheimpflug-rule follows the graphical derivation described by *[Donges and Noll 1993]*. In doing so, the correct tiled plane (refer to Figure A-19) is then described by a line equation in a rectangular coordinate system spun in the centre of the lens and with the axis *u´* and *v´*.

On the object side the coordinates of two points are described by the coordinates *v, u* and on the image side by the coordinates *v´, u´*. The two points P1 and P2 lie on the light ray that is described universally by the equation

$$u = m_{LR} * u_0$$ **Formula A-21: light ray line.**

The lens transforms $P_1(v_1,u_1)$ and $P_2(v_2,u_2)$ that lie on the light ray to $P_1´(v´_1,u´_1)$ and $P_2´(v´_2,u´_2)$ that lie on the tilted image plane in the Scheimpflug arrangement. This can be expressed as a transformation of the line equation of the light ray to a line equation of the tilted image plane through the mapping function:

Image scale $$\beta = \frac{v}{v´}$$ **Formula A-22: Image scale.**

Mapping function $$\frac{1}{v} - \frac{1}{v´} = \frac{1}{f}$$ **Formula A-23: Mapping function.**

Converting Formula A-23 to $$\beta = \frac{v´}{v} = \frac{u´}{u} \rightarrow u = \frac{u´*v}{v´}$$ gives *u*

Converting Formula A-22 to $$v = \frac{v´ * f´}{f - v´}$$ gives *v*

Using *u* and *v* in Formula A-21 and dissolving to u´ results in the equation of the tilted detector plane satisfying the Scheimpflug-rule:

$$u' = v' * \left(m_{LR} - \frac{u_0}{f}\right) + u_0$$

Formula A--24: Tilted detector plane satisfying the Scheimpflug rule.

From this equation the tilting angle can be derived easily, i.e. for the construction or adjustment of special tilt/shift lenses or lens adapters.

Certificate of Ethical Approval

Applicant:

Marc Kuehn

Project Title:

The automatic detection and rectification of surface and aesthetic defects in the production of wooden panels.

This is to certify that the above named applicant has completed the Coventry University Ethical Approval process and their project has been confirmed and approved as Low Risk

Date of approval:

04 August 2015

Project Reference Number:

P35875